Study on Geomagnetic Transfer Function of Japan Islands(Dissertation_全文)

AUTHOR(S):

Fujiwara, Satoshi

主論文

Study on Geomagnetic Transfer Function of Japan Islands

Satoshi FUJIWARA

Geographical Survey Institute, Tsukuba 305-0811, Japan

Contents

ABSTRACT

Geomagnetic signals observed at the surface of the Earth have information on underground conductive structure of the Earth. As the geomagnetic transfer function is calculated from the geomagnetic signals and related to conductive structure of the Earth, it is one of the most useful and efficient methods for geomagnetic investigations. Repeated measurements of the Earth's time varying magnetic field have been made across Japan by the Geographical Survey Institute. Such measurements are known as the first order geomagnetic survey. There are 105 geomagnetic stations located uniformly across the whole area of Japan. Since 1987, triaxial fluxgate magnetometers have been used to obtain one-minute data at almost all stations. From the geomagnetic data, transfer functions were determined for each station. Traditional vertical field transfer functions of wide period range (from 4 min to 128 min) were obtained, making use of the interstation method which is robust against artificial magnetic and electric noises. Additionally, we calculated transfer functions for the horizontal field. The distribution of the transfer functions can be used to form a reference map of geomagnetic induction in Japan. Moreover, the distribution of the horizontal transfer functions in Japan has been examined for the first time. After eliminating the effect of the sea water using thin-sheet models, large regional anomalies are found to remain. These anomalies are diagnostic of the resistivity structure and show patterns of current channeling in Japan. We examined temporal changes of the transfer functions in order to detect conductivity changes associated with crustal activities such as occurrence of earthquakes and volcanic activities. Using the geomagnetic data observed at observatories and first order geomagnetic stations, changes of the transfer functions were obtained. Although we did not find changes of the transfer functions associated with crustal activities at the observatories, we detected temporal changes that possibly associated with occurrence of a large earthquake at the first order geomagnetic stations using the interstation transfer functions.

1. Introduction

1.1 Conductive Anomaly and Transfer Functions

Geomagnetic temporal variations (primary magnetic fields) cause induction currents in the Earth, which is regarded as a conductor. Secondary magnetic fields are generated by these induction currents and coupled geomagnetic variations of the primary and secondary variations are observed at the surface of the earth in general. The induction currents are affected by conductive (the reciprocal of resistive) structure of the Earth. For example, as conductivity becomes higher, the induction currents and the secondary geomagnetic variations become larger. The source of the geomagnetic variations is electric currents in the ionosphere and magnetosphere of the Earth. In general, geomagnetic variations originated in the Earth's ionosphere in mid latitude are almost composed of horizontal fields and there is little vertical field (Lilly, 1974). If conductive structure of the Earth is homogeneous, in other words, there is no conductive anomaly (CA) (Figure 1-1 (a)), the vertical component of the geomagnetic variation is not observed on the surface of the Earth. On the contrary, when a good conductor (low resistivity) exists in a rather homogeneous conductive structure (Figure 1-1 (b)), the vertical component of the geomagnetic variations appears. As an indicator of the conductive anomaly, we can often use $\Delta Z/\Delta H$, where ΔZ is the vertical component of geomagnetic variations, and ΔH is the horizontal component (the geomagnetic north component). In or to the south of a good conductor, $\Delta Z/\Delta H$ has a negative value, in or to the north of a good conductor, $\Delta Z/\Delta H$ has a positive value (Figure 1-1 (b)), and on the center of the good conductor, $\Delta Z/\Delta H$ has almost zero value. Therefore $\Delta Z/\Delta H$ shows horizontal contrasts of the conductive structure, and it can be used for geophysical investigation.

It has been known that ΔZ at Greenwich and Paris had the opposite sign during geomagnetic storms (van Bemmelen, 1908; Chapman and Bartels, 1940). Schmidt (1909) pointed out that changes of ΔZ at Potsdam and Seddin (they apart from each other only 13 km)

were quite different. Since 1950's it has been known that the vertical components of geomagnetic variations at periods shorter than several hours differ in amplitude and phase significantly from one place to another in Japan. Figure 1-2 shows a typical example of simultaneous observations by CA research group in Japan (Rikitake, 1971). In the figure, the horizontal component (H) and the declination (D) show small differences for all stations, but unusually large variations of the vertical component were observed along the Pacific coast in the central Japan and reversed variation was observed at the northern end of the Honshu. Such differences can be used to map conductive anomalies and have been studied by many researchers in Japan (e.g. Rikitake, 1966). Figure 1-3 shows the geographical distribution of $\Delta Z/\Delta H$. Rikitake (1969) accounted for large CA in central Japan and northeastern Japan by assuming an undulation of a mantle conducting layer (Figure 1-4), as it was thought that these CA had a close relation to the conductive structure of the upper mantle.

An empirical linear relation among the three components of geomagnetic short-period variations (e.g. 'Bay type' variations) can be derived and widely used:

$$\Delta Z = A \cdot \Delta X + B \cdot \Delta Y \qquad (1\text{-}1)$$

where ΔX, ΔY and ΔZ are the geographic north, east and vertical components of geomagnetic variations, respectively. Mathematically complex Fourier components (ΔH instead of ΔX, and ΔD (declination) instead of ΔY are conventionally used in CA studies, but in this study we rotated the axis from the geomagnetic coordinate to the geographic coordinate using the results of precise declination observation [see section 2.1.]. The true geographical expression is much better for the interpretation of the CA structure.). This relation is interpreted as a linear system that has two inputs of ΔX and ΔY, and an output ΔZ. The coefficients A and B are constants that are specific to a given station although they

depend on frequencies. Since they have information on CA of the Earth, they are also called the CA transfer functions. The transfer functions represent anomalies of the vertical field. Rikitake and Yokoyama (1955) interpreted Eq. 1-1 as indicating a plane in which the vector of magnetic variation is confined and the plane is called the Rikitake and Yokoyama plane. This plane is also interpreted as magnetic lines, as shown in Figure 1-1. Parkinson (1959, 1962) introduced an arrow representation of the transfer functions, called the Parkinson vector, can be derived by projecting a vector which is normal to the Rikitake and Yokoyama plane onto the Earth's surface. In these days, a representation using an arrow called the induction arrow is often used to illustrate the transfer functions. The transfer functions are usually expressed as the induction arrows, A is southward direction and B is westward direction. The induction arrows are similar to the Parkinson vectors, only the length is slightly different. The induction arrows are commonly used as a method of estimating conductive structure. Using the transfer functions at a station, we can estimate conductive structure in the crust and upper mantle beneath and around the station.

In general, the transfer functions are frequency-depend complex functions. This is because geomagnetic variations of longer periods can penetrate into thicker parts of the Earth but on the other hand those of shorter period are attenuated due to induced eddy currents and can penetrate into only thinner parts of the Earth. This behavior is called the skin effect, and the skin depth is the typical depth at which amplitudes of the input geomagnetic variation becomes $1/e$. The skin depth d (m) is given by:

$$d = 503\sqrt{\rho T} \tag{1-2}$$

where ρ denotes resistivity in ohm·m and T denotes period in seconds. This frequency dependence is derived from vertical anomalies of conductive structure. There is a phase shift

of the geomagnetic response of the Earth, which means a complex function. Their real and imaginary parts are designated with suffixes u and v, respectively:

$$A(f)=Au(f)+iAv(f) \tag{1-3}$$

$$B(f)=Bu(f)+iBv(f) \tag{1-4}$$

where f is frequency (Hz). In general, the imaginary part is smaller than the real part.

Local features of the transfer functions have been extensively studied in Japan (observed induction arrows were compiled by Handa *et al.*, 1992, and Bapat *et al.*, 1993), but a nation-wide survey has not been previously attempted.

1.2. Origin of the Variation of the External Field

The geomagnetic transfer functions is researched using magnetvariation fields, and we should pay attention to the nature of the geomagnetic fields themselves, at least approximately. Although artificially controlled electromagnetic sources are sometimes used for geophysical soundings, they are basically free from assumption of the source field. As the artificial source power is, however, limited, there is limitation of the maximum depth and the area of soundings.

In mid- and low-latitudes, rather regular daily variations of the geomagnetic field are found and it is called the solar quiet daily variation (*Sq*). The *Sq* field is generated by elctric dynamo in the ionosphere. A typical *Sq* variation is recognized on April 3, 1993 shown in Figure 1-5. In this study, we didn't use *Sq* variations because they have lower frequencies than we concerned.

A Large disturbance of the geomagnetic field is sometimes recognized, and it is called a geomagnetic storm. A typical geomagnetic storm observed at Mizusawa is also seen in Figure 1-5, and at the beginning of the geomagnetic storm the horizontal component suddenly increases as shown in the figure. The geomagnetic storm is caused by high-energy plasma, ejected at the time of explosions on the sun's surface, collides with the magnetosphere and compress it. The initial phase of the geomagnetic storm is considered to deformation of the magnetosphere due to plasma compression and the main and recovery phase of the storm are generated by equatorial ring current which initially develop and gradually decay at distances of 5 or 6 earth-radii (Rikitake and Honkura, 1985). A geomagnetic storm occurs generally about once per 29 days (depends on solar rotation) and the variations caused by a typical geomagnetic storm continues more than a few days.

Substorm variations (bay-type variations) of the geomagnetic field are frequently found in magnetograms (e.g. Figure 1-2). These variations are caused by a strong current in the auroral zone. Besides them, temporal geomagnetic variations with periods from 0.1 s to 1000 s

sometimes recognized and are called geomagnetic pulsations (micropulsations). Figure 1-6 shows the relationship between period and power spectrum for the geomagnetic pulsations. Geomagnetic pulsations have relational interactions between solar wind plasma and the Earth's magnetosphere. The periods of geomagnetic pulsations are related to the dimensions of the magnetosphere and its resonance cavity (Rikitake and Honkura, 1985). The geomagnetic pulsations give rise to significant induction currents only in those layers of the Earth's crust and these phenomena are used in the geomagnetic soundings.

In this study, the geomagnetic variations with periods from 4 min to 128 min are mainly analyzed. Though practical geomagnetic variations above mentioned can not be completely uniform on the Earth's surface, they are regarded as quasi-uniform over large areas, particularly in mid-latitudes (Lilley, 1974). We can consider that the scale length of sources concerned may be much greater than the scale length of anomalies of the local conductive structure of the Earth. A schematic diagram of the actual geophysical situation and the uniform-field model is shown in Figure 1-7 (after Lilley, 1974).

1.3. Effect of Sea Water

The electrical resistivity of sea water is about 0.3 Ω m, which is one of the lowest resistors (the highest conductors) around shallow part of the Earth. Therefore short-period geomagnetic variations have high sensitivity to sea water, and the ocean distribution not a little affects the transfer functions. As Japan is surrounded with oceans, the sea water effect on the transfer function study cannot be neglected. The so-called coast, island, peninsula and channeling effects are typical examples of the effect of sea water.

(a) Coastal Effect

A coastline is a clear boundary separating a low resistive sea from a high resistive land. The induced electric currents tend to flow in sea water, and the currents make large anomalies in the vertical geomagnetic field. Since the induction arrows tend to point towards high conductor, the induction arrows are often perpendicular to the coast line and point towards sea.

(b) Island and Peninsula Effect

Island and peninsula effects are considered a kind of the coastal effects. In a small island and a tip of a peninsula, large anomalies of the transfer functions are often found. Figure 1-8 shows a typical example of the island effect observed on Oshima Island, a small volcanic island situated south of the central Japan (Sasai, 1967, 1968). For a bay-type variation, the Z variation at the southern part of the island is almost the same with the H variation, while that in the central island is very small and that at the northern part has opposite sign (Figure 1-8 (a)). Figure 1-8 (b) shows Parkinson vectors in the island, and they tend to point towards the ocean.

(c) Channeling Effect

The channeling effect is also one of the coast effect. In a narrow strait, concentration of induced electric currents often occurs. Therefore the phase of anomalous Z variation at one side of a strait often shows opposite to that to another.

1.4. Horizontal Transfer Functions

The study of the transfer functions has been usually focused on the anomalies of the vertical field component. However, anomalies of the horizontal field component were also observed at some stations. Nishida (1981) found that the amplitudes of horizontal fields at selected stations in Hokkaido were 1.8 times as large as those at a reference station. However, the study of horizontal anomalies has been less than that of the vertical because there are two difficulties; first in synchronizing clocks at two separate stations, and secondly in defining a reference 'normal field'.

Anomalies of the horizontal component correspond to shallow low resistivity structure, as they attenuate more rapidly than the vertical anomalies with increasing distance from the structure of interest (e.g. Rikitake and Honkura, 1985). In other words, the anomalous horizontal fields are more localized in comparison with the anomalous vertical fields, and therefore the study of the anomalous horizontal fields may provide additional information on the resistivity structure of the Earth. This study is the first attempt to determine the distribution of the horizontal anomalies over the whole of Japan.

1.5. Temporal Changes of the Transfer Functions

As mentioned above, the transfer functions of the geomagnetic fields are primarily used for investigations of the conductive structure of the Earth. If electric conductivity of rocks beneath an observations station changes, some temporal changes of the transfer functions are expected at the station. In a seismic active region, it is expected that the electric conductive structure in a certain region may change due to changes of tectonic stresses, temperature, chemical composition, or due to dilatancy phenomena (Scholz *et al.*, 1973), underground water flow (Mizutani and Ishido, 1976) and other phenomena.

As for changes of resistivity of rocks, a large amount of changes in electrical resistivity are observed as a function of compressive stress in a variety of crystalline rocks (Brace and Orange, 1968). In the majority of rocks (see Figure 1-9), resistivity first increase in a small amount slightly up to about half of the fracture stress, while a reverse effect is noted for rocks that are partially saturated. Beyond half and particularly within about 20 % of the fracture stress, resistivity drops typically by an order of magnitude. This sharp decrease of resistivity corresponds closely to an increase in porosity, which takes place under compressive stress.

Yanagihara(1972) pointed out that the ratio of $\Delta Z/\Delta H$ ($\fallingdotseq A$) underwent a temporal change at the Kakioka Magnetic Observatory (Figure 1-10) and that the minimum value of $\Delta Z/\Delta H$ took place in association with the great Kanto earthquake (1923, M= 7.9). Such evidence that temporal changes of the transfer functions occurred in association with occurrence of earthquakes has been reported (e.g., Miyakoshi, 1975; Yanagihara and Nagano, 1976; Rikitake, 1979; Fujiwara and Sumitomo, 1988; Fujiwara *et al.*, 1994). Therefore monitoring the temporal changes of the transfer functions are thought to be one of the possible means of prediction of earthquakes, and for this purpose the transfer functions are continuously monitored at several places in Japan (Honkura, 1979; Shiraki, 1980; Sano *et al.*, 1982; Fujita, 1989). Not only the traditional transfer functions, but also the horizontal transfer functions have been used to detect precursory changes associated with earthquakes. Honkura and Taira (1983) found that the amplitudes of the horizontal geomagnetic variations changed in association with crustal uplift in Izu Peninsula, Japan (Figure 1-11).

Rikitake (1976) pointed out that geomagnetic variations having a period of a few minutes might be useful for detecting conductivity changes corresponding to earthquake occurrences. Although Beamish (1982) detected change of the conductive anomaly preceding an earthquake using the horizontal transfer functions. There was no precursor, however, at longer periods

than 10 min (Figure 1-12). In this study, we examined the changes of the transfer functions at periods of wide range.

2. Data

2.1. First Order Geomagnetic Survey

The Geographical Survey Institute has carried out the geomagnetic surveys with almost regular intervals in Japan since 1949 in order to investigate the geographical distribution of the geomagnetic secular variation (Geographical Survey Institute, 1951, 1995). Such measurements are known as the first order geomagnetic survey. There are 105 geomagnetic stations that uniformly cover the whole of Japan (Figure 2-1 and Table 2-1). Observations are carried out every 2 or 5 years.

Since 1987, triaxial fluxgate magnetometers have been introduced to collect one-minute data at almost all the stations (Otaki and Tsukahara, 1990). The triaxial fluxgate magnetometer is a variometer that measures the changes of three-components of the geomagnetic field, consisting of the sensor, the control unit and the recorder. The measuring process of the fluxgate magnetometer is as follows; an alternative magnetic field of a fundamental frequency is applied to the sensor through the first coil and the distorted induced current is observed in the second coil. The amplitude of the bi-harmonic frequency in the second coil is in proportion to the magnetic field. In the actual measurement, the bias magnetic field is applied to compensate the geomagnetic field, and then very small residue between the geomagnetic field and the compensating bias field is measured. The sensor element of each component consists of a pair of cores made of high permeable materials such as permalloy with coils wounding around them, and each axis of three-element cores is perpendicular to each other.

This instrument has a temperature dependence of 0.2 nT/ºC for the sensor and 0.1 nT/ºC for the control unit, with a stability of 0.1 nT/day and resolution of 0.1 nT. The sensor is mounted on gimbals so that Z is aligned with the vertical direction by gravity, and the sensor case is buried to reduce the effects of ambient temperature changes (Photos 2-1, 2-2, and 2-3).

Timing accuracy is within 3 seconds, so we can get simultaneous data with the permanent geomagnetic observatories. Typical magnetograms observed at the first order geomagnetic stations are shown in Figure 2-2. At some stations, artificial noises of a few nT are found in Z component (cf. Figures 2-2 (b), (f), and (i)).

The observations and analyses in this study have the following features:

(a) The first order geomagnetic stations are uniformly distributed over the whole of Japan.

(b) Instruments of observations and the method of analyses are quite common for each of the first order geomagnetic station.

(c) Since the absolute declinations are precisely measured at all station, induction arrows are referred to the true geographical coordinates.

(d) As we regularly repeat at the first order geomagnetic survey at a station every 2 or 5 years, the time variations of the transfer functions at the station can be obtained.

2.2. Geomagnetic Observatory

We have also used data from a number of permanent geomagnetic observatories. The Geographical Survey Institute operates geomagnetic observatories at Mizusawa (MIZ or MZS), Kanozan (KNZ) and Tsukuba (TKB) (see Figure 2-1). Mizusawa Geodetic Observatory is situated in Mizusawa city, Iwate prefecture, the north-eastern part of Japan. Kanozan Geodetic Observatory is situated in Kimitsu city, in the Boso Peninsula, the central part of Japan. Absolute observations in the geomagnetic filed are performed in a absolute observation hut once per week at each observatory. The declination and the inclination are measured with GSI type magnetometers (using a rotating coil detector), or a DIM type magnetometer (a fluxgate magnetometer theodolite). The total intensity is continuously observed with the proton precession magnetometer at each observatory. Geomagnetic variation meters are also operated in magnetically quiet variation huts at each observatory, in which three components (*H, D* and *Z*) of the geomagnetic are measured digitally every minute, with a least count of 0.1 nT.

In addition, we used data from other observatories and permanent stations, namely Kakioka (KAK), Memanbetsu (MMB), Kanoya (KNY), Matsuzaki (MTZ) and Omaezaki (OMZ), which are operated by the Japan Meteorological Agency, and Yatsugatake (YAT), which is operated by the Earthquake Research Institute, the University of Tokyo.

3. Data Analyses

3.1. Transfer Functions

The usual transfer functions, A and B, can be derived simply from Eq. (1-1). In this study, however, we refine Eq. (1-1) by making use of data from different observation sites. This approach is known as the interstation method. Using the interstation method, we can also calculate horizontal transfer functions.

Geomagnetic variations observed at a field station can be separated into a normal part and anomalous one. The normal part is composed of both an external field and an internal field that arises from induced current flowing in a 'normal' Earth structure. On the other hand, the anomalous part is attributed only to an internal field that arises from induced current flowing in an 'anomalous' Earth structure (Beamish, 1982).

The interstation transfer functions are written using these normal and anomalous parts:

$$\begin{pmatrix} \Delta X_s \\ \Delta Y_s \\ \Delta Z_s \end{pmatrix} = \begin{pmatrix} \Delta X_n \\ \Delta Y_n \\ \Delta Z_n \end{pmatrix} + \begin{pmatrix} \Delta X_a \\ \Delta Y_a \\ \Delta Z_a \end{pmatrix} = \begin{pmatrix} \Delta X_n \\ \Delta Y_n \\ \Delta Z_n \end{pmatrix} + \begin{pmatrix} C & D & G \\ E & F & H \\ A & B & I \end{pmatrix} \cdot \begin{pmatrix} \Delta X_n \\ \Delta Y_n \\ \Delta Z_n \end{pmatrix} + \begin{pmatrix} \delta X \\ \delta Y \\ \delta Z \end{pmatrix} \tag{3-1}$$

where A,B,C,D,E,F,G,H and I are the interstation transfer functions and δX, δY and δZ are uncorrelated parts of the corresponding components (Schmucker, 1970), including observational errors. ΔXs, ΔYs and ΔZs are the three components of geomagnetic variations of an observation site; ΔXa, ΔYa and ΔZa are anomalous components, ΔXn, ΔYn and ΔZn are normal components.

Now we assume that ΔZn, δX, δY and δZ are negligibly small and the normal field is observed at the reference station. Then we get:

$$\begin{pmatrix} \Delta X_s \\ \Delta Y_s \\ \Delta Z_s \end{pmatrix} = \begin{pmatrix} \Delta X_r \\ \Delta Y_r \\ 0 \end{pmatrix} + \begin{pmatrix} C & D \\ E & F \\ A & B \end{pmatrix} \cdot \begin{pmatrix} \Delta X_r \\ \Delta Y_r \end{pmatrix} = \begin{pmatrix} C+1 & D \\ E & F+1 \\ A & B \end{pmatrix} \cdot \begin{pmatrix} \Delta X_r \\ \Delta Y_r \end{pmatrix} \qquad (3\text{-}2)$$

where ΔXr and ΔYr are the horizontal components of geomagnetic variations of the reference station.

To calculate the interstation transfer functions, synchronous observations at the field station and the reference station are needed. Time differences of sampling of the observations at each first order geomagnetic station is within 3 seconds, which is sufficiently accurate to calculate the interstation transfer functions of both the geomagnetic vertical and horizontal fields, since we calculated the transfer functions for the periods from 4 min to 128 min and the phase error is at most 5 degrees (3 sec / 4 min).

We selected Kakioka as the reference observatory because Kakioka is situated in the central part of Japan and we can always use reliable data for any duration of all the field observations.

When there are local noises in the data of a station, we can reduce the effect of the noise using data at other stations. This technique is called the remote reference method, which was developed in magnetotelluric studies (Gamble *et al.*, 1979). In this study, we have calculated the interstation transfer functions by a method similar to the remote reference method. The interstation method is effective if there are noises that are not coherent from one station to another. However, the method sometimes does not work well if either the noise is coherent or if the input external signal is incoherent. Since the smallest distance in this study between the observation sites and the reference station Kakioka is 18 km (TKB) and coherent artificial noise was not found, the effect of coherent noises is negligible. The maximum distance in this study almost one thousand kilometers. Since the wavelength of substorm events is several thousand kilometers at mid-latitude (Camfield and Gough, 1975), we can assume that Kakioka and the

field stations are within the same external field. Table 3-1 shows squared coherency of the three components of the geomagnetic field between Kakioka and other observatories. Generally, the squared coherency of the horizontal field is greater than 0.8 except for that at Kanozan at shorter periods (probably attributing to artificial noises which are clearly seen in the data of Kanozan). The coherency is at least 0.85 between Kakioka and Memanbetsu in northern Japan. As the input signal of the reference horizontal field is coherent, and local anomalous fields and noises are generally small at both the reference station and the field stations, the interstation method can be utilized in this study to reduce the effect of noises. In section 5.1, the choice of Kakioka as the reference station will be further discussed.

3.2. Method of Analysis

In this study, the transfer functions are obtained by making use of the power spectrum analysis method (Everett and Hyndman, 1967). We can get the transfer functions using the following formula:

$$A = \frac{P_{ZsXr} \cdot P_{YrYr} - P_{YrXr} \cdot P_{ZsYr}}{P_{XrXr} \cdot P_{YrYr} - P_{XrYr} \cdot P_{YrXr}} \tag{3-3}$$

$$B = \frac{P_{ZsYr} \cdot P_{XrXr} - P_{XrYr} \cdot P_{ZsXr}}{P_{XrXr} \cdot P_{YrYr} - P_{XrYr} \cdot P_{YrXr}} \tag{3-4}$$

$$C = \frac{P_{XsXr} \cdot P_{YrYr} - P_{YrXr} \cdot P_{XsYr}}{P_{XrXr} \cdot P_{YrYr} - P_{XrYr} \cdot P_{YrXr}} - 1 \tag{3-5}$$

$$D = \frac{P_{XsYr} \cdot P_{XrXr} - P_{XrYr} \cdot P_{XsXr}}{P_{XrXr} \cdot P_{YrYr} - P_{XrYr} \cdot P_{YrXr}} \tag{3-6}$$

$$E = \frac{P_{YsXr} \cdot P_{YrYr} - P_{YrXr} \cdot P_{YsYr}}{P_{XrXr} \cdot P_{YrYr} - P_{XrYr} \cdot P_{YrXr}} \tag{3-7}$$

$$F = \frac{P_{YsYr} \cdot P_{XrXr} - P_{XrYr} \cdot P_{YsXr}}{P_{XrXr} \cdot P_{YrYr} - P_{XrYr} \cdot P_{YrXr}} - 1 \tag{3-8}$$

where P_{XrXr}, P_{YrYr} denote the auto-power spectra and P_{XrYr}, P_{YrXr}, P_{XsXr}, P_{YsXr}, and P_{ZsYr} etc. the cross-power spectra.

Figure 3-1 shows a flow chart of the analysis in this study. Initially, the raw data of three components of the geomagnetic variations were individually checked by visual inspection of time series and we eliminated bad data. They were then rotated to the geographical

coordinate and partitioned into the 8-hour data segments. A digital high-pass filter (cut off period of 140 min) and the hanning window were applied to each partitioned data set. Auto- and cross-power spectra for each data segment were then calculated using FFT, and were smoothed out in frequency. Transfer functions are generally obtained by averaging a subset of the transfer functions that are selected on the basis of the signal power and the coherency. However, in this study a simpler method was used in which we calculated the transfer functions using auto- and cross-power spectra for all stacked data. Confidence intervals (95 %) were estimated by the method described by Bendat and Piersol (1971).

3.3. Evaluation of the Accuracy of the Transfer Functions

As the transfer functions are possibly affected by external ΔZ, coherent temporal changes of the geomagnetic transfer functions are sometimes found at two stations which are distant from each other (Sano *et al.*, 1982). Geomagnetic activities change frequently with time and therefore it has been argued that transfer functions are unstable, particularly when the power of the external horizontal field is small or the coherency between ΔX and ΔY is large (Shiraki, 1980). In this section, we discuss the accuracy of the transfer functions at the first order geomagnetic stations.

Figure 3-2 shows the standard deviation of the transfer functions A and B at Kakioka with increasing numbers of stacked data. The one data is calculated from a data length of 8 hours. It is clear that the standard deviation becomes smaller as the stacking number becomes larger. As the duration of continuous observations is about 40 hours or more at each first order geomagnetic station, we checked the standard deviations of A and B at each observatory using power spectral estimates from 5 data segments (40 hours). In Figure 3-3, it can be seen that the accuracy of the transfer function is frequency dependent, and individually varies in the observatories. The accuracy (estimated by the standard deviation) of B at the period of 128 min is the worst, and is about 0.1. We note that secular variations and seasonal variations in the observatories' transfer functions (Fujita, 1989) will tend to increase the standard deviations. The average confidence intervals of all first order geomagnetic stations are at most 0.04 of B at periods of 128 min and 4 min. The confidence estimates of the transfer functions at the first order geomagnetic stations are therefore smaller than that due to the secular and the seasonal variations. For all stations and observatories the accuracy is better than 0.1 which is sufficient to examine the nation wide distribution of transfer functions.

4. Geographical Distributions of the Transfer Functions in Japan

4.1. Results at First Order Geomagnetic Stations

(a) Induction Arrows

We have two types of the transfer functions from the single-station and interstation methods. The single-station transfer functions As and Bs, which are defined in Eq. (1-1), are given by

$$\Delta Z_s = A_s \cdot \Delta X_s + B_s \cdot \Delta Y_s \tag{4-1}$$

Similarly, the interstation transfer functions Ai and Bi, which are defined in Eq. (3-2), are given by

$$\Delta Z_s = A_i \cdot \Delta X_r + B_i \cdot \Delta Y_r \tag{4-2}$$

In Eq. (1-1), ΔX and ΔY are considered as normal fields, and the anomalous horizontal fields are regarded to be negligibly small. However, we have found that large anomalies of horizontal fields that cannot be neglected exist in some places. From Eqs. (3-2) and (4-1) we have

$$A_s = A_r = \frac{A_i \cdot F - B_i \cdot E}{C \cdot F - D \cdot E} \tag{4-3}$$

$$B_s = B_r = \frac{B_i \cdot C - A_i \cdot D}{C \cdot F - D \cdot E} \tag{4-4}$$

In these equations, *As* and *Bs* are re-defined using only the interstation transfer functions. Hereafter we call induction arrows composed of *As* and *Bs* in Eqs.(4-3) and (4-4) the remote reference induction arrows (*Ar* and *Br*).

Figure 4-1 shows the single-station induction arrows *As* and *Bs* in Eq.(4-1) and Figure 4-2 shows the remote reference induction arrows *Ar* and *Br* in Eqs.(4-3) and (4-4) for a comparison. At a glance, the single-station induction arrows are quite similar to the remote reference induction arrows, because the input external fields have high coherency and are almost the same at Kakioka and the stations (Table 3-1).

There are temporal fluctuations of a few nT at periods of shorter than a few tens of minutes at some stations. They are mainly caused by leaked currents from DC electric railways. Artificial noises dominate the transfer functions at some stations and it is difficult to remove such effects automatically using single-station data only. However, using the interstation method, we can estimate the noise contamination. For example, in Figure 4-1, single-station induction arrows of a few stations (e.g. No. 5 Imazu and No. 45 Inuyama) have quite unusual values as compared with those of the neighboring stations due to artificial noise. By use of a remote reference, induction arrows become more consistent with neighboring stations or can be rejected because of large estimated errors (note that when the estimated standard deviations are greater than 0.2, transfer functions are not used). The remote reference induction arrows were therefore used in this study instead of the traditional single-station induction arrows.

Figure 4-3 shows frequency dependences of the transfer functions at observatories and averages frequency responses of the transfer functions at all stations and observatories. It is interesting that the averages *Au* becomes smaller as the period becomes smaller whereas *Bu* becomes larger.

(b) Horizontal Transfer Functions

Since the horizontal transfer functions *C, D, E* and *F* include information of anomalous fields in conductivity, they can be used to estimate electrical resistivity structures of the Earth. There are several methods of portraying these horizontal transfer functions on a map that displays anomalous magnetic fields or electrical resistivity structures. However, an optimum method has not yet been found (Lilley, 1974). In this paper we have used and refined a method, developed by Beamish (1982), of plotting the anomalous horizontal field rotation ellipses. The purpose of this graphical method is to summarize the response of ΔXs and ΔYs compared with ΔXr and ΔYr. We assume a regional horizontal fields ΔXr and ΔYr at the reference station which results in anomalous horizontal fields ΔXa and ΔYa at field stations.

The horizontal field at a field station,

$$\mathbf{s} = (\Delta X_s, \Delta Y_s), \tag{4-5}$$

is divided into the reference (normal) field,

$$\mathbf{r} = (\Delta X_r, \Delta Y_r), \tag{4-6}$$

and the anomalous field,

$$\mathbf{a} = (\Delta X_a, \Delta Y_a). \tag{4-7}$$

Therefore,

$$\mathbf{s} = \mathbf{r} + \mathbf{a} = \mathbf{r} + \begin{pmatrix} C & D \\ E & F \end{pmatrix} \mathbf{r} \quad . \tag{4-8}$$

Now let us define vector **r** which has unit amplitude and zero phase so that it is normalized according to an external reference field. Hence,

$$\mathbf{r} = (\sin\theta, \cos\theta) \quad , \tag{4-9}$$

so $|\mathbf{r}|=1$, $0^{\circ} \leq \theta < 360^{\circ}$, and

$$\mathbf{s} = \begin{pmatrix} \sin\theta \\ \cos\theta \end{pmatrix} + \begin{pmatrix} C & D \\ E & F \end{pmatrix} \begin{pmatrix} \sin\theta \\ \cos\theta \end{pmatrix} \quad , \tag{4-10}$$

$$\mathbf{a} = \begin{pmatrix} C & D \\ E & F \end{pmatrix} \begin{pmatrix} \sin\theta \\ \cos\theta \end{pmatrix} \quad . \tag{4-11}$$

s and **a** are also regarded as vectors. Tops of these **s** and **a** can be plotted as a point in a plane (Figure 4-4 (a)). As the angle θ changes, each points will trace out the locus of an ellipse. The radii of the ellipses are proportional to the anomalous field, which is induced by anomalous currents in the Earth. Further we define the anomalous horizontal field rotation ellipses as locus of **a**. Figure 4-4 (b) shows an example of the anomalous ellipse of the horizontal transfer functions. In this expression, a bold line shows $|\mathbf{s}|>1$ and a broken line shows $|\mathbf{s}|<1$. The direction of the anomalous current flow, which tends to coincide with the strike direction of low resistivity anisotropy, is normal to the major or minor axis of the anomalous ellipses of the horizontal transfer functions.

The regional resistivity structure causes the directional anomaly of electric currents, e.g. through channeling effects. Although the geomagnetic variations induce currents normal to

the geomagnetic variations, the direction of electric current is actually deflected by local and regional resistivity structures. We have added a new expression of this directional anomaly of currents to the anomalous ellipses of the horizontal transfer functions. The anomalous fields **a** of θ=180º (west) and θ=270º (south) are written in terms of the anomalous ellipse as

$$\theta = 180° \rightarrow \begin{pmatrix} \Delta X_r \\ \Delta Y_r \end{pmatrix} = \begin{pmatrix} 0 \\ -1 \end{pmatrix} \rightarrow \begin{pmatrix} \Delta X_a \\ \Delta Y_a \end{pmatrix} = \begin{pmatrix} -D \\ -F \end{pmatrix} \tag{4-12}$$

$$\theta = 270° \rightarrow \begin{pmatrix} \Delta X_r \\ \Delta Y_r \end{pmatrix} = \begin{pmatrix} -1 \\ 0 \end{pmatrix} \rightarrow \begin{pmatrix} \Delta X_a \\ \Delta Y_a \end{pmatrix} = \begin{pmatrix} -C \\ -E \end{pmatrix} \tag{4-13}$$

Then

$$\mathbf{a}_{west} = (-D,-F) \tag{4-14}$$

$$\mathbf{a}_{south} = (-C,-E) \tag{4-15}$$

These variables can be used to interpret the anomalous current (Figure 4-4 (c)).

Figures 4-5 and 4-6 shows the observed anomalous ellipses of the horizontal transfer functions at all stations. Each element of the horizontal transfer functions *C, D, E* and *F* has a real (Figure 4-5) and imaginary part (Figure 4-6). Since the imaginary part is much smaller than the real part, we will mainly use the real part in the following discussion.

4.2. Thin-sheet Modeling

As sea water has low electrical resistivity, the ocean effect on the transfer functions can be large (see section 1.3.). To remove the ocean effect we applied numerical calculation using McKirdy *et al.*'s (1985) thin-sheet algorithm. In a similar study, Chamalaun and McKnight (1993) applied this method in New Zealand. The resistivity structure of the crust is too complex to model and so we estimated only the sea water effect in this study, as a first approximation.

McKirdy *et al.*'s (1985) method includes a thin layer (known as a thin-sheet) of laterally varying conductance overlying a layered resistivity structure, representing the crust and upper mantle. In this study, the layer just below the thin-sheet is 80 km thick and has a resistivity of 250 ohm·m, and the bottom layer is a half space with resistivity of 10 ohm·m. In this model, the upper layer represents the upper lithosphere and the lower layer represents the lower lithosphere and the asthenosphere (e.g. Filloux, 1980; Bapat *et al.*, 1993). The resistivity and the thickness of the layer just below the surface thin-sheet are very important parameters in the sense that,

(1) the resistivity governs penetration of poloidal electric currents in the thin-sheet into the substratum, and

(2) the thickness determines to what extent toroidal electric currents within the thin-sheet mutually couple with those within deep conductors.

Bapat *et al.* (1993) conducted thin-sheet model studies using a similar 1D structure (a 80 km thick lithosphere and an asthenospheric conductor of 10 ohm·m) beneath the thin-sheets though they used different thin-sheet algorithm based on Vasseur and Weidelt (1977) and a value of 1000 ohm·m as the resistivity of the layer just below the thin-sheet. We used 250 ohm·m for the sake of a finer grid spacing since all the lengths appeared in the thin-sheet calculations were normalized by the skin depth in the layer just below the thin-sheet. (It results in a coarse grid

spacing if we put a high resistivity layer beneath the thin-sheet.) Coarseness of the numerical grids tends to result in smaller vertical magnetic components and consequently smaller amplitudes of the calculated induction arrows (Agarwal and Weaver, 1989) since vertical magnetic component is closely related to horizontal spatial derivatives of horizontal electric components by Faraday's law of induction ;

$$\partial Ey/\partial x - \partial Ex/\partial y = -i\omega\mu Z. \tag{4-16}$$

It, however, was also examined by several direct comparisons that introduction of a higher resistivity layer did not yield any significant differences in the calculated induction arrows. It also turned out, in the course of such examination, that damping by the deep conductor through mutual coupling governed the amplitudes of the calculated induction arrows rather than the resistivity value itself. It is not necessarily bad approximation to assume the regional 1D structure around Japan by a 80 km thick lithosphere and an asthenospheric conductor of 10 ohm·m beneath, though it is fairly difficult to give a proper 1D substratum beneath the Japanese islands where intense lateral conductivity contrasts are expected due mainly to subduction of the oceanic plates (the Pacific plate and the Philippine Sea plate).

The boundary condition on the outer boundaries of the grids are;

$$\partial\sigma/\partial x \rightarrow 0 \text{ as } |x| \rightarrow \infty \tag{4-17}$$

and

$$\partial\sigma/\partial y \rightarrow 0 \text{ as } |y| \rightarrow \infty, \tag{4-18}$$

in which σ is the thin-sheet conductance, and x and y are the horizontal coordinates. This condition allows 2D distribution of the surface conductances at lateral infinity, viz., the

condition can be regarded as 'Neumann-type' boundary condition rather than 'Dirichlet' in terms of boundary value problems.

We used a model comprising 51 by 51 grids that covers the Japanese island and the oceans surrounding the Japanese island. Each grid cell size is approximately 40 km × 40 km and the conductance of each cell is calculated from the ocean depths, assuming the resistivity of sea water to be 0.3 ohm·m and the land to be 1000 ohm·m. The depth grouping used in this study is in Table 4-2 and the resultant conductance distribution is shown in Figure 4-7.

Model calculations were done only at periods of 128, 64 and 32 min because the thin-sheet assumption breaks down at periods shorter than 32 min. At short periods, the external fields are significantly attenuated within the ocean, which implies that the ocean is too thick to be modeled by any thin-sheets. Figures 4-8, 9, and 10 show the calculated remote reference induction arrows and the anomalous ellipses of the horizontal transfer functions of the real and imaginary parts, respectively.

4.3. Differences between the Observed Transfer Functions and the Thin-sheet Model Transfer Functions

In this study, we regarded the induction arrows and the horizontal transfer functions as 'vectors', which can be treated linearly. However, this treatment is not strictly correct (Weaver and Agarwal, 1991) because anomalous geomagnetic fields made by several conductors are coupled mutually and not separable. Bapat *et al.* (1993) and Chamalaun and McKnight (1993) treated the induction arrows as true vectors and removed the sea water effect from the induction arrows by subtracting the model calculated induction arrows assuming that the mutual coupling is weak compared with the self-induction by a primary source field. In a similar manner, we can expect that the difference between the observed transfer functions and the thin-sheet model transfer functions shows the effect of removing the sea water.

Histograms of transfer functions of observations and residuals (the observation minus the model) at the period of 128, 64, and 32 min are shown in Figure 4-11. Although the mean values of observed A, C and F at the period of the 32 min are more than 0.1, those of the residuals are less than 0.1. The standard deviations of both A and B of the residuals are smaller than those observed. If the resistivity anomalies are randomly distributed and the thin-sheet model is able to reproduce the effect of sea water, then the mean of residuals would become 0 and the standard deviations would become small. However, the standard deviations of the horizontal transfer functions were not improved. This suggests that the effect of sea water on the horizontal transfer functions is less than that on the vertical transfer functions.

The residual induction arrows and anomalous ellipses of real part and imaginary part, which are the difference between those of the observation and those of the thin-sheet model, are shown in Figures 4-12, 13, and 14, respectively. Residual induction arrows generally become smaller, except in some anomalous regions (e.g. southern Hokkaido District, Kanto District and southern Kyushu District), but the effect of the ocean on the anomalous ellipses is smaller.

5. Interpretation of the Distribution of the Transfer Functions in Japan

5.1. Induction Arrows and Anomalous Horizontal Field

(a) Interpretation of Induction Arrows and Anomalous Horizontal Field

Induction arrows are commonly used in Geomagnetic Depth Sounding (GDS) studies. The induction arrows indicate lateral variations in anomalous electric currents while the horizontal transfer functions represent anomalous currents beneath the station. The maximum of the anomalous horizontal field is located just above the induced current concentration. Although electric currents may be directly induced in low resistivity regions (good conductors), currents may also be channeled. Therefore we must pay attention to the current flow in addition to anomalous conductors themselves.

(b) Selection of the Reference Station

As discussed previously, the reference station should be a 'normal' station, in the sense that it should be situated above horizontally stratified resistivity structure, and sufficiently distant from any lateral discontinuities (Banks, 1973). From this definition, the coherence between any pair of the components ΔX, ΔY and ΔZ should be zero. Since ΔX and ΔZ of Kakioka have high coherency, we did not use ΔZ of Kakioka in the remote-reference calculation.

We considered Kakioka as a suitable reference station for the following reasons. As the horizontal transfer functions in inland parts of Tohoku District are small (Figures 4-5 and 6), we can assume that the horizontal fields measured at Kakioka are the same as that of the other stations in Tohoku District. In addition, we can not find systematic anomalies in northern and southern Japan where there are great distances from Kakioka. The high coherency of the

horizontal components between Kakioka and other observatories (Table 3-1) also supports the selection as a reference station.

(c) Effects of Sea Water and Sediments

A contribution to the anomalous magnetic field is provided by induced electric currents in sea water, known as the coast, island and peninsula effects. Such effects were estimated in this study using the thin-sheet algorithm, although the effects of complex and small scale coast lines could not be modeled accurately and we are restricted to periods longer than 32 min.

The coast effect arises due to concentration of induced currents in the ocean, which produces large anomalous vertical fields near the coast. Since coastlines often run parallel to tectonic structures, such as plate boundaries, we must pay attention to the interpretation of the coast effect.

The anomalous ellipses of the horizontal transfer functions in an island or a peninsula show frequency dependence that they become smaller at shorter periods. Especially at the island stations such as No. 85 Tanegashima and No. 87 Saigou, and peninsula stations such as No. 47 Tanabe and No. 72 Nakamura, the horizontal transfer functions show large attenuation at shorter periods. This effect is similar to that observed by ocean bottom magnetometer studies (e.g. Filloux, 1967). Magnetic field variations at shorter periods are attenuated at the seafloor because sea water has low resistivity. The mechanism of the island and peninsula effect on the horizontal transfer functions is different from that of the ocean bottom case. As electric currents tend to flow into sea water around an island or a peninsula and don't tend to flow just under the island or the peninsula, the horizontal magnetic field becomes smaller in the island or the peninsula, especially at shorter periods. A schematic explanation of electric current around an island is shown in Figure 5-1.

At No. 33 Ishinomaki, No. 34 Sakata, No. 42 Choushi and Kanozan, the anomalous ellipses of the horizontal transfer functions show large anisotropy at shorter periods associated with the Sendai plain, the Shonai plain and the Kanto plain, respectively. The shorter axes of the ellipses are parallel to the plains and perpendicular to the coast lines. Furthermore, at No. 34 Sakata the induction arrows at shorter periods than 32 min in Figure 4-2 point to the north and this can be explained by the low resistivity sediments of the Shonai plain. They also show frequency dependence. These phenomena are probably explained by concentration of currents in the sediments from the ocean.

5.2. Discussion with Respect to the Three Districts

Figure 5-2 shows topographic features in eastern Japan. Generally, regions below 100 m coincide with plains usually covered by low resistivity sedimentary layers.

(a) Hokkaido and Tohoku District

Hokkaido is situated at the junction of two island arcs, the Northeastern Japanese arc and the Kurile arc. Nishida (1976, 1977a, 1977b, 1981, 1982) studied the anomalies of geomagnetic variations in Hokkaido, and Kato (1968) found the northeastern Japan anomaly, which lies just south of Hokkaido. The northeastern Japan anomaly was interpreted in terms of a channeling of electric currents between the Pacific Ocean and the Japan Sea through the Tsugaru Strait (e.g. Rikitake and Honkura, 1985), although Avdeev *et al.* (1995) showed that induction arrows at 256 sec period could not be fully explained only by the channeling.

Figure 4-12 shows that there are the large residual induction arrows that point to the northeast at the sites along the eastern coast of southern Hokkaido, No. 27 Shimokita and No. 28 Hachinohe in northeastern Japan (Tohoku District). Figure 4-13 shows that there are strong anomalous horizontal transfer functions along the Ishikari plain. The current that flows into and out of the Ishikari plain can produce large induction arrows and the horizontal transfer functions (Nishida, 1976, 1981).

Nishida (1982) concluded that a low resistivity layer exists at a depth range of 30 to 70 km beneath the inner part of the Volcanic Front of the northeastern Japanese arc. He also concluded that the effect of the low resistivity layer, situated at the west of the Ishikari plain, cancels the ΔZ component which occurs from the surface sediment layer. Although this conclusion seems to coincide with the observed horizontal transfer functions (Figure 4-5), the residual horizontal transfer functions (Figure 4-13) at the periods of 64 and 128 min of No. 18, No. 23, No. 25, No. 26, and No. 80 in the southwestern Hokkaido are not so anomalous, except

for the anomalies associated with the Ishikari plain. The residual induction arrows at No. 25 and No. 80 (Figure 4-12) are small and the residual anomalous ellipses No. 26, No. 27, No. 80 and No. 81 (Figure 4-13) show that the current along the Tsugaru Strait is small at longer periods. In this region, the depth of the Moho discontinuity is about 35 km and the plate boundary is deeper than 100 km (Miyamachi *et al.*, 1993, Figure 5-3). In Tohoku and Chubu districts, low resistivity layers exist between the Conrad discontinuity and the Moho discontinuity beneath around the Volcanic Front (e.g. Utada, 1987). Residual transfer functions are small and the effect of the low resistivity layer is not dominant at longer periods. Therefore, there is a possibility that the low resistivity layer exists at a depth shallower than the Moho discontinuity in southern Hokkaido.

Figure 4-13 shows that there are large anomalies of the horizontal transfer functions in northern and eastern Hokkaido. Nishida (1981) pointed out that this region is characterized by large horizontal fields that may be explained by the sediments of the Cenozoic group.

By contrast, in northeastern Japan, anomalies of the horizontal transfer functions are smaller. The Ishikari plain and the Konsen plain in Hokkaido are both adjacent to ocean and current channeling may occur through the sediments. Anomalies of the horizontal transfer functions in the northeastern Japan are small, as less current channeling occurs.

(b) Kanto and Chubu District

In the early 1950's, a significant variation of the vertical component was observed at Kakioka in northern Kanto District. It was the first study of the so-called central Japan anomaly (Rikitake, 1966). Honkura (1985) showed that this central Japan anomaly is primarily accounted for by surface sediments and sea water, although no significant information on the crustal and mantle resistivity structure could be derived. Bapat *et al.* (1993) also showed that the central Japan anomaly can be explained primarily by the sea effect and local anomalies of the sedimentary layer using a thin-sheet model. However, the distribution of geomagnetic stations in their study does not cover all Kanto District, particularly in and around the Izu peninsula. Yanagihara and Yokouchi (1965) and Honkura (1985) showed that there are large currents in the thick sediment in the Kanto plain. In the northern Kanto District, the large residual induction arrows at No. 40 Utsunomiya and TKB are accounted for by these currents.

Most anomalies in the northern Kanto District can be explained by the sediment layer and sea water effect. However, in the southern Kanto District and the Izu peninsula, there are large residual induction arrows that point to the south, far off the Izu peninsula. Although all the sea water effects can not be entirely removed due to the complicated coast lines, the residual induction arrows are too large to be explained by the sediment and sea water effects alone. The Kanto District is divided into three tectonic plates (the Philippine Sea, Eurasian and Pacific plates) and two island arcs (the Izu-Ogasawara, which subducts beneath the other island arc, the Japan arc) (Ishida, 1992). At sea, the upper layer of the plates has low resistivity, which significantly affects the induction arrows (Utada, 1987). Figure 5-4 shows the plate boundary between the Philippine Sea plate and the Eurasian plate and depth of each plates (Ishida, 1992). The residual induction arrows in the southern Kanto District point toward the Philippine Sea

plate (Figure 4-12). It follows that the effect of the Philippine Sea plate on the induction arrows is probably large in southern Kanto District.

The observed and residual induction arrows at No. 39 Tookamachi and No. 97 Tochigi point to the southwest. Induced electric currents in the sediment layer in the Kanto plain tend to flow parallel to the NW-SE trend of thick sediments (Yanagihara and Yokouchi, 1965). Therefore, these currents probably flow from the northern edge of the Kanto plain to the Japan Sea. Similarly, Figure 4-5 shows that the regional general current flows in a NW-SE direction in Chubu inland District and is approximately uniform. This current flows between the Pacific Ocean and the Japan Sea through this region. From a 2D study of geomagnetic induction, Utada (1987) showed that there are low resistivity layers in the lower crust above the Moho discontinuity beneath and around the Volcanic Front, and the current flowing in the upper surface of the Philippine Sea plate probably flows into there. The NW-SE current in the Izu peninsula (Figure 4-13, just above the northern tip of the Philippine Sea plate) also supports this hypothesis. Figure 5-5 shows a schematic explanation of the electric currents in Kanto and Chubu District associated with the Philippine Sea plate.

On the other hand, the low resistivity layers of the Pacific plate east of the Kanto District can not be detected and their effect on the transfer functions should be small. This is because the Pacific plate subducts under the Philippine Sea plate, and the large electric current concentrates in the Philippine Sea plate is nearer than that of the Pacific plate.

In the southern Kii peninsula, the residual induction arrows shown in Figure 4-12 point to the south but they are small. However, Bapat *et al.* (1993) showed an opposite result that there are the large residual induction arrows in the southern Kii peninsula. Fujita (1994) concluded that low resistivity layer of 10 ohm·m exists below the Pacific Ocean near the tip of the Kii peninsula, using MT and GDS methods. We cannot make a direct comparison with these conclusions because there are no first order geomagnetic stations at the tip of the Kii

peninsula. However, it seems reasonable to suppose that low resistivity layer does not exist just below the Kii peninsula. This hypothesis is supported by the fact that the horizontal transfer functions are small in the southern Kii peninsula.

(c) Chugoku and Kyushu District

In Chugoku, northern and central Kyushu, most induction arrows point to the west (Research Group for Crustal Resistivity Structure, Japan, 1989; Handa *et al.*, 1992) and the residual induction arrows (Figure 4-12) also support this tendency. Handa *et al.* (1992) suggested that there are low resistivity layers beneath the Yellow Sea (to the west of Kyushu) and that current channeling occurs, possibly in the Tsushima strait (to the north of Kyushu). It is interesting that the residual induction arrows in southern Kyushu point to the southwest and they are larger than those of northern and central Kyushu (Figure 4-12). Although the station No. 85 Tanegashima is situated in northeastern part of Tanegashima island, induction arrows do not show the island effect at longer periods and point to the south. Moreover, the anomalous ellipses of the horizontal transfer functions in Kyushu suggest that there are East-West currents. Therefore, such East-West currents in southern Kyushu and southern off Kyushu most probably produce the anomalies of the transfer functions in southern Kyushu.

6. Temporal Changes of the Transfer Functions

The purpose of this chapter is to clarify temporal changes of the transfer functions. We examined two kinds of the transfer functions, first long time changes at the observatories, second temporal changes observed at first order geomagnetic stations in association with a big earthquake.

As the transfer functions are possibly affected by the external ΔZ, similar changes of the geomagnetic transfer functions are sometimes found at two stations at a great distance (Sano *et al.*, 1982). Therefore it is important to monitor changes of the transfer functions at several stations simultaneously.

6.1. Temporal Changes of the Transfer Functions at Observatories

6.1.1. Results from 1989 to 1992

We obtained the temporal changes of the single-station transfer functions at Mizusawa, Kakioka, Tsukuba and Kanozan at periods of 128, 64, 32, 16, 8 and 4 min during the period from 1989 to 1992. At each observatory, the semimonthly transfer functions at each period are shown in Figure 6-2. Error bars show the 95% confidence intervals (Bendat and Piersol, 1971). Some error bars are relatively large because of low signal to noise ratio (S/N) mainly due to artificial noises.

From Figure 6-2 it is clear that there are some significant changes that are above the 95% confidence intervals. Common changes are significant at the all observatories at the periods of 128 min and 64 min. The transfer functions at the period of 32 min have the smallest error and the most stable, however, common seasonal changes are also clearly found.

Though the cause of the seasonal changes is not clear, Sano (1980) and Shiraki (1980) suggested influence of the common external field. At any rate, it is important to compare

temporal changes of the transfer functions at several stations in order to remove the effect of common seasonal change.

At Tsukuba and Kanozan, the changes of *Au* at the period 4 min show almost the same amplitude but the changes have negative correlation. Examining Figure 6-2 more carefully, it is found that the changes of *Au* at Kakioka and Tsukuba, and those of *Bu* at Kakioka, Tsukuba and Kanozan have positive correlation. Table 3-1 shows correlation coefficients of the temporal changes of the transfer functions *Au* and *Bu* between Tsukuba and other observatories.

6.1.2. Results in Southern Kanto District in 1989

Figure 6-3 shows temporal changes of the single-station transfer functions in southern Kanto district in 1989. At Tsukuba and Omaezaki, the changes of *Au* and *Bu* at the period 4 min have negative correlation. On the contrary, at Tsukuba and Yatsugatake, the changes of *Au* at a period 4 min have positive correlation and those of *Bu* have negative correlation. The imaginary parts, *Av* and *Bv* do not show large changes but those of Tsukuba and Omaezaki show large changes. The changes from July 1989 to August 1989 are quite large. Difference induction arrows of these changes of the transfer functions are shown in Figure 6-4. In this figure, the difference arrows point towards the same inner part of Kanto district. This fact can be explained by assuming that the conductivity in the inner part of Kanto district changed in summer 1989, however, they seem too large. In section 5.2., it is shown that there are large channeling currents in the Kanto plain and it is possible that the changes of direction or quantity of the channeling currents may cause the temporal changes of the transfer functions shown in Figure 6-3.

6.1.3 Comparison with Other Geophysical Data

In order to make clear origins of the temporal changes of the transfer functions shown in Figure 6-3, especially at periods of 4 and 8 min, the following comparison with other geophysical data was done.

(a) Underground Water Level, Rain Fall and Sea Level

Underground water flow has close relationship with the conductivity of the region (Mizutani and Ishido, 1976). Figure 6-5 shows the underground water level observed at Tsukuba (the distance between the geomagnetic observation hut in Tsukuba and the underground water level gauge is about 100 m). There is sedimentary layer having high conductivity as thick as several 100 m at Tsukuba. In addition, monthly precipitation in Kanto district is shown in Figure 6-6.

As the sea water has very high conductivity compared with the crust, it has much contribution on the transfer functions. The Japan Current (Kuroshio) flows northeast from the Philippines along the eastern coast of Japan. The Kuroshio varies in speed and tends to stray from its usual course. It is about 80 km wide and reaches speeds of about 3.5 knots. As the induced current flows in the sea water, changes of the speed and course of the Kuroshio can affect sea level and the transfer functions. Figure 6-7 shows the daily mean sea level at Aburatsubo at the Miura peninsula facing the western Pacific Ocean. The location of Abratsubo is shown in Figure 6-6 (b).

Judging from the Figures 6-5, 6, and 7, the underground water, the precipitation and the sea water level had no relation to the temporal change of the transfer functions in Kanto district in 1989.

(b) Relationships between the Changes of the Transfer Functions and those of the Seismicity

Changes of stress field in crust of the Earth can cause changes of the conductive structure of the Earth. Since the stress field has influence on the seismicity in the region, the transfer functions are possibly related to the seismicity.

The changes of the transfer functions in 1989 are remarkable. There was no large earthquake from 1989 to 1992 in Kanto district. We examined the relationship between the changes of the transfer functions and those of seismic activity in fairy broad regions. Figure 6-8 (a) shows the cumulative numbers of earthquakes in the shadowed region shown in Figure 6-8 (b). We assume that the cumulative number of earthquakes represents a rate of seismicity in the region. In July 1989, an earthquake swarm occurred at eastern off Ito city, in the Izu peninsula, and seismicity in Kanto district were changed and became active. The seismic activity in the shadowed region in Figure 6-8 (a) increases clearly in the middle of August, 1989. This change of seismicity coincides with the changes of the transfer functions. Therefore it looks that the seismicity has a relationship with the transfer functions of the observatories in Kanto district. Changes of the stress field that cause the changes of the seismicity directly or indirectly may cause changes of conductive structure.

(c) K-Index

To estimate effects of the external geomagnetic field on the transfer functions, K-indices at Kakioka are used. The K-index is one of indices that show the geomagnetic activity. Figure 6-9 (a) shows the monthly K-indices at Kakioka and the transfer functions at Kanozan and Figure 6-9 (b) shows correlation between the K-indices and the transfer functions at Kanozan. In this comparison, there is likely relationship between the changes of the K-indices and those of the transfer functions. Though K-index does not represent all features of the external geomagnetic field, it is clear that the external field affects the transfer functions in Kanto district. A possible mechanism that explains the changes of the transfer functions will be discussed in the section 6.1.5.

6.1.4. Interstation Transfer Functions at Kanozan

The temporal changes of interstation transfer functions at Kanozan with the reference station Kakioka are shown in Figure 6-10. At the longer periods of 128 min and 64 min, the temporal changes of the interstation transfer functions are almost the same as those of the single-station transfer functions. This simply means that the horizontal field at Kanozan is quite similar to that at Kakioka and the noise is very small. This feature is also found at the period of 32 min, however, large error bars at the period of 8 min show the estimation of the transfer functions is not accurate. In particular at the period of 4 min, there are much larger errors in the interstation transfer functions than in the single-station transfer functions. These large error bars suggest low coherency of the horizontal field between Kanozan and Kakioka at the shorter periods. This tendency is also found at other observatories, Mizusawa, Tsukuba and Omaezaki.

6.1.5. Possible Cause of the Change of the Transfer Functions in Kanto District

There are three possible causes by which temporal changes of the transfer functions occur. First, the transfer functions are changeable due to contamination of the external ΔZ that originates in the ionosphere or the magnetosphere of the Earth. Second, the transfer functions are responsible to some changes of conductive structure beneath and around a station. The last, some apparent changes are usually introduced in process of observations or analyses. The external ΔZ, if exists, likely makes common changes of the transfer functions at the every station concerned in Japan region, because the external signals have so long wave lengths that the stations are included under the same external field. Sano *et al.* (1982) reported that there are common changes among stations distant more than 1000 km from each other. The common seasonal changes at the longer periods should be occurred by the external field.

Next we discuss the cause of the temporal changes shown in Figure 6-3. Since Tsukuba is about 80 km away from Kanozan, common artificial noise can not be contained and common external geomagnetic field should be contained. Though the common changes at the periods of 128 min and 64 min that are almost the same at all observatories can be simply explained as the result of external field, those at the period of 4 min which amplitude and direction are different each other can not be explained as the direct influence of the common external field.

At shorter periods, the temporal changes are large in Kanto district. Fujita (1989) showed those of daily scattering at Kakioka are larger than those at Kanoya and Memanbetsu. Artificial noises such as leaked currents from electric railways can cause those fluctuations and we found such artificial noise in the data at Kanozan. Figure 6-11 shows average amplitude of the three geomagnetic components at each observatory. The amplitude of X component at the period of 4 min at Kanozan is much larger than those at other observatories, and it is caused by artificial noises. The noises at Kakioka are fairly small (less than 1 nT), however, the average amplitude of signal at the period of 4 min is only 2 nT and the S/N is not big. Figure 6-12

shows coherency squared of the horizontal geomagnetic components between Kakioka and other observatories. In spite of great distances from Kakioka to Memanbetsu and Kanoya, almost all the coherency squared is greater than 0.8 except for that of Kanozan at shorter periods. Since leaked currents from DC railways has major direction peculiar to each station (Fujiwara *et al.*, 1986), the geomagnetic noise caused by the leaked currents will make a bias in the transfer functions. The bias will become larger as the external signal becomes smaller. Therefore the K-index and the transfer functions have correlation. In the case of the interstation transfer functions, the transfer functions do not change very largely but error bars become large in July 1989. The large error bars suggest that the coherency between the input external horizontal field at Kakioka and the output vertical field at Kanozan is small, that is mainly caused by low power of the input external field, which is supported by the fact that the K-index at Kakioka in July is very small.

In conclusion, the temporal changes in Kanto district in 1989 at the shorter periods are probably caused by the mixed of the activity of the common external geomagnetic field and the artificial noises at each observatory.

Meanwhile, a rather long time decrease of *Bu* at the period of 4 min is found at Kakioka and Tsukuba in 1990, and it recovered suddenly at the beginning 1991 (Figure 6-2). This change coincides with the change of seismicity around Kakioka and Tsukuba (Figure 6-13) but no changes of the transfer functions are found at Kanozan. Since the noise level at Kakioka and Tsukuba is much smaller than that at Kanozan, these changes aren't probably caused by artificial noises. Further investigation is needed to clarify the cause of these changes.

6.2. Temporal Changes of the Transfer Functions Associated with the 1993 South-western off Hokkaido Earthquake

In this chapter, we use only the interstation transfer functions.

6.2.1. The 1993 Southwestern off Hokkaido Earthquake

A large earthquake occurred in southwestern off Hokkaido, Japan on July 12, 1993. It was registered a magnitude of 7.2 on the Richter scale. After the earthquake, the Geographical Survey Institute carried out the first order geomagnetic survey around southwestern part of Hokkaido to detect geomagnetic phenomena associated with the earthquake (Fujiwara *et al.*, 1994). Figure 6-14 shows the aftershock region (Research Group For Aftershocks Of the July 12, 1993, Hokkiado-nansei-oki Earthquake, 1993) and the geomagnetic stations concerned with this survey.

6.2.2. Changes of the Transfer Functions Associated with the Earthquake

We got transfer functions of the three first order geomagnetic stations that had two observations, before and after the earthquake. Although time of the observations after the earthquake was within one month after the occurrence, those of before it were, July 1990 at No. 18 Furubira, June 1992 at No. 25 Imakane and June 1993 at No. 80 Fukushima. As all the observations were done in summer, the effect of the seasonal changes are probably small. We calculated the interstation transfer functions, and Kakioka was the reference station.

Figure 6-14 (a) shows the induction arrows. The induction arrows represent geographical contrast of anomalous currents. Electric currents possibly exist to the direction the induction arrow points.

At the period of 64 min, the induction arrow at No. 25 Imakane became smaller after the earthquake and the change is beyond the 95 % confidence interval, however, no significant

change is found at the shorter period of 16 min. This implies that the conductivity of western part of No. 25 Imakane became smaller after the earthquake.

Honkura and Taira (1983) examined temporal changes of the amplitudes of the horizontal field and crustal movements. They found that there is good correlation between them. In this study, we also used the horizontal transfer functions that include the same kind of information. We express in Figure 6-14 (b) the horizontal transfer functions as an arrow, *Cu* is southward direction and *Fu* is westward direction. This arrow approximately means anomalous horizontal field and electric current flows just beneath the station perpendicular to the arrow and the strength of the current is proportional to the length of the arrow. From Figure 6-14 (b), we can find that the WNW-ESE current beneath No. 18 Furubira became larger after the earthquake, on the contrary, the current beneath No. 25 Imakane became smaller. The internal anomalous field is produced by electric currents induced in the Earth. Though the electric currents are directly induced in high conductive regions (good conductors), the currents usually flow to or from other good conductors. These phenomena are called 'channeling effect'. Therefore we must pay attention to the current flow in addition to anomalous conductors.

6.2.3. Model Simulation

We will discuss models of the change of conductive structure that can account for the temporal changes of the transfer functions in association with the 1993 southwestern off Hokkaido earthquake.

Two-dimensional model simulations using a computer program of Jones and Pascoe (1971) and Pascoe and Jones (1972) were carried out to estimate the region size and the quantity of conductivity change. Williamson *et al.* (1974) pointed out that the program of Jones and Pascoe (1971) had an error in the finite deference representation. However, Jones and Thomson (1974) has shown that its effect on calculated results is much decrease when a slowly changing grid is used. Since this model simulation was used for rough estimation and showing possible cause of the time change of the transfer functions, Jones and Pascoe's method had enough accuracy for this study.

First, it is supposed that the conductivity changed near the stations. If there are active faults near the stations, conductivity change possibly occurs in the active faults (Sumitomo and Noritomi, 1986). If conductivity changes in the region width 1 km and thickness 1 km, the conductivity change is required more than one hundred times to account for the changes of induction arrows. However, it appears difficult to be supposed that such large changes occurred near each station and active faults have not been found near the stations (Research Group for active Faults of Japan, 1991). Moreover, the frequency dependence at the periods of 64 and 16 min can not be explained.

Second, a more possible model is proposed that conductivity changed in the aftershocks region. If conductivity changes in the region width 20 km and thickness 10 km as shown in Figure 6-15 (b), the conductivity change is required 100 times to account for the changes of induction arrows. This model can explain the frequency dependence at the periods both 64 min and 16 min. Brace and Orange (1968) reported that the rock partially saturated with water

shows a remarkable increase in the conductivity when a mechanical stress is applied to the rock. If such a phenomenon occurs in the region, the induction arrows in southwestern Hokkaido region show the changes.

The changes in Figure 6-13 imply the possibility that the conductivity of the aftershock region became smaller. The increase of electric current beneath No. 18 Furubira and the decrease of it beneath No. 25 Imakane can be explained by that the current that had flowed in the aftershock region changed its pass caused by the decrease of the conductivity of the aftershock region. This model simulation only presents one possibility and we can not conclude any finite models.

7. Concluding Remarks

We have determined a nation wide distribution of geomagnetic transfer functions around Japan, for both the vertical field and the horizontal field, using the interstation method. We also estimated the effect of sea water using the thin-sheet method. As the coastlines of Japan are complex, the model calculation could be improved by using a finer mesh or by considering a smaller area. However, the residual transfer functions show large anomalies that can not be explained by the effect of the coastlines alone. Current channeling in sedimentary layers may account for some of the observed anomalies. The large anomaly in southern Kanto District is most likely related to the existence of the Philippine Sea plate.

Since we have not had large earthquakes and volcanic activities near the observatories within the period of the data used in this study, we could not find any changes associated with crustal activities at the observatories. The changes at the longer periods of 128, 64, and 32 min are often due to the external field and those at the shorter periods are occasionally due to the complex of the external field and the artificial noise. Since the transfer functions at shorter periods are often affected by artificial noises, the single-station transfer functions tend to show apparent changes. Therefore checking contamination of artificial noise is necessary and using the interstation transfer functions is useful for this purpose. We found that there were changes of the transfer functions associated with the 1993 southwestern off Hokkaido earthquake at the first order geomagnetic stations. This is possibly because the conductivity of the aftershocks region changed.

This thesis is based on following published papers;

1. Geomagnetic transfer functions in Japan obtained by first order geomagnetic survey, *Journal of Geomagnetism and Geoelectricity*, Vol. **48**, 1071-1101, 1996, S. Fujiwara and H. Toh.
2. Temporal changes of geomagnetic transfer functions using data obtained mainly by the Geographical Survey Institute, *Bulletin of the Geographical Survey Institute,* No. **42**, 1-25,1996, S. Fujiwara.

Acknowledgments

The author wishes to my sincere thanks to Professors N. Sumitomo and N. Oshiman of Kyoto University for critical discussions and supporting studies. The author also greatly thanks to Dr. H. Toh of Tokyo University for supporting the analyses of the thin sheet model and helpful suggestions. The author is grateful to Dr. G. S. Heinson for reading the manuscript and making a number of helpful suggestions. The author wishes to thank the members of Geomagnetic section and Mizusawa and Kanozan Observatories of the Geographical Survey Institute who made efforts to get geomagnetic data used in this study. The author thanks Kakioka Magnetic Observatory, the Japan Meteorological Agency, for providing Memanbetsu, Kakioka, Kanoya, Omaezaki and Matsuzaki data, Yatsugatake Magnetic Observatory, the Earthquake Research Institute, the University of Tokyo, for providing Yatsugatake data.

REFERENCES

Agarwal, A. K., and J. T. Weaver, Regional electromagnetic induction around the Indian peninsula and Sri Lanka; a three-dimensional numerical model study using the thin sheet approximation, *Phys. Earth Planet. Inter.*, **54**, 320-331, 1989.

Avdeev, D. B., Y. Ogawa, A. V. Kuvshinov, and O. V. Pankratov, An interpretation of magnetovariational data in the northern Tohoku District, Japan, using multi sheet modelling, *J. Geomag. Geoelectr.*, **47**, 405-410, 1995.

Banks, R. J., Data processing and interpretation in geomagnetic deep sounding, *Phys. Earth Planet. Inter.*, **7**, 339-348, 1973.

Bapat, V. J., J. Segawa, Y. Honkura, and P. Tarits, Numerical estimation of the sea effect on the distribution of induction arrows in the Japanese island arc, *Phys. Earth Planet. Inter.*, **81**, 215-229, 1993.

Beamish, D., A geomagnetic precursor to the 1979 Carlisle earthquake, *Geophys. J. R. astr. Soc.*, **68**, 531-543, 1982.

van Bemmelen, W., The starting impluse of magnetic disturbances, *Koninkl. Ned. Akad. Wetenschap.*, Proc., Ser. B, **11**, 773-782, 1908.

Bendat, J. S., and A. G. Piersol, *Random data: Analysis and measurements*, 407pp., Wiley-Interscience, New York, 1971.

Brace, W. F., and A. S. Orange, Further studies of the effect of pressure on electrical resistivity of rocks, *J. Geophys. Res.*, **73**, 5407-5420, 1968.

Camfield, P. A., and D. I. Gough, Anomalies in daily variation magnetic fields and structure under north-western United States and south-western Canada, *Geophysics J. R. astr. Soc.*, **41**, 193-218, 1975.

Chamalaun, F. H., and J. D. McKnight, A New Zealand wide magnetometer array study, *J. Geomag. Geoelectr.*, **45**, 741-759, 1993.

Chapman, S., and J. Barteles, Geomagnetism, Oxford Univ. Press, London, 1049pp, 1940.

Everett, J. E., and R. D. Hyndman, Geomagnetic variations and electrical conductivity structure in south-western Australia, *Phys. Earth Planet. Inter.*, **1**, 24-34, 1967.

Filloux, J. H., An ocean bottom, D-component magnetometer, *Geophysics*, **32**, 978-987, 1967.

Filloux, J. H., Magnetotelluric soundings over the northeast Pacific may reveal spatial dependence of depth and conductance of the asthenosphere, *Earth Planet. Sci. Lett.*, **46**, 244-252, 1980.

Fujita, K., The study of the electrical resistivity structure beneath the Kii-peninsula using the electromagnetic method, Ph. D. thesis, 121pp., Kobe university, 1994.

Fujita, S., Monitoring of time change of conductivity anomaly transfer functions at Japanese magnetic observatory network, *Mem. Kakioka Mag. Obs.*, **23**, 2, 53-87, 1989.

Fujiwara, S., N. Sumitomo, and I. Shiozaki, Some characteristics of artificial earth current leaked from electric railways and their application to electrical soundings (2) (in Japanese), *'Tsukumo Tigaku' Rep. Geoscience, Kyoto Univ.*, **21**, 8-16, 1986.

Fujiwara, S., and N. Sumitomo, Conductivity anomaly observation near the Yanagase fault (3) - relation between the changes of transfer functions and the seismicity in southwest Japan - (in Japanese), *1988 Proceedings of Conductivity Anomaly Symposium*, 157-166, 1988.

Fujiwara, S., T. Minato, M. Tsuzuku, and Y. Nakahori, The geomagnetic change associated with the 1993 southwestern off Hokkaido earthquake (in Japanese), *Biannual Rep. Geograph. Surv. Inst.*, **81**, 1-7, 1994.

Gamble, T. D., W. M. Goubau, and J. Clarke, Magnetotellurics with a remote magnetic reference, *Geophysics*, **44**, 53-68, 1979.

Geographical Survey Institute, Magnetic survey of Japan 1948-1951, , *Bull. Geograph. Surv. Inst.*, **2**, Parts 2-3, 121-166, 1951, and **3**, Parts 2-4, 119-148, 1951.

Geographical Survey Institute, First order geomagnetic survey in Japan from 1949 to 1994, *Technical Rep. Geograph. Surv. Inst.*, **B4-12**, 174 pp., 1995.

Handa, S., Y. Tanaka, and A. Suzuki, The electrical high conductivity layer beneath the northern Okinawa trough, inferred from geomagnetic depth sounding in northern and central Kyushu, Japan, *J. Geomag. Geoelectr.*, **44**, 505-520, 1992.

Honkura, Y., Observations of short-period geomagnetic variations at Nakaizu(2):changes in transfer functions associated with the Izu-Oshima-Kinkai earthquake of 1978, *Bull. Earthq. Res. Inst., Univ. Tokyo*, **54**, 477-490, 1979.

Honkura, Y., and S. Taira, Changes in the amplitudes of short-period geomagnetic variations as observed in association with crustal uplift in the Izu peninsula, Japan, *Earthq. Predic. Res.*, **2**, 115-125, 1983.

Honkura, Y., Perturbation of induced electric currents by surface conductivity inhomogeneity with special reference to anomalous behavior of short-period geomagnetic variations in the Kanto Plain, *J. Geomag. Geoelectr.*, **37**, 627-641, 1985.

Ishida, M., Geometry and relative motion of the Philippine Sea plate and Pacific plate beneath the Kanto-Tokai district, Japan, *J. Geophys. Research*, **97**, B1, 489-513, 1992.

Ishikawa, Y., K. Matsumura, H. Yokoyama, and H. Matsumoto, SEIS-PC -its outline, *Geol. Data Processing* (in Japanese), **10**, 19-34, 1985.

Jones, F. W., and L. J. Pascoe, A general computer program to determine the perturbation of alternating electric currents in a two-dimensional model of a region of uniform conductivity with an embedded inhomogeneity, *Geophys. J. R. astr. Soc.*, **24**, 3-30, 1971.

Jones, F. W., and D. J. Thomson, A discussion of the finite difference method in computer modelling of electrical conductivity structures. A reply to the discussion by Williamson, Hewlett and Tammemagi, *Geophys. J. R. astro. Soc.,* **37**, 537-544, 1974.

Kato, Y., Northeastern Japan anomaly of the upper mantle (in Japanese), *Proc. Conductivity Anomaly Symposium*, 19-31, 1968.

Kaufman, A. A., and G. V. Keller, *The magnetotelluric sounding method*, 595 pp., Elsevier Sci. Pub. Co., Amsterdam, 1981.

Lilley, F. E. M., Analysis of the geomagnetic induction tensor, *Phys. Earth Planet. Inter.*, **8**, 301-316, 1974.

McKirdy, D. McA., J. T. Weaver, and T.W. Dawson, Induction in a thin sheet of variable conductance at the surface of a stratified earth; -II. Three-dimensional theory, *Geophys. J. R. astr. Soc.*, **80**, 177-194, 1985.

Miyakoshi, J., Secular variation of Parkinson vectors in a seismically active region of Middle Asia, *J. Fac. Gen. Educ., Tottori Univ.*, **8**, 209-218, 1975.

Miyamachi, H., M. Kasahara, S. Suzuki, H. Okada, K. Tanaka, and A. Hasegawa, Three-dimensional velocity structure beneath northern Japan (in Japanese), *Abstracts 1993 fall meeting of the seismological soc. Japan,* 335, 1993.

Mizutani, H., and T. Ishido, A new interpretation of magnetic field variation associated with the Matsushiro earthquakes, *J. Geomag. Geoelectr.*, **2**, 179-188, 1976.

Nishida, Y., Conductivity anomalies in the southern half of Hokkaido, Japan, *J. Geomag. Geoelectr.*, **28**, 375-394, 1976.

Nishida, Y., Conductivity anomalies in and around the Ishikari Plain, Hokkaido (in Japanese with English abstract), *Geophys. Bull. Hokkaido Univ.*, **36**, 17-28, 1977a.

Nishida, Y., Observations of geomagnetic and geoelectric variations along the north-south profile of Hokkaido (in Japanese with English abstract), *Geophys. Bull. Hokkaido Univ.*, **36**, 29-40, 1977b.

Nishida, Y., Anomalous behavior in the horizontal components of geomagnetic variations in Hokkaido, Japan, *J. Geomag. Geoelectr.*, **33**, 197-204, 1981.

Nishida, Y., Conductivity structure in and around Hokkaido, Japan as revealed by the period dependence of the CA transfer functions, *J. Geomag. Geoelectr.*, **34**, 453-465, 1982.

Otaki, M., and K. Tsukahara, Geomagnetic Survey with the Triaxial Fluxgate Magnetometer, *Bull. Geograph. Surv. Inst.*, **35**, 1-9, 1990.

Parkinson, W. D., Directions of rapid geomagnetic fluctuations, *Geophys. J. R. astr. Soc.*, **2**, 1-14, 1959.

Parkinson, W. D., The influence of continents an oceans on geomagnetic variations, *Geophys. J. R. astr. Soc.*, **4**, 441-449, 1962.

Pascoe, L. J., and F. W. Jones, Boundary conditions and calculation of surface values for the general two-dimetional electromagnetic induction problem, *Geophys. J. R. astro. Soc.*, **27**, 179-193, 1972.

Research Group for active Faults of Japan, *Active faults in Japan (revised edition)* (in Japanese with English summary), 437pp, University of Tokyo Press, 1991.

Research Group for Crustal Resistivity Structure, Japan, The crustal resistivity structure in the Chugoku District , Japan (preliminary report) (in Japanese), *Proc. Conductivity Anomaly Symposium,* 49-54, 1989.

Research Group for aftershocks of the July 12, 1993, Hokkiado-nansei-oki Earthquake, Geometry of the aftershocks of the July 12, 1993, Hokkiado-nansei-oki Earthquake, *Abstracts of the 1993 Fall meeting of the Seismological Society of Japan*, 15, 1993.

Rikitake, T., Electromagnetism and the Earth's interior, 308 pp., Elsevier, Amsterdam, 1966.

Rikitake, T., The undulation of an electrically conductive layer beneath the islands of Japan, *Tectonophysics*, **7**, 257-264, 1969.

Rikitake, T., Electric conductivity anomaly in the earth's crust and mantle, *Earth-Sci, Rev.*, **7**, 35-65, 1971.

Rikitake, T., Crustal dilatancy and geomagnetic variations of short period, *J. Geomag. Geoelectr.*, **28**, 145-156, 1976.

Rikitake, T., Changes in direction of magnetic vector of short-period geomagnetic variations before the 1972 Sitka, Alaska, earthquake, *J. Geomag. Geoelectr.*, **31**, 441-448, 1979.

Rikitake, T., and Y. Honkura, Solid earth geomagnetism, 384 pp., Terra Scientific Publishing Company, Tokyo, Japan, 1985.

Rikitake, T., and I. Yokoyama, The anomalous behavior of geomagnetic variations of short period in Japan and its relation to the subterranean structure, *Bull. Earthq. Res. Inst., Univ. Tokyo,* **33**, 297-331, 1955.

Sano, Y., Time changes of transfer functions at Kakioka related to earthquake occurrences (I), *Geophys. Mag.*, **40**, 91-111, 1980.

Sano, Y., K. Nakaya, T. Kurihara, and S. Nakajima, Simultaneous comparisons of CA transfer functions among Memanbetsu, Iwaki, Kakioka and Kanoya (in Japanese with English abstract), *Mem. Kakioka Mag. Obs.*, **19**, 53-68, 1982.

Sasai, Y, Spatial dependence of short-period geomagnetic fluctuations on Oshima Island (1), *Bull. Earthq. Res. Inst., Univ. Tokyo*, **45**, 137-157, 1967.

Sasai, Y, Spatial dependence of short-period geomagnetic fluctuations on Oshima Island (2), *Bull. Earthq. Res. Inst., Univ. Tokyo*, **46**, 907-926, 1968.

Scholz, C.H., L. R. Sykes, and Y. P. Aggarwal, Earthquake prediction: A physical basis, *Science*, **181**, 803-810, 1973.

Schmidt, A, Die magnetische Storung am 25 September 1909 zu Potsdam und Seddin, *Meteorol. Z.*, **26**, 509-511, 1909.

Schmucker, U., Anomalies of geomagnetic variations in the southwestern United States, *Bull. Scripps Inst. Oceanogr.*, **13**, 165 pp., 1970.

Shiraki, M., Monitoring of the time change in transfer functions in the central Japan conductivity anomaly, *J. Geomag. Geoelectr.*, **32**, 637-648, 1980.

Sumitomo, N., and K. Noritomi, Synchronous precursors in the electrical earth resistivity and the geomagnetic field in relation to an earthquake near the Yamasaki fault, southwest Japan, *J. Geomag. Geoelectr.*, **38**, 971-989, 1986.

Utada, H., A direct inversion method for two-dimensional modelling in the geomagnetic induction problem, Ph. D. thesis, 409 pp., University of Tokyo, 1987.

Vasseur, G., and P. Weidelt, Bimodal electromagnetic induction in non-uniform thin sheets with an application to the northern Pyrenean induction anomaly, *Geophys. J. R. astr. Soc.*, **51**, 669-690, 1977.

Weaver, J. T., and A. K. Agarwal, Is addition of induction vectors meaningful?, *Phys. Earth Planet. Inter.*, **65**, 267-275, 1991.

Williamson, K., C. Hewlett, and H. Y. Tammemagi, Computer modelling of electrical conductivity structures, *Geophys. J. R. astr. Soc.*, **37**, 533, 1974.

Yanagihara, K., Secular variation of the electrical conductivity anomaly in the central part of Japan, *Mem. Kakioka Mag. Obs.*, **15**, 1-11, 1972.

Yanagihara, K., and T. Nagano, Time change of transfer function in the Central Japan anomaly of conductivity with special reference to earthquake occurrences, *J. Geomag. Geoelectr.*, **28**, 157-163, 1976.

Yanagihara, K., and T. Yokouchi, Local anomaly of earth-currents and earth-resistivity (in Japanese with English abstract), *Mem. Kakioka Mag. Obs.*, **12**, 105-113, 1965.

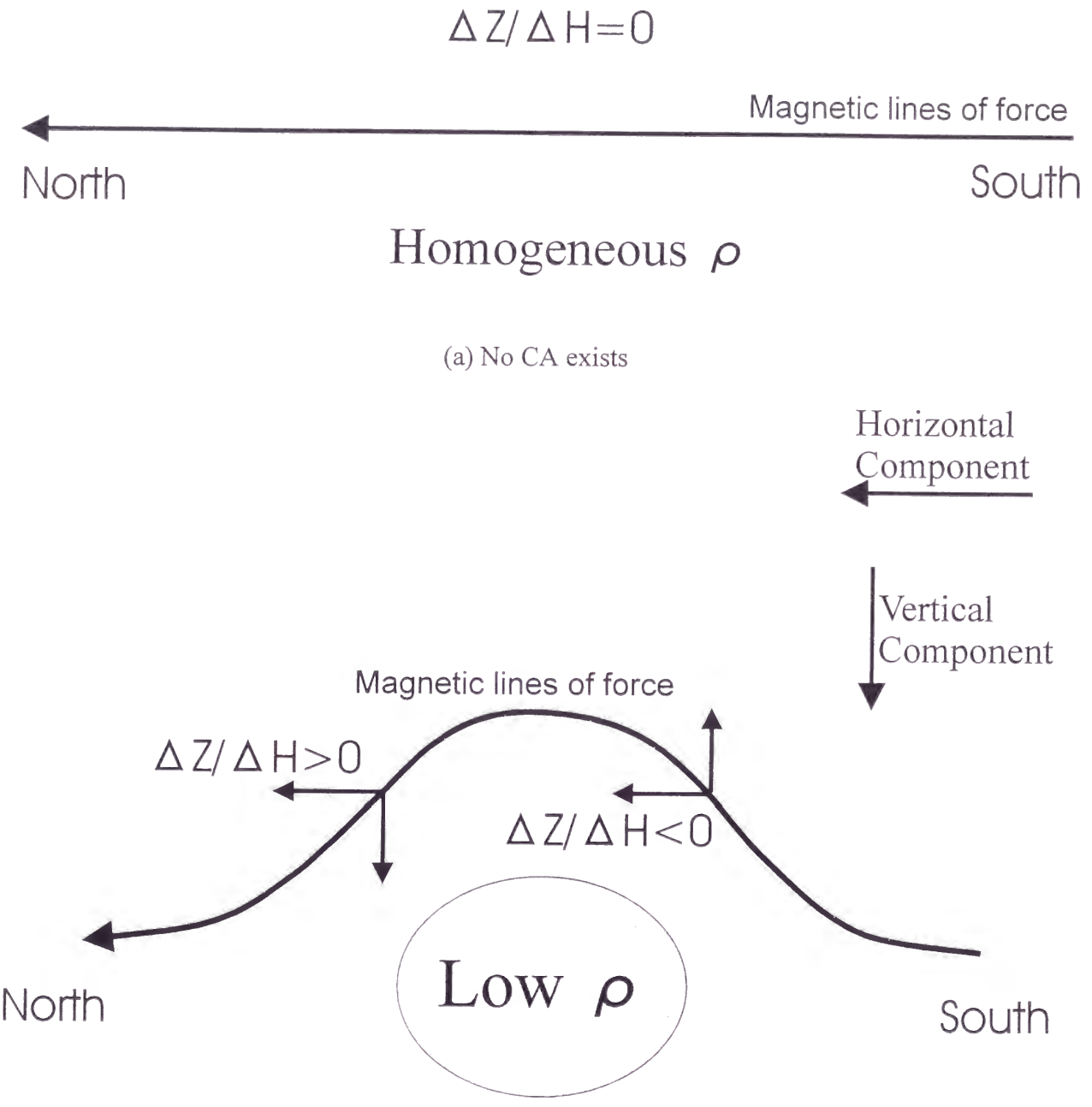

(a) No CA exists

(b) CA exists

Figure 1-1 Schematic explanation of conductive anomaly.
Arrows show changes of the geomagnetic field.

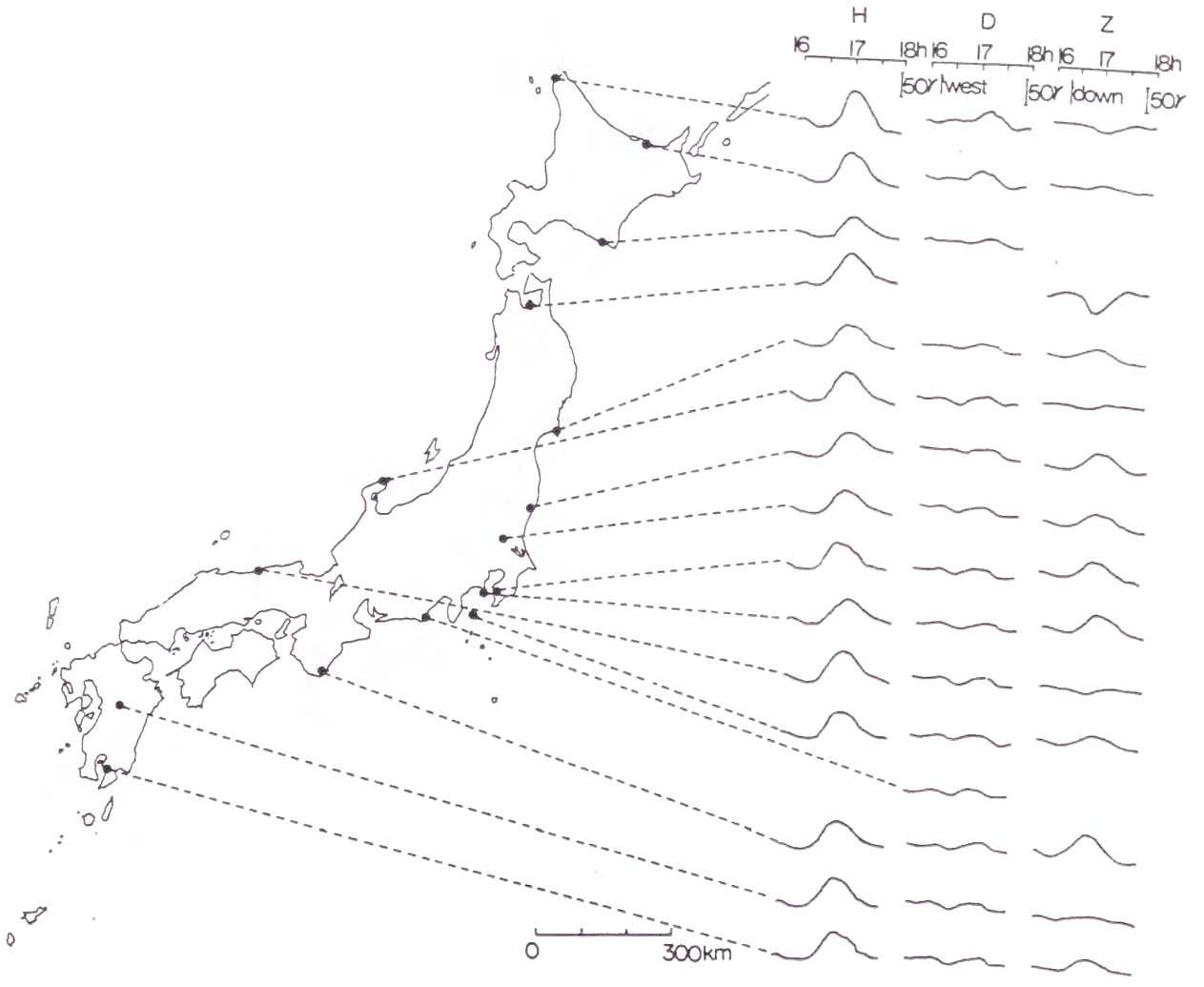

Figure 1-2 Geomagnetic bay on March 30, 1964 as observed simultaneously by a network of magnetic observatories, permanent and temporary, in Japan (after Rikitake, 1971).

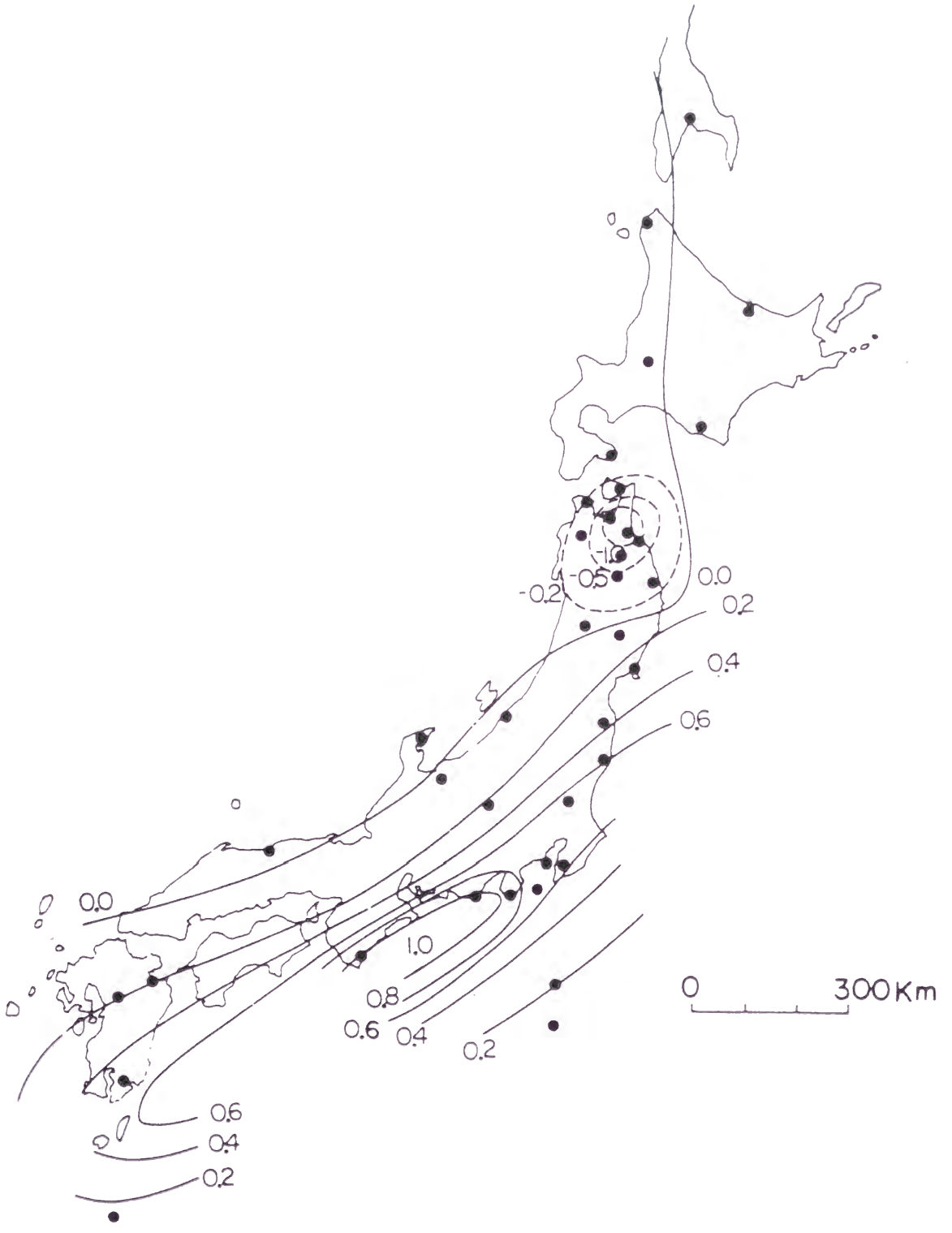

Figure 1-3 The $\Delta Z/\Delta H$ value distribution for geomagnetic bays and similar changes (after Rikitake, 1969).

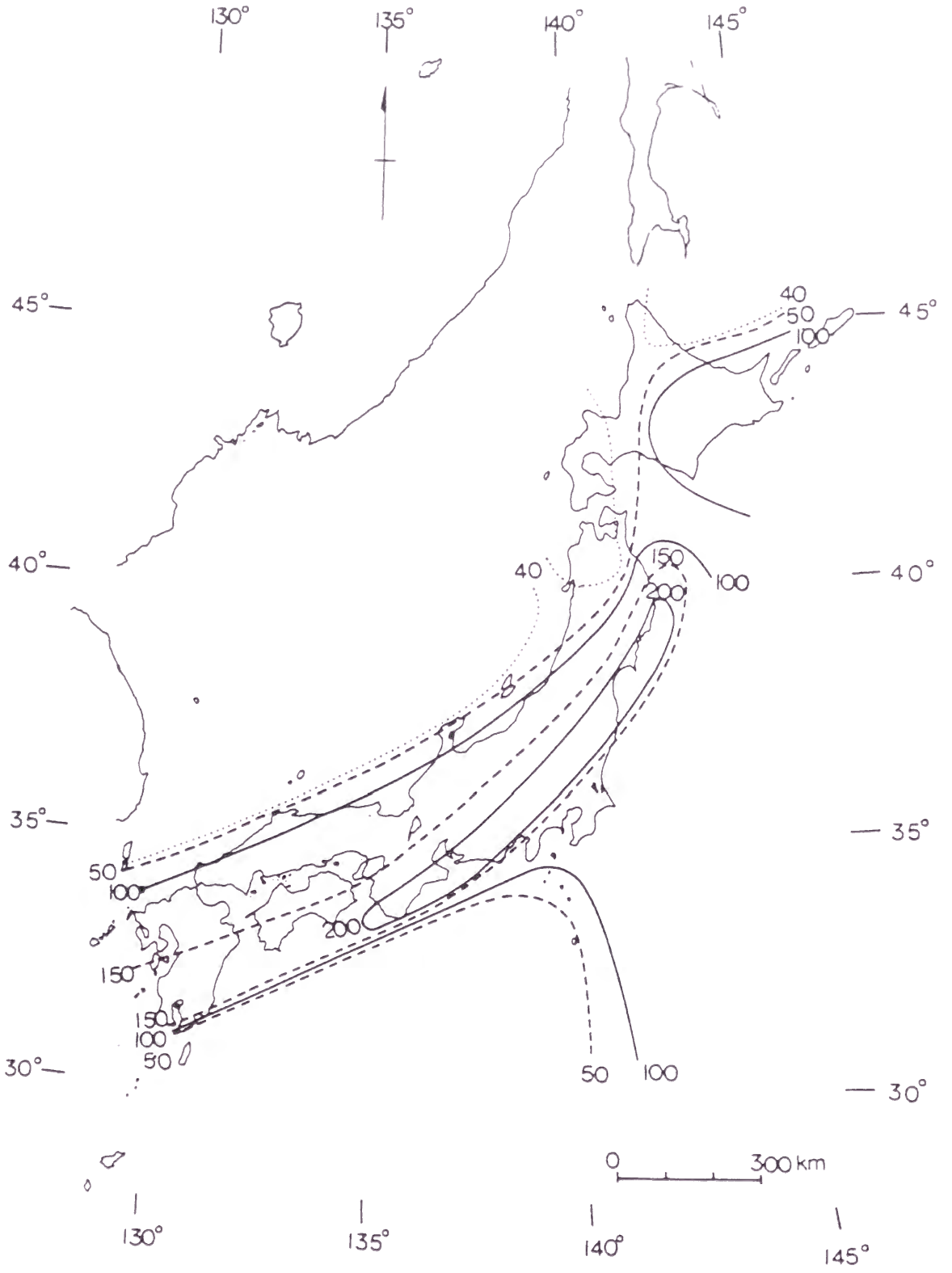

Figure 1-4 The depth in km of the mantle layer of high conductivity as deduced from the $\Delta Z/\Delta H$ value distribution in Japan (after Rikitake, 1969).

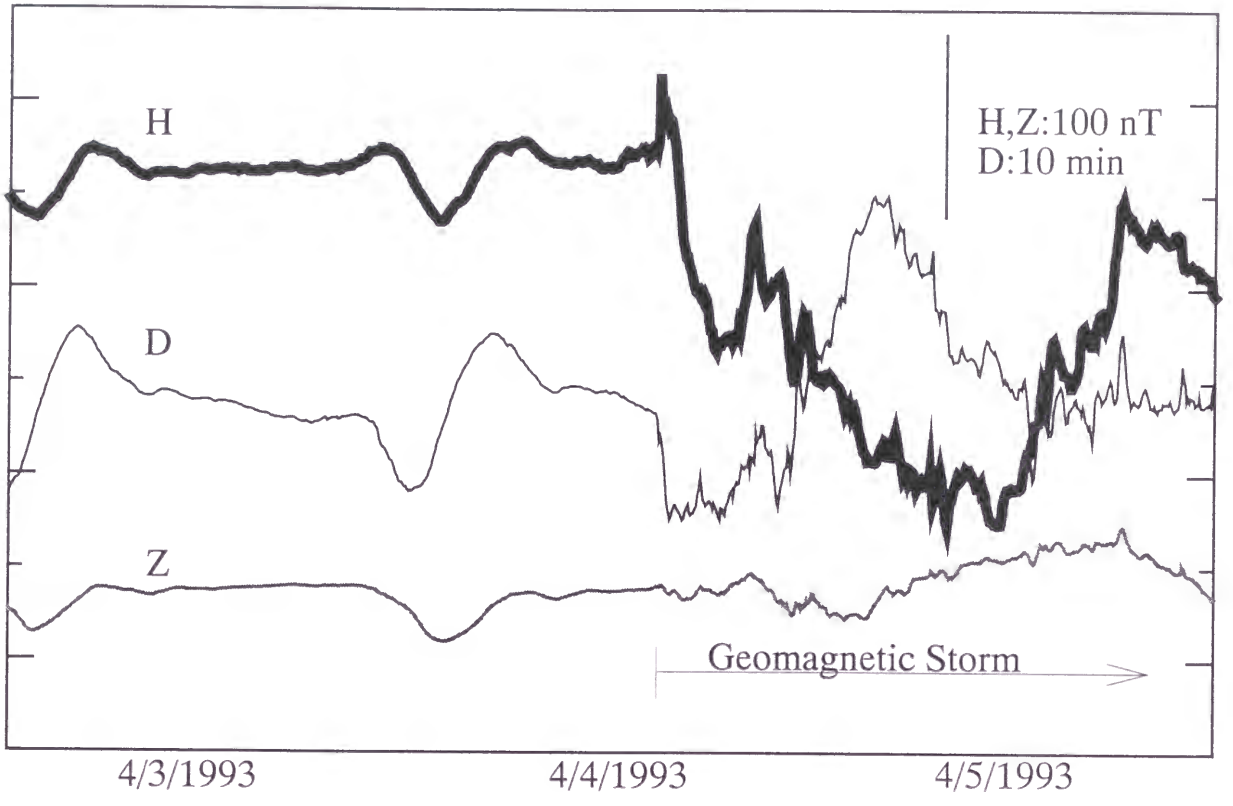

Figure 1-5 Geomagnetic Variations observed at Mizusawa

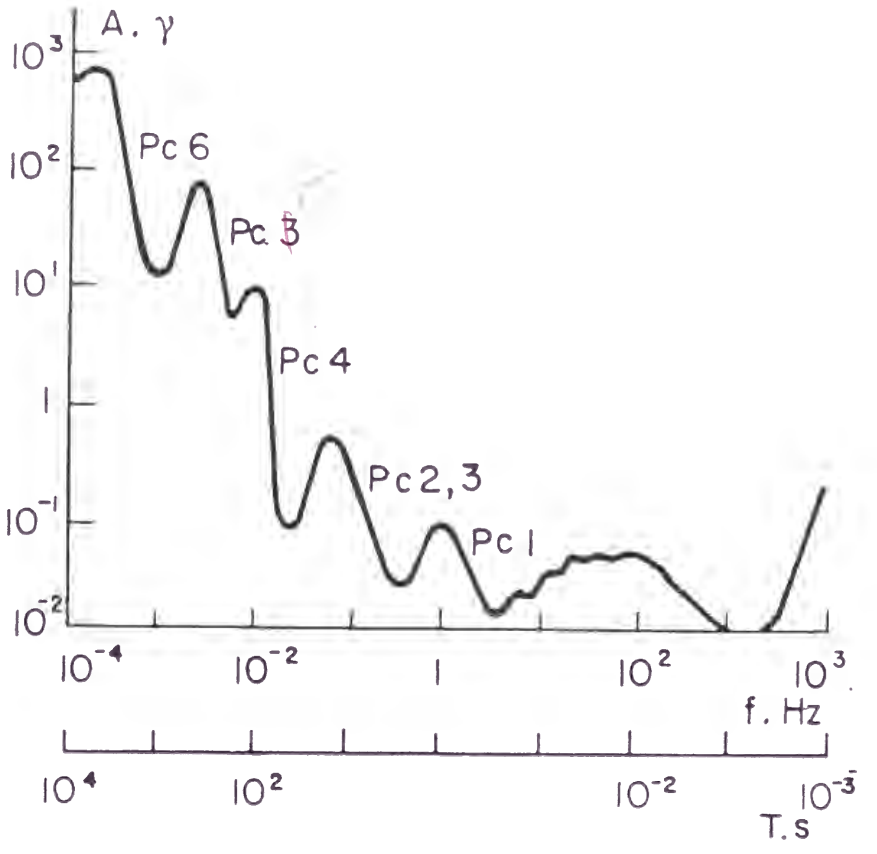

Figure 1-6 Spectrum of Pc geomagnetic pulsations (after Kaufman and Keller, 1981).

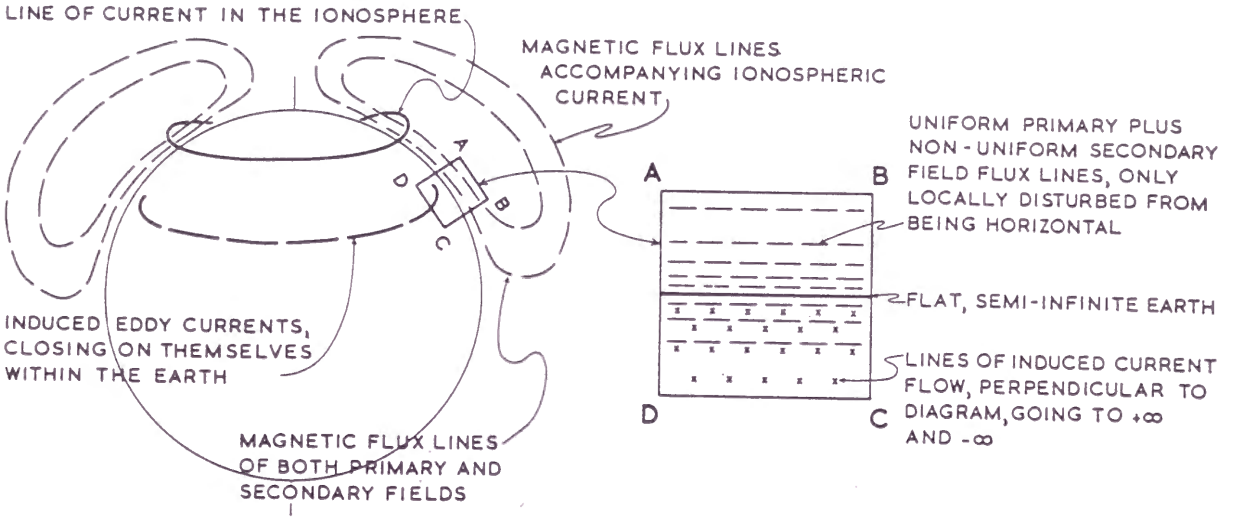

Figure 1-7 Schematic diagram of the approximation involved in modeling geomagnetic induction due to ionosphere currents by a uniform primary field and a semi-infinite half space (after Lilley, 1974).

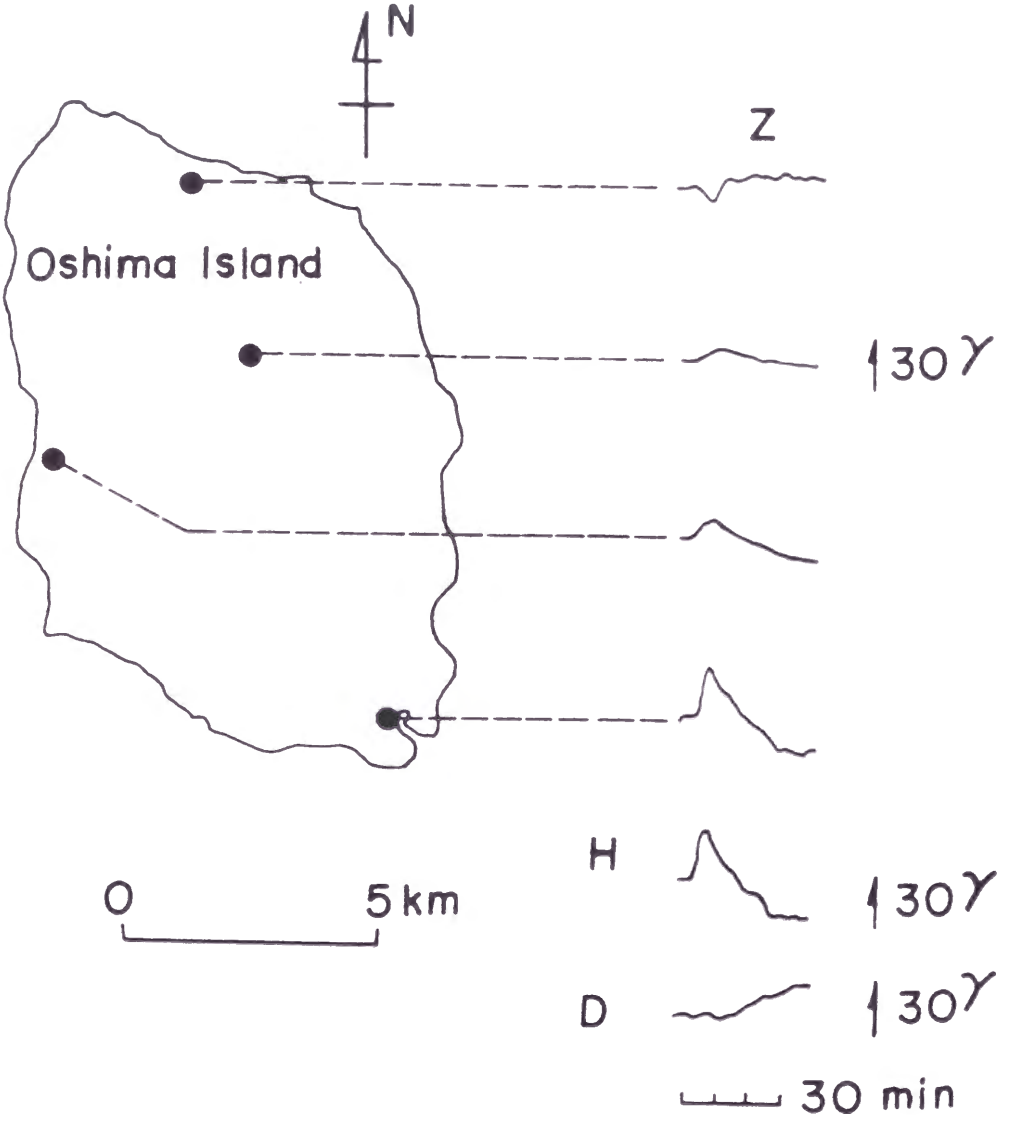

Figure 1-8 (a) An example of simultaneous sudden storm commencement magnetograms at for stations on Oshima Island. Changes in the horizontal intensity (H) and declination (D) are almost the same throughout the stations (after Sasai, 1967).

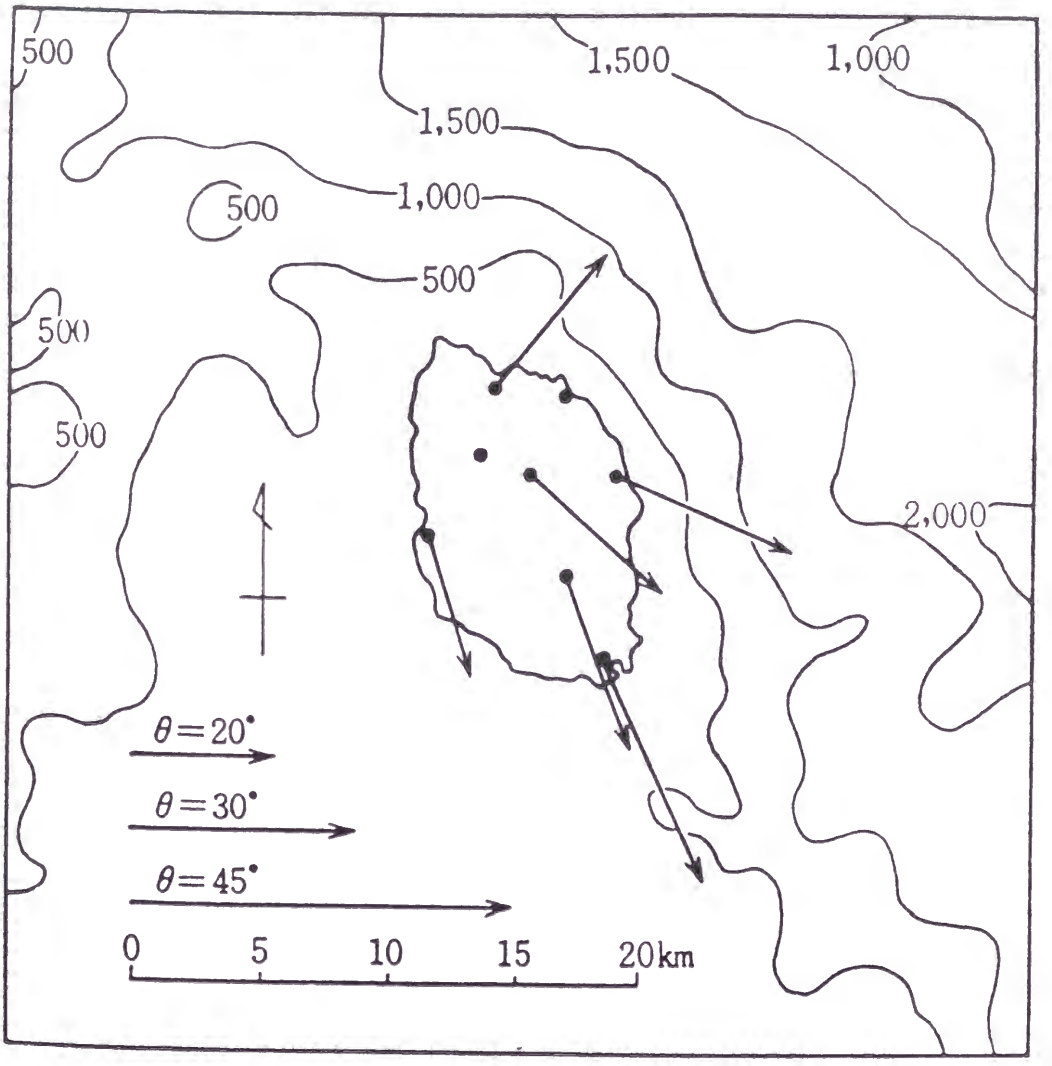

Figure 1-8 (b) Parkinson vectors on Oshima Island (after Sasai, 1968). Bathymetric contours are given in meters.

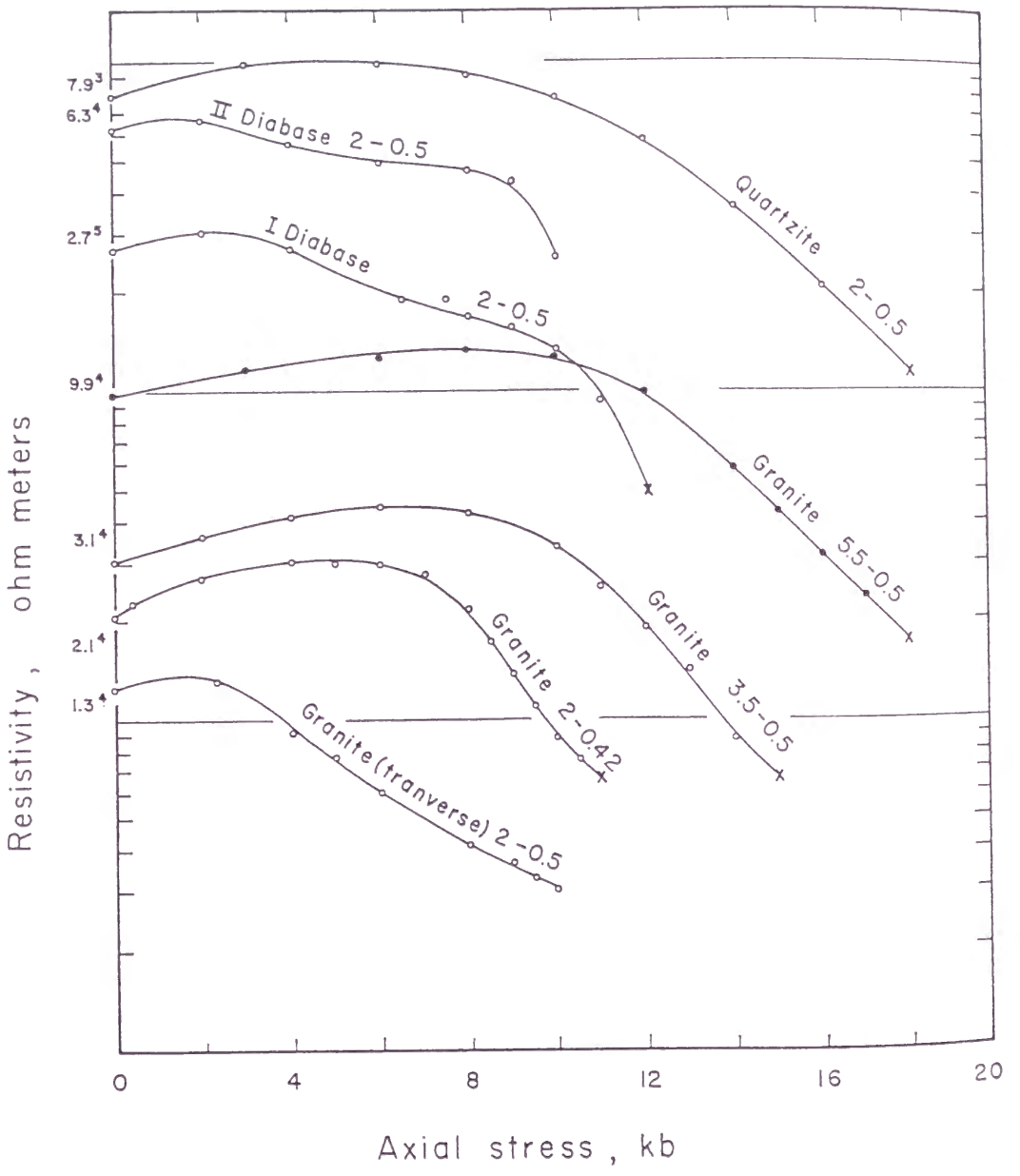

Figure 1-9 Resistivity as a function of axial stress (after Brace and Orange, 1968). The numbers after the rock name are the confining and pore pressure, respectively, in kilobars.

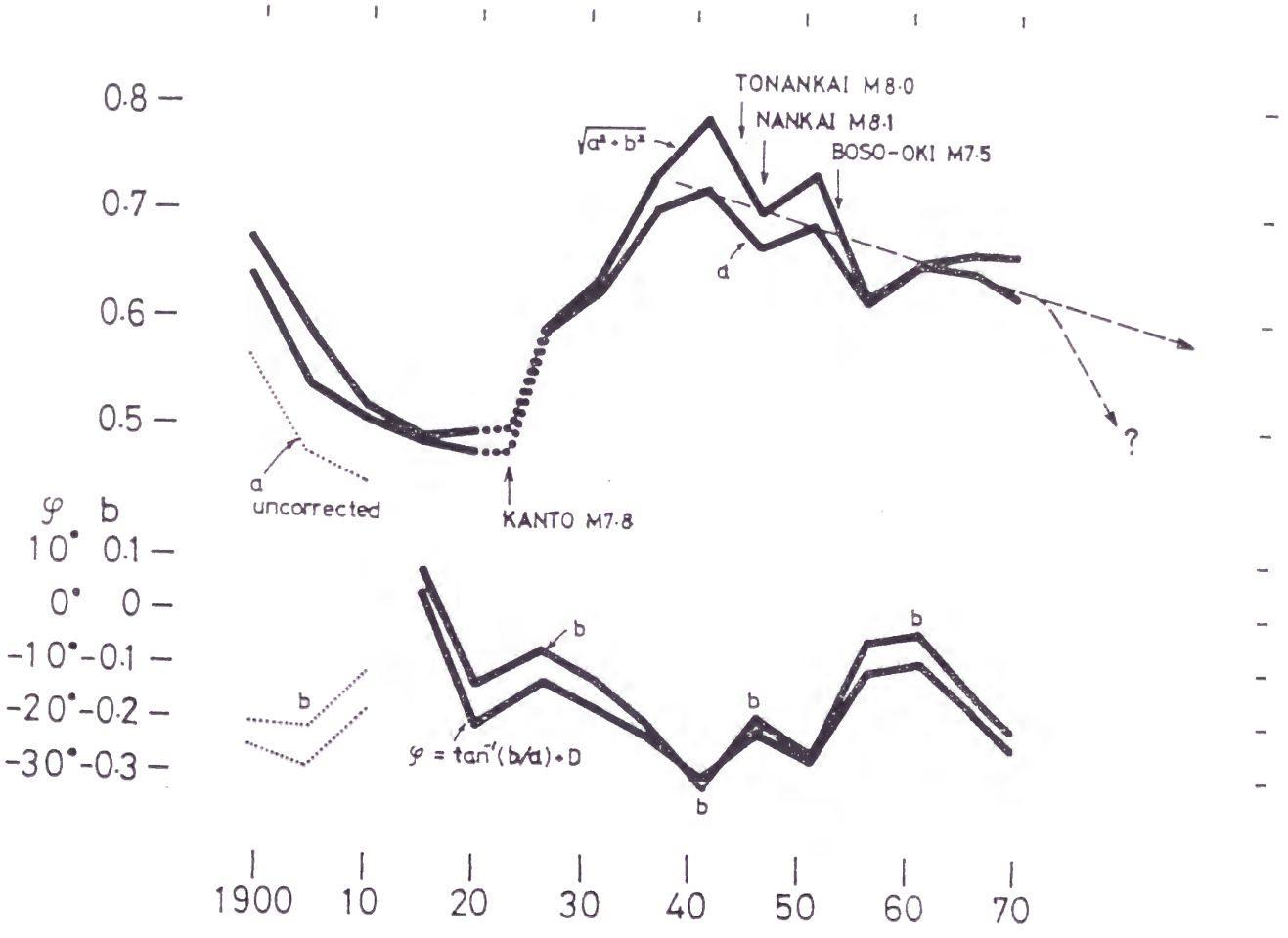

Figure 1-10 Secular variations of A and B values at Kakioka Magnetic Observatory (after Yanagihara, 1972).

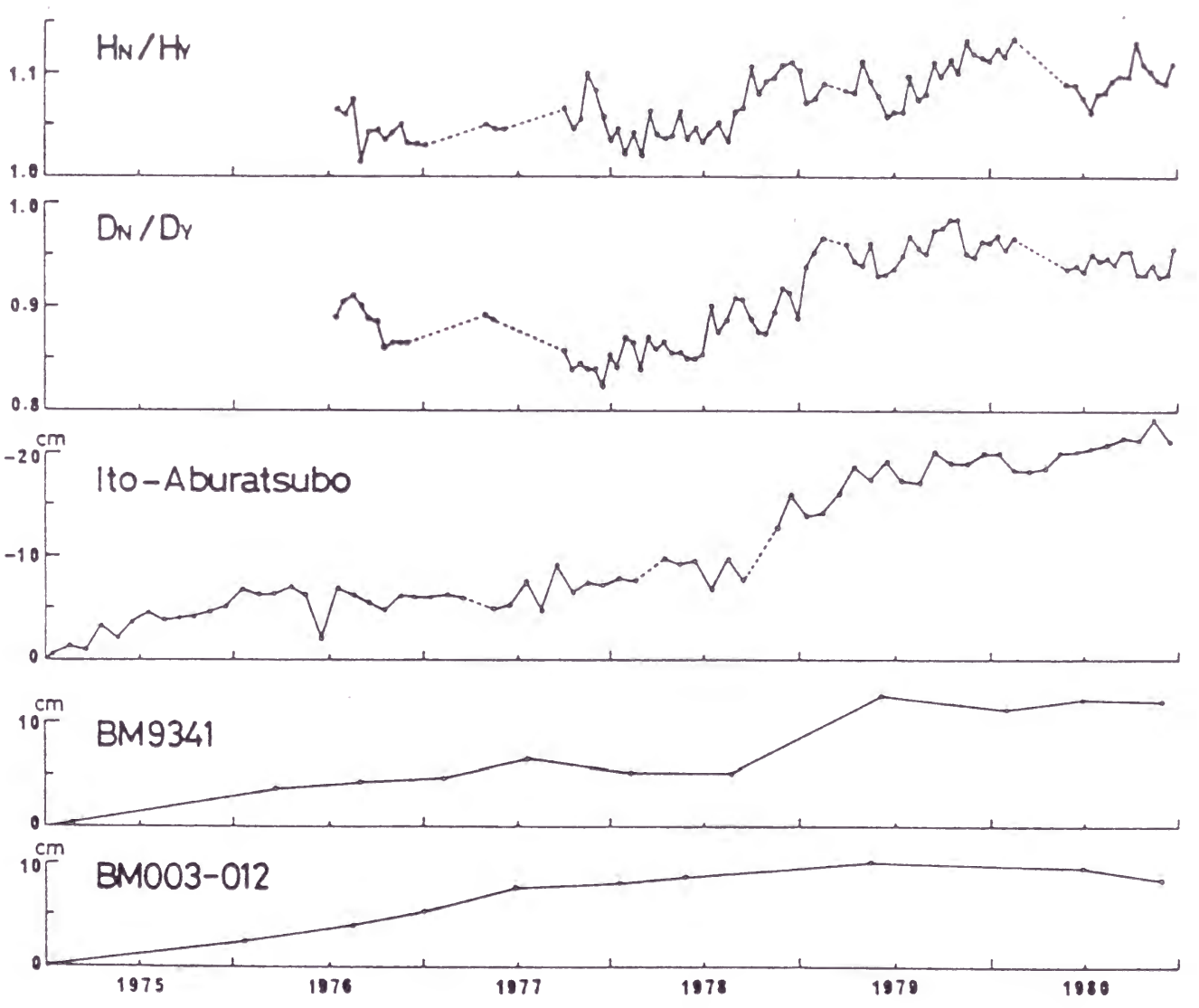

Figure 1-11 Amplitude ratios of short-period geomagnetic variations at Naka-izu relative to the Yatsugatake Magnetic Observatory for the *H* and *D* components, mean sea-level at Ito relative to Aburatsubo, leveling data at bench marks (after Honkura and Taira, 1983).

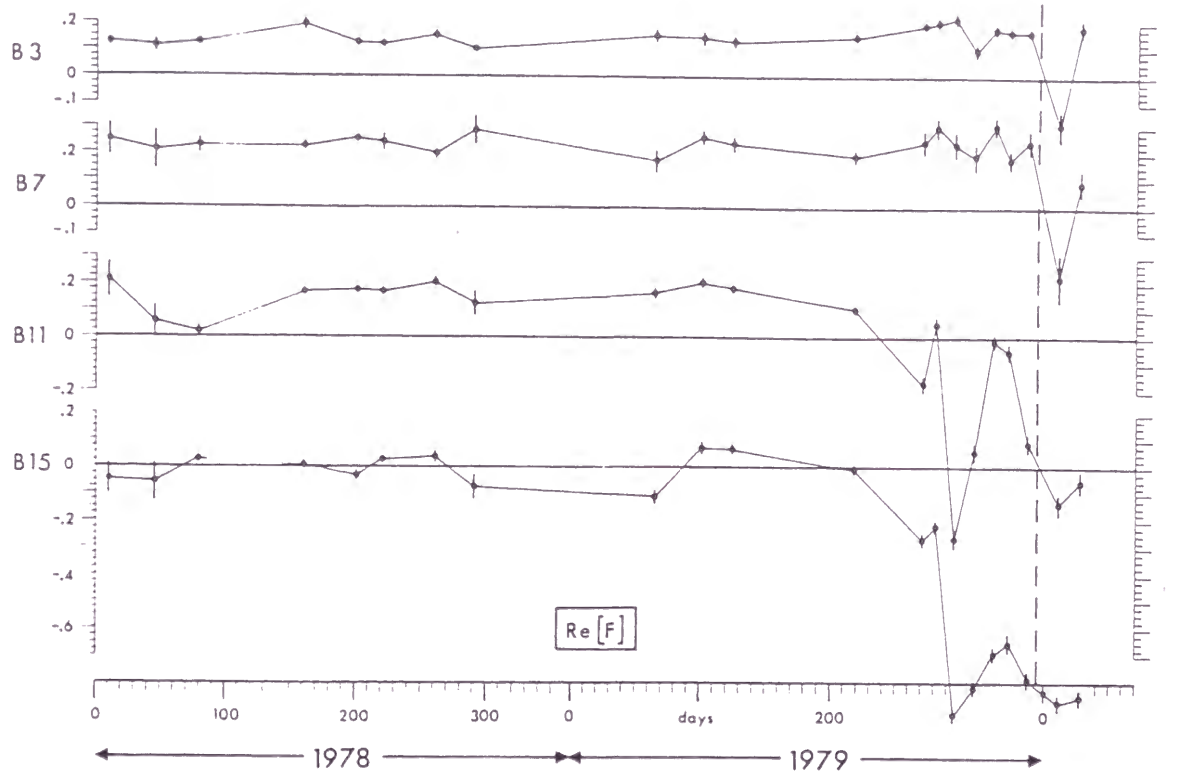

(a)

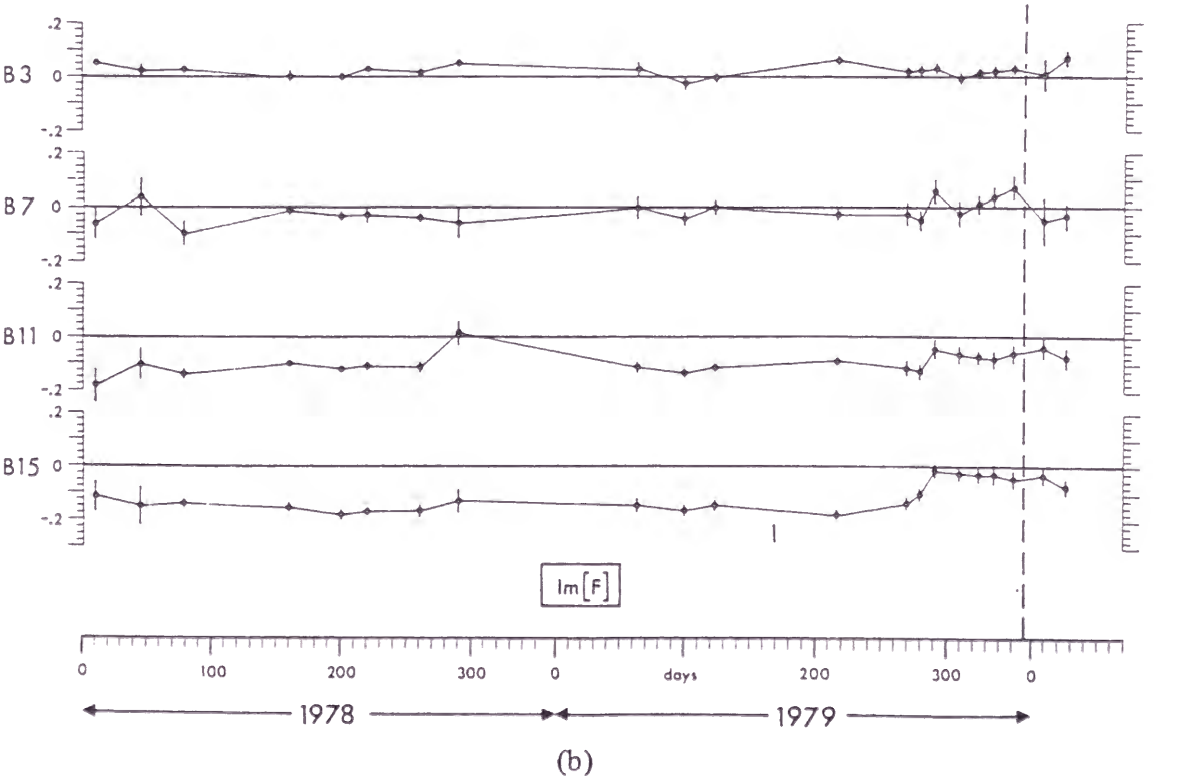

(b)

Figure 1-12 Estimates of inter-station horizontal field transfer function F during 1978 and 1979 for four period ranges: B3(4000-2000 s), B7(1000-600 s), B11(250-150 s) and B15(70-50 s). All error bars are +/- 1 SD. The occurrence of the Boxing Day earthquake (M=5) is shown as the broken line. (after Beamish, 1982)

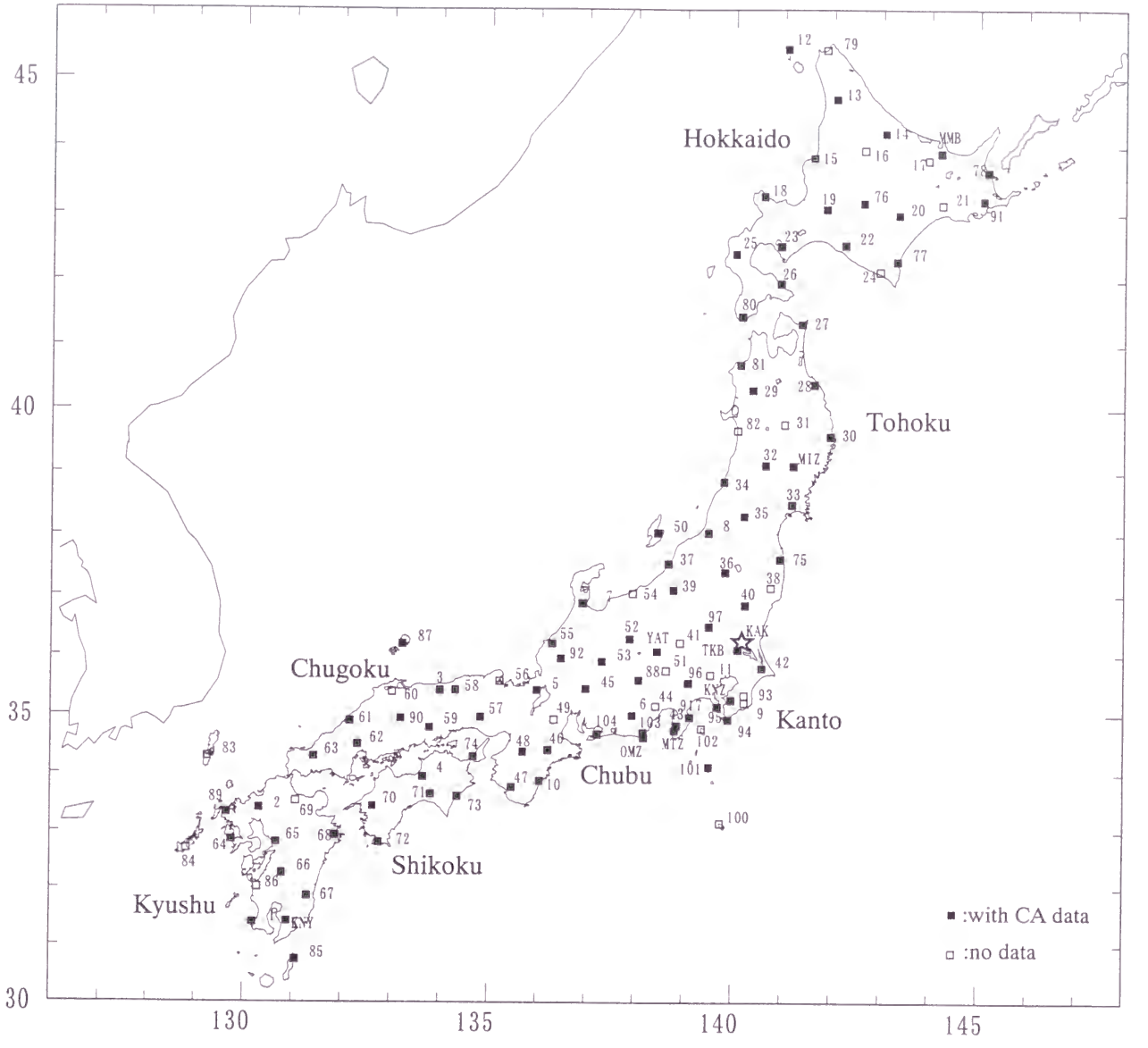

Figure 2-1 Locations of the first order geomagnetic stations and the geomagnetic observatories

Table 2-1 Names and locations of the first order geomagnetic stations and the observatories

Num	Name	Japanese name	Latitude deg	Latitude min	Longitude deg	Longitude min
1	KAGOSHIMA	鹿児島	31	23.7	130	10.8
2	SEBURIYAMA	背振山	33	25.0	130	18.5
3	KURAYOSHI	倉吉	35	24.6	133	59.8
4	KAWANOE	川之江	33	56.6	133	39.3
5	IMAZU	今津	35	24.7	135	59.4
6	HAMAMATSU	浜松	34	59.3	137	56.5
7	HIMI	氷見	36	52.1	136	55.2
8	SHIBATA	新発田	38	1.3	139	28.9
9	KATSUURA	勝浦	35	11.9	140	14.1
10	KUMANO	熊野	33	52.4	136	3.1
11	MITAKA	三鷹	35	40.4	139	33.0
12	REBUNTOU	礼文島	45	25.4	141	2.7
13	NAKAGAWA	中川	44	42.0	142	2.3
14	TAKINOUE	滝ノ上	44	12.0	143	2.5
15	RUMOI	留萌	43	50.4	141	35.5
16	ASAHIKAWA	旭川	43	57.1	142	37.3
17	KITAMI	北見	43	47.8	143	56.2
18	FURUBIRA	古平	43	16.2	140	34.7
19	IWAMIZAWA	岩見沢	43	4.6	141	51.2
20	OBIHIRO	帯広	42	59.2	143	20.1
21	KUSHIRO	釧路	43	8.3	144	13.4
22	MONBETSU	門別	42	31.8	142	13.9
23	DATE	伊達	42	30.9	140	55.8
24	SAMANI	様似	42	8.0	142	57.1
25	IMAKANE	今金	42	24.2	140	.7
26	KAYABE	茅部	41	57.4	140	55.6
27	SHIMOKITA	下北	41	19.9	141	22.3
28	HACHINOHE	八戸	40	23.7	141	37.6
29	OODATE	大館	40	18.4	140	22.3
30	MIYAKO	宮古	39	34.5	141	57.5
31	MORIOKA	盛岡	39	46.3	141	2.0
32	YOKOTE	横手	39	7.2	140	38.6
33	ISHINOMAKI	石巻	38	29.3	141	11.1
34	SAKATA	酒田	38	50.8	139	47.6
35	YAMAGATA	山形	38	18.0	140	13.1
36	WAKAMATSU	若松	37	22.6	139	49.5
37	IZUMOZAKI	出雲崎	37	30.7	138	39.8
38	IWAKI	いわき	37	7.6	140	46.0
39	TOOKAMACHI	十日町	37	5.2	138	46.3
40	UTSUNOMIYA	宇都宮	36	50.3	140	14.5
41	TOMIOKA	富岡	36	12.5	138	55.2
42	CHOUSHI	銚子	35	47.4	140	35.2
43	NISHIIZU	西伊豆	34	49.3	138	50.8
44	SHIMIZU	清水	35	9.0	138	25.5
45	INUYAMA	犬山	35	26.3	136	58.8
46	MIE	三重	34	24.2	136	13.4
47	TANABE	田辺	33	45.6	135	28.3
48	GOJOU	五条	34	22.3	135	42.2
49	KOUGA	甲賀	34	54.8	136	21.0
50	RYOUZU	両津	38	.9	138	27.2
51	KOUFU	甲府	35	44.6	138	37.7
52	MATSUMOTO	松本	36	15.9	137	52.9
53	TAKAYAMA	高山	35	54.0	137	19.2
54	ITOIGAWA	糸魚川	37	1.4	137	56.7
55	FUKUI	福井	36	11.7	136	18.1
56	MIYAZU	宮津	35	33.7	135	13.4
57	HIMEJI	姫路	34	57.6	134	50.0
58	TOTTORI	鳥取	35	24.8	134	18.7
59	OKAYAMA	岡山	34	46.7	133	47.4
60	MATSUE	松江	35	22.9	133	1.4
61	HAMADA	浜田	34	53.6	132	10.1
62	HIROSHIMA	広島	34	29.6	132	19.4
63	YAMAGUCHI	山口	34	17.4	131	25.3
64	NAGASAKI	長崎	32	51.3	129	45.1
65	KUMAMOTO	熊本	32	49.0	130	39.6
66	HITOYOSHI	人吉	32	15.6	130	46.6
67	MIYAZAKI	宮崎	31	51.6	131	17.6
68	SAEKI	佐伯	32	55.7	131	52.5
69	NAKATSU	中津	33	31.5	131	3.7
70	OOZU	大洲	33	26.3	132	38.2
71	KOUCHI	高知	33	38.5	133	48.8
72	NAKAMURA	中村	32	48.4	132	45.6
73	OOSATO	大里	33	35.9	134	22.0
74	AWAJI	淡路島	34	17.2	134	40.8
75	HARANOMACHI	原ノ町	37	35.7	140	57.2
76	IKUTORA	幾寅	43	9.8	142	36.4
77	HIROO	広尾	42	17.3	143	17.4
78	SHIBETSU	標津	43	38.0	145	10.2
79	WAKKANAI	稚内	45	24.6	141	49.8
80	FUKUSHIMA	福島	41	26.7	140	8.6
81	GOSHOGAWARA	五所川原	40	41.8	140	6.9
82	AKITA	秋田	39	39.8	140	4.3
83	TSUSHIMA	対島	34	16.8	129	14.4
84	FUKUE	福江	32	41.3	128	49.4
85	TANEGASHIMA	種子島	30	43.9	131	4.1
86	IZUMI	出水	32	1.2	130	16.6
87	SAIGOU	西郷	36	11.5	133	13.5
88	IIDA	飯田	35	35.1	138	3.9
89	SASEBO	佐世保	33	20.0	129	38.6
90	TOUJOU	東城	34	56.4	133	12.2
91	NEMURO	根室	43	12.2	145	4.5
92	OONO	大野	35	57.0	136	29.0
93	CHIBA	千葉	35	20.1	140	13.6
94	TATEYAMA	館山	34	55.3	139	53.9
95	KENZAKI	剣崎	35	8.3	139	40.7
96	TANZAWA	丹沢	35	32.2	139	5.3
97	TOCHIGI	栃木	36	28.6	139	29.9
98	CHICHIJIMA	父島	27	3.5	142	13.1
99	OKINAWA	沖縄	26	38.9	128	14.5
100	HACHIJOUJIMA	八丈島	33	8.5	139	44.7
101	MIYAKEJIMA	三宅島	34	7.0	139	30.7
102	IZUOOSHIMA	伊豆大島	34	46.1	139	21.6
103	OMAEZAKI	御前崎	34	41.7	138	9.7
104	MIKAWA	三河	34	39.9	137	13.4
105	ISHIGAKIJIMA	石垣島	24	22.2	124	11.5
917	ITOU	伊東	34	57.5	139	6.8
KNZ	Kanozan	鹿野山	35	15.2	139	57.5
MIZ	Mizusawa	水沢	39	6.5	141	12.4
TKB	Tsukuba	つくば	36	6.1	140	5.5
KAK	Kakioka	柿岡	36	13.8	140	11.4
KNY	Kanoya	鹿屋	31	25.2	130	52.9
MMB	Memanbetsu	女満別	43	54.5	144	11.6
MTZ	Matsuzaki	松崎	34	44.0	138	48.0
OMZ	Omaezaki	御前崎	34	37.0	138	11.0
YAT	Yatsugatake	八ケ岳	36	4.1	138	26.6

Photo 2-1 A sensor of a fluxgate magnetometer in a digged hole

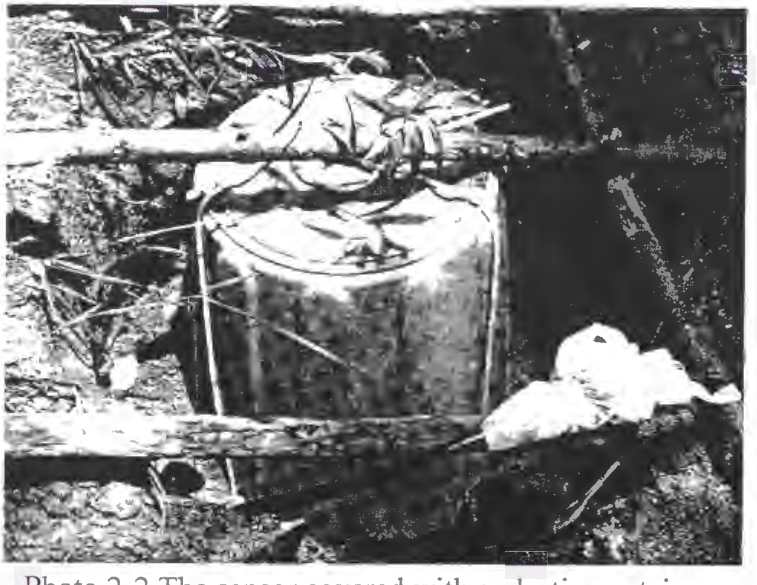

Photo 2-2 The sensor covered with a plastic container

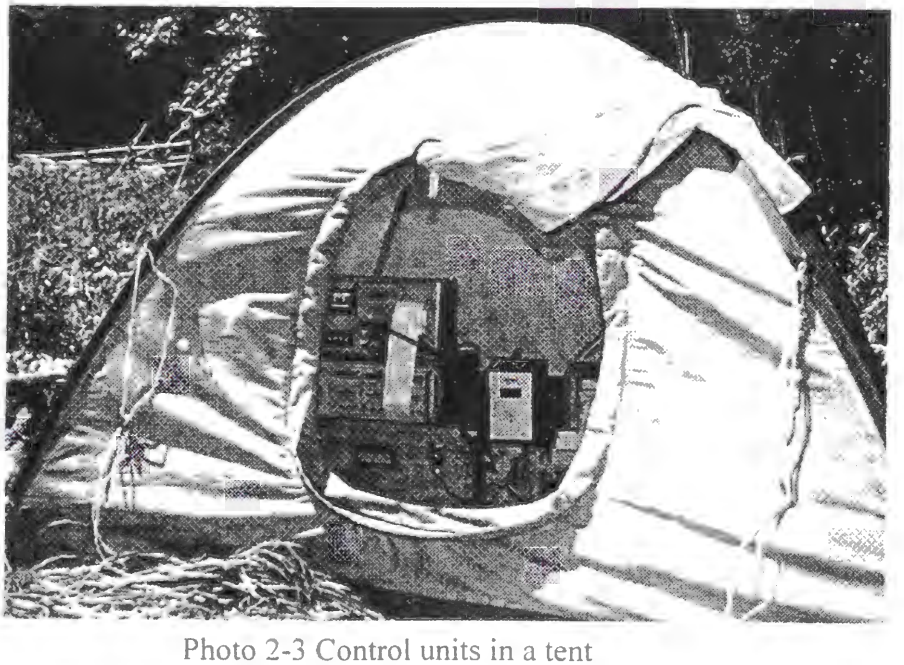

Photo 2-3 Control units in a tent

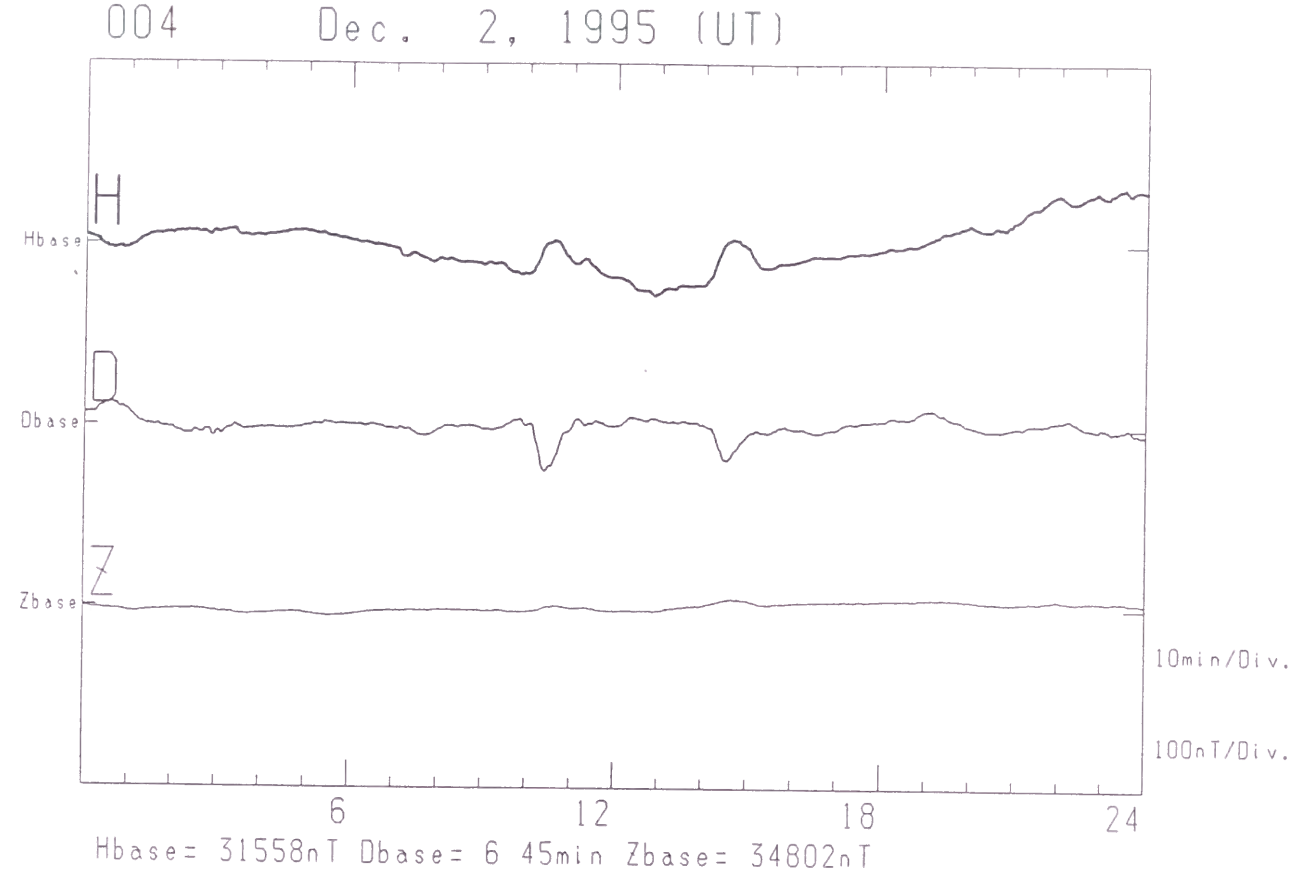

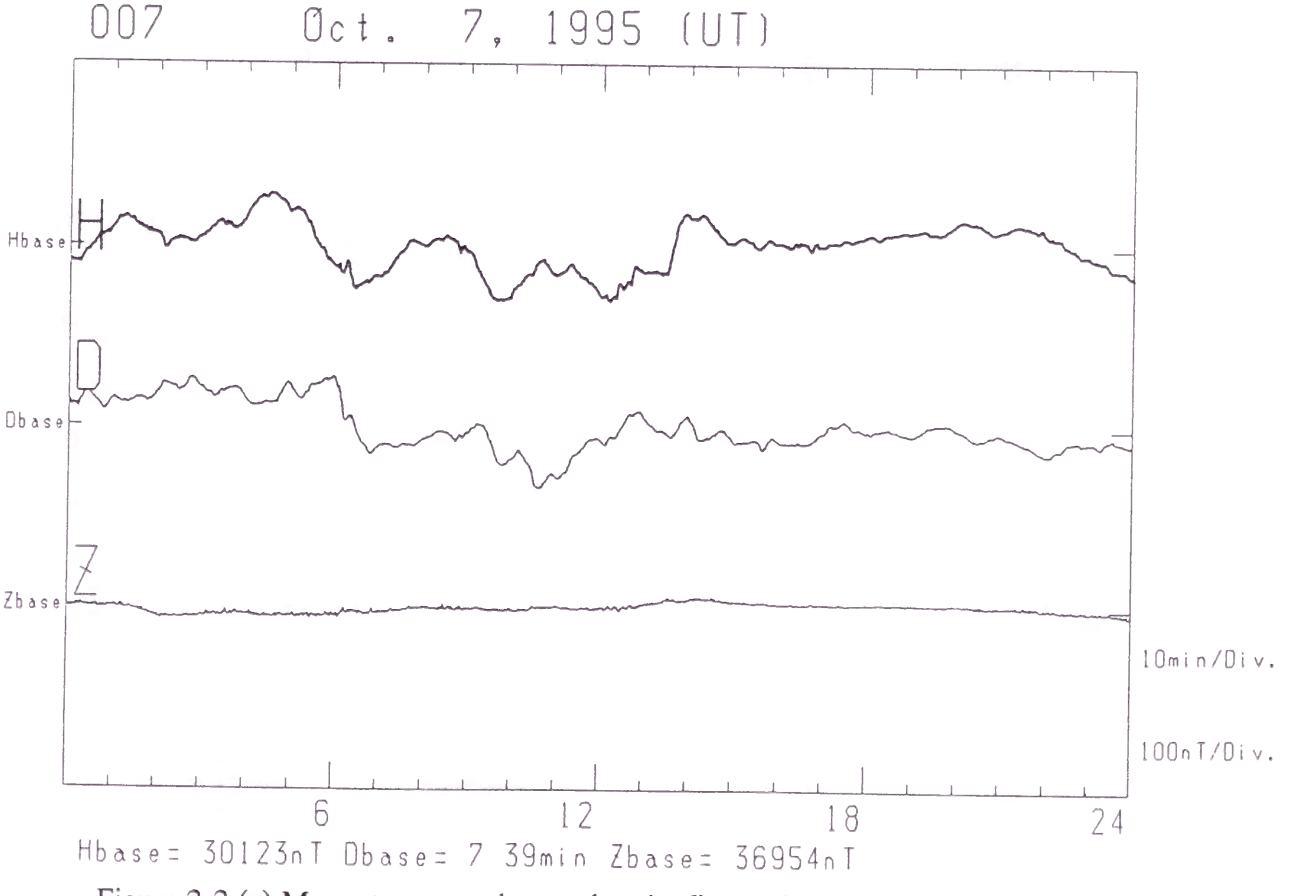

Figure 2-2 (a) Magnetograms observed at the first order geomagnetic stations

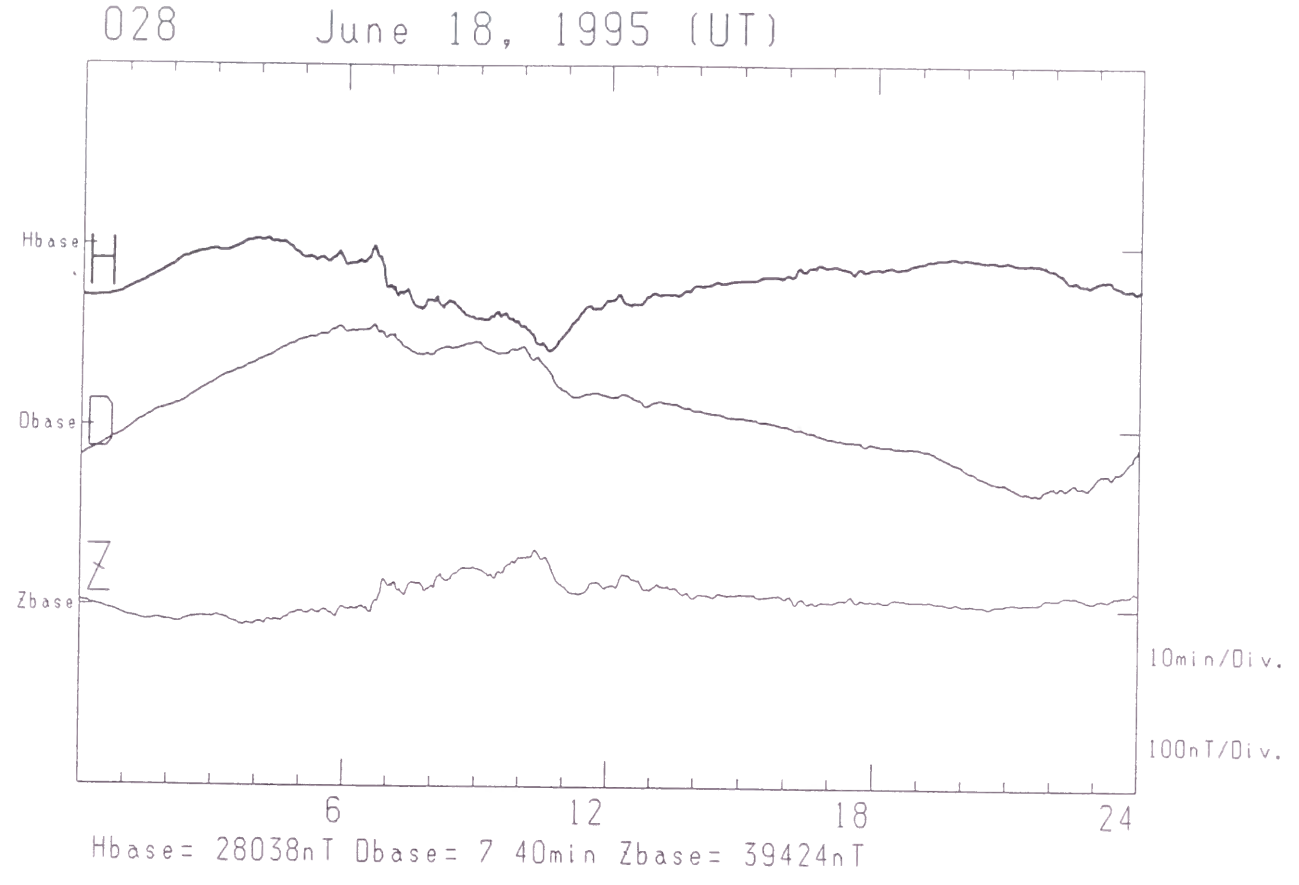

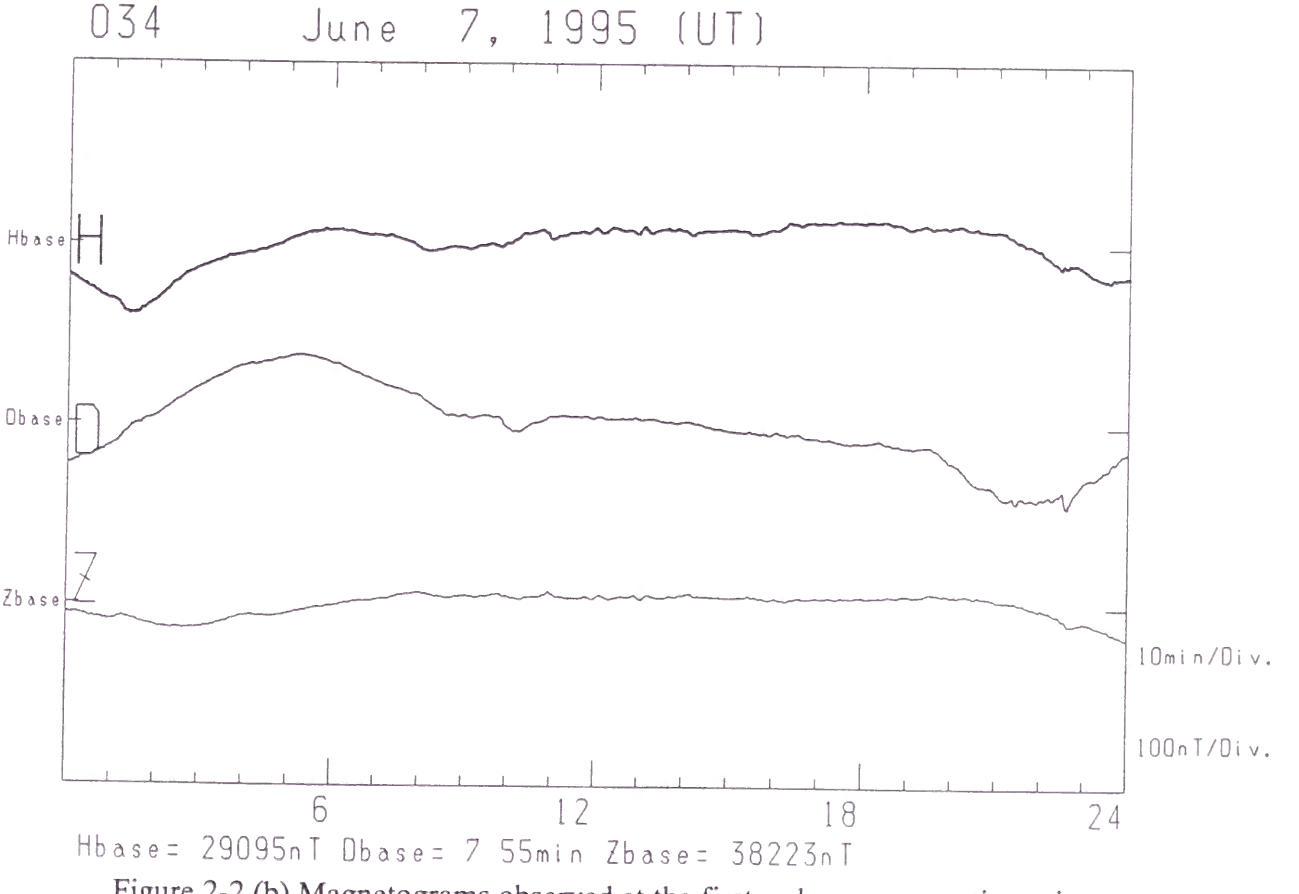

Figure 2-2 (b) Magnetograms observed at the first order geomagnetic stations

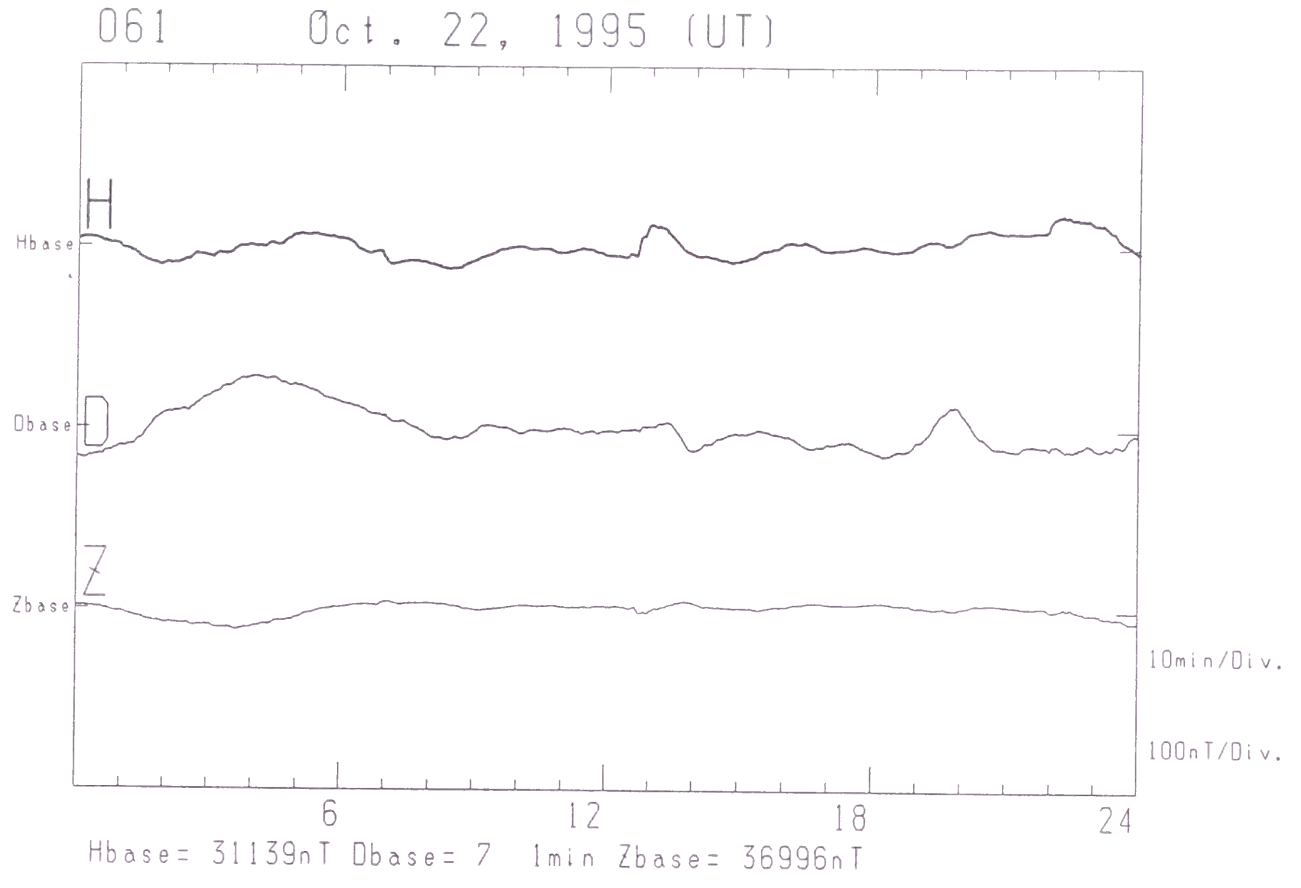

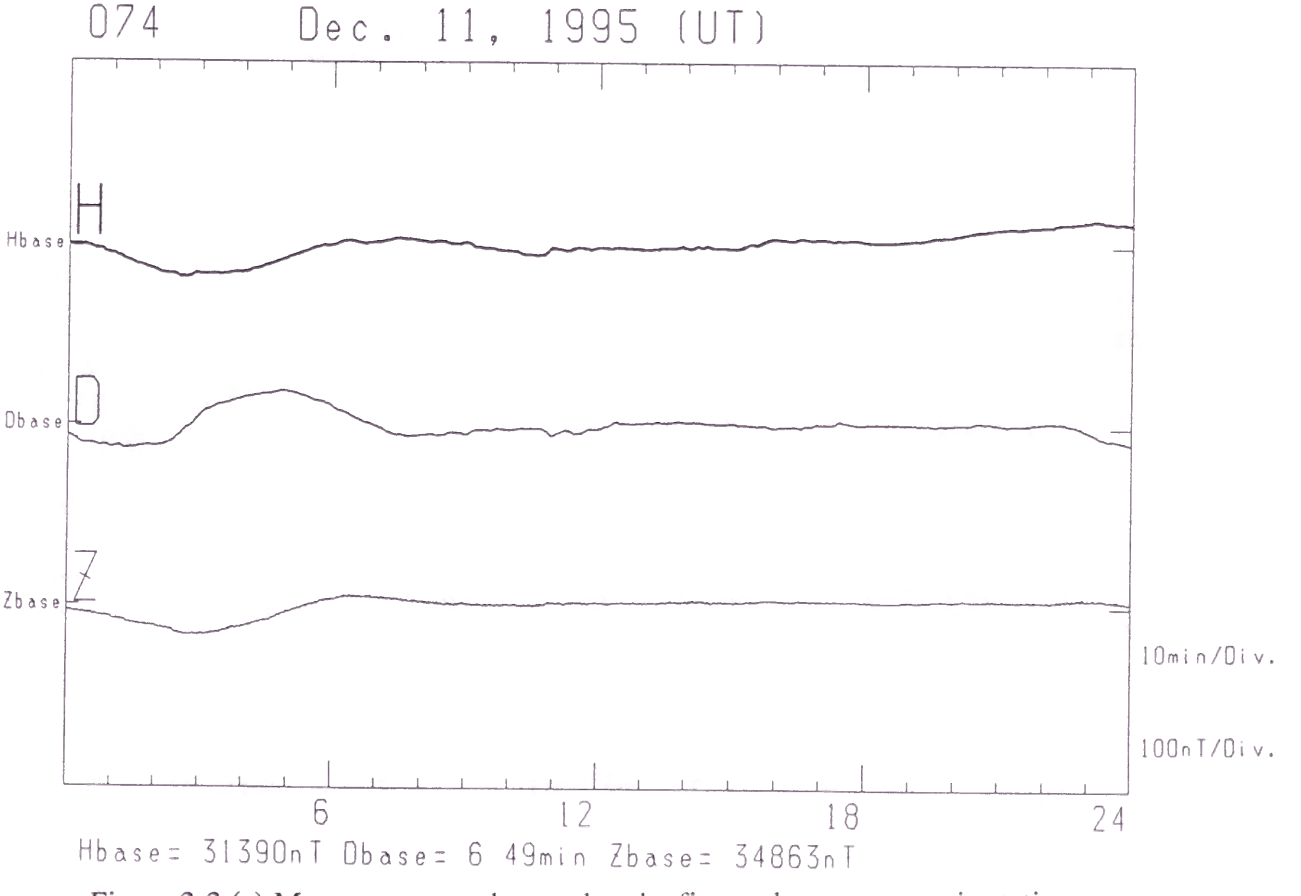

Figure 2-2 (c) Magnetograms observed at the first order geomagnetic stations

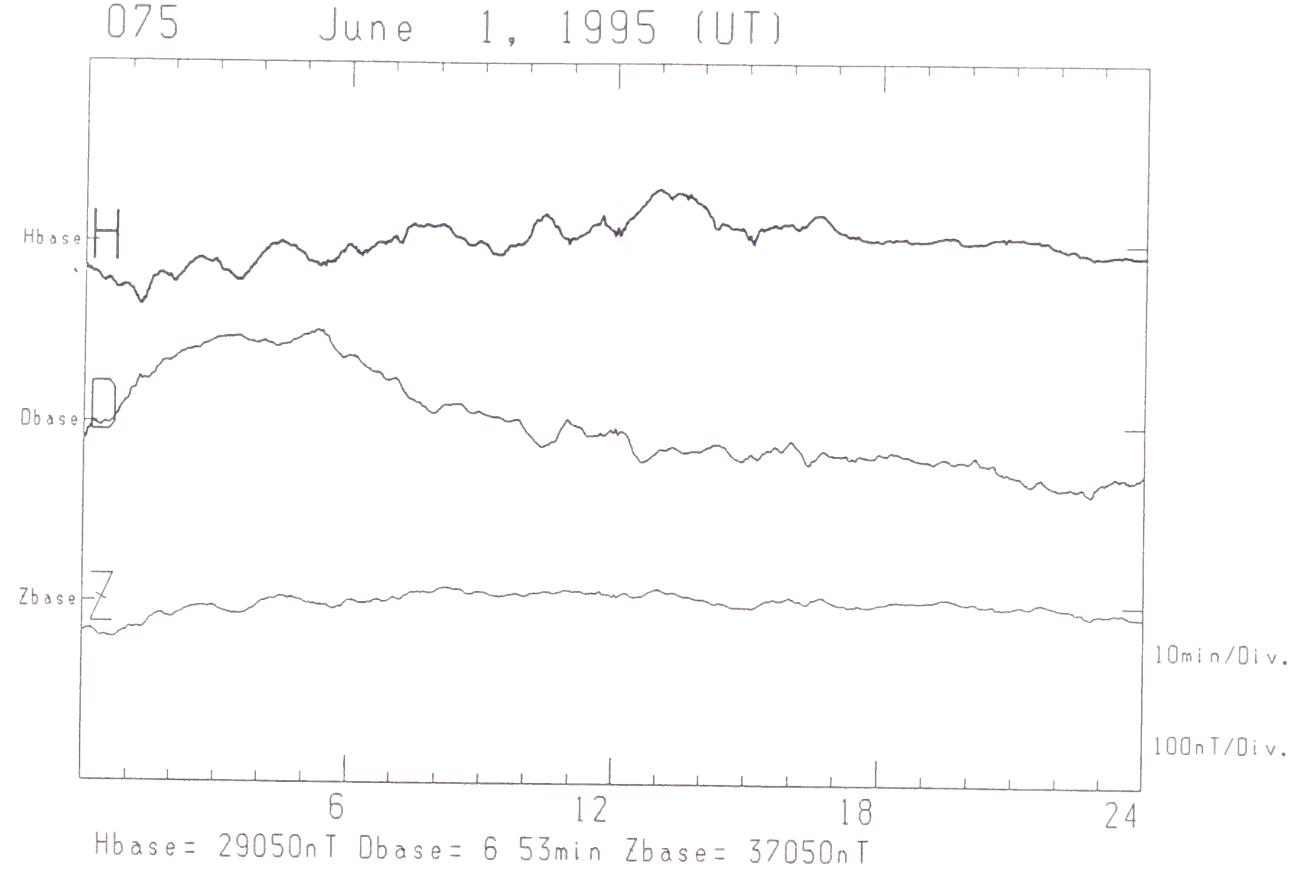

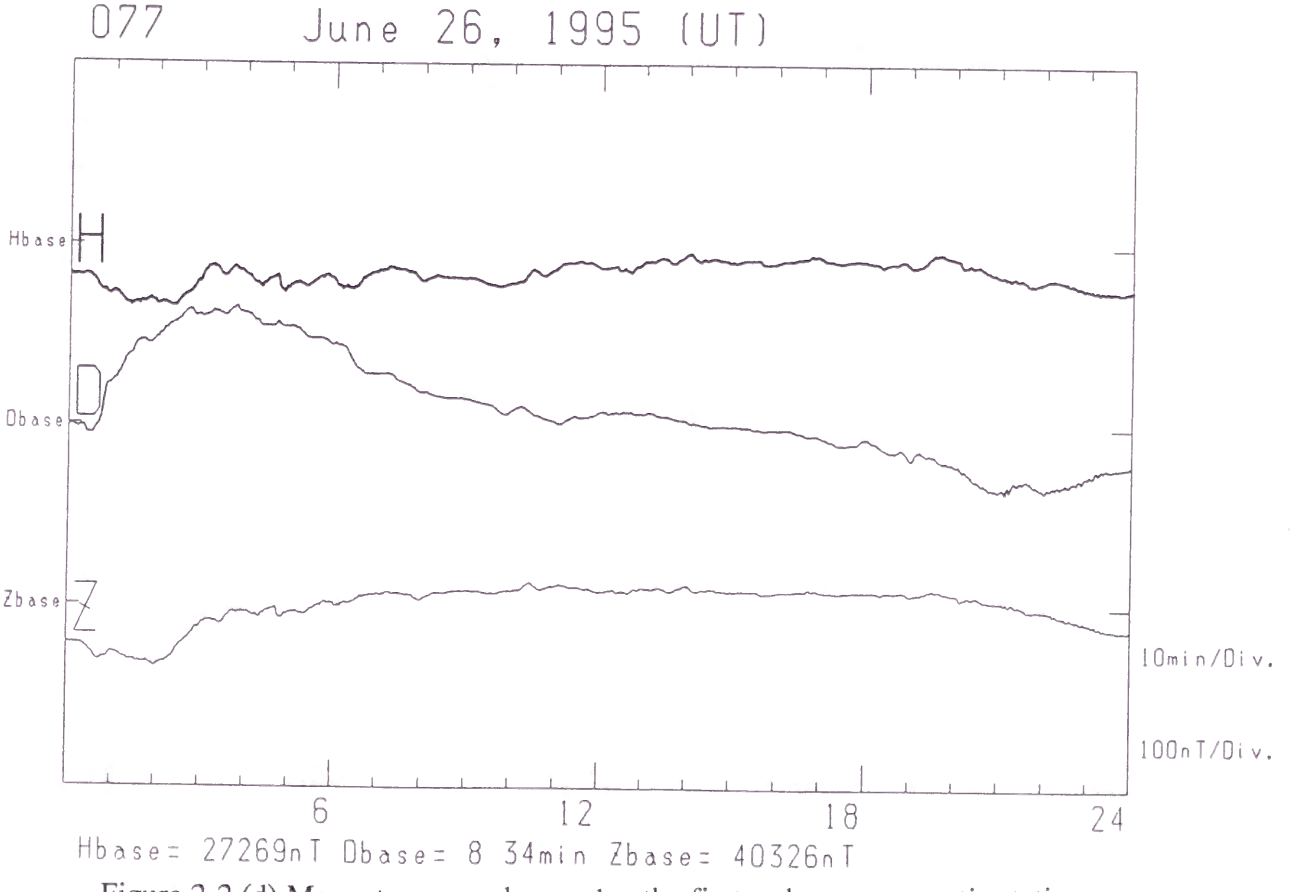

Figure 2-2 (d) Magnetograms observed at the first order geomagnetic stations

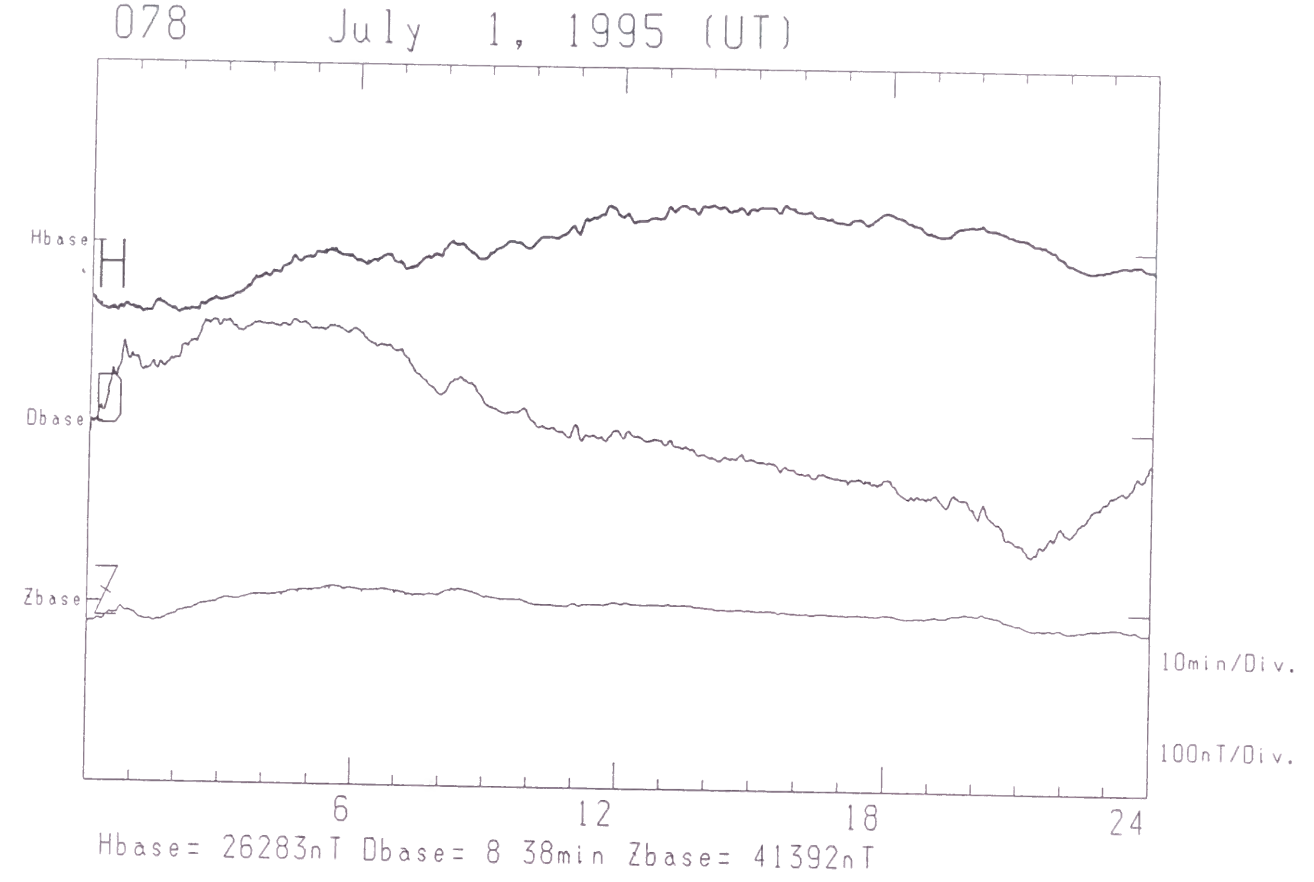

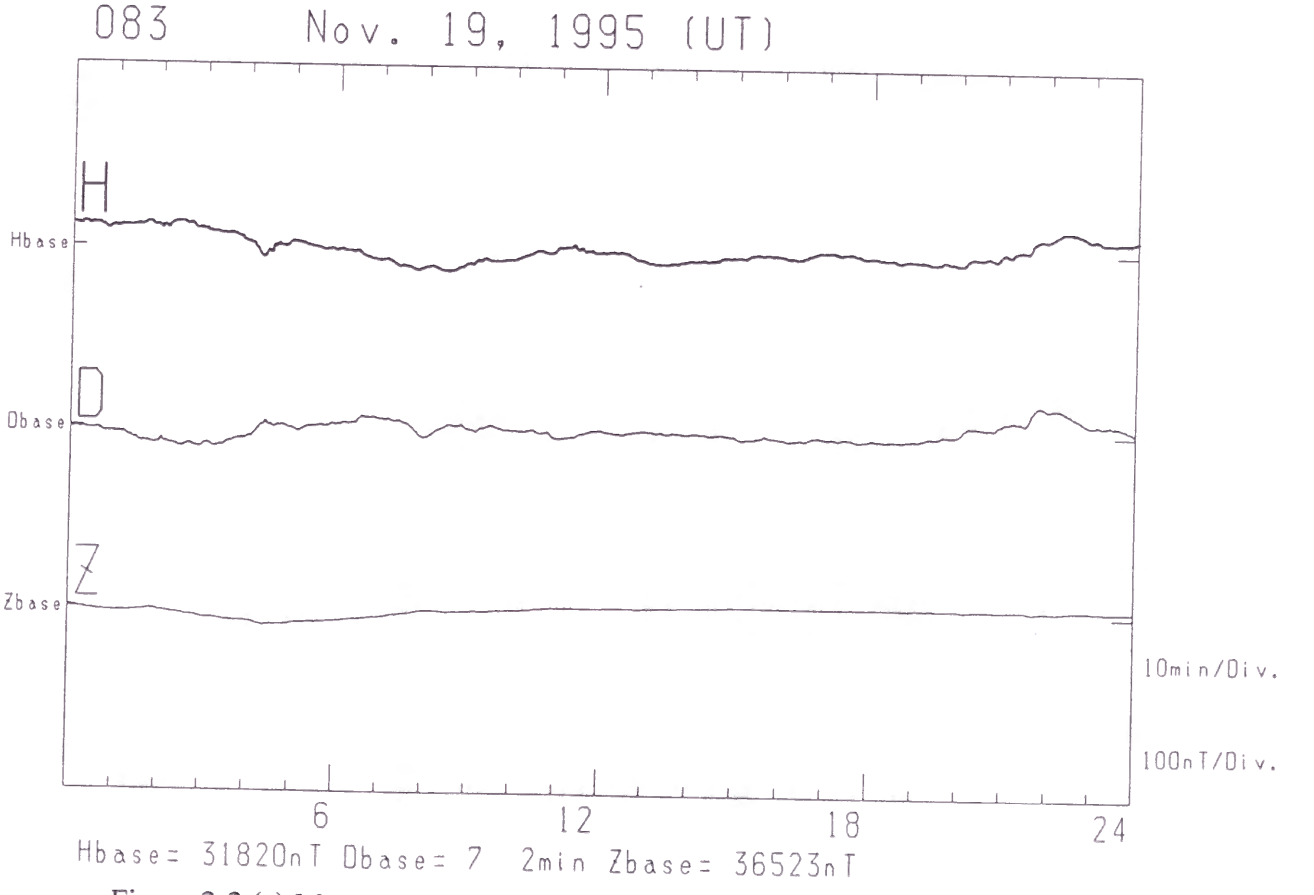

Figure 2-2 (e) Magnetograms observed at the first order geomagnetic stations

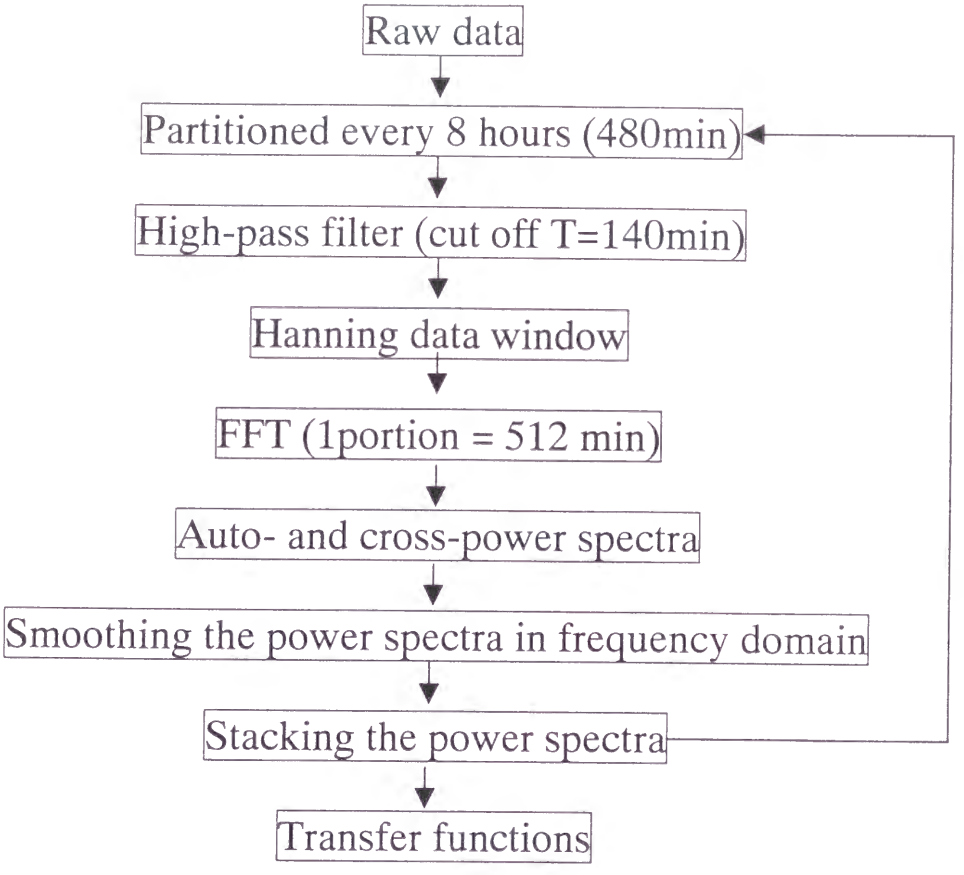

Figure 3-1 A flow chart of the analysis

Table 3-1 Coherency squared of each component between KAK and each observatory (June 1993)

	MMB			MIZ			KNZ			KNY		
	X	Y	Z	X	Y	Z	X	Y	Z	X	Y	Z
128 min	.91	.87	.10	.95	.95	.16	.99	.98	.95	.94	.82	.63
64 min	.91	.89	.11	.95	.95	.19	.99	.98	.95	.94	.85	.67
32 min	.85	.94	.14	.98	.98	.05	.98	.97	.92	.94	.88	.65
16 min	.88	.94	.03	.99	.98	.11	.98	.92	.83	.97	.92	.76
8 min	.86	.96	.09	.98	.98	.31	.94	.79	.48	.95	.94	.73
4 min	.90	.88	.02	.93	.86	.28	.53	.26	.06	.93	.82	.53

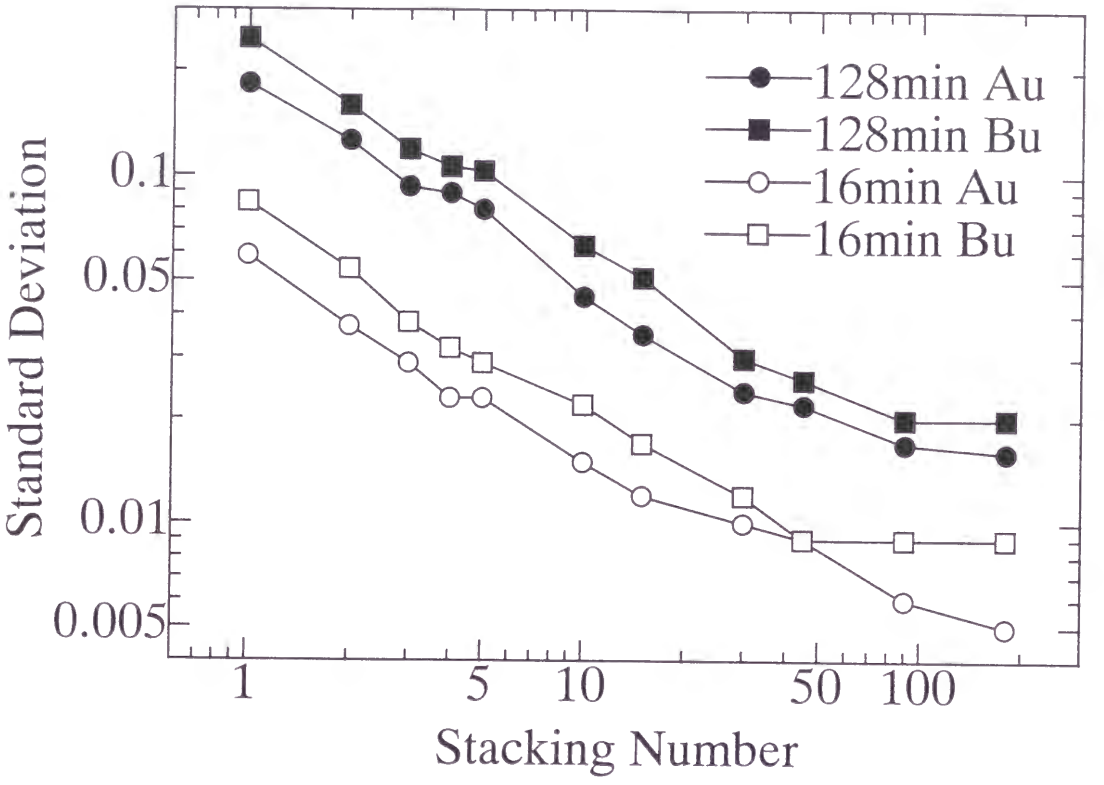

Figure 3-2 Standard deviations of the transfer function A and B at Kakioka according to stacking number in 1989

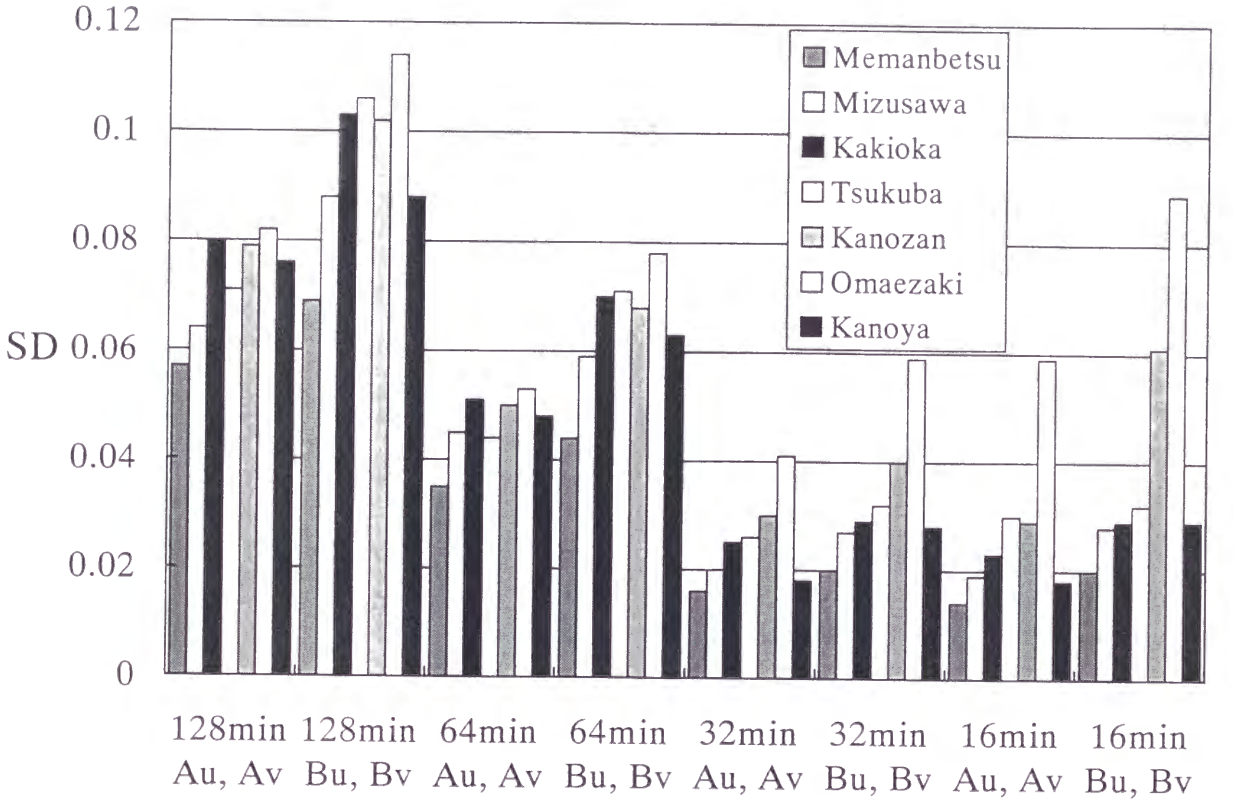

Figure 3-3 Standard deviations of the transfer function A and B at each observatory. Each transfer function was calculated from 40 hour data (5 stacking).

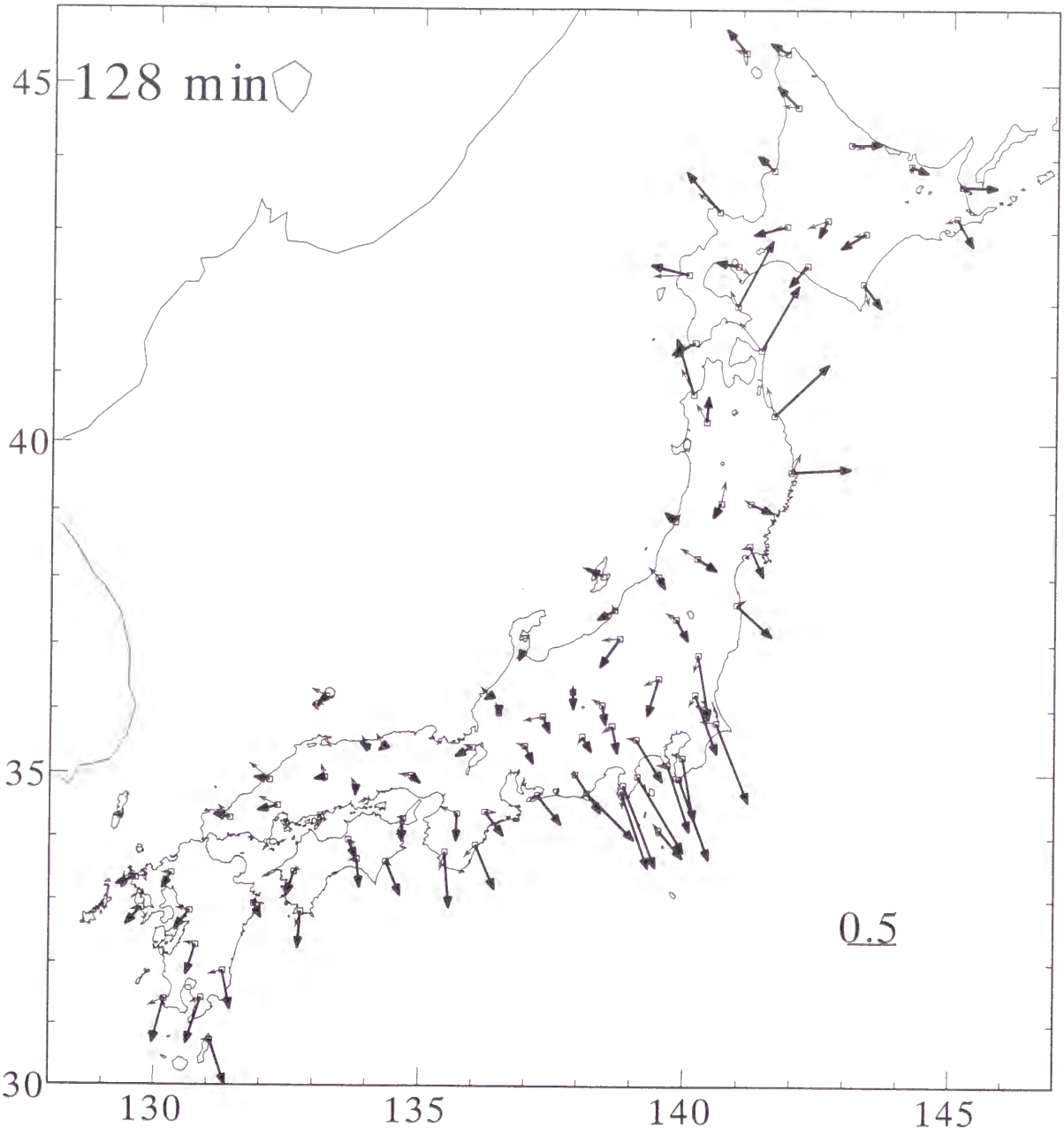

Figure 4-1 (a) Single-station induction arrows
The thick line with a large arrowhead shows a real part (*Au* and *Bu*) and the thin line with a small arrowhead shows an imaginary part (*Av* and *Bv*).

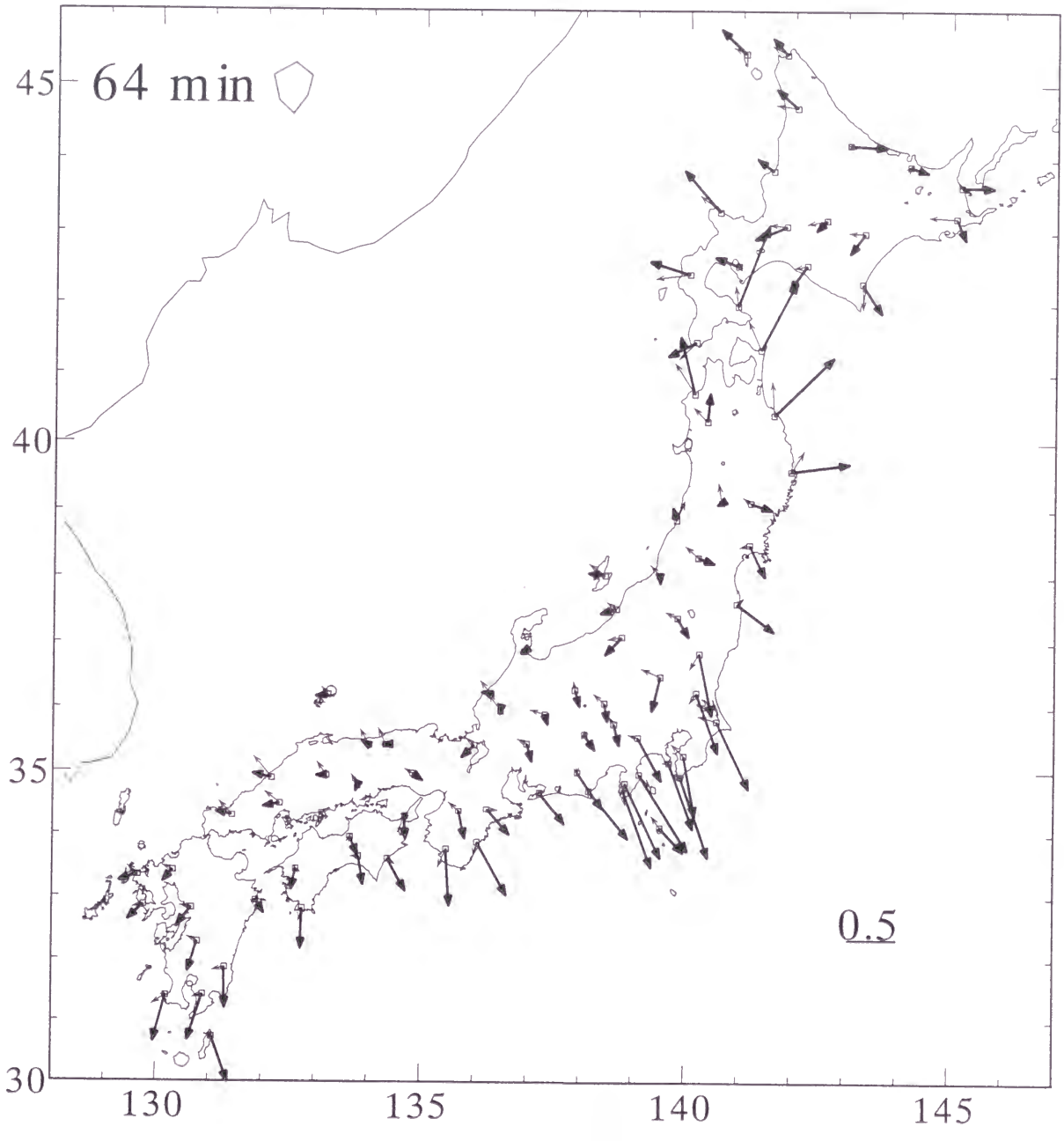

Figure 4-1 (b) Single-station induction arrows
The thick line with a large arrowhead shows a real part (*Au* and *Bu*) and the thin line with a small arrowhead shows an imaginary part (*Av* and *Bv*).

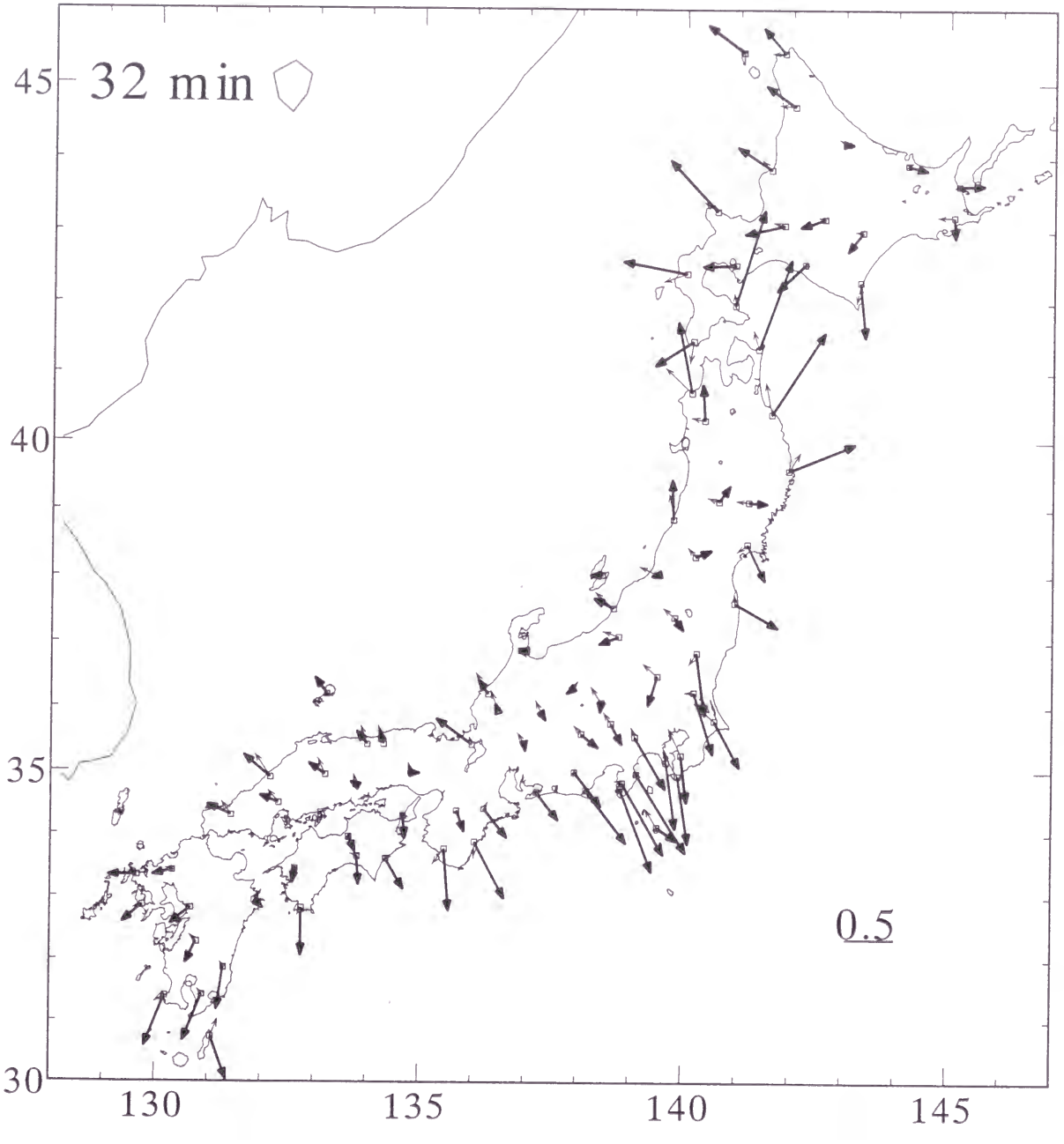

Figure 4-1 (c) Single-station induction arrows
The thick line with a large arrowhead shows a real part (*Au* and *Bu*) and the thin line with a small arrowhead shows an imaginary part (*Av* and *Bv*).

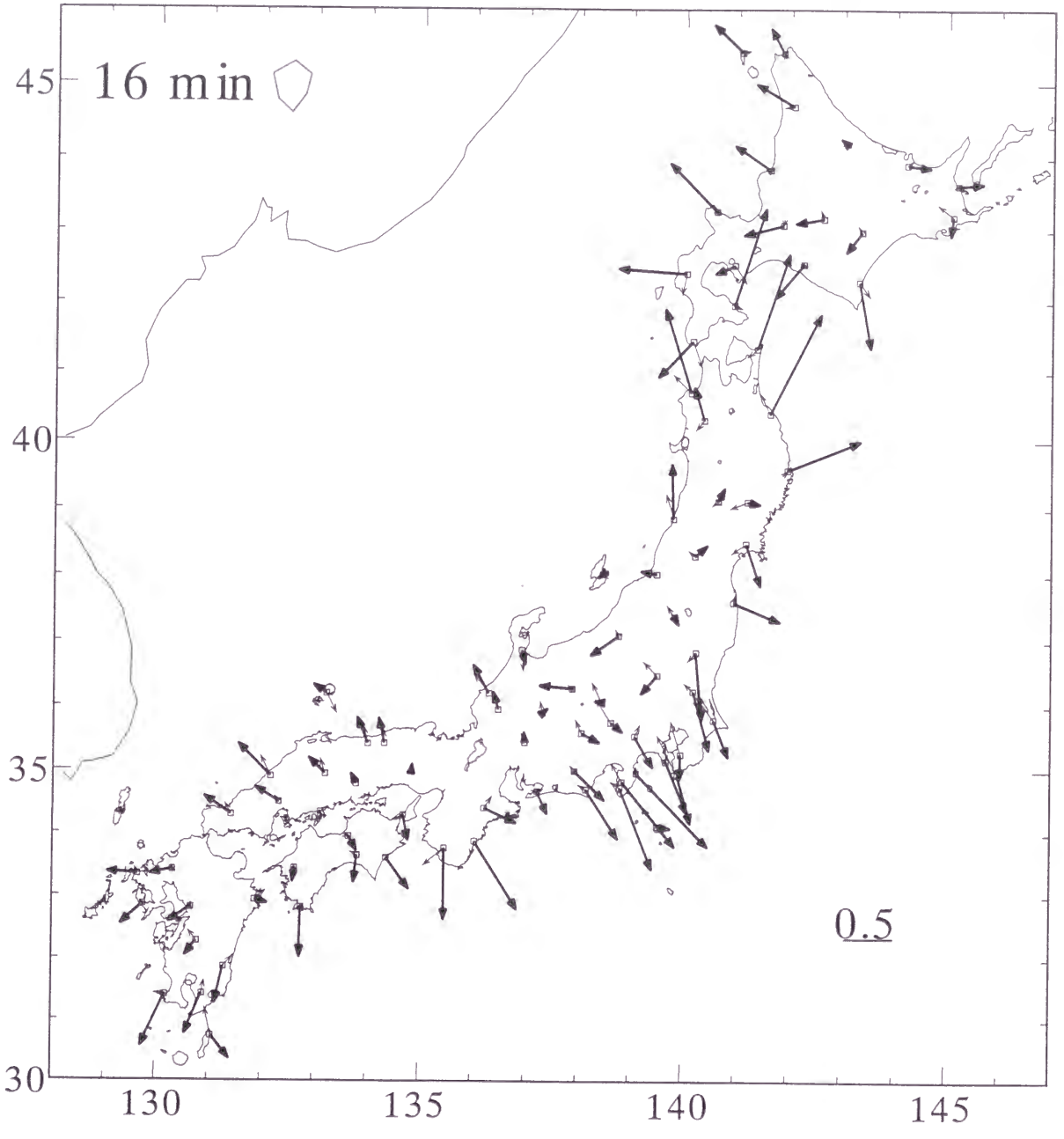

Figure 4-1 (d) Single-station induction arrows
The thick line with a large arrowhead shows a real part (*Au* and *Bu*) and the thin line with a small arrowhead shows an imaginary part (*Av* and *Bv*).

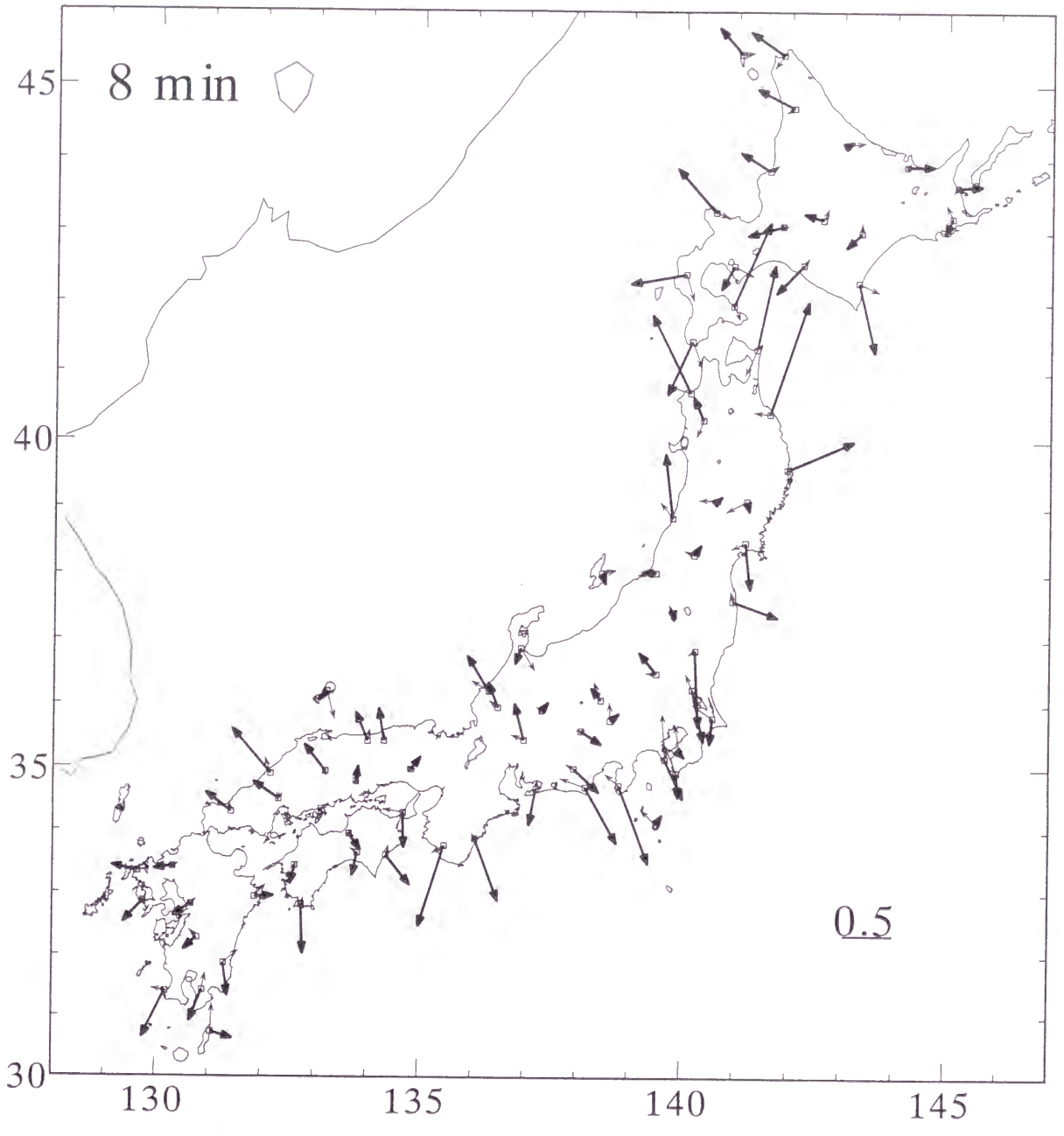

Figure 4-1 (e) Single-station induction arrows
The thick line with a large arrowhead shows a real part (*Au* and *Bu*) and the thin line with a small arrowhead shows an imaginary part (*Av* and *Bv*).

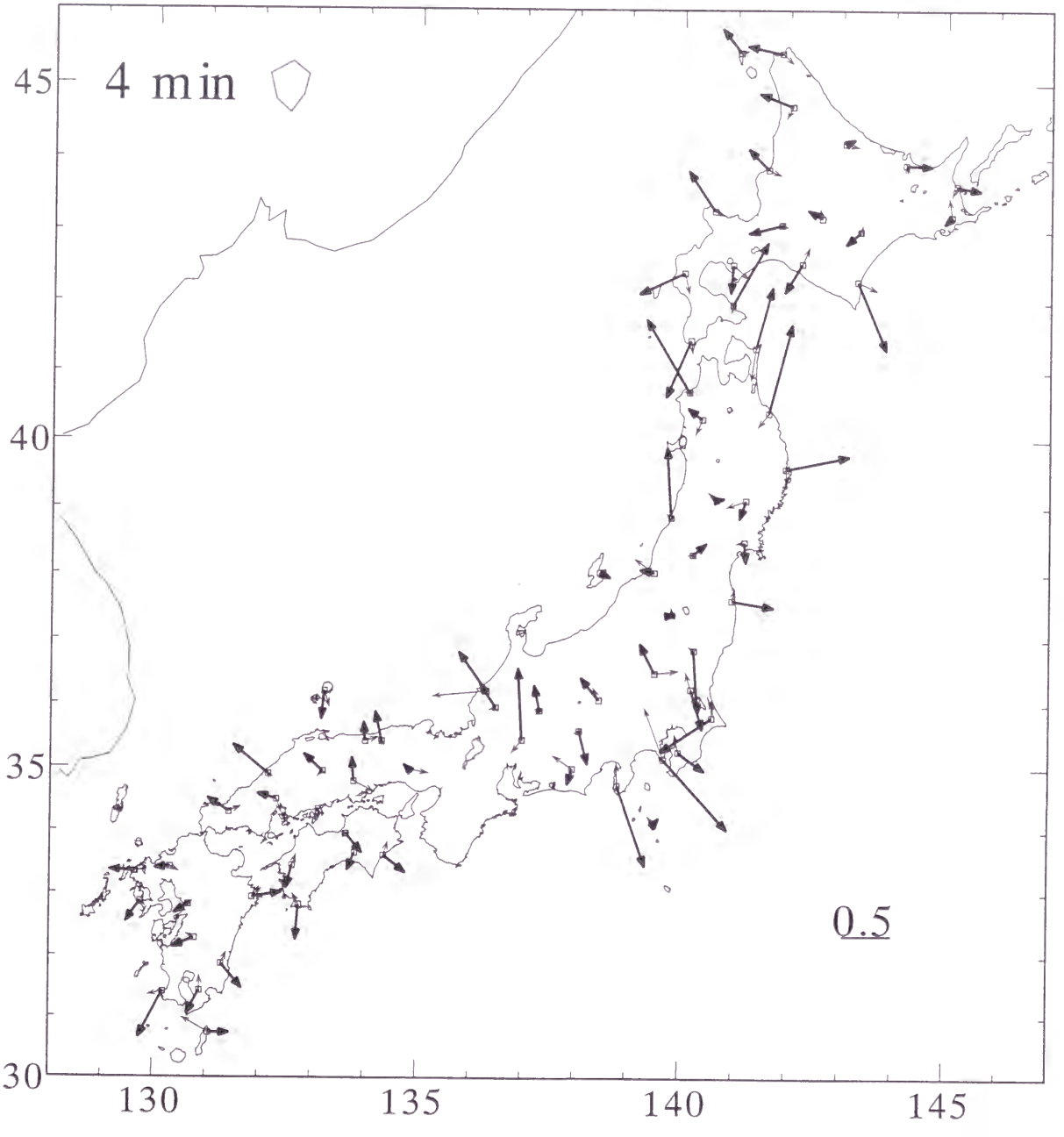

Figure 4-1 (f) Single-station induction arrows
The thick line with a large arrowhead shows a real part (*Au* and *Bu*) and the thin line with a small arrowhead shows an imaginary part (*Av* and *Bv*).

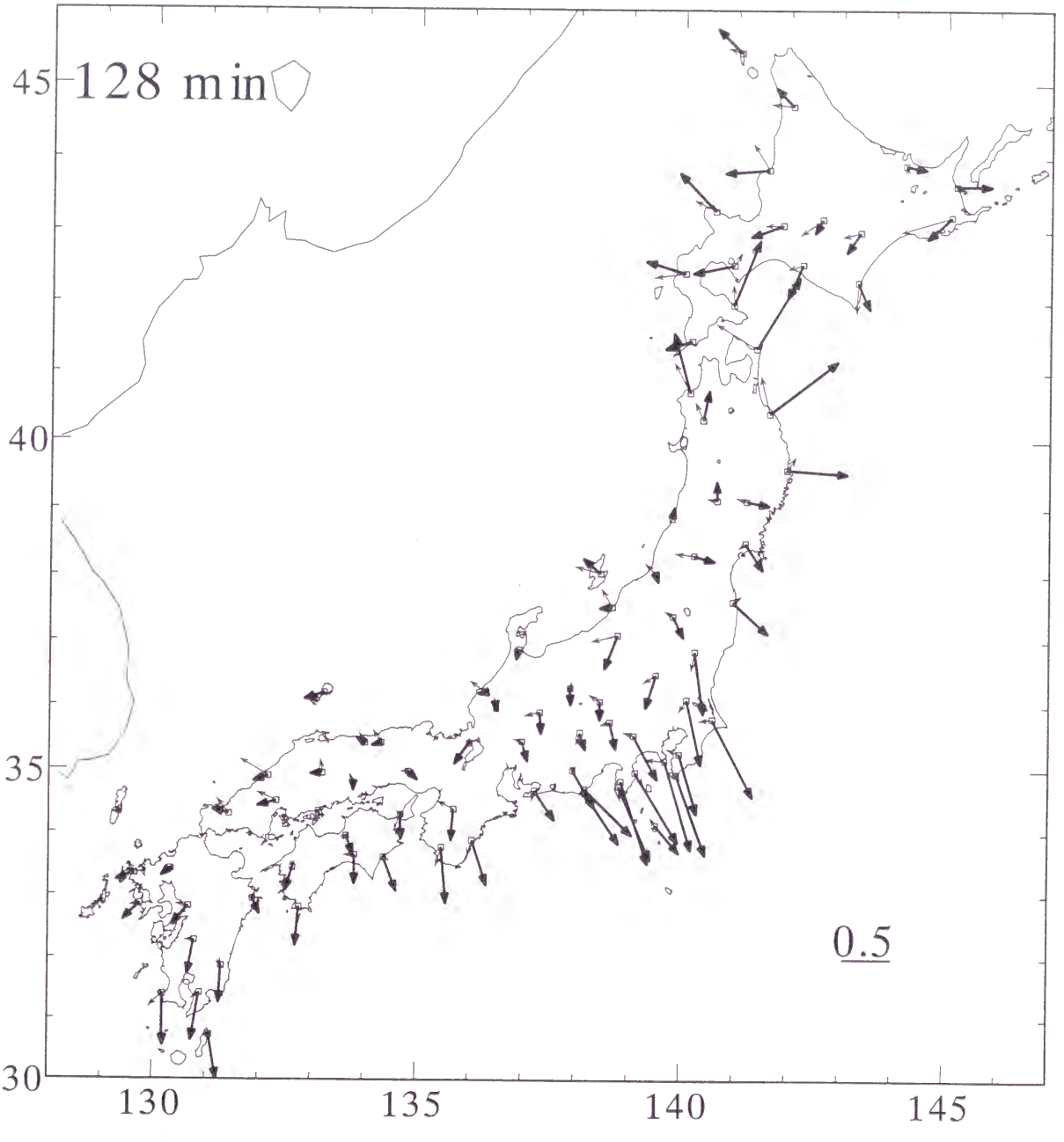

Figure 4-2 (a) Observed remote reference induction arrows. The thick line with a large arrowhead shows a real part and the thin line with a small arrowhead shows an imaginary part.

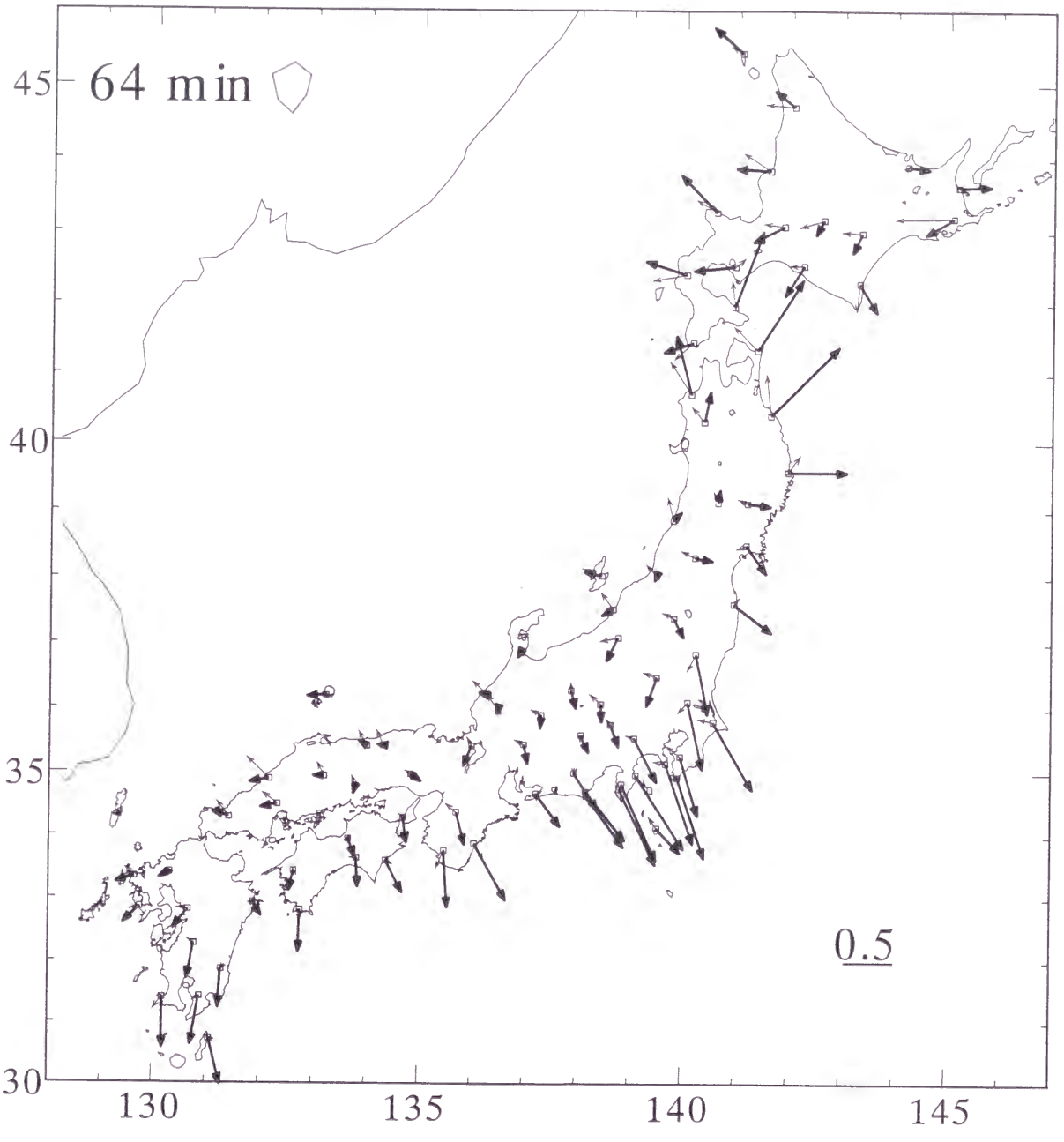

Figure 4-2 (b) Observed remote reference induction arrows. The thick line with a large arrowhead shows a real part and the thin line with a small arrowhead shows an imaginary part.

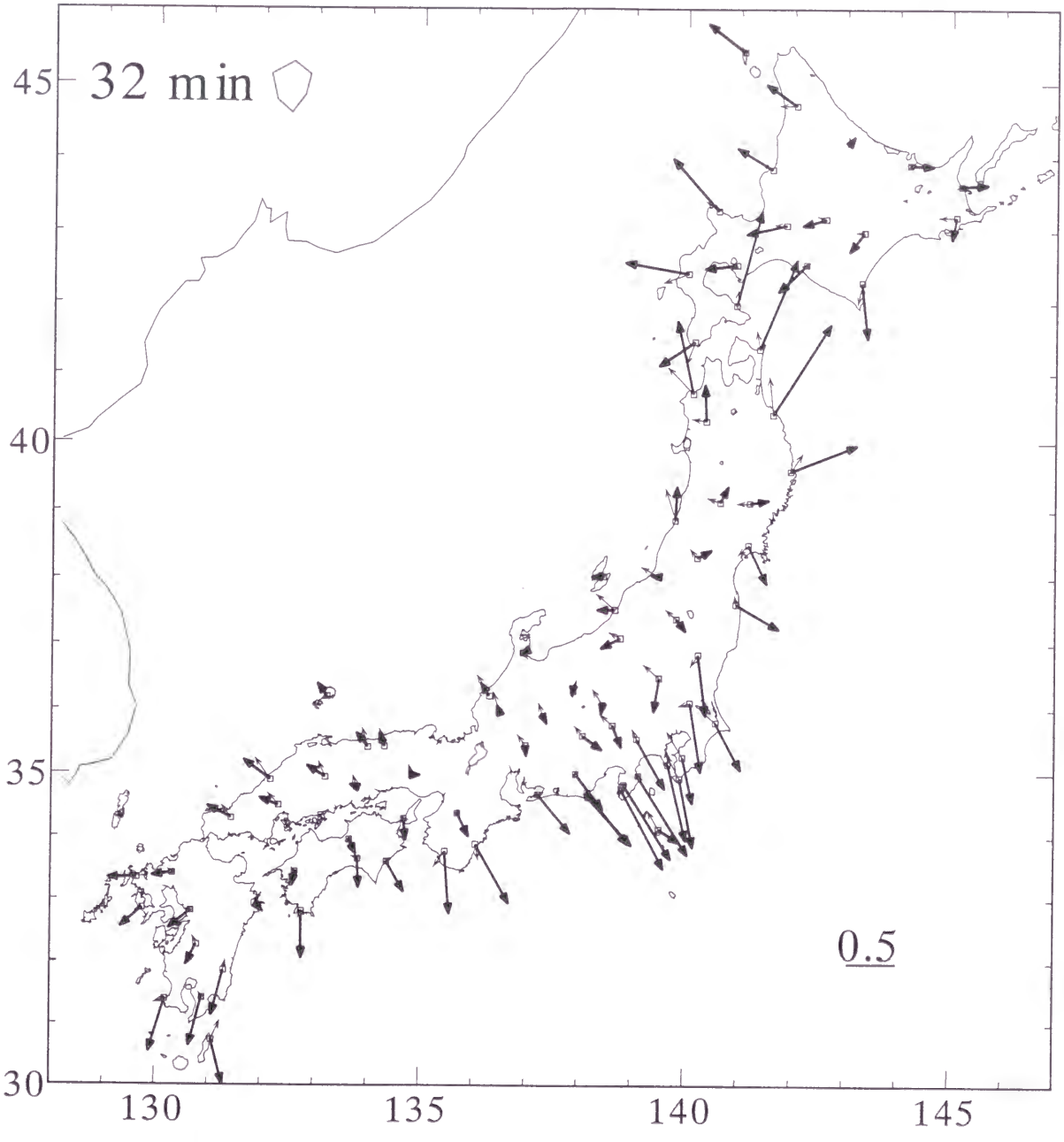

Figure 4-2 (c) Observed remote reference induction arrows. The thick line with a large arrowhead shows a real part and the thin line with a small arrowhead shows an imaginary part.

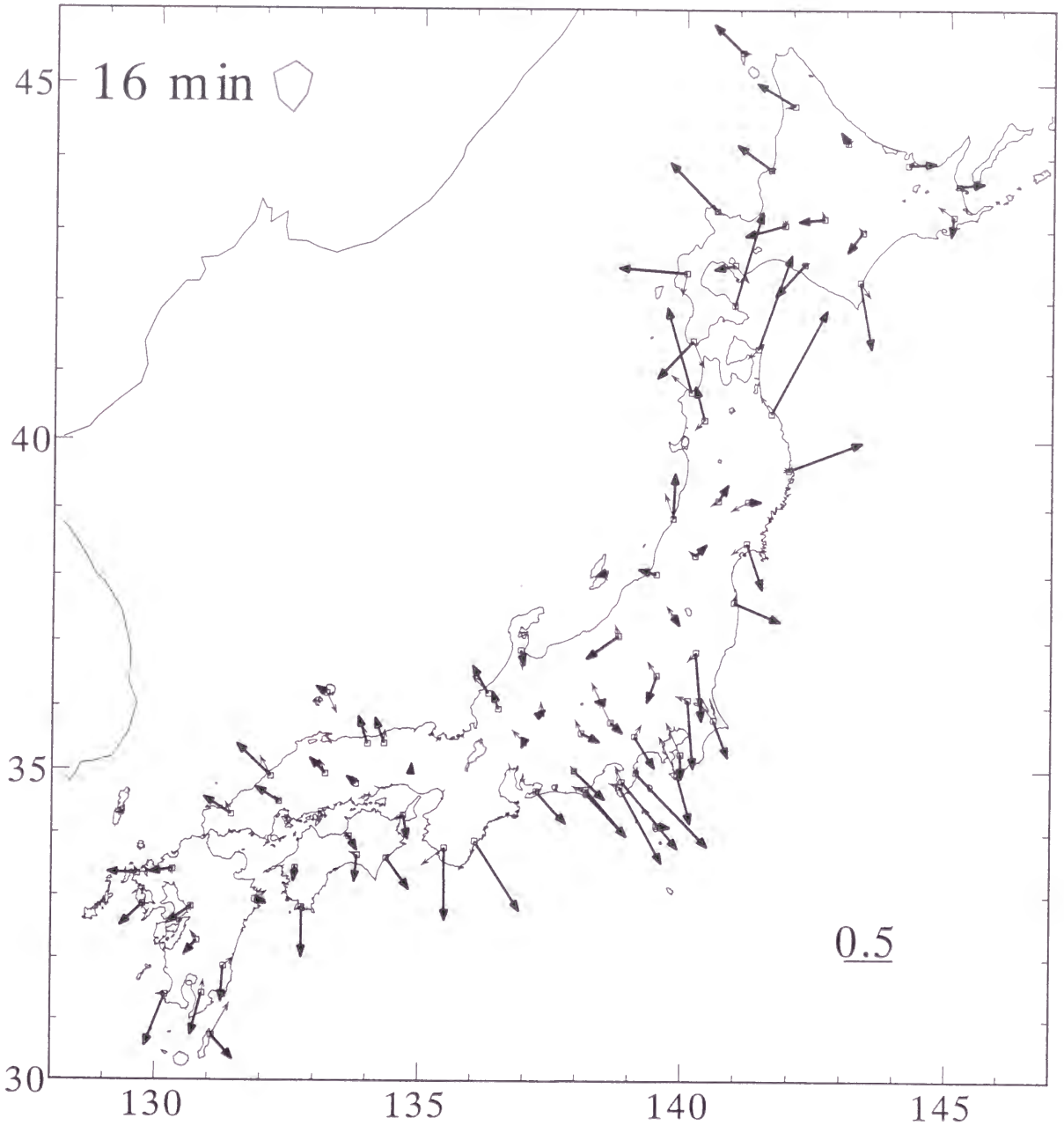

Figure 4-2 (d) Observed remote reference induction arrows. The thick line with a large arrowhead shows a real part and the thin line with a small arrowhead shows an imaginary part.

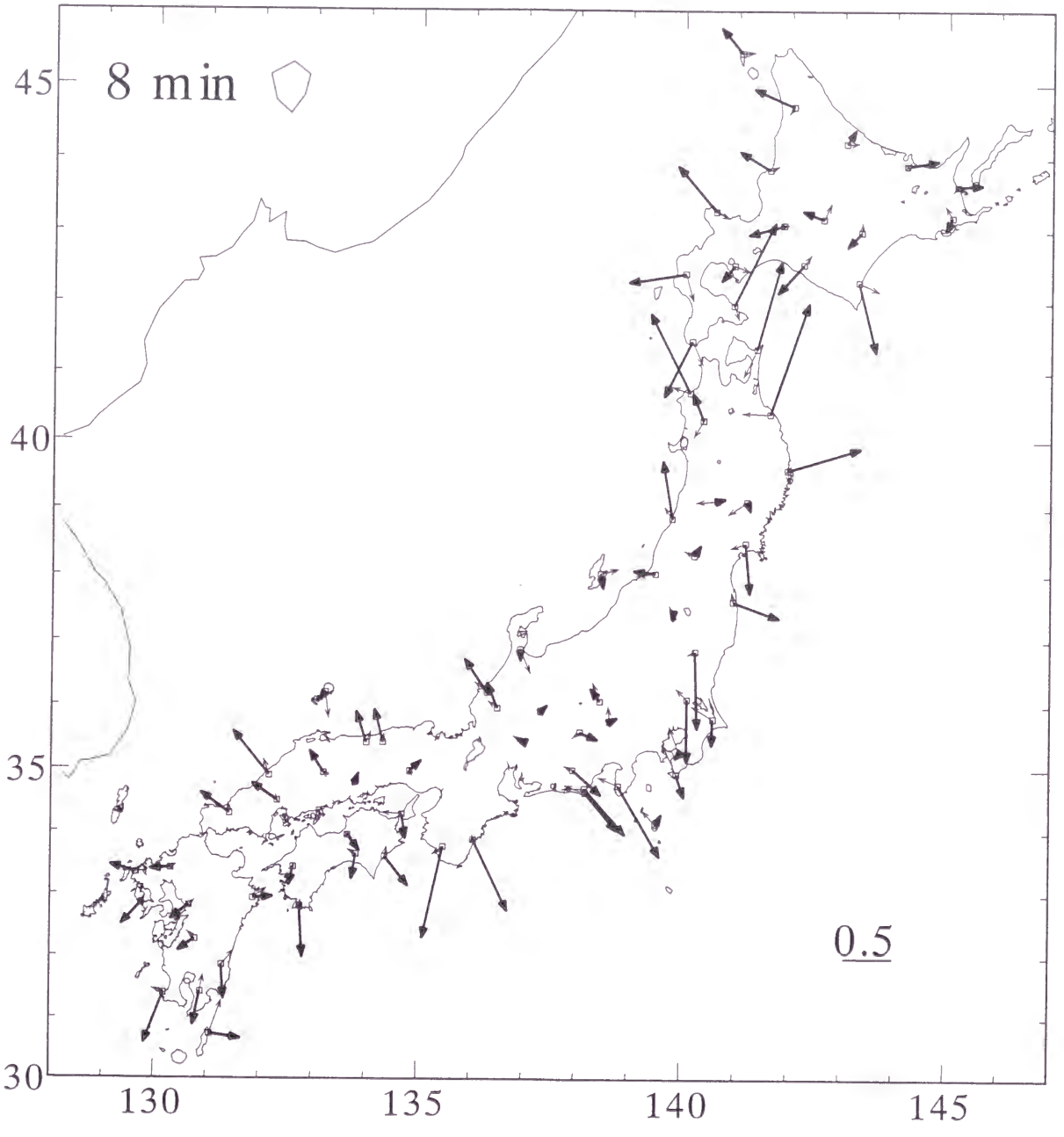

Figure 4-2 (e) Observed remote reference induction arrows. The thick line with a large arrowhead shows a real part and the thin line with a small arrowhead shows an imaginary part.

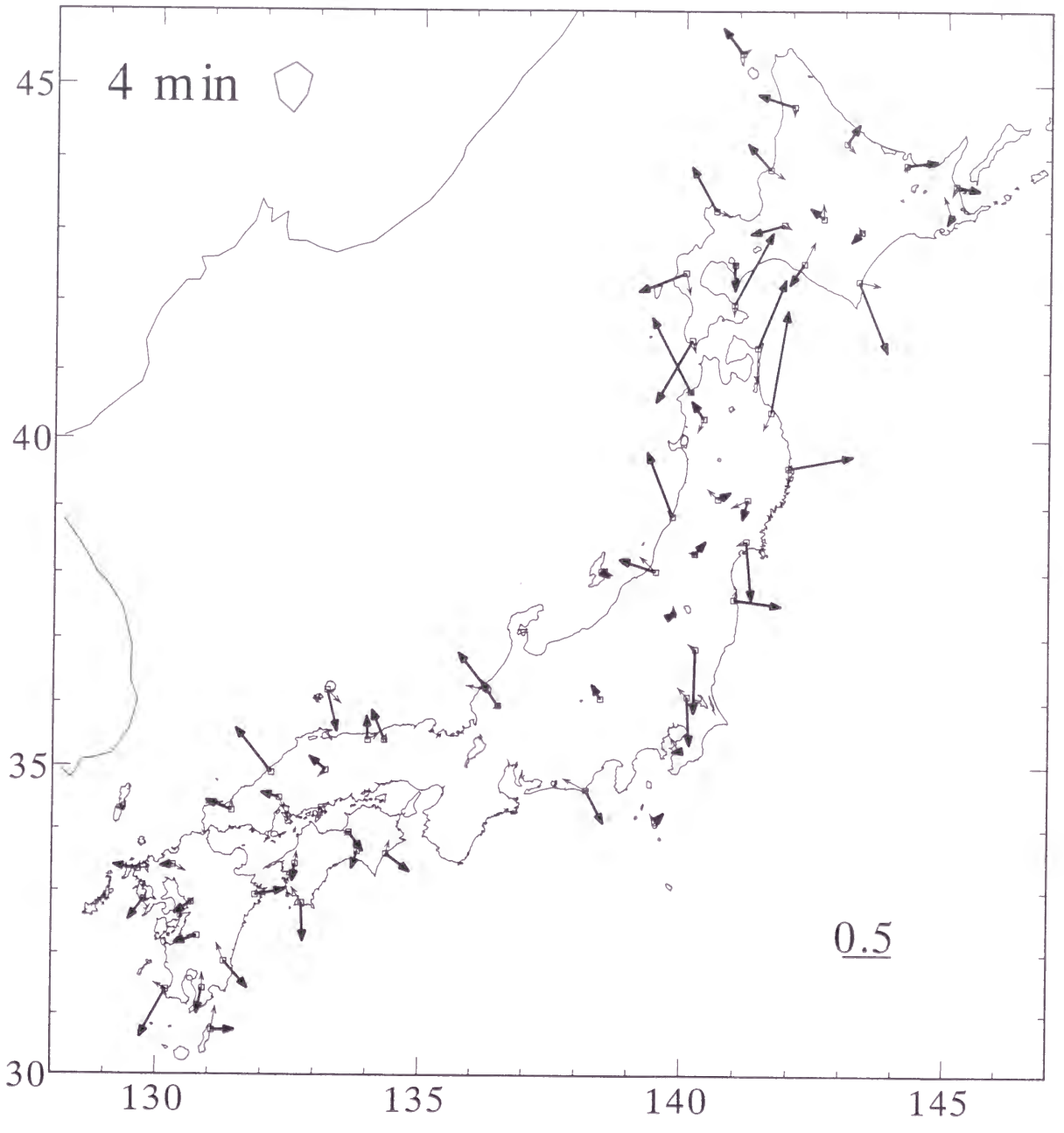

Figure 4-2 (f) Observed remote reference induction arrows. The thick line with a large arrowhead shows a real part and the thin line with a small arrowhead shows an imaginary part.

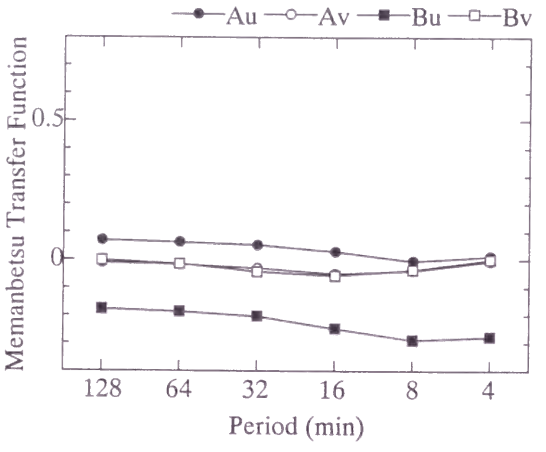

(a) Memanbetsu

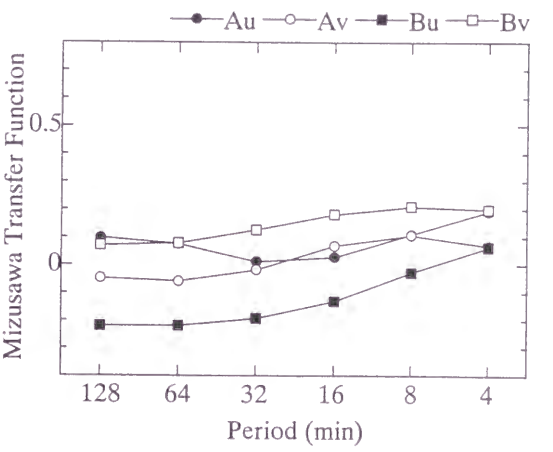

(b) Mizusawa

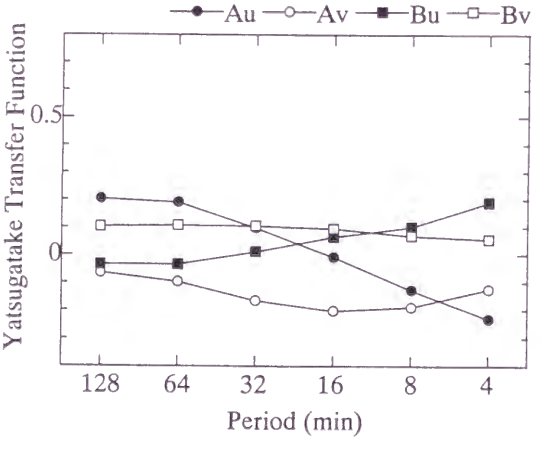

(c) Yatsugatake

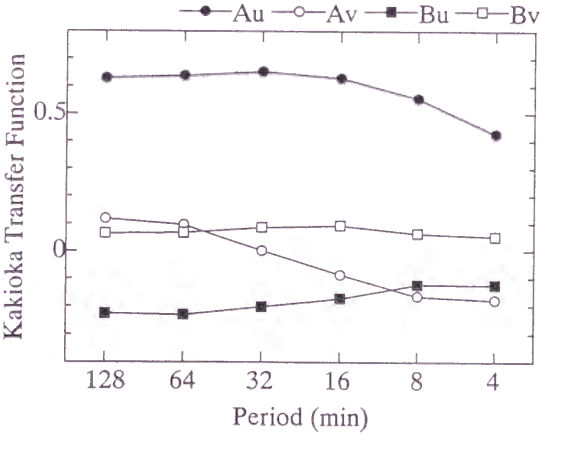

(d) Kakioka

Figure 4-3 (a)-(d) Frequency dependence of the transfer functions at observatories

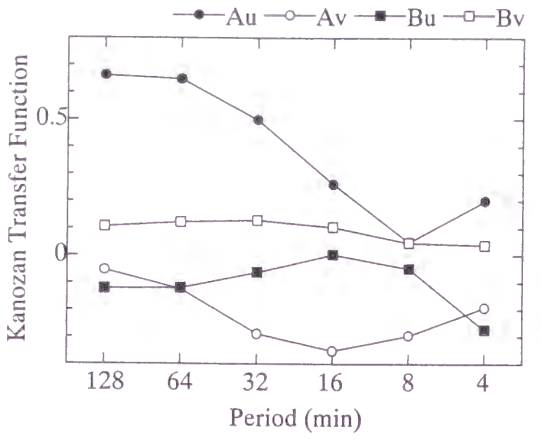

(e) Kanozan

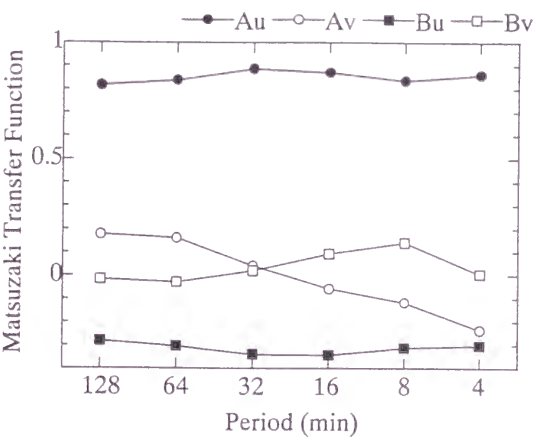

(f) Matsuzaki

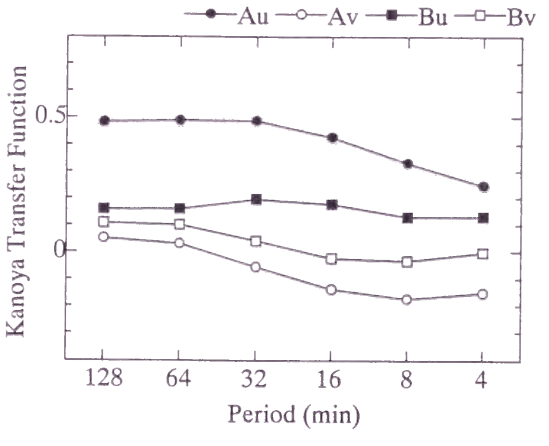

(g) Kanoya

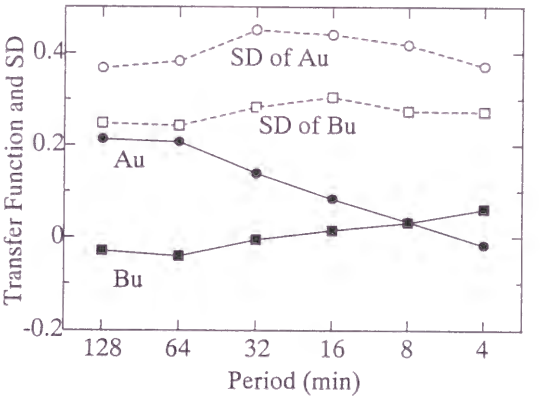

(h) Average of all stations and observatories

Figure 4-3 (e)-(g) Frequency dependence of the transfer functions at observatories
(h) Average frequency responce of the transfer function at all stations and observatories

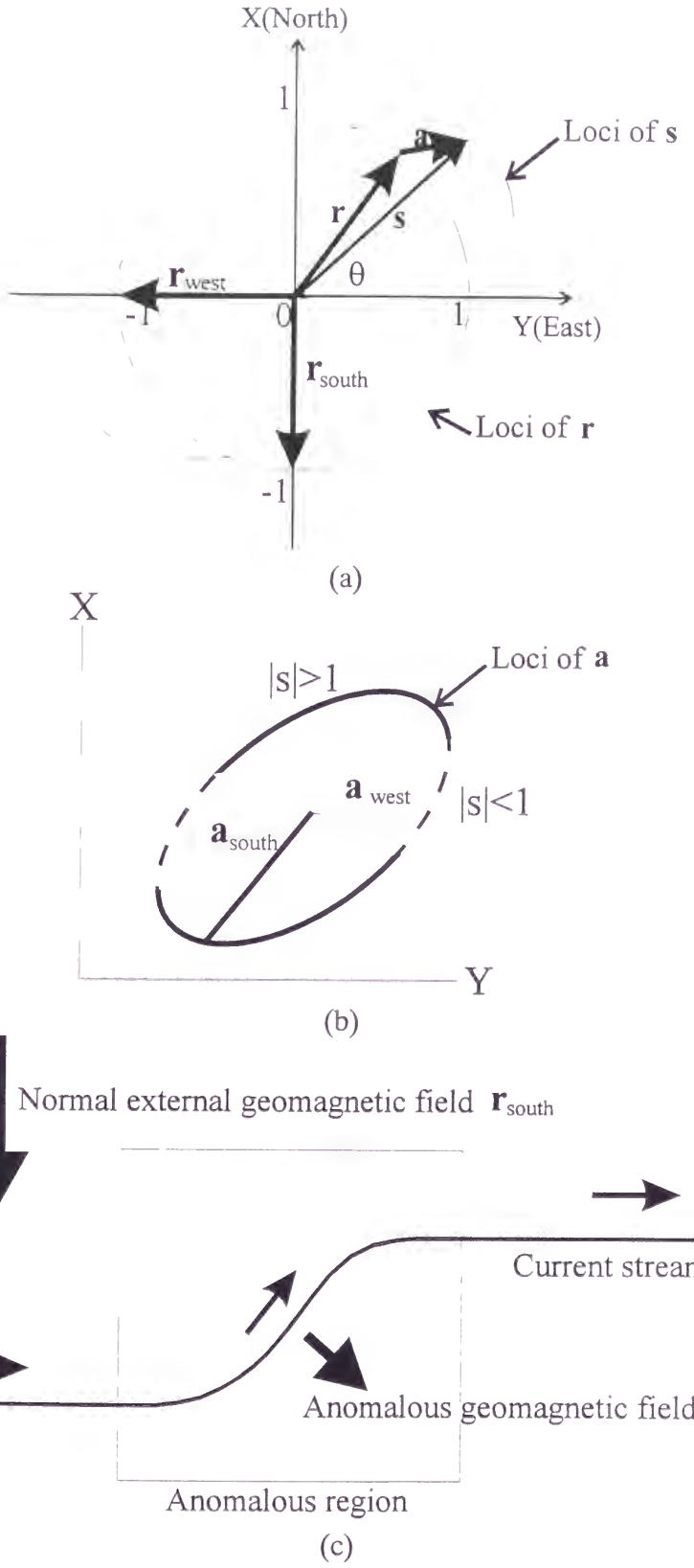

Figure 4-4 (a) Expression of horizontal transfer functions
(b) Anomalous ellipse of the horizontal transfer function
Thick line of the ellipse shows |s|>1 and broken line shows |s|<1.
(c) Schematic explanation of normal and anomalous field and current

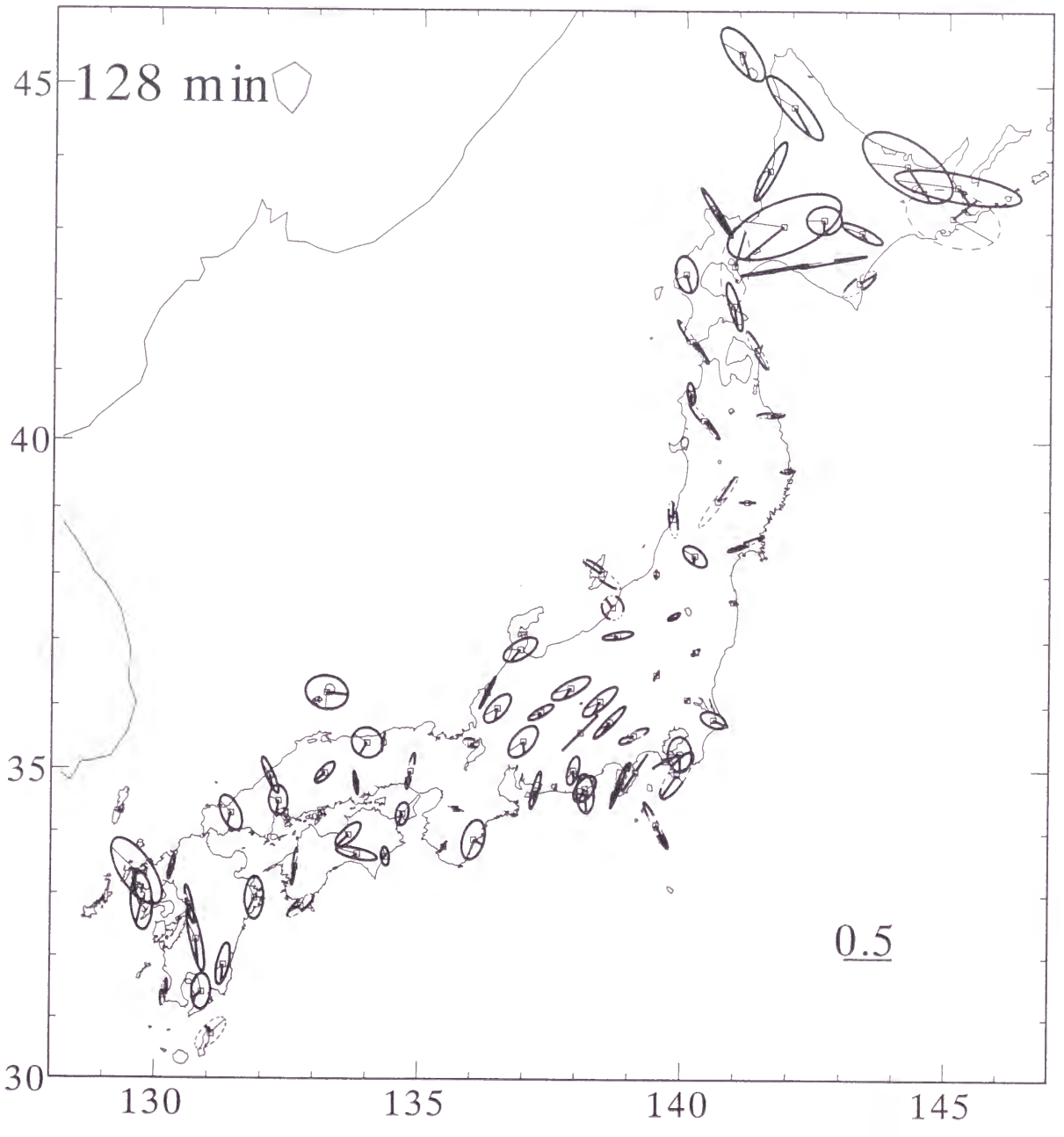

Figure 4-5 (a) Observed anomalous ellipses of horizontal transfer functions (real part)

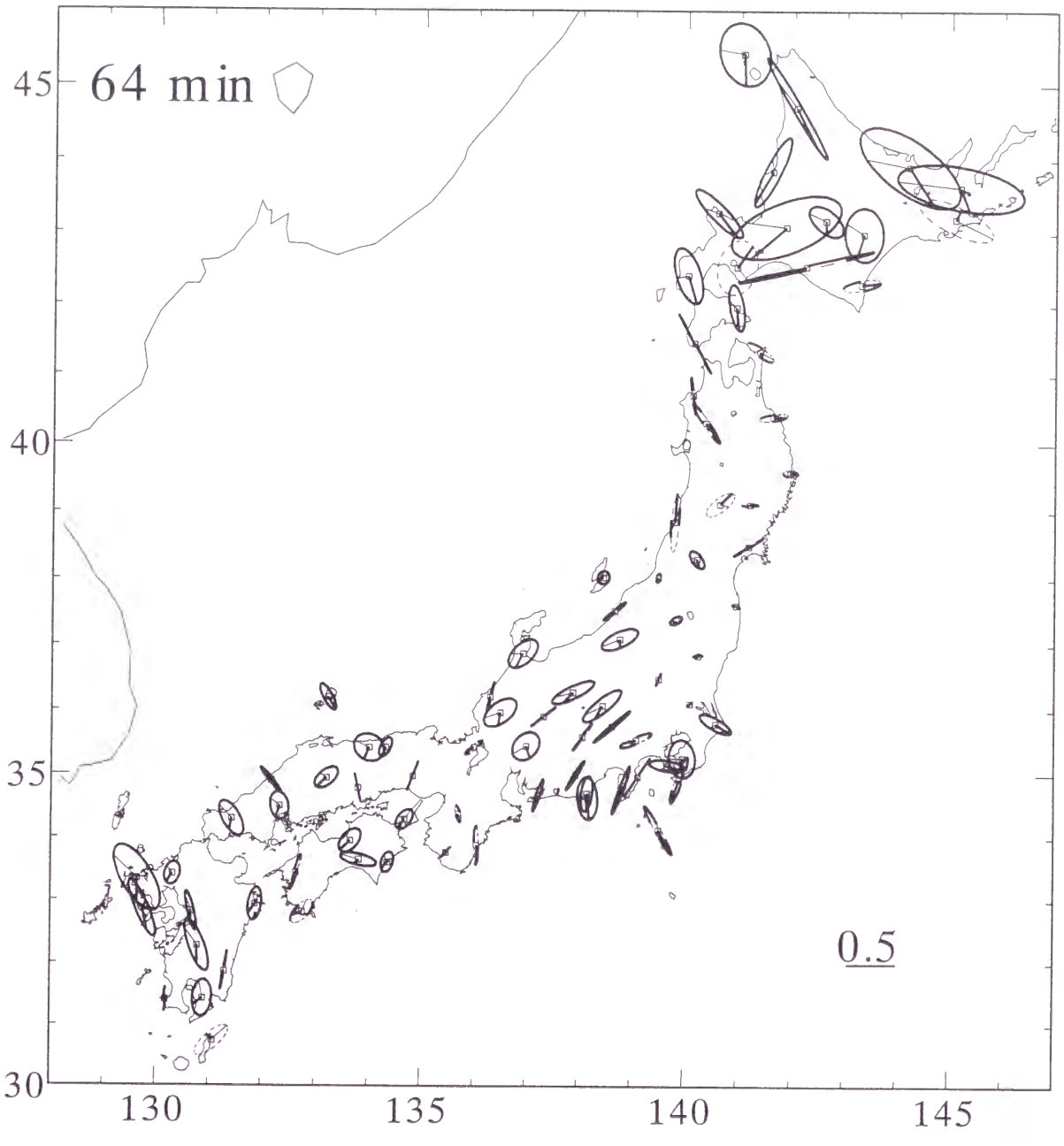

Figure 4-5 (b) Observed anomalous ellipses of horizontal transfer functions (real part)

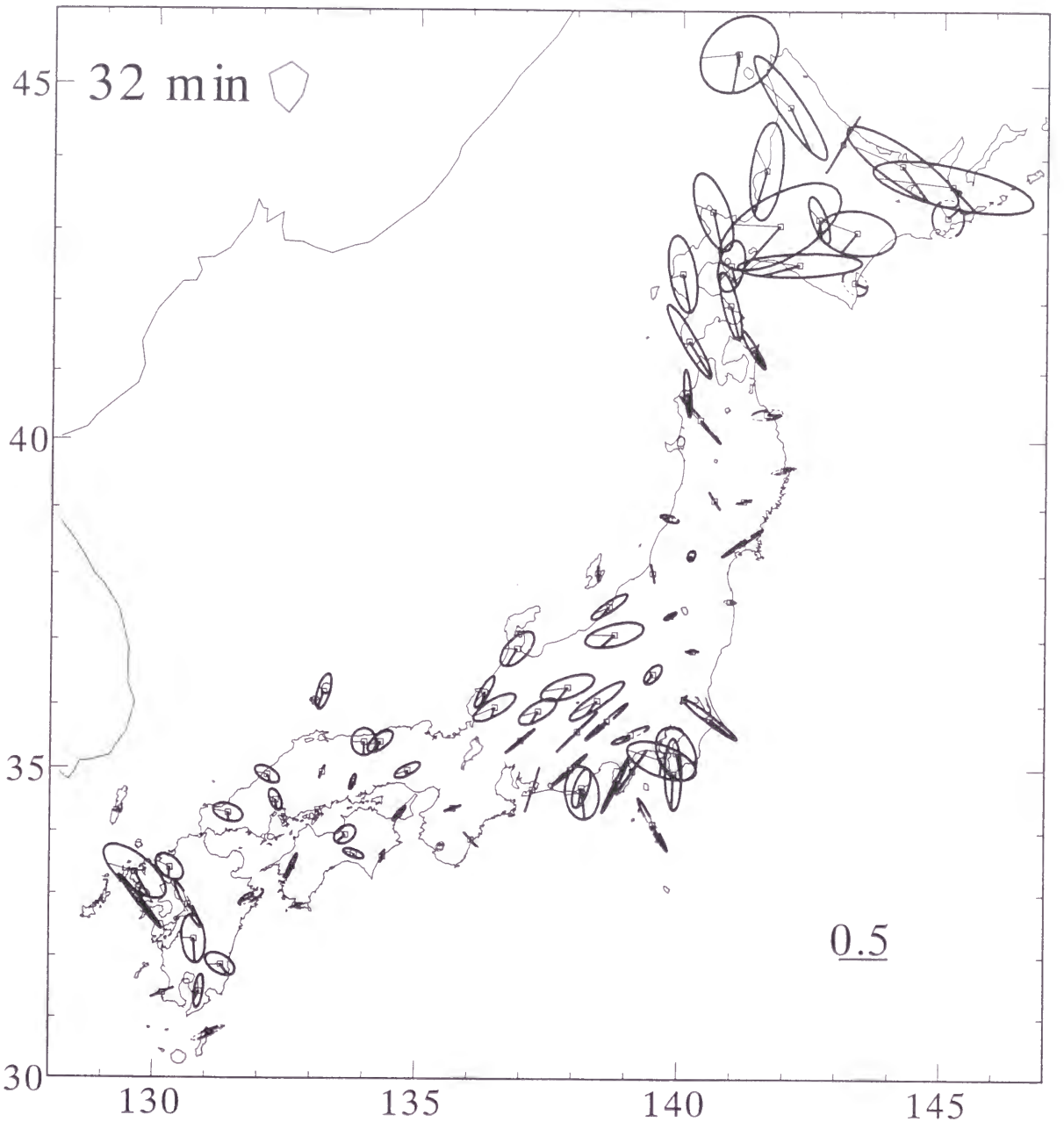

Figure 4-5 (c) Observed anomalous ellipses of horizontal transfer functions (real part)

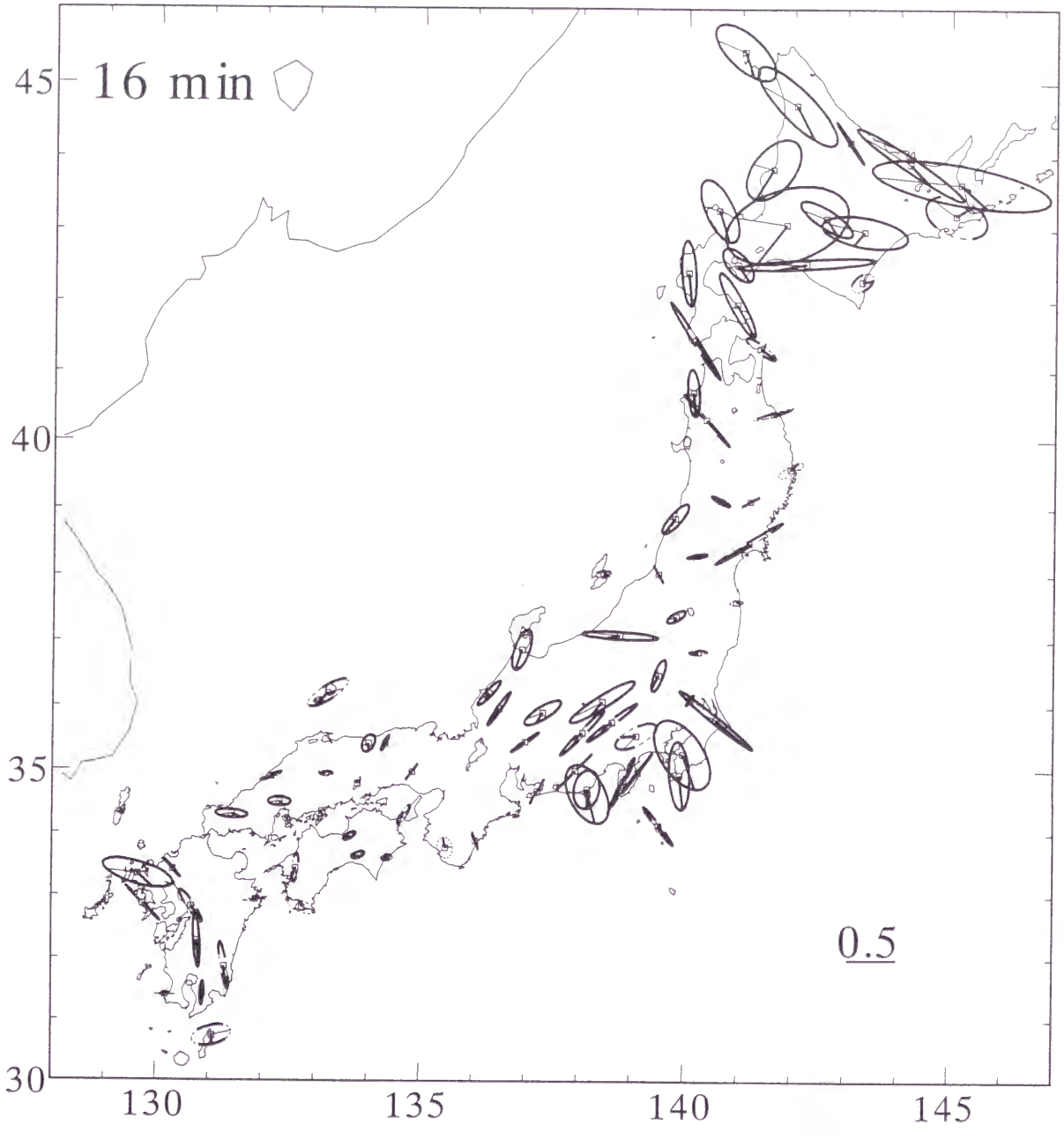

Figure 4-5 (d) Observed anomalous ellipses of horizontal transfer functions (real part)

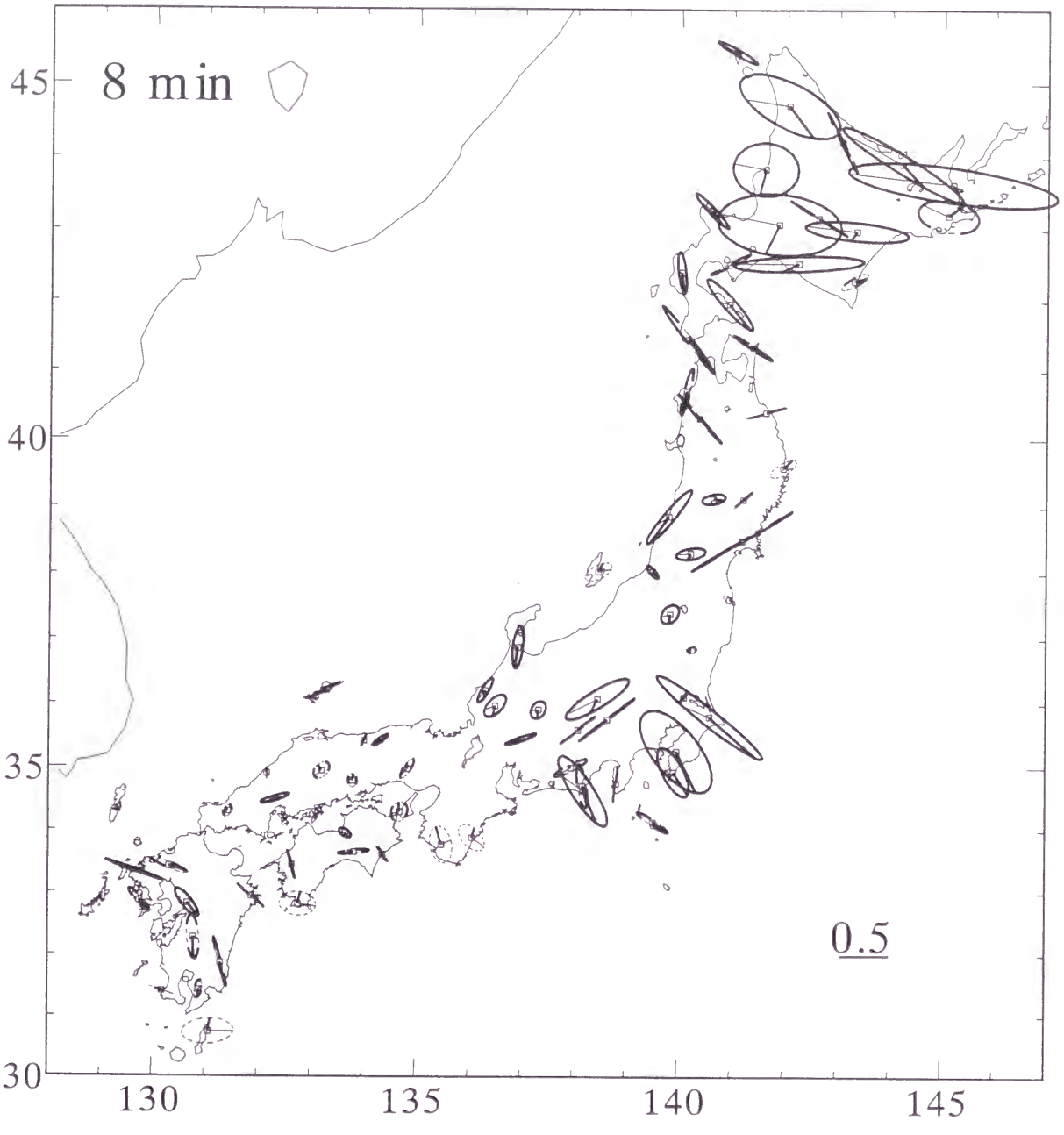

Figure 4-5 (e) Observed anomalous ellipses of horizontal transfer functions (real part)

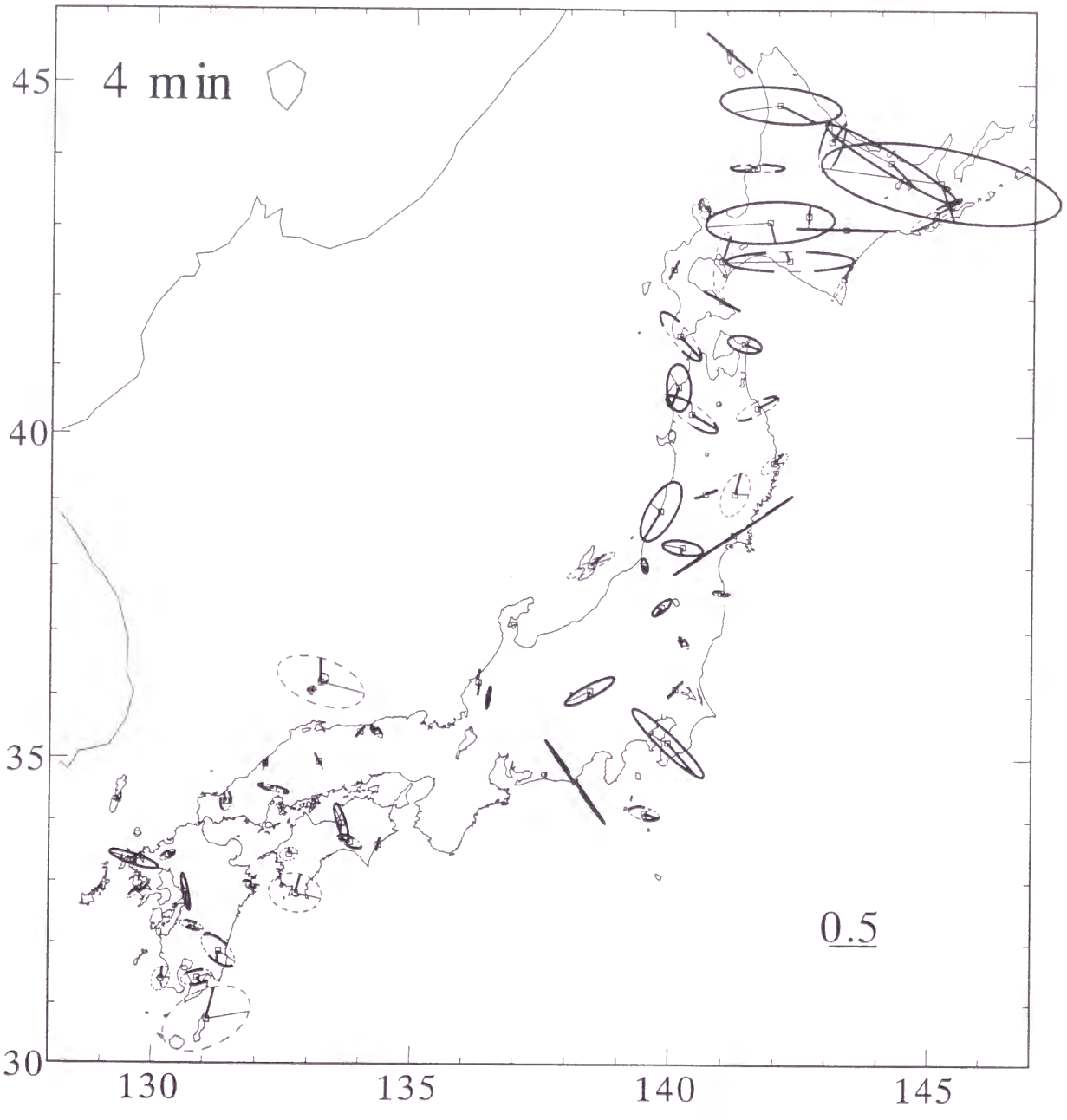

Figure 4-5 (f) Observed anomalous ellipses of horizontal transfer functions (real part)

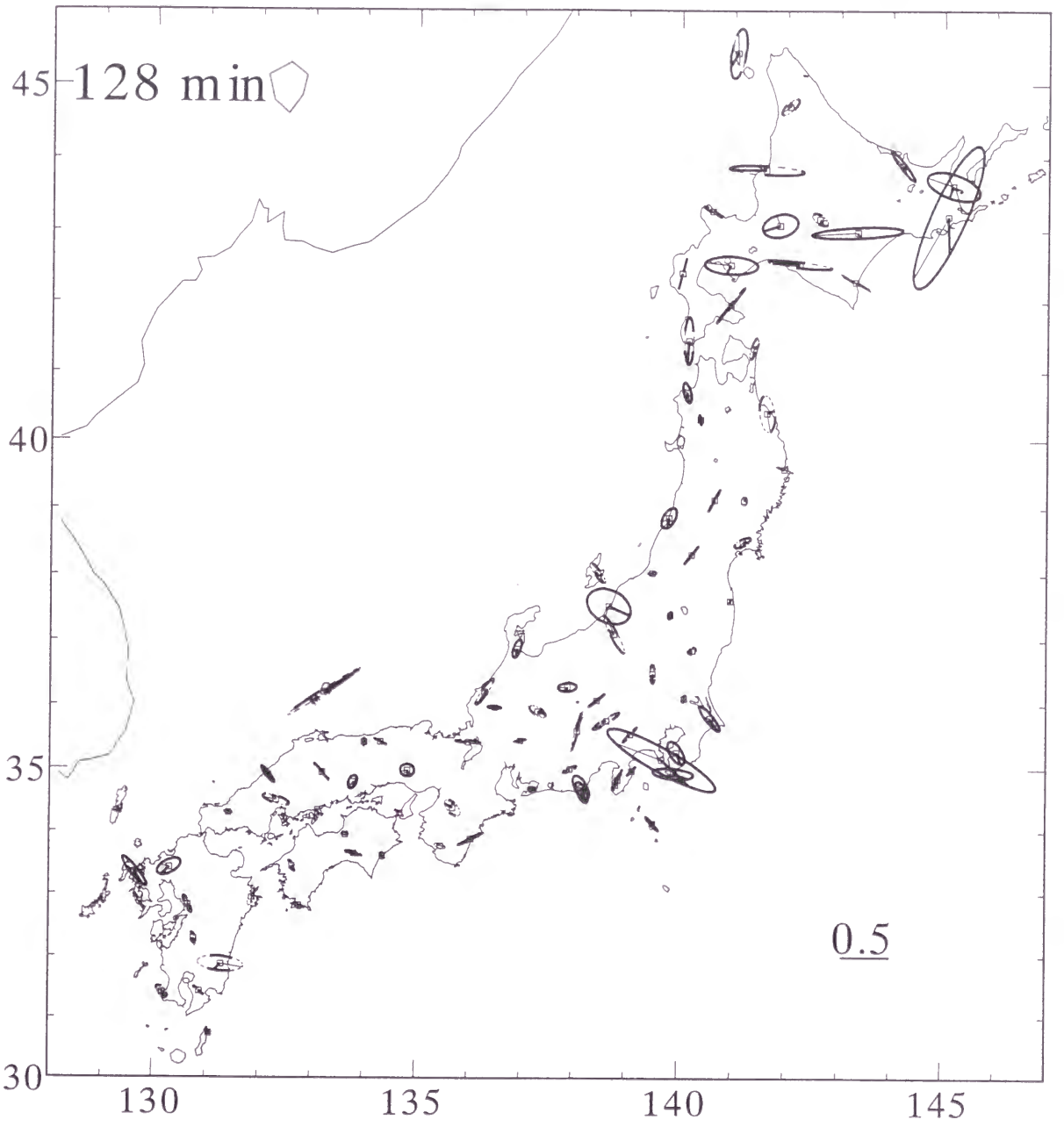

Figure 4-6 (a) Observed anomalous ellipses of horizontal transfer functions (imaginary part)

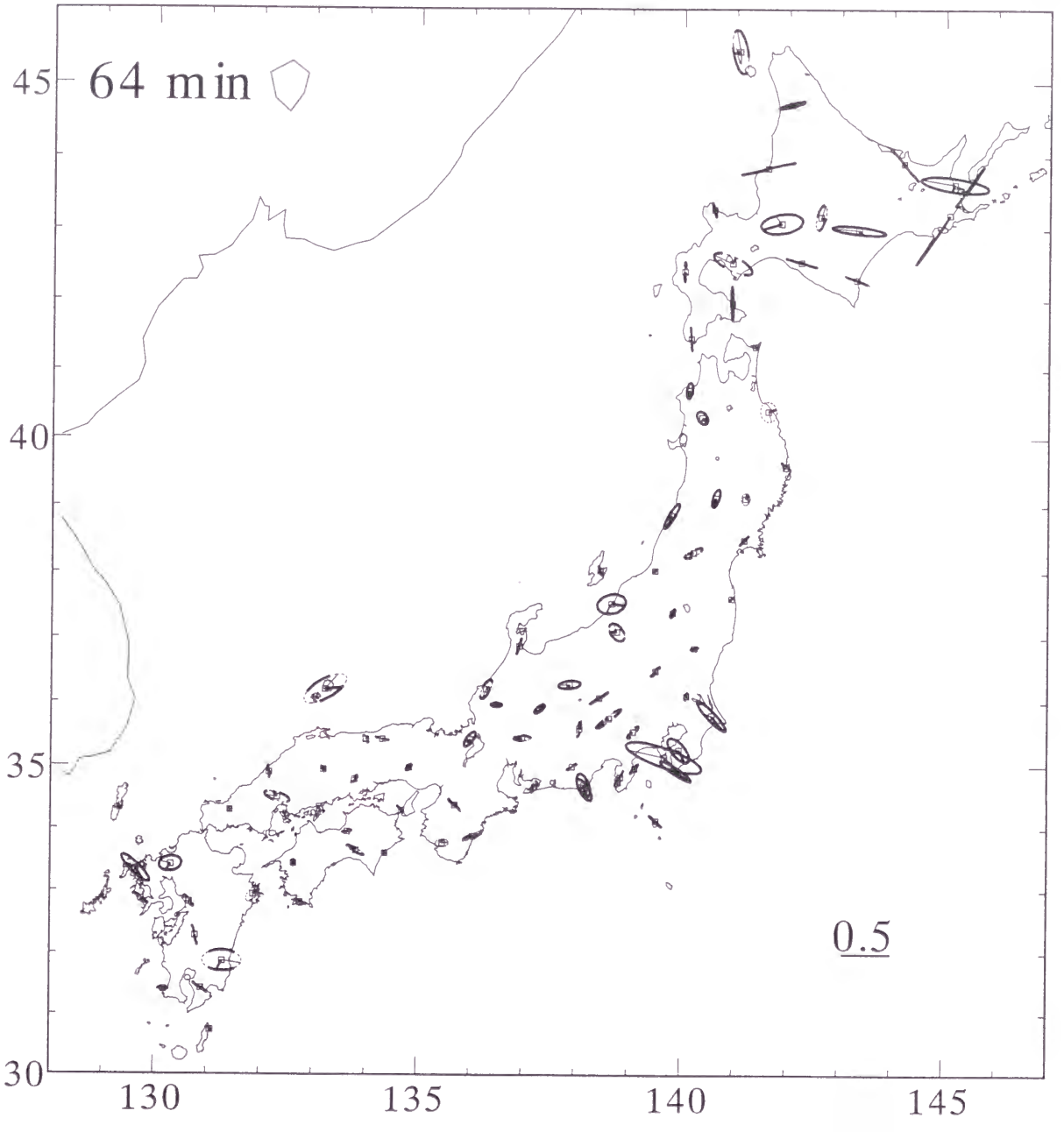

Figure 4-6 (b) Observed anomalous ellipses of horizontal transfer functions (imaginary part)

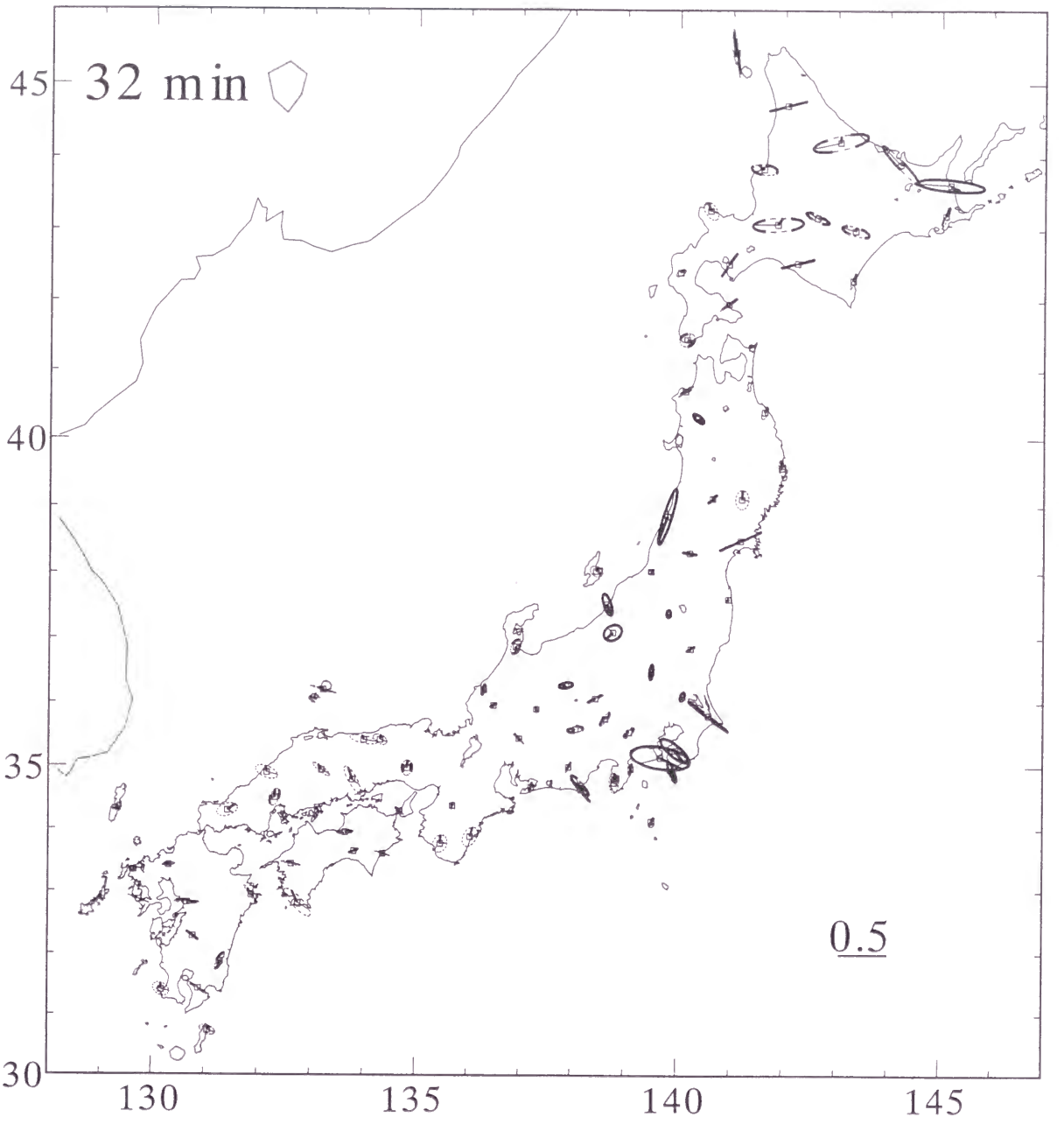

Figure 4-6 (c) Observed anomalous ellipses of horizontal transfer functions (imaginary part)

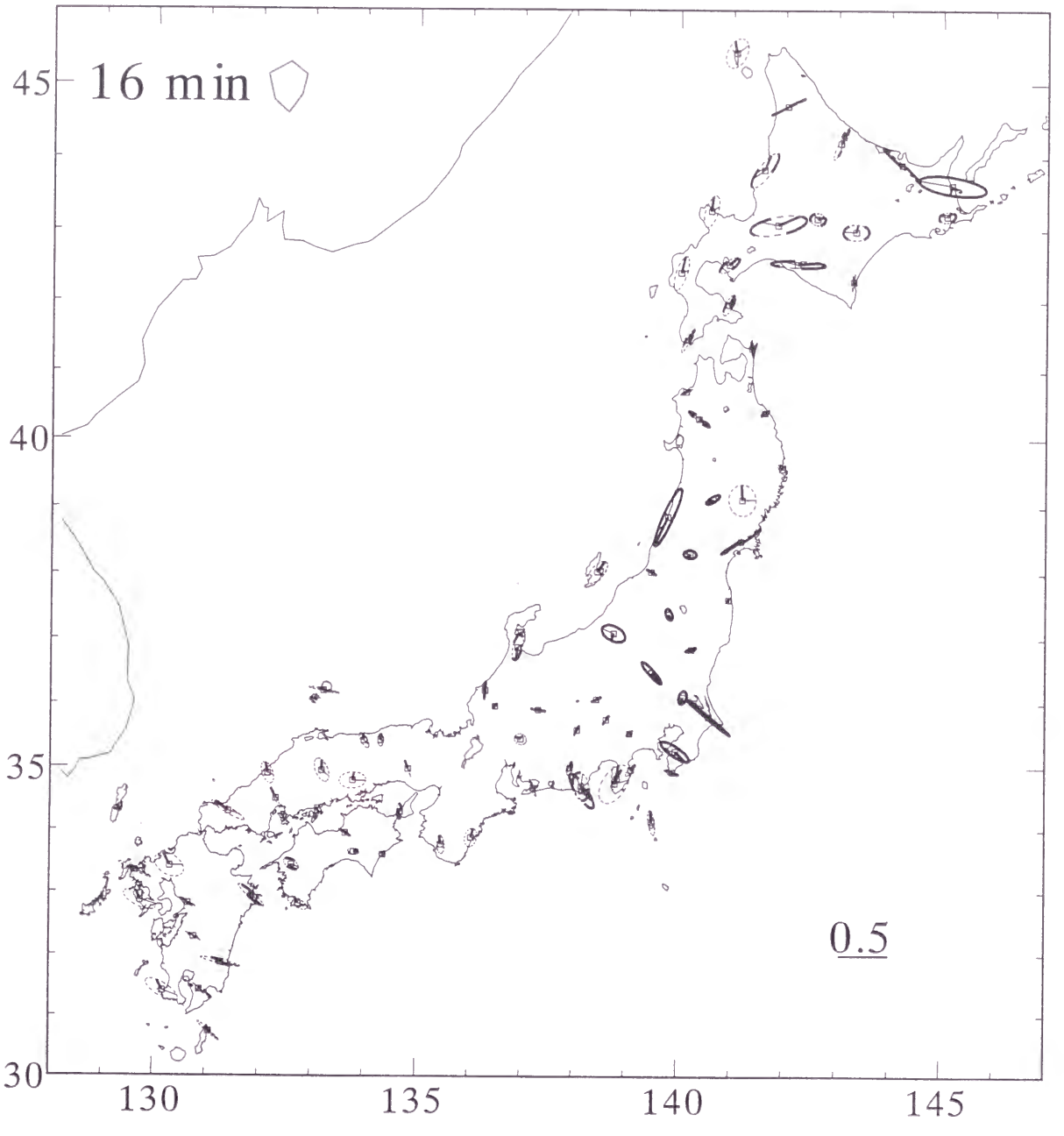

Figure 4-6 (d) Observed anomalous ellipses of horizontal transfer functions (imaginary part)

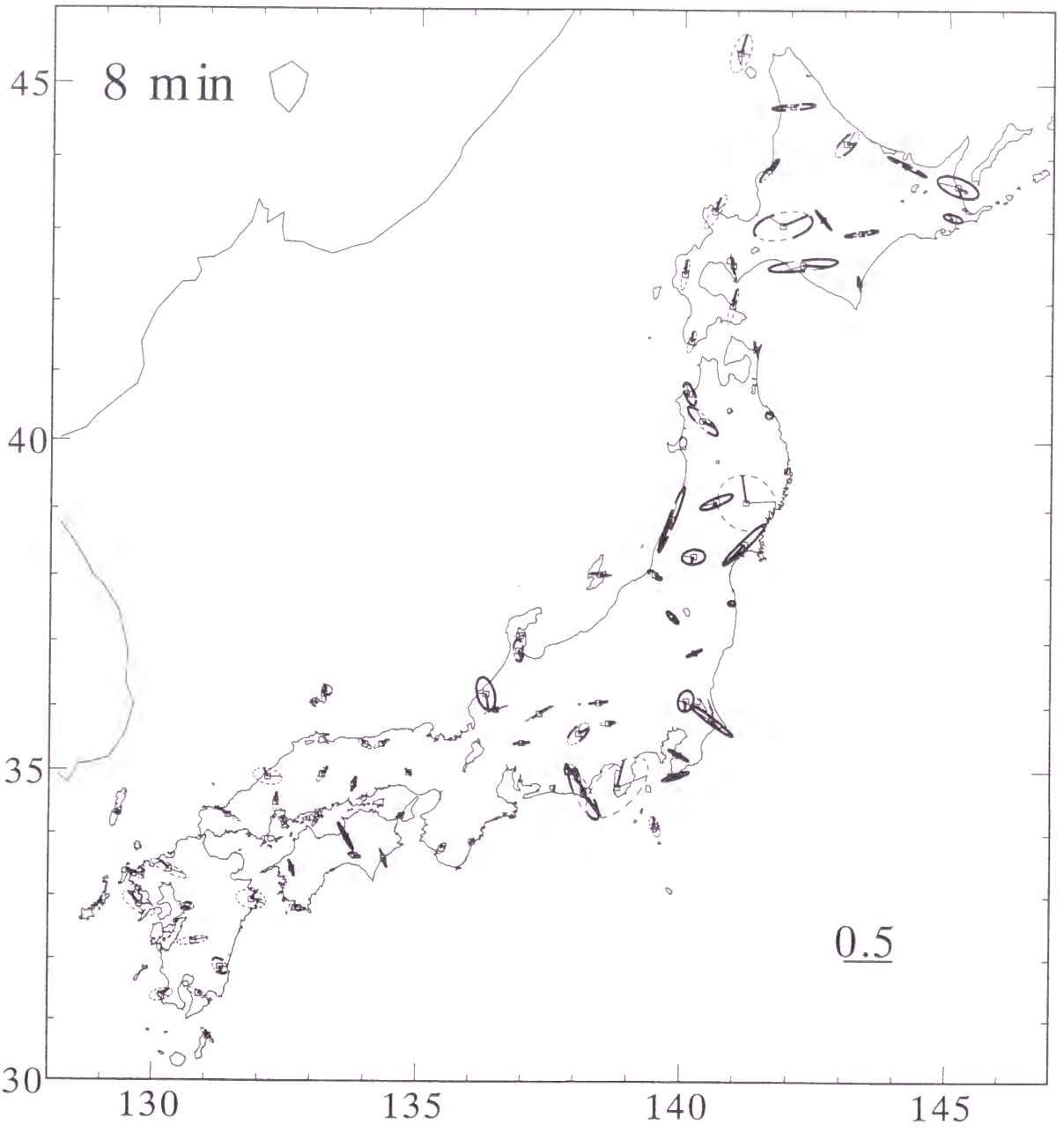

Figure 4-6 (e) Observed anomalous ellipses of horizontal transfer functions (imaginary part)

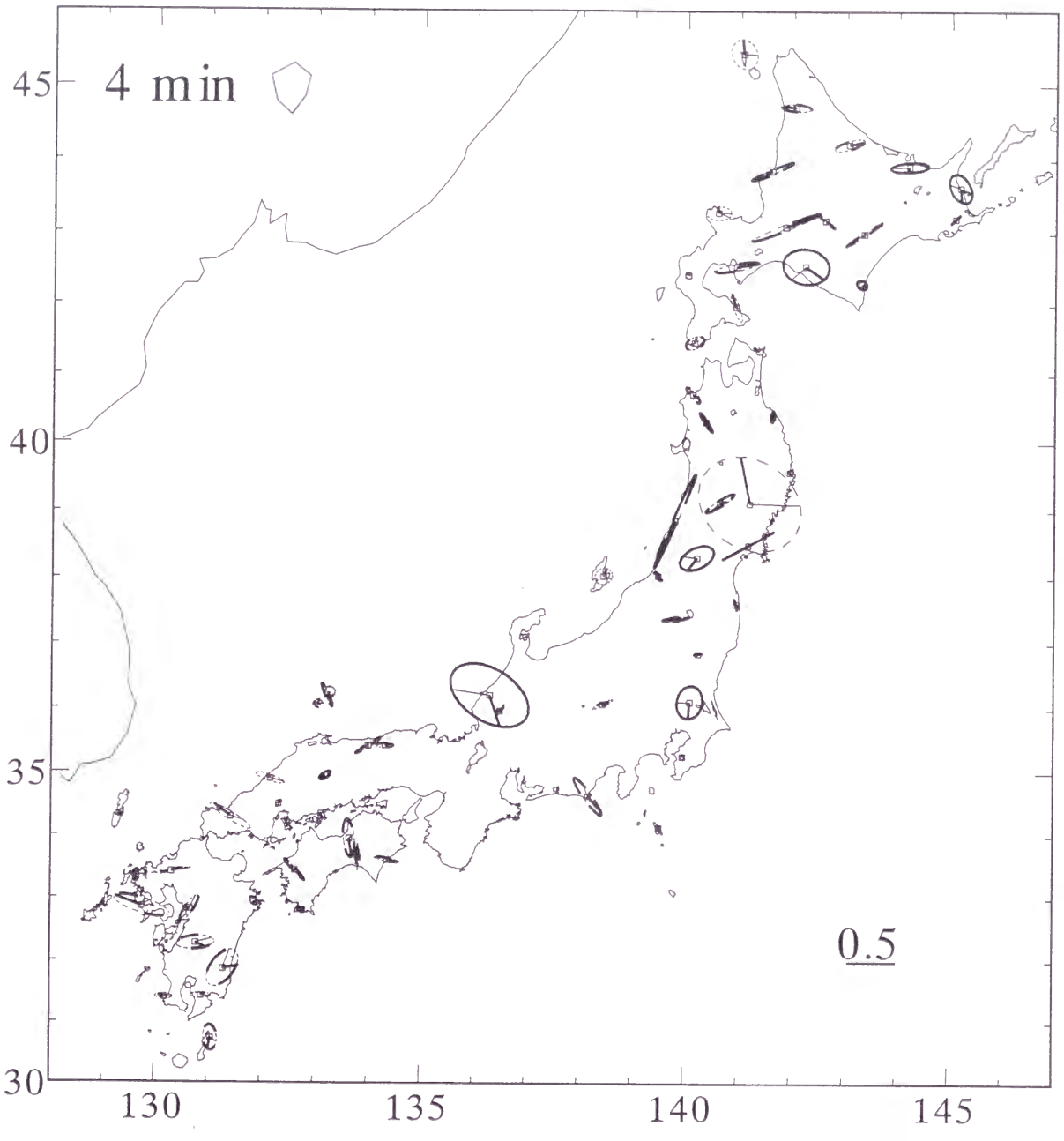

Figure 4-6 (f) Observed anomalous ellipses of horizontal transfer functions (imaginary part)

Table 4-1 Observed interstation geomagnetic transfer functions at the first order geomagnetic stations and geomagnetic observatories in Japan

128 min

	Lat ° '	Lon ° '	Cu	Cv	Du	Dv	ErrC	ErrD	Eu	Ev	Fu	Fv	ErrE	ErrF	Au	Av	Bu	Bv	ErrA	ErrB
1	31. 237	130. 108	. 979	. 054	−. 104	−. 083	. 053	. 053	. 033	−. 056	. 976	−. 015	. 171	. 021	. 560	. 197	−. 133	. 086	. 063	. 021
2	33. 250	130. 185	1. 124	. 086	−. 039	−. 015	. 089	. 092	. 037	. 083	1. 011	. 093	. 104	. 108	. 091	. 013	. 085	. 037	. 065	. 067
3	35. 246	133. 598	1. 133	. 000	−. 090	. 037	. 049	. 053	. 081	−. 016	1. 143	. 005	. 048	. 052	−. 054	−. 116	. 100	. 071	. 056	. 060
4	33. 566	133. 393	1. 122	. 003	−. 050	. 001	. 018	. 015	. 126	−. 017	1. 050	. 028	. 093	. 017	. 218	−. 015	−. 085	−. 020	. 017	. 017
5	35. 247	135. 594	1. 047	. 014	. 001	−. 002	. 119	. 107	−. 025	−. 097	. 913	. 090	. 174	. 157	. 229	−. 058	. 143	. 011	. 200	. 181
6	34. 593	137. 565	1. 105	. 004	. 104	. 035	. 022	. 027	−. 006	. 040	1. 076	. 038	. 072	. 032	. 465	−. 017	−. 171	. 070	. 052	. 033
7	36. 521	136. 552	1. 131	. 092	. 001	. 031	. 057	. 045	. 108	. 015	1. 144	. 047	. 049	. 038	. 117	. 076	. 025	. 066	. 086	. 068
8	38. 013	139. 289	1. 044	. 000	. 013	. 007	. 041	. 050	. 002	−. 034	. 994	. 016	. 035	. 042	. 092	−. 111	−. 029	. 102	. 075	. 091
12	45. 254	141. 027	1. 256	. 143	−. 125	−. 224	. 185	. 215	−. 079	. 087	1. 220	. 008	. 145	. 168	−. 345	−. 082	. 327	. 221	. 099	. 115
13	44. 420	142. 023	1. 301	−. 061	−. 157	. 059	. 086	. 091	−. 167	−. 007	1. 244	. 091	. 184	. 088	−. 289	−. 060	. 244	. 290	. 058	. 082
15	43. 504	141. 355	1. 306	−. 003	−. 061	−. 051	. 239	. 236	. 165	. 371	1. 046	. 131	. 338	. 333	. 060	−. 154	. 451	. 252	. 219	. 216
18	43. 162	140. 347	1. 240	. 055	−. 097	−. 002	. 080	. 081	−. 138	−. 088	1. 095	. 027	. 118	. 061	−. 526	−. 229	. 453	. 262	. 070	. 072
19	43. 046	141. 510	1. 346	. 056	−. 058	−. 111	. 070	. 091	. 421	. 182	1. 423	. 042	. 134	. 107	. 273	. 149	. 467	. 267	. 055	. 087
20	42. 592	143. 201	1. 086	. 056	−. 077	. 026	. 094	. 135	−. 058	−. 020	1. 210	. 487	. 170	. 129	. 223	. 045	. 070	. 300	. 086	. 103
22	42. 318	142. 139	1. 085	−. 019	. 061	−. 044	. 085	. 103	. 471	. 296	1. 456	. 155	. 157	. 122	. 414	. 165	. 231	. 237	. 055	. 077
23	42. 309	140. 558	. 628	. 091	. 219	−. 027	. 208	. 304	−. 103	. 051	. 885	. 276	. 128	. 187	. 027	−. 040	. 416	. 025	. 149	. 218
25	42. 242	140. 007	1. 185	. 093	. 053	. 125	. 052	. 057	−. 058	. 025	1. 104	. 031	. 070	. 040	−. 185	. 026	. 438	. 358	. 049	. 045
26	41. 574	140. 556	1. 232	. 185	−. 113	−. 015	. 044	. 040	−. 038	. 147	1. 080	. 002	. 117	. 030	−. 794	−. 424	−. 222	. 038	. 066	. 027
27	41. 199	141. 223	1. 005	−. 030	. 210	. 110	. 129	. 186	. 039	−. 038	. 881	. 027	. 102	. 148	−. 766	−. 206	−. 538	. 222	. 126	. 181
28	40. 237	141. 376	1. 008	−. 034	−. 026	. 193	. 070	. 053	−. 126	−. 075	. 907	−. 032	. 058	. 028	−. 478	−. 338	−. 553	. 011	. 073	. 047
29	40. 184	140. 223	1. 149	. 049	. 121	−. 015	. 044	. 050	−. 147	−. 006	. 935	. 012	. 122	. 035	−. 337	−. 236	−. 100	. 057	. 049	. 034
30	39. 345	141. 575	1. 002	−. 031	. 019	. 011	. 056	. 049	−. 078	. 073	. 996	−. 057	. 048	. 042	. 094	−. 173	−. 641	−. 053	. 120	. 105
32	39. 072	140. 386	. 728	. 055	−. 051	. 099	. 209	. 184	−. 183	. 025	. 906	. 056	. 111	. 098	−. 148	−. 047	. 009	. 067	. 221	. 195

Table 4-1 (continued.)

128 min

	Lat ° '	Lon ° '	Cu	Cv	Du	Dv	ErrC	ErrD	Eu	Ev	Fu	Fv	ErrE	ErrF	Au	Av	Bu	Bv	ErrA	ErrB
33	38. 293	141. 111	1. 056	−. 007	. 062	. 055	. 030	. 034	. 166	−. 071	1. 095	. 049	. 124	. 030	. 279	. 074	−. 191	. 082	. 044	. 030
34	38. 508	139. 476	. 816	. 100	−. 080	. 042	. 101	. 104	−. 001	. 012	1. 050	. 080	. 058	. 044	−. 084	−. 099	−. 013	−. 006	. 084	. 083
35	38. 180	140. 131	1. 087	. 062	−. 074	. 069	. 137	. 162	. 014	. 045	1. 126	. 056	. 082	. 097	. 058	−. 031	−. 258	. 204	. 166	. 196
36	37. 226	139. 495	1. 034	. 029	. 025	. 024	. 012	. 016	. 016	−. 006	1. 063	. 021	. 041	. 013	. 235	−. 046	−. 112	. 088	. 026	. 011
37	37. 307	138. 398	. 898	. 096	. 080	. 165	. 149	. 068	. 078	−. 226	1. 084	. 056	. 105	. 047	. 063	−. 189	. 165	. 108	. 313	. 141
39	37. 052	138. 463	1. 045	−. 056	. 011	−. 191	. 120	. 140	. 055	. 069	1. 153	. 089	. 191	. 223	. 363	. 070	. 148	. 251	. 202	. 236
40	36. 503	140. 145	1. 004	−. 006	. 033	. 033	. 024	. 034	. 032	. 037	1. 026	. 017	. 019	. 026	. 666	. 184	−. 080	. 066	. 096	. 135
41	36. 125	138. 552	1. 080	−. 007	. 087	. 033	. 110	. 162	. 187	. 056	. 942	. 122	. 106	. 157	−. 153	−. 025	. 486	. 173	. 184	. 273
42	35. 474	140. 352	1. 062	. 132	. 065	−. 022	. 049	. 080	−. 129	−. 087	1. 039	. 065	. 042	. 070	. 942	. 140	−. 397	. 095	. 119	. 196
45	35. 263	136. 588	1. 133	. 019	. 160	−. 087	. 106	. 094	−. 011	. 064	1. 203	. 041	. 094	. 084	. 198	−. 028	−. 111	. 173	. 128	. 114
47	33. 456	135. 283	1. 025	−. 029	−. 057	. 011	. 021	. 026	. 010	. 013	. 953	−. 060	. 027	. 033	. 615	. 177	−. 082	. 054	. 037	. 044
48	34. 223	135. 422	1. 007	−. 048	. 030	−. 074	. 084	. 069	. 010	. 085	. 911	. 007	. 067	. 055	. 321	−. 099	. 028	. 124	. 147	. 122
50	38. 009	138. 272	. 864	. 008	−. 084	. 110	. 109	. 075	. 201	. 034	1. 024	−. 078	. 111	. 077	−. 110	−. 007	. 231	. 242	. 106	. 073
51	35. 446	138. 377	1. 135	. 006	. 109	. 091	. 044	. 047	. 089	. 054	1. 142	. 128	. 046	. 049	. 314	. 037	−. 060	. 123	. 115	. 123
53	35. 540	137. 192	1. 060	. 025	. 059	. 059	. 075	. 084	. 026	−. 083	1. 131	−. 031	. 084	. 094	. 254	. 046	−. 001	. 189	. 097	. 108
55	36. 117	136. 181	1. 152	−. 008	. 073	. 152	. 045	. 079	. 072	−. 043	1. 070	. 083	. 071	. 124	. 096	−. 163	. 004	. 227	. 065	. 114
57	34. 579	134. 497	1. 147	. 065	. 124	. 014	. 054	. 056	. 050	−. 018	1. 003	. 073	. 092	. 095	. 104	. 009	−. 088	. 060	. 093	. 096
58	35. 248	134. 187	1. 098	. 021	. 015	−. 013	. 027	. 035	. 017	−. 068	1. 037	−. 019	. 135	. 045	. 053	−. 145	. 097	. 078	. 029	. 032
59	34. 467	133. 474	1. 095	. 017	−. 080	. 069	. 060	. 059	−. 003	−. 040	1. 026	. 029	. 074	. 073	. 090	−. 098	−. 001	. 050	. 059	. 059
61	34. 536	132. 101	1. 146	. 045	−. 127	−. 076	. 049	. 070	−. 031	−. 009	1. 087	. 070	. 065	. 092	. 071	−. 205	. 126	. 346	. 090	. 128
62	34. 296	132. 194	1. 157	−. 051	−. 041	−. 028	. 035	. 051	. 021	. 039	1. 097	. 135	. 042	. 062	. 051	−. 095	. 184	. 244	. 049	. 072
63	34. 174	131. 253	1. 113	. 002	−. 158	−. 009	. 026	. 027	. 036	. 026	1. 118	. 027	. 065	. 043	−. 086	−. 175	. 198	. 159	. 034	. 037
64	32. 513	129. 451	1. 242	. 085	−. 182	−. 004	. 027	. 029	. 056	−. 055	1. 100	−. 008	. 090	. 036	. 237	. 040	. 168	. 104	. 021	. 026

Table 4-1 (continued.)

128 min

	Lat ° '	Lon ° '	Cu	Cv	Du	Dv	ErrC	ErrD	Eu	Ev	Fu	Fv	ErrE	ErrF	Au	Av	Bu	Bv	ErrA	ErrB
65	32. 490	130. 396	1. 134	. 068	−. 176	−. 031	. 058	. 091	. 001	−. 047	1. 155	. 007	. 092	. 143	. 217	−. 010	. 178	. 134	. 046	. 072
66	32. 156	130. 466	1. 281	. 047	−. 191	. 037	. 108	. 118	−. 027	. 003	1. 092	−. 030	. 148	. 163	. 450	. 015	. 012	. 107	. 092	. 101
67	31. 516	131. 176	1. 204	. 071	. 077	. 040	. 069	. 085	. 015	. 064	1. 073	−. 233	. 098	. 120	. 476	. 039	. 052	. 006	. 084	. 103
68	32. 557	131. 525	1. 166	−. 064	−. 156	. 063	. 078	. 051	. 070	−. 041	1. 070	−. 002	. 073	. 047	. 183	. 030	−. 108	−. 009	. 044	. 029
70	33. 263	132. 382	1. 182	. 050	−. 070	. 023	. 055	. 060	. 018	−. 015	. 973	−. 031	. 044	. 049	. 290	. 024	. 055	. 003	. 043	. 047
71	33. 385	133. 488	1. 043	−. 014	−. 058	−. 021	. 060	. 067	. 059	. 090	1. 210	. 019	. 052	. 059	. 314	. 004	−. 018	. 124	. 055	. 061
72	32. 484	132. 456	1. 122	−. 028	−. 175	−. 011	. 088	. 143	. 130	. 063	. 883	−. 115	. 099	. 160	. 463	. 158	−. 008	. 006	. 084	. 136
73	33. 359	134. 220	1. 033	. 017	−. 096	−. 027	. 046	. 061	. 038	. 005	1. 023	. 006	. 044	. 059	. 367	. 033	−. 174	−. 067	. 046	. 061
74	34. 172	134. 408	1. 120	−. 038	−. 045	−. 008	. 064	. 068	. 042	. 045	1. 057	−. 017	. 074	. 079	. 292	−. 045	−. 020	. 035	. 070	. 074
76	43. 098	142. 364	1. 149	. 065	. 000	. 010	. 271	. 161	. 005	−. 039	1. 182	−. 073	. 136	. 081	. 167	. 193	. 114	. 268	. 200	. 119
78	43. 380	145. 102	1. 170	. 116	−. 081	−. 100	. 153	. 127	−. 133	. 050	1. 674	. 280	. 136	. 113	. 054	−. 043	−. 632	−. 067	. 092	. 076
80	41. 267	140. 086	1. 188	. 246	. 129	. 058	. 070	. 085	−. 155	. 014	. 936	−. 046	. 086	. 070	. 022	. 181	. 271	. 201	. 072	. 076
81	40. 418	140. 069	1. 113	. 105	−. 035	−. 023	. 137	. 205	−. 002	−. 014	1. 041	. 043	. 114	. 170	−. 666	−. 419	. 187	. 205	. 120	. 179
85	30. 440	131. 040	. 921	. 001	−. 151	−. 024	. 048	. 075	. 054	. 016	. 849	. 015	. 075	. 118	. 431	. 012	−. 141	. 029	. 055	. 087
87	36. 115	133. 135	1. 027	−. 234	. 178	−. 106	. 215	. 166	−. 225	−. 371	1. 012	−. 120	. 227	. 176	. 051	−. 047	. 235	. 019	. 132	. 102
88	35. 351	138. 039	1. 176	−. 160	−. 062	. 146	. 111	. 062	. 174	−. 056	. 940	. 028	. 099	. 055	. 224	. 116	−. 083	. 053	. 135	. 076
89	33. 199	129. 386	1. 247	. 147	−. 255	−. 060	. 080	. 056	. 018	−. 095	1. 274	. 094	. 097	. 068	. 116	−. 134	. 222	. 126	. 079	. 056
90	34. 564	133. 122	1. 101	. 002	−. 051	−. 088	. 061	. 091	. 103	. 004	1. 028	. 078	. 054	. 081	. 025	−. 143	. 118	. 037	. 048	. 072
91	43. 122	145. 045	. 791	. 382	. 238	. 650	. 261	. 244	−. 261	−. 012	. 565	. 376	. 214	. 200	. 064	. 067	−. 102	. 584	. 251	. 235
92	35. 570	136. 290	1. 131	. 012	. 079	. 004	. 035	. 045	. 027	−. 046	1. 140	. 056	. 053	. 067	. 033	−. 110	−. 002	. 006	. 091	. 115
94	34. 553	139. 539	1. 241	. 053	. 069	. 027	. 054	. 101	. 162	−. 152	. 935	. 146	. 062	. 118	1. 006	. 134	−. 229	−. 050	. 064	. 120
96	35. 322	139. 053	1. 021	. 013	. 083	. 080	. 032	. 047	. 114	. 024	1. 106	. 070	. 040	. 059	. 443	−. 023	−. 247	. 124	. 088	. 129
97	36. 286	139. 299	1. 046	. 093	−. 014	. 034	. 083	. 093	. 027	. 007	. 995	−. 025	. 051	. 057	. 362	. 117	. 103	. 137	. 116	. 130

Table 4-1 (continued.)

128 min

	Lat ° '	Lon ° '	Cu	Cv	Du	Dv	ErrC	ErrD	Eu	Ev	Fu	Fv	ErrE	ErrF	Au	Av	Bu	Bv	ErrA	ErrB
101	34. 070	139. 307	1. 242	. 065	−. 055	−. 035	. 014	. 018	−. 130	−. 052	. 990	. 042	. 014	. 019	. 405	−. 069	−. 269	. 033	. 024	. 032
103	34. 417	138. 097	1. 140	. 128	−. 009	−. 015	. 044	. 072	. 069	−. 045	1. 100	. 076	. 047	. 077	. 523	. 155	−. 558	. 010	. 085	. 139
104	34. 399	137. 134	1. 142	. 023	. 145	−. 009	. 082	. 084	. 012	. 002	1. 060	. 042	. 070	. 072	. 357	. 119	−. 179	. 028	. 073	. 075
917	34. 575	139. 068	1. 146	. 029	. 133	. 035	. 011	. 015	. 095	. 023	1. 084	. 038	. 026	. 014	. 814	. 157	−. 400	−. 072	. 048	. 015
201	35. 152	139. 575	1. 188	. 123	−. 002	−. 008	. 014	. 017	−. 003	−. 050	1. 125	. 075	. 010	. 012	. 773	. 028	−. 222	. 118	. 025	. 030
202	39. 065	141. 124	1. 000	−. 047	. 001	. 019	. 017	. 020	−. 074	−. 015	1. 030	−. 032	. 013	. 015	. 064	−. 041	−. 239	. 107	. 021	. 024
203	36. 061	140. 055	1. 021	. 034	. 004	. 006	. 006	. 007	. 022	. 011	1. 004	. 011	. 002	. 002	. 704	. 146	−. 153	. 085	. 023	. 027
204	31. 252	130. 529	1. 087	. 044	−. 168	−. 007	. 017	. 017	. 091	−. 050	1. 039	−. 001	. 022	. 022	. 560	. 090	. 006	. 069	. 015	. 015
205	43. 545	144. 116	1. 373	. 087	−. 042	−. 135	. 024	. 024	−. 252	−. 035	1. 415	. 124	. 022	. 022	. 112	. 003	−. 312	−. 031	. 012	. 012
206	34. 440	138. 480	1. 188	. 021	. 142	. 051	. 016	. 018	. 056	. 022	1. 069	. 014	. 017	. 018	. 912	. 179	−. 261	. 039	. 033	. 037
208	34. 370	138. 110	1. 213	. 109	. 006	−. 021	. 016	. 019	−. 012	−. 029	1. 092	. 058	. 018	. 021	. 645	. 147	−. 385	−. 044	. 027	. 031
209	36. 041	138. 266	1. 137	. 030	. 087	. 060	. 009	. 011	. 077	. 030	1. 166	. 077	. 015	. 017	. 223	−. 065	. 015	. 128	. 022	. 026

Table 4-1 (continued.)

64 min

	Lat ° '	Lon ° '	Cu	Cv	Du	Dv	ErrC	ErrD	Eu	Ev	Fu	Fv	ErrE	ErrF	Au	Av	Bu	Bv	ErrA	ErrB
1	31. 237	130. 108	1. 075	. 002	−. 034	−. 029	. 039	. 034	−. 003	−. 053	. 996	. 012	. 148	. 025	. 619	. 143	−. 110	. 060	. 043	. 027
2	33. 250	130. 185	1. 101	. 078	−. 067	−. 022	. 087	. 101	. 060	. 048	1. 056	. 108	. 104	. 121	. 078	−. 015	. 110	. 042	. 075	. 088
3	35. 246	133. 598	1. 129	−. 011	−. 069	. 048	. 045	. 050	. 052	−. 022	1. 150	−. 027	. 049	. 054	−. 056	−. 172	. 109	. 103	. 044	. 050
4	33. 566	133. 393	1. 104	−. 003	−. 069	. 010	. 016	. 014	. 102	−. 024	1. 054	. 041	. 073	. 017	. 205	−. 031	−. 091	−. 017	. 017	. 017
5	35. 247	135. 594	1. 006	. 062	. 075	. 047	. 100	. 086	. 044	. 010	1. 078	. 063	. 161	. 138	. 227	−. 068	. 111	. 059	. 175	. 150
6	34. 593	137. 565	1. 104	−. 006	. 111	. 028	. 017	. 020	. 055	. 001	1. 085	. 036	. 054	. 031	. 420	−. 006	−. 215	. 038	. 041	. 033
7	36. 521	136. 552	1. 152	. 080	. 005	. 019	. 045	. 034	. 081	. 024	1. 135	. 009	. 040	. 030	. 064	. 007	. 032	. 040	. 075	. 056
8	38. 013	139. 289	1. 040	−. 002	. 023	. 003	. 034	. 041	. 019	−. 015	. 986	. 008	. 035	. 042	. 054	−. 123	. 019	. 101	. 068	. 080
12	45. 254	141. 027	1. 331	. 021	−. 048	−. 236	. 150	. 190	−. 009	. 074	1. 266	. 042	. 121	. 153	−. 373	−. 081	. 372	. 236	. 075	. 095
13	44. 420	142. 023	1. 424	. 020	−. 320	. 034	. 082	. 097	−. 218	. 007	1. 233	. 136	. 180	. 098	−. 291	−. 108	. 271	. 403	. 049	. 079
15	43. 504	141. 355	1. 336	. 062	−. 142	. 018	. 212	. 193	. 193	. 275	1. 015	. 052	. 229	. 208	−. 031	−. 096	. 360	. 336	. 153	. 139
18	43. 162	140. 347	1. 246	. 067	−. 059	−. 034	. 082	. 071	−. 189	−. 015	1. 163	. 016	. 137	. 053	−. 545	−. 235	. 459	. 276	. 070	. 061
19	43. 046	141. 510	1. 332	. 059	−. 051	−. 088	. 057	. 075	. 386	. 209	1. 430	. 075	. 111	. 093	. 299	. 116	. 435	. 314	. 044	. 072
20	42. 592	143. 201	1. 255	. 044	−. 119	−. 025	. 077	. 110	. 083	−. 044	1. 187	. 284	. 150	. 118	. 276	. 003	. 032	. 270	. 063	. 085
22	42. 318	142. 139	1. 096	−. 035	. 140	−. 031	. 066	. 087	. 471	. 115	1. 532	. 110	. 091	. 092	. 424	. 079	. 338	. 241	. 039	. 065
23	42. 309	140. 558	. 771	−. 068	. 173	−. 095	. 232	. 276	−. 158	−. 031	. 857	. 201	. 170	. 202	−. 040	−. 067	. 393	−. 016	. 187	. 222
25	42. 242	140. 007	1. 293	. 087	. 022	. 061	. 047	. 050	−. 087	. 008	1. 126	−. 008	. 067	. 036	−. 224	. 036	. 479	. 389	. 038	. 033
26	41. 574	140. 556	1. 238	. 180	−. 052	−. 025	. 042	. 044	−. 021	−. 002	1. 080	. 011	. 123	. 031	−. 924	−. 480	−. 285	. 065	. 063	. 027
27	41. 199	141. 223	1. 070	. 000	. 075	−. 013	. 121	. 181	−. 027	−. 009	. 859	. 041	. 101	. 151	−. 783	−. 273	−. 476	. 186	. 119	. 178
28	40. 237	141. 376	. 997	−. 033	−. 042	. 104	. 077	. 055	−. 133	−. 081	. 924	−. 034	. 053	. 026	−. 636	−. 358	−. 582	. 011	. 063	. 045
29	40. 184	140. 223	1. 192	. 050	. 086	. 048	. 042	. 046	−. 144	−. 055	. 976	. 025	. 154	. 036	−. 354	−. 219	−. 086	. 097	. 041	. 036
30	39. 345	141. 575	1. 005	−. 060	. 040	. 020	. 046	. 044	−. 077	. 037	. 989	−. 039	. 043	. 042	. 045	−. 190	−. 617	−. 105	. 102	. 097
32	39. 072	140. 386	. 875	. 095	. 019	. 007	. 176	. 153	−. 122	. 024	. 914	. 039	. 126	. 109	−. 105	−. 120	−. 024	. 037	. 169	. 147

Table 4-1 (continued.)

64 min

	Lat ° '	Lon ° '	Cu	Cv	Du	Dv	ErrC	ErrD	Eu	Ev	Fu	Fv	ErrE	ErrF	Au	Av	Bu	Bv	ErrA	ErrB
33	38. 293	141. 111	1. 085	. 027	. 042	. 040	. 028	. 033	. 131	. 021	1. 077	. 041	. 136	. 031	. 296	. 057	−. 220	. 114	. 038	. 027
34	38. 508	139. 476	. 688	. 099	. 035	. 089	. 113	. 124	−. 019	. 030	1. 044	. 079	. 053	. 045	−. 035	−. 180	−. 079	. 039	. 086	. 082
35	38. 180	140. 131	1. 090	. 008	−. 026	. 055	. 097	. 134	−. 026	. 068	1. 074	. 064	. 059	. 082	. 033	−. 095	−. 204	. 144	. 117	. 161
36	37. 226	139. 495	1. 044	. 037	. 013	. 027	. 010	. 013	. 016	. 005	1. 062	. 028	. 035	. 011	. 210	−. 056	−. 107	. 126	. 019	. 010
37	37. 307	138. 398	1. 040	. 016	. 087	. 104	. 126	. 066	. 069	−. 143	1. 094	. 051	. 114	. 059	. 097	−. 193	. 146	. 136	. 251	. 131
39	37. 052	138. 463	1. 089	−. 004	. 074	−. 095	. 124	. 150	. 000	. 075	1. 192	. 035	. 172	. 209	. 254	. 047	. 161	. 205	. 142	. 172
40	36. 503	140. 145	. 999	. 001	. 007	. 014	. 019	. 027	. 035	. 041	1. 033	. 009	. 016	. 022	. 634	. 171	−. 133	. 101	. 093	. 129
42	35. 474	140. 352	1. 101	. 158	. 034	−. 032	. 040	. 047	−. 156	−. 127	1. 058	. 088	. 048	. 057	. 889	. 109	−. 430	. 107	. 115	. 136
45	35. 263	136. 588	1. 060	. 015	. 102	−. 027	. 088	. 069	−. 043	. 093	1. 127	. 033	. 085	. 067	. 222	−. 086	−. 030	. 155	. 102	. 080
47	33. 456	135. 283	1. 024	−. 043	−. 057	−. 006	. 024	. 025	. 018	. 003	. 940	−. 068	. 026	. 027	. 630	. 163	−. 064	. 064	. 032	. 033
48	34. 223	135. 422	1. 029	−. 074	. 088	−. 005	. 071	. 071	. 017	. 067	. 967	. 015	. 065	. 066	. 340	−. 123	−. 059	. 093	. 127	. 128
50	38. 009	138. 272	1. 025	−. 008	−. 064	. 055	. 083	. 074	. 060	. 016	1. 018	−. 027	. 075	. 067	−. 032	−. 062	. 196	. 199	. 084	. 075
51	35. 446	138. 377	1. 121	. 005	. 116	. 103	. 039	. 041	. 119	. 045	1. 150	. 122	. 050	. 052	. 251	−. 062	−. 074	. 058	. 120	. 125
53	35. 540	137. 192	1. 044	. 001	. 089	. 048	. 064	. 079	. 062	−. 037	1. 114	. 042	. 085	. 104	. 149	−. 050	. 022	. 120	. 086	. 105
55	36. 117	136. 181	1. 139	. 018	. 056	. 136	. 032	. 067	. 039	−. 045	1. 083	. 084	. 062	. 129	−. 003	−. 185	. 057	. 197	. 045	. 094
57	34. 579	134. 497	1. 121	. 011	. 089	. 032	. 053	. 060	. 046	−. 013	1. 035	. 031	. 077	. 087	. 085	−. 039	−. 103	. 053	. 072	. 081
58	35. 248	134. 187	1. 098	. 007	. 003	−. 014	. 029	. 033	. 035	−. 068	1. 082	−. 020	. 120	. 041	. 012	−. 169	. 064	. 072	. 031	. 030
59	34. 467	133. 474	1. 101	−. 019	−. 105	. 032	. 041	. 051	−. 021	−. 039	1. 022	. 011	. 064	. 078	. 088	−. 121	. 015	. 051	. 039	. 048
61	34. 536	132. 101	1. 112	. 043	−. 076	−. 049	. 067	. 071	−. 073	−. 008	1. 080	−. 002	. 069	. 073	. 042	−. 265	. 201	. 259	. 105	. 111
62	34. 296	132. 194	1. 129	−. 057	−. 074	−. 019	. 038	. 055	. 034	. 042	1. 091	. 126	. 041	. 058	. 035	−. 125	. 165	. 195	. 033	. 048
63	34. 174	131. 253	1. 110	−. 005	−. 149	−. 008	. 024	. 027	. 022	. 001	1. 147	. 021	. 071	. 049	−. 085	−. 186	. 197	. 167	. 027	. 032
64	32. 513	129. 451	1. 234	. 055	−. 188	−. 004	. 026	. 026	−. 049	−. 076	1. 133	−. 019	. 078	. 033	. 214	. 030	. 171	. 102	. 017	. 025
65	32. 490	130. 396	1. 146	. 031	−. 172	−. 012	. 047	. 089	. 001	−. 049	1. 167	. 047	. 061	. 117	. 219	−. 018	. 137	. 132	. 029	. 055

Table 4-1 (continued.)

64 min

	Lat ° '	Lon ° '	Cu	Cv	Du	Dv	ErrC	ErrD	Eu	Ev	Fu	Fv	ErrE	ErrF	Au	Av	Bu	Bv	ErrA	ErrB
66	32. 156	130. 466	1. 195	. 062	−. 180	. 071	. 086	. 098	−. 008	−. 012	1. 127	−. 023	. 132	. 150	. 436	−. 026	. 019	. 101	. 077	. 087
67	31. 516	131. 176	1. 182	. 108	. 085	. 030	. 063	. 077	. 034	. 049	1. 009	−. 201	. 082	. 100	. 481	. 064	. 066	. 019	. 088	. 106
68	32. 557	131. 525	1. 104	−. 049	−. 138	. 066	. 071	. 053	. 069	−. 071	1. 025	−. 001	. 081	. 060	. 151	−. 022	−. 107	−. 009	. 040	. 030
70	33. 263	132. 382	1. 175	. 030	−. 052	−. 005	. 054	. 052	. 046	−. 003	. 966	−. 016	. 053	. 051	. 256	−. 017	. 032	. 002	. 040	. 039
71	33. 385	133. 488	1. 049	−. 016	−. 054	−. 049	. 051	. 053	. 048	. 060	1. 182	. 063	. 060	. 062	. 321	−. 004	−. 037	. 061	. 059	. 061
72	32. 484	132. 456	1. 062	−. 024	−. 187	−. 015	. 075	. 108	. 109	. 059	. 889	−. 095	. 084	. 121	. 453	. 129	−. 044	−. 009	. 065	. 093
73	33. 359	134. 220	1. 074	. 004	−. 076	. 017	. 047	. 063	. 061	. 006	1. 030	−. 019	. 050	. 067	. 357	. 036	−. 210	−. 058	. 046	. 061
74	34. 172	134. 408	1. 102	−. 052	−. 031	. 011	. 054	. 054	. 067	. 048	1. 065	−. 011	. 077	. 076	. 287	−. 052	−. 051	. 040	. 065	. 064
76	43. 098	142. 364	1. 137	. 043	−. 089	−. 128	. 208	. 174	−. 001	−. 034	1. 181	−. 045	. 102	. 086	. 180	. 087	. 106	. 266	. 126	. 105
78	43. 380	145. 102	1. 242	. 066	−. 074	−. 057	. 127	. 105	−. 093	. 038	1. 666	. 358	. 123	. 102	. 021	−. 075	−. 586	−. 044	. 085	. 070
80	41. 267	140. 086	1. 284	. 102	. 126	. 069	. 079	. 079	−. 159	−. 006	. 938	−. 006	. 100	. 065	. 076	. 202	. 292	. 212	. 075	. 066
81	40. 418	140. 069	1. 193	. 077	. 020	. 031	. 081	. 136	−. 022	−. 003	. 988	. 035	. 084	. 141	−. 714	−. 466	. 147	. 204	. 076	. 127
85	30. 440	131. 040	. 943	. 004	−. 151	−. 023	. 050	. 071	. 058	−. 005	. 834	−. 001	. 070	. 099	. 453	−. 011	−. 175	. 007	. 051	. 073
87	36. 115	133. 135	1. 130	−. 016	. 048	−. 157	. 156	. 127	−. 080	−. 179	1. 027	−. 138	. 177	. 145	−. 001	−. 070	. 204	. 006	. 101	. 083
88	35. 351	138. 039	1. 135	−. 058	. 039	. 076	. 099	. 068	. 100	−. 028	1. 017	. 007	. 094	. 064	. 208	. 068	−. 082	. 024	. 114	. 079
89	33. 199	129. 386	1. 261	. 127	−. 231	−. 068	. 070	. 065	−. 001	−. 084	1. 248	. 123	. 087	. 081	. 101	−. 121	. 219	. 162	. 058	. 053
90	34. 564	133. 122	1. 102	−. 007	−. 045	−. 036	. 058	. 075	. 104	−. 010	1. 067	. 012	. 073	. 095	. 012	−. 146	. 117	. 082	. 039	. 051
91	43. 122	145. 045	. 875	. 148	. 186	. 496	. 242	. 291	−. 067	. 092	. 612	. 347	. 187	. 225	. 072	. 022	−. 007	. 569	. 195	. 234
92	35. 570	136. 290	1. 138	. 022	. 060	. 002	. 038	. 043	. 025	−. 008	1. 172	. 061	. 051	. 058	. 042	−. 200	. 003	. 125	. 065	. 074
94	34. 553	139. 539	1. 241	. 107	. 046	−. 025	. 048	. 078	. 091	−. 135	. 975	. 092	. 078	. 129	1. 049	. 102	−. 244	−. 009	. 061	. 099
96	35. 322	139. 053	1. 031	. 007	. 073	. 063	. 024	. 033	. 129	. 035	1. 101	. 047	. 032	. 044	. 445	−. 025	−. 233	. 106	. 070	. 095
97	36. 286	139. 299	1. 062	. 047	. 016	. 020	. 083	. 082	. 027	. 046	1. 003	. 001	. 068	. 067	. 324	−. 030	. 112	. 140	. 150	. 147
101	34. 070	139. 307	1. 248	. 056	−. 072	−. 024	. 015	. 018	−. 146	−. 056	1. 008	. 030	. 015	. 018	. 377	−. 135	−. 274	. 074	. 026	. 030

Table 4-1 (continued.)

64 min

	Lat °	'	Lon °	'	Cu	Cv	Du	Dv	ErrC	ErrD	Eu	Ev	Fu	Fv	ErrE	ErrF	Au	Av	Bu	Bv	ErrA	ErrB
103	34.	417	138.	097	1. 178	. 122	. 057	−. 007	. 037	. 044	. 002	−. 035	1. 063	. 064	. 046	. 055	. 604	. 134	−. 414	−. 026	. 077	. 092
104	34.	399	137.	134	1. 130	−. 021	. 112	. 057	. 075	. 086	. 028	. 018	1. 053	. 027	. 064	. 072	. 393	. 067	−. 235	. 011	. 063	. 072
917	34.	575	139.	068	1. 151	. 027	. 134	. 041	. 012	. 014	. 098	. 013	1. 086	. 040	. 025	. 011	. 856	. 144	−. 446	−. 097	. 043	. 013
201	35.	152	139.	575	1. 202	. 130	−. 003	−. 019	. 012	. 014	−. 009	−. 067	1. 137	. 095	. 010	. 011	. 785	−. 042	−. 230	. 131	. 021	. 025
202	39.	065	141.	124	1. 003	−. 061	. 009	. 018	. 015	. 017	−. 076	−. 017	1. 029	−. 043	. 011	. 013	. 047	−. 052	−. 242	. 115	. 017	. 020
203	36.	061	140.	055	1. 023	. 036	. 003	. 002	. 004	. 005	. 024	. 012	1. 005	. 014	. 002	. 002	. 723	. 137	−. 159	. 099	. 019	. 022
204	31.	252	130.	529	1. 082	. 050	−. 178	. 013	. 015	. 015	. 097	−. 069	1. 031	−. 007	. 021	. 020	. 569	. 075	. 001	. 067	. 012	. 012
205	43.	545	144.	116	1. 415	. 044	−. 086	−. 168	. 023	. 022	−. 272	−. 033	1. 464	. 145	. 021	. 021	. 106	−. 008	−. 332	−. 060	. 011	. 011
206	34.	440	138.	480	1. 189	−. 007	. 158	. 050	. 014	. 016	. 054	. 022	1. 078	. 009	. 013	. 015	. 940	. 146	−. 291	. 023	. 028	. 031
208	34.	370	138.	110	1. 226	. 110	. 017	−. 039	. 014	. 016	−. 019	−. 036	1. 106	. 071	. 016	. 019	. 667	. 127	−. 427	−. 065	. 023	. 027
209	36.	041	138.	266	1. 142	. 027	. 097	. 056	. 008	. 009	. 082	. 034	1. 184	. 090	. 013	. 016	. 214	−. 102	. 002	. 130	. 019	. 022

Table 4-1 (continued.)

32 min

	Lat ° '	Lon ° '	Cu	Cv	Du	Dv	ErrC	ErrD	Eu	Ev	Fu	Fv	ErrE	ErrF	Au	Av	Bu	Bv	ErrA	ErrB
1	31. 237	130. 108	1. 038	−. 018	. 002	. 006	. 027	. 025	. 109	. 003	. 921	−. 087	. 112	. 038	. 591	. 013	. 135	. 092	. 037	. 034
2	33. 250	130. 185	1. 122	−. 006	−. 070	−. 015	. 072	. 069	. 006	. 048	1. 148	−. 048	. 135	. 129	. 034	−. 029	. 238	. 041	. 051	. 049
3	35. 246	133. 598	1. 144	−. 044	. 001	. 024	. 041	. 055	−. 001	. 014	1. 131	−. 144	. 037	. 050	−. 175	−. 213	. 145	. 047	. 036	. 049
4	33. 566	133. 393	1. 085	. 001	−. 052	. 017	. 015	. 014	. 091	−. 080	1. 070	−. 008	. 065	. 018	. 155	−. 032	−. 081	−. 013	. 012	. 015
6	34. 593	137. 565	1. 080	−. 064	. 157	. 006	. 021	. 019	. 110	−. 028	1. 159	. 005	. 053	. 024	. 375	−. 054	−. 268	−. 018	. 032	. 027
7	36. 521	136. 552	1. 186	. 064	−. 001	−. 039	. 032	. 029	. 113	−. 003	1. 141	−. 058	. 043	. 040	. 007	. 063	. 019	−. 060	. 068	. 062
8	38. 013	139. 289	1. 080	−. 007	. 050	. 015	. 032	. 030	−. 015	−. 029	. 989	−. 007	. 035	. 032	−. 006	−. 112	. 074	. 173	. 063	. 058
12	45. 254	141. 027	1. 412	−. 158	. 041	−. 201	. 114	. 105	. 068	. 011	1. 409	. 032	. 092	. 085	−. 405	−. 024	. 513	. 114	. 050	. 046
13	44. 420	142. 023	1. 464	−. 028	−. 295	. 042	. 057	. 059	−. 220	−. 108	1. 327	. 160	. 112	. 056	−. 377	−. 073	. 457	. 276	. 034	. 044
14	44. 120	143. 025	1. 202	−. 076	−. 220	. 062	. 220	. 294	. 112	−. 003	. 863	. 294	. 181	. 242	−. 092	−. 069	−. 029	. 006	. 191	. 255
15	43. 504	141. 355	1. 459	−. 057	−. 245	. 013	. 065	. 080	. 129	. 068	1. 120	. 117	. 113	. 072	−. 288	−. 053	. 451	. 200	. 053	. 056
18	43. 162	140. 347	1. 402	−. 096	−. 080	. 007	. 057	. 031	−. 090	. 032	1. 194	−. 070	. 087	. 023	−. 825	−. 087	. 634	. 131	. 047	. 031
19	43. 046	141. 510	1. 464	−. 074	−. 018	. 001	. 048	. 061	. 404	−. 052	1. 504	. 263	. 088	. 063	. 315	. 011	. 589	. 293	. 038	. 053
20	42. 592	143. 201	1. 199	−. 045	−. 130	−. 045	. 034	. 055	. 167	−. 011	1. 372	. 145	. 072	. 060	. 264	−. 005	. 176	. 121	. 030	. 044
22	42. 318	142. 139	1. 110	−. 020	−. 059	. 038	. 057	. 099	. 409	−. 067	1. 520	. 157	. 080	. 097	. 441	. 001	. 419	. 127	. 033	. 062
23	42. 309	140. 558	1. 211	−. 103	. 171	. 070	. 144	. 148	−. 054	−. 077	1. 135	. 045	. 151	. 156	. 036	. 014	. 384	. 100	. 143	. 147
25	42. 242	140. 007	1. 406	−. 037	. 045	−. 010	. 024	. 031	−. 078	−. 019	1. 132	−. 048	. 056	. 025	−. 207	. 097	. 761	. 268	. 023	. 020
26	41. 574	140. 556	1. 358	−. 066	. 023	−. 014	. 032	. 037	−. 094	−. 091	1. 077	−. 015	. 057	. 022	−1. 336	−. 125	−. 307	−. 002	. 040	. 023
27	41. 199	141. 223	1. 204	−. 038	. 022	−. 018	. 085	. 110	−. 124	. 021	1. 030	−. 018	. 071	. 092	−1. 091	−. 206	−. 419	. 050	. 078	. 101
28	40. 237	141. 376	1. 005	−. 057	−. 058	. 040	. 052	. 041	−. 150	−. 034	. 921	−. 015	. 041	. 022	−. 892	−. 330	−. 479	. 030	. 046	. 034
29	40. 184	140. 223	1. 246	. 051	. 022	. 004	. 023	. 031	−. 209	−. 044	. 961	. 040	. 107	. 026	−. 469	−. 084	. 000	. 137	. 020	. 021
30	39. 345	141. 575	. 965	−. 093	. 004	. 005	. 031	. 038	−. 113	. 013	. 924	−. 034	. 027	. 032	−. 203	−. 150	−. 646	−. 092	. 067	. 081
32	39. 072	140. 386	1. 089	−. 008	. 005	. 040	. 069	. 089	−. 057	−. 020	. 996	. 040	. 058	. 075	−. 174	−. 057	−. 087	. 118	. 079	. 102

Table 4-1 (continued.)

32 min

	Lat ° '	Lon ° '	Cu	Cv	Du	Dv	ErrC	ErrD	Eu	Ev	Fu	Fv	ErrE	ErrF	Au	Av	Bu	Bv	ErrA	ErrB
33	38. 293	141. 111	1. 140	. 099	. 044	. 014	. 025	. 024	. 194	. 213	1. 092	. 038	. 138	. 018	. 392	. 126	−. 198	. 116	. 021	. 017
34	38. 508	139. 476	1. 000	. 275	−. 042	−. 113	. 086	. 083	. 075	. 099	1. 058	. 009	. 040	. 030	−. 278	−. 424	−. 040	. 161	. 076	. 077
35	38. 180	140. 131	1. 053	−. 009	. 014	−. 006	. 049	. 059	. 003	. 059	1. 042	. 042	. 036	. 044	−. 091	−. 107	−. 158	. 067	. 051	. 061
36	37. 226	139. 495	1. 035	. 037	. 022	. 019	. 009	. 011	. 029	−. 007	1. 059	. 022	. 024	. 010	. 134	−. 091	−. 097	. 115	. 014	. 010
37	37. 307	138. 398	1. 110	. 116	. 081	−. 002	. 112	. 095	. 085	−. 033	1. 171	. 042	. 091	. 077	. 043	−. 176	. 207	. 219	. 245	. 206
39	37. 052	138. 463	1. 136	. 067	. 002	−. 053	. 111	. 141	. 153	. 075	1. 268	. 059	. 118	. 149	. 145	−. 029	. 243	. 148	. 158	. 200
40	36. 503	140. 145	. 990	. 012	. 008	. 021	. 016	. 019	. 054	. 026	1. 038	. 029	. 021	. 026	. 635	. 123	−. 084	. 093	. 050	. 063
42	35. 474	140. 352	1. 218	. 151	−. 035	−. 056	. 027	. 031	−. 268	−. 190	1. 110	. 088	. 035	. 040	. 735	−. 101	−. 334	. 139	. 052	. 059
45	35. 263	136. 588	1. 085	−. 023	. 117	. 021	. 075	. 088	. 086	. 052	1. 135	. 039	. 055	. 065	. 127	−. 135	. 011	. 080	. 103	. 121
47	33. 456	135. 283	. 957	−. 093	−. 030	−. 007	. 028	. 034	. 016	−. 008	. 954	−. 078	. 031	. 038	. 645	. 090	−. 057	. 103	. 036	. 043
48	34. 223	135. 422	1. 015	−. 025	. 026	−. 029	. 114	. 106	. 028	. 000	1. 079	−. 014	. 078	. 074	. 249	. 033	−. 120	−. 031	. 208	. 195
50	38. 009	138. 272	1. 078	−. 052	−. 010	. 027	. 076	. 054	. 001	−. 013	. 994	−. 064	. 055	. 039	. 004	−. 047	. 126	. 034	. 055	. 039
51	35. 446	138. 377	1. 089	−. 025	. 176	. 063	. 021	. 032	. 130	. 008	1. 181	. 048	. 030	. 047	. 233	−. 113	−. 071	. 137	. 071	. 111
53	35. 540	137. 192	1. 130	−. 017	. 053	. 032	. 057	. 072	. 077	. 001	1. 186	−. 004	. 094	. 117	. 085	−. 146	−. 038	. 051	. 065	. 080
55	36. 117	136. 181	1. 123	. 040	. 098	. 060	. 019	. 044	. 032	−. 006	1. 100	. 034	. 032	. 073	−. 145	−. 259	. 094	. 119	. 040	. 093
57	34. 579	134. 497	1. 064	−. 082	. 056	−. 014	. 041	. 043	. 009	−. 010	1. 135	. 053	. 060	. 062	−. 009	−. 110	−. 102	. 020	. 047	. 048
58	35. 248	134. 187	1. 111	−. 043	. 022	. 024	. 020	. 021	. 047	−. 009	1. 127	−. 086	. 049	. 028	−. 164	−. 200	. 064	. 054	. 023	. 027
59	34. 467	133. 474	1. 070	−. 129	−. 039	. 060	. 027	. 047	. 036	. 042	1. 009	−. 076	. 040	. 070	−. 043	−. 119	. 079	. 034	. 030	. 054
61	34. 536	132. 101	1. 091	−. 066	−. 025	. 032	. 051	. 047	−. 041	. 010	1. 123	−. 117	. 077	. 070	−. 258	−. 234	. 344	. 143	. 067	. 061
62	34. 296	132. 194	1. 108	−. 086	−. 032	. 035	. 031	. 033	−. 017	−. 005	1. 068	. 054	. 042	. 045	−. 097	−. 136	. 210	. 125	. 025	. 026
63	34. 174	131. 253	1. 090	−. 064	−. 007	. 035	. 023	. 026	−. 010	−. 085	1. 182	−. 090	. 092	. 047	−. 155	−. 147	. 301	. 090	. 024	. 025
64	32. 513	129. 451	1. 228	. 003	−. 174	. 044	. 022	. 027	−. 159	−. 005	1. 164	−. 114	. 054	. 031	. 212	. 026	. 238	. 062	. 009	. 021
65	32. 490	130. 396	1. 201	. 024	−. 166	−. 066	. 059	. 069	−. 126	−. 088	1. 083	−. 034	. 100	. 117	. 192	−. 032	. 212	. 032	. 025	. 029

Table 4-1 (continued.)

32 min

	Lat ° '	Lon ° '	Cu	Cv	Du	Dv	ErrC	ErrD	Eu	Ev	Fu	Fv	ErrE	ErrF	Au	Av	Bu	Bv	ErrA	ErrB
66	32. 156	130. 466	1. 252	. 042	−. 005	−. 004	. 065	. 044	−. 020	−. 056	1. 126	. 006	. 098	. 066	. 257	−. 107	. 119	. 046	. 066	. 044
67	31. 516	131. 176	1. 122	. 072	. 012	−. 046	. 066	. 087	−. 087	. 017	1. 131	−. 048	. 076	. 100	. 528	−. 076	. 141	−. 050	. 064	. 085
68	32. 557	131. 525	1. 065	−. 063	−. 050	. 077	. 040	. 037	. 132	. 032	. 998	−. 065	. 052	. 048	. 075	−. 105	−. 090	−. 037	. 021	. 019
70	33. 263	132. 382	1. 128	−. 018	−. 025	. 016	. 045	. 056	. 060	. 039	1. 011	−. 094	. 056	. 070	. 164	−. 045	. 026	. 026	. 030	. 038
71	33. 385	133. 488	1. 046	−. 015	−. 029	. 009	. 040	. 049	−. 012	−. 034	1. 109	. 025	. 042	. 051	. 318	−. 035	−. 021	. 066	. 031	. 038
72	32. 484	132. 456	1. 019	−. 146	−. 050	. 098	. 054	. 054	. 029	. 056	. 849	−. 123	. 052	. 052	. 504	−. 008	−. 011	. 072	. 053	. 053
73	33. 359	134. 220	1. 056	−. 006	−. 028	. 025	. 044	. 044	. 016	. 031	. 977	−. 075	. 041	. 042	. 337	−. 033	−. 191	−. 025	. 034	. 034
74	34. 172	134. 408	1. 057	−. 038	. 054	. 013	. 046	. 040	. 027	. 042	1. 063	−. 020	. 051	. 045	. 241	−. 027	−. 014	. 023	. 070	. 062
76	43. 098	142. 364	1. 210	. 000	−. 131	−. 064	. 091	. 108	−. 027	−. 067	1. 113	. 102	. 118	. 140	. 084	−. 054	. 254	. 118	. 083	. 099
78	43. 380	145. 102	1. 260	. 066	−. 098	−. 022	. 078	. 074	−. 251	−. 069	1. 826	. 358	. 148	. 141	. 054	. 021	−. 511	−. 006	. 046	. 044
80	41. 267	140. 086	1. 381	. 016	. 083	−. 070	. 052	. 053	−. 232	−. 072	1. 036	−. 034	. 064	. 040	. 266	. 270	. 429	. 082	. 046	. 045
81	40. 418	140. 069	1. 249	. 003	. 043	−. 058	. 071	. 046	−. 027	. 022	1. 032	−. 075	. 050	. 032	−. 963	−. 354	. 146	. 294	. 086	. 055
85	30. 440	131. 040	1. 039	−. 041	−. 073	. 032	. 050	. 046	. 022	−. 013	. 821	−. 081	. 049	. 045	. 474	−. 224	−. 134	−. 032	. 049	. 045
87	36. 115	133. 135	1. 181	. 001	−. 050	. 040	. 072	. 071	. 065	. 025	1. 053	−. 131	. 104	. 103	−. 153	. 048	. 114	. 050	. 087	. 086
88	35. 351	138. 039	1. 142	−. 012	. 156	. 032	. 054	. 052	. 146	. 066	1. 155	. 050	. 079	. 076	. 133	−. 117	−. 210	. 070	. 063	. 061
89	33. 199	129. 386	1. 277	−. 015	−. 080	. 022	. 076	. 081	−. 156	−. 034	1. 297	. 000	. 108	. 114	−. 040	−. 121	. 400	. 110	. 041	. 044
90	34. 564	133. 122	1. 056	−. 053	. 030	. 048	. 052	. 051	. 029	. 030	1. 008	−. 084	. 070	. 069	−. 132	−. 154	. 197	. 043	. 047	. 046
91	43. 122	145. 045	. 879	−. 097	−. 161	. 047	. 090	. 131	−. 135	−. 027	1. 106	. 034	. 097	. 140	. 200	−. 047	. 005	. 210	. 083	. 121
92	35. 570	136. 290	1. 116	. 009	. 095	. 015	. 023	. 028	. 040	. 015	1. 221	. 029	. 050	. 059	−. 069	−. 222	. 025	. 059	. 042	. 050
94	34. 553	139. 539	1. 375	. 113	−. 081	. 008	. 038	. 081	. 013	−. 043	1. 086	. 023	. 037	. 079	1. 032	−. 255	−. 215	. 165	. 074	. 157
96	35. 322	139. 053	1. 046	−. 011	. 084	. 048	. 036	. 055	. 153	. 022	1. 122	. 044	. 033	. 051	. 503	−. 114	−. 288	. 053	. 093	. 143
97	36. 286	139. 299	1. 097	. 077	−. 032	−. 028	. 107	. 108	. 079	. 015	1. 052	. 017	. 062	. 062	. 403	−. 110	. 039	. 164	. 079	. 079
101	34. 070	139. 307	1. 267	−. 044	−. 087	. 017	. 017	. 019	−. 156	−. 030	1. 018	. 004	. 014	. 016	. 208	−. 265	−. 225	. 133	. 027	. 031

Table 4-1 (continued.)

32 min

	Lat ° '	Lon ° '	Cu	Cv	Du	Dv	ErrC	ErrD	Eu	Ev	Fu	Fv	ErrE	ErrF	Au	Av	Bu	Bv	ErrA	ErrB
103	34. 417	138. 097	1. 202	. 064	. 052	−. 087	. 033	. 035	. 038	−. 085	1. 092	. 044	. 053	. 055	. 642	. 111	−. 436	−. 040	. 073	. 077
104	34. 399	137. 134	1. 114	−. 020	. 203	. 053	. 102	. 099	. 039	−. 001	1. 064	. 011	. 063	. 061	. 448	−. 009	−. 281	−. 020	. 092	. 090
917	34. 575	139. 068	1. 171	−. 034	. 159	. 050	. 025	. 025	. 112	−. 018	1. 112	. 014	. 023	. 023	. 924	. 008	−. 452	−. 007	. 094	. 092
201	35. 152	139. 575	1. 283	. 127	−. 020	−. 026	. 012	. 014	−. 053	−. 099	1. 208	. 109	. 012	. 013	. 678	−. 287	−. 165	. 174	. 017	. 020
202	39. 065	141. 124	. 988	−. 104	. 012	. 007	. 009	. 011	−. 084	−. 008	1. 020	−. 070	. 008	. 009	−. 010	−. 006	−. 188	. 148	. 009	. 011
203	36. 061	140. 055	1. 038	. 047	. 003	−. 002	. 003	. 003	. 030	. 014	1. 009	. 022	. 002	. 002	. 755	. 066	−. 118	. 113	. 012	. 014
204	31. 252	130. 529	1. 115	. 004	−. 137	. 069	. 016	. 016	. 052	−. 010	1. 012	−. 095	. 019	. 018	. 572	−. 054	. 071	. 059	. 009	. 009
205	43. 545	144. 116	1. 365	−. 027	−. 221	−. 204	. 028	. 028	−. 275	−. 028	1. 535	. 196	. 023	. 022	. 079	−. 027	−. 371	−. 115	. 010	. 010
206	34. 440	138. 480	1. 187	−. 105	. 223	. 025	. 010	. 011	. 072	−. 010	1. 124	−. 049	. 010	. 011	. 964	−. 031	−. 314	. 067	. 027	. 029
208	34. 370	138. 110	1. 284	. 088	. 022	−. 080	. 010	. 012	−. 031	−. 077	1. 179	. 060	. 014	. 016	. 674	. 035	−. 530	−. 017	. 018	. 021
209	36. 041	138. 266	1. 154	. 004	. 142	. 041	. 007	. 008	. 117	. 017	1. 263	. 073	. 010	. 011	. 109	−. 174	. 028	. 113	. 012	. 015

Table 4-1 (continued.)

16 min

	Lat ° ,	Lon ° ,	Cu	Cv	Du	Dv	ErrC	ErrD	Eu	Ev	Fu	Fv	ErrE	ErrF	Au	Av	Bu	Bv	ErrA	ErrB
1	31. 237	130. 108	1. 034	−. 102	. 031	. 065	. 033	. 027	. 060	. 052	. 866	−. 170	. 101	. 038	. 574	−. 021	. 197	. 067	. 034	. 031
2	33. 250	130. 185	1. 069	−. 127	−. 064	. 002	. 126	. 131	−. 052	. 058	1. 062	−. 145	. 097	. 101	. 023	−. 009	. 248	−. 041	. 050	. 052
3	35. 246	133. 598	1. 087	−. 061	. 032	. 053	. 046	. 060	. 001	. 003	1. 071	−. 053	. 050	. 064	−. 322	−. 179	. 105	. 027	. 055	. 071
4	33. 566	133. 393	1. 042	. 027	−. 010	. 031	. 016	. 018	. 055	−. 041	1. 034	−. 035	. 062	. 022	. 147	. 017	−. 088	−. 015	. 014	. 017
6	34. 593	137. 565	1. 061	−. 074	. 172	−. 041	. 022	. 029	. 046	−. 025	1. 158	. 022	. 070	. 031	. 305	−. 077	−. 341	. 012	. 035	. 026
7	36. 521	136. 552	1. 213	. 130	−. 017	−. 036	. 039	. 041	. 070	. 013	1. 078	−. 057	. 040	. 042	. 163	. 257	−. 040	−. 025	. 107	. 112
8	38. 013	139. 289	1. 059	. 027	. 066	. 002	. 031	. 036	−. 032	−. 045	. 967	−. 006	. 024	. 029	−. 050	−. 039	. 178	. 135	. 069	. 081
12	45. 254	141. 027	1. 270	−. 130	−. 129	−. 087	. 115	. 148	−. 093	. 025	1. 304	−. 116	. 099	. 127	−. 400	. 057	. 422	−. 096	. 057	. 074
13	44. 420	142. 023	1. 358	−. 038	−. 219	. 079	. 042	. 052	−. 185	−. 084	1. 379	. 156	. 072	. 044	−. 390	−. 026	. 589	. 185	. 025	. 030
14	44. 120	143. 025	1. 142	−. 154	−. 168	. 072	. 116	. 149	−. 084	−. 083	1. 119	. 003	. 088	. 113	−. 135	. 028	. 101	−. 003	. 097	. 125
15	43. 504	141. 355	1. 313	−. 159	−. 060	. 092	. 049	. 075	. 189	−. 064	1. 219	. 132	. 073	. 061	−. 277	−. 009	. 449	−. 020	. 044	. 045
18	43. 162	140. 347	1. 326	−. 160	−. 051	−. 054	. 038	. 032	−. 101	−. 021	1. 175	−. 080	. 047	. 019	−. 723	. 114	. 605	−. 076	. 038	. 027
19	43. 046	141. 510	1. 408	−. 104	−. 076	−. 037	. 032	. 052	. 318	−. 231	1. 565	. 193	. 070	. 055	. 292	−. 088	. 635	. 073	. 025	. 037
20	42. 592	143. 201	1. 132	−. 085	−. 112	−. 010	. 024	. 040	. 122	−. 020	1. 437	. 136	. 040	. 041	. 253	−. 079	. 198	. 084	. 019	. 031
22	42. 318	142. 139	1. 065	−. 017	. 013	−. 036	. 042	. 077	. 369	−. 214	1. 627	. 193	. 060	. 076	. 459	−. 101	. 503	−. 008	. 020	. 044
23	42. 309	140. 558	1. 176	−. 086	. 028	−. 010	. 125	. 122	−. 119	−. 087	1. 111	. 063	. 134	. 131	. 033	. 192	. 251	−. 129	. 102	. 100
25	42. 242	140. 007	1. 343	−. 177	. 053	−. 035	. 021	. 031	−. 032	−. 039	1. 070	−. 070	. 036	. 019	−. 059	. 279	. 775	. 017	. 020	. 017
26	41. 574	140. 556	1. 339	−. 107	. 028	−. 037	. 022	. 033	−. 180	−. 060	1. 064	. 022	. 026	. 021	−1. 262	. 166	−. 328	. 034	. 027	. 022
27	41. 199	141. 223	1. 109	−. 059	−. 041	−. 075	. 056	. 090	−. 154	−. 004	. 982	. 009	. 043	. 069	−1. 038	. 147	−. 291	. 170	. 061	. 098
28	40. 237	141. 376	. 949	−. 030	−. 045	−. 021	. 036	. 027	−. 190	−. 046	. 907	−. 006	. 051	. 017	−. 934	−. 154	−. 481	. 143	. 063	. 027
29	40. 184	140. 223	1. 274	. 059	. 035	−. 060	. 019	. 023	−. 239	−. 098	. 988	. 052	. 082	. 018	−. 468	. 069	. 082	. 126	. 016	. 017
30	39. 345	141. 575	. 919	−. 055	−. 021	. 009	. 027	. 028	−. 077	. 019	. 893	−. 040	. 025	. 026	−. 209	. 008	−. 682	. 012	. 056	. 058

Table 4-1 (continued.)

16 min

	Lat ° '	Lon ° '	Cu	Cv	Du	Dv	ErrC	ErrD	Eu	Ev	Fu	Fv	ErrE	ErrF	Au	Av	Bu	Bv	ErrA	ErrB
32	39.072	140.386	1.055	.034	−.005	.038	.078	.095	−.085	.002	1.048	.076	.063	.077	−.171	.033	−.115	.065	.087	.106
33	38.293	141.111	1.197	.131	.098	.025	.023	.026	.329	.199	1.117	.067	.092	.017	.478	.216	−.149	.189	.016	.015
34	38.508	139.476	1.159	.300	−.002	−.063	.055	.056	.117	.141	1.076	.031	.024	.023	−.488	−.446	−.040	.122	.060	.060
35	38.180	140.131	1.019	.044	.014	−.010	.036	.057	.016	.009	1.104	.069	.027	.043	−.120	−.061	−.138	.064	.043	.067
36	37.226	139.495	1.059	.061	.031	.004	.008	.012	.030	−.019	1.091	.035	.032	.013	.099	−.111	−.061	.077	.012	.011
39	37.052	138.463	1.028	.073	−.036	−.056	.144	.161	.156	.024	1.367	.124	.186	.208	.305	−.085	.435	.078	.183	.205
40	36.503	140.145	.992	.023	.020	.000	.011	.017	.077	.042	1.048	.037	.024	.036	.714	.108	−.053	.090	.032	.048
42	35.474	140.352	1.303	.177	−.079	−.075	.023	.031	−.353	−.202	1.151	.112	.026	.035	.647	−.282	−.241	.183	.049	.067
45	35.263	136.588	1.004	.026	.106	−.079	.162	.153	.049	.060	1.138	−.034	.084	.079	.052	−.166	−.058	.126	.179	.169
47	33.456	135.283	.890	−.099	−.012	−.011	.033	.044	.019	.013	.920	−.039	.035	.047	.697	.088	−.004	.204	.048	.064
50	38.009	138.272	1.020	−.116	−.030	.022	.082	.066	−.050	−.084	.936	−.069	.051	.041	.019	.047	.050	−.050	.057	.046
51	35.446	138.377	1.084	−.049	.187	.013	.027	.030	.147	−.038	1.217	.006	.040	.044	.090	−.241	−.125	.104	.111	.121
53	35.540	137.192	1.112	.013	.070	.001	.092	.114	.073	−.074	1.180	.003	.145	.179	−.030	−.127	−.043	−.005	.082	.101
55	36.117	136.181	1.109	.107	.084	.010	.022	.035	.050	.008	1.105	.018	.029	.047	−.306	−.226	.170	.170	.046	.074
57	34.579	134.497	1.014	−.087	.085	.020	.051	.074	.012	.031	1.063	−.010	.073	.105	−.089	−.066	−.014	−.022	.082	.118
58	35.248	134.187	1.070	−.059	.048	.002	.018	.021	.026	−.007	1.038	−.054	.084	.036	−.291	−.148	.074	−.002	.026	.030
59	34.467	133.474	.962	−.086	−.060	.004	.037	.060	.000	−.014	.960	−.141	.052	.084	−.080	−.065	.100	.021	.058	.094
61	34.536	132.101	.986	−.112	.043	.023	.027	.037	−.067	.019	1.087	−.064	.041	.056	−.388	−.165	.380	.075	.042	.057
62	34.296	132.194	1.047	−.111	.014	.006	.024	.048	−.040	.050	1.113	−.017	.037	.074	−.179	−.027	.264	.032	.025	.050
63	34.174	131.253	1.027	−.100	.023	.050	.026	.030	−.101	.131	1.131	−.124	.104	.047	−.261	−.096	.332	.015	.031	.027
64	32.513	129.451	1.184	−.096	.014	.048	.020	.027	−.179	.037	.998	−.169	.120	.050	.234	.042	.241	−.023	.014	.028
65	32.490	130.396	1.175	.023	−.043	.003	.044	.059	−.120	−.012	1.065	−.033	.079	.106	.177	−.038	.239	−.016	.020	.027
66	32.156	130.466	1.250	.001	.126	.044	.056	.084	−.029	−.012	1.023	−.076	.062	.094	.178	−.126	.160	.049	.036	.055

Table 4-1 (continued.)

16 min

	Lat ° '	Lon ° '	Cu	Cv	Du	Dv	ErrC	ErrD	Eu	Ev	Fu	Fv	ErrE	ErrF	Au	Av	Bu	Bv	ErrA	ErrB
67	31.516	131.176	1.238	.008	.069	.051	.061	.116	-.030	.054	.957	-.202	.051	.097	.466	-.100	.033	-.089	.051	.097
68	32.557	131.525	1.013	-.004	-.019	.122	.050	.065	.015	.047	.874	-.130	.070	.092	.046	-.094	-.110	-.083	.027	.036
70	33.263	132.382	1.116	.049	.102	.035	.051	.064	.031	.002	.985	-.080	.050	.062	.159	-.024	.032	.009	.039	.049
71	33.385	133.488	1.033	-.004	.021	.032	.038	.056	.000	-.054	1.069	-.024	.044	.066	.292	-.036	.041	.092	.031	.045
72	32.484	132.456	.952	-.070	.071	.059	.060	.072	-.003	.028	.869	-.103	.053	.065	.506	-.014	.060	.073	.050	.061
73	33.359	134.220	1.015	-.019	.024	-.003	.048	.074	.057	.009	.968	-.037	.044	.069	.323	-.043	-.229	-.043	.041	.064
74	34.172	134.408	.987	-.026	.106	.082	.039	.048	.030	.027	1.061	.002	.045	.056	.248	.041	-.029	.134	.076	.094
76	43.098	142.364	1.165	-.027	-.096	-.059	.096	.087	-.111	-.071	1.249	.041	.104	.094	.001	-.116	.325	.054	.098	.089
78	43.380	145.102	1.250	.090	-.093	-.062	.090	.089	-.283	.027	1.907	.359	.134	.133	.039	-.001	-.522	-.021	.034	.034
80	41.267	140.086	1.404	-.119	.051	-.050	.037	.041	-.263	-.071	1.000	-.004	.055	.031	.484	.332	.402	-.119	.040	.032
81	40.418	140.069	1.250	.017	.022	-.026	.036	.032	-.023	.037	1.059	-.053	.041	.036	-1.131	-.247	.260	.228	.066	.058
85	30.440	131.040	1.101	-.040	-.048	.096	.058	.057	-.013	.023	.792	-.112	.053	.052	.269	-.383	-.178	-.081	.067	.065
87	36.115	133.135	1.144	-.023	-.041	.027	.077	.072	.132	.059	.832	-.151	.115	.107	-.056	.230	.075	-.110	.076	.071
88	35.351	138.039	1.093	-.045	.218	.030	.114	.075	.127	-.029	1.193	.013	.131	.087	.075	-.141	-.203	.040	.152	.101
89	33.199	129.386	1.152	-.038	-.034	.079	.086	.080	-.163	.035	1.336	-.172	.091	.085	-.075	-.076	.437	-.008	.042	.039
90	34.564	133.122	.983	-.106	.009	.065	.053	.044	.038	-.004	1.057	-.079	.065	.054	-.172	-.123	.184	.040	.066	.055
91	43.122	145.045	.878	-.053	-.189	-.018	.093	.090	-.191	-.047	1.267	.076	.076	.074	.174	-.150	-.020	.233	.088	.085
92	35.570	136.290	1.130	-.028	.122	.015	.026	.029	.068	-.010	1.103	.018	.063	.071	-.206	-.171	.046	.024	.046	.052
94	34.553	139.539	1.359	.020	.063	-.012	.045	.077	-.039	-.062	1.100	.002	.044	.074	.719	-.556	-.126	.176	.068	.115
96	35.322	139.053	1.009	-.035	.141	.012	.054	.070	.166	-.014	1.137	.024	.050	.064	.299	-.142	-.191	-.096	.127	.163
97	36.286	139.299	1.149	.114	-.080	.031	.151	.189	.074	-.105	1.018	.014	.083	.104	.359	-.139	.083	.117	.125	.156
101	34.070	139.307	1.193	-.125	-.067	.048	.018	.021	-.154	.007	1.025	-.038	.016	.019	.014	-.264	-.130	.154	.038	.043
103	34.417	138.097	1.202	.064	.046	-.137	.049	.052	-.010	-.085	1.137	-.019	.143	.149	.618	.035	-.466	.048	.105	.109

Table 4-1 (continued.)

16 min

	Lat ° '	Lon ° '	Cu	Cv	Du	Dv	ErrC	ErrD	Eu	Ev	Fu	Fv	ErrE	ErrF	Au	Av	Bu	Bv	ErrA	ErrB
104	34. 399	137. 134	1. 017	−. 062	. 130	. 072	. 145	. 200	. 014	. 012	1. 074	−. 036	. 082	. 113	. 349	−. 009	−. 289	. 078	. 130	. 179
917	34. 575	139. 068	1. 128	−. 063	. 170	. 009	. 040	. 063	. 087	−. 050	1. 130	−. 023	. 025	. 040	. 816	−. 083	−. 720	−. 006	. 136	. 217
201	35. 152	139. 575	1. 368	. 108	−. 035	−. 019	. 016	. 019	−. 131	−. 108	1. 265	. 103	. 016	. 019	. 404	−. 458	−. 041	. 192	. 020	. 025
202	39. 065	141. 124	. 951	−. 168	. 012	−. 005	. 008	. 010	−. 092	. 007	1. 020	−. 145	. 006	. 008	. 026	. 070	−. 105	. 195	. 007	. 009
203	36. 061	140. 055	1. 054	. 070	. 000	. 000	. 003	. 004	. 039	. 013	1. 009	. 043	. 003	. 004	. 762	. 004	−. 065	. 120	. 010	. 013
204	31. 252	130. 529	1. 124	−. 011	−. 033	. 094	. 015	. 018	. 011	−. 014	1. 016	−. 143	. 015	. 019	. 497	−. 164	. 117	. 011	. 008	. 010
205	43. 545	144. 116	1. 219	−. 032	−. 315	−. 176	. 026	. 032	−. 212	. 012	1. 532	. 198	. 019	. 023	. 035	−. 057	−. 436	−. 132	. 009	. 011
206	34. 440	138. 480	1. 114	−. 202	. 253	−. 044	. 011	. 012	. 055	−. 046	1. 120	−. 156	. 013	. 015	. 877	−. 182	−. 284	. 137	. 041	. 045
208	34. 370	138. 110	1. 313	. 100	−. 032	−. 156	. 013	. 015	−. 085	−. 119	1. 215	. 056	. 022	. 026	. 656	−. 035	−. 551	. 089	. 025	. 030
209	36. 041	138. 266	1. 149	−. 010	. 169	. 020	. 006	. 007	. 122	−. 037	1. 318	. 030	. 010	. 012	. 003	−. 221	. 077	. 097	. 014	. 017

Table 4-1 (continued.)

8 min

	Lat ° '	Lon ° '	Cu	Cv	Du	Dv	ErrC	ErrD	Eu	Ev	Fu	Fv	ErrE	ErrF	Au	Av	Bu	Bv	ErrA	ErrB
1	31.237	130.108	.976	-.058	.049	.016	.035	.029	.066	-.087	.913	-.079	.136	.040	.558	-.101	.197	.085	.047	.041
2	33.250	130.185	1.060	-.083	.065	.061	.140	.141	-.179	.075	.917	-.175	.136	.137	-.023	-.007	.190	-.082	.060	.061
3	35.246	133.598	1.052	-.047	.010	.022	.060	.106	.024	.025	1.006	-.063	.056	.099	-.344	-.105	.100	-.062	.065	.115
4	33.566	133.393	1.050	.141	-.015	-.021	.022	.023	-.016	-.074	1.062	.030	.060	.026	.166	.063	-.133	-.054	.019	.017
6	34.593	137.565	.965	-.064	.093	-.071	.046	.048	.031	-.048	1.155	.049	.098	.045	.247	-.047	-.313	.035	.057	.050
7	36.521	136.552	1.225	.107	-.035	-.046	.060	.073	.032	-.028	1.049	-.045	.070	.085	.119	.309	-.006	-.123	.174	.209
8	38.013	139.289	1.067	.037	.017	-.036	.041	.046	-.056	-.071	1.023	.007	.044	.050	-.030	-.007	.232	.194	.125	.141
12	45.254	141.027	1.061	-.207	-.104	.012	.075	.098	-.048	-.064	1.201	-.095	.073	.095	-.306	.036	.279	-.162	.066	.086
13	44.420	142.023	1.336	-.033	-.071	.012	.048	.062	-.252	-.057	1.467	.218	.109	.077	-.349	.060	.617	.159	.041	.050
14	44.120	143.025	1.157	-.014	-.280	-.133	.225	.241	-.064	-.093	1.147	-.084	.142	.151	-.176	.006	-.075	-.107	.149	.160
15	43.504	141.355	1.275	-.124	-.064	.046	.086	.086	.066	-.079	1.339	.063	.134	.072	-.238	-.057	.446	-.093	.059	.056
18	43.162	140.347	1.151	-.150	-.108	-.097	.042	.035	-.111	-.056	1.139	-.105	.077	.029	-.593	.137	.500	-.149	.039	.034
19	43.046	141.510	1.306	-.120	-.117	-.097	.031	.062	.148	-.264	1.637	.152	.062	.067	.174	-.122	.593	-.016	.022	.043
20	42.592	143.201	1.090	-.031	-.064	.018	.041	.056	.068	-.070	1.542	.161	.103	.064	.171	-.123	.220	.021	.032	.044
22	42.318	142.139	1.083	.010	.000	.069	.057	.081	.187	-.256	1.660	.253	.074	.083	.359	-.184	.467	-.030	.026	.048
23	42.309	140.558	.969	-.099	.107	.084	.161	.132	-.090	.030	1.191	-.012	.181	.148	.153	.057	.169	-.161	.159	.130
25	42.242	140.007	1.221	-.157	-.009	-.052	.025	.029	-.022	-.020	1.041	-.041	.037	.020	.146	.311	.628	-.111	.025	.023
26	41.574	140.556	1.268	-.179	-.034	-.071	.038	.046	-.217	-.035	1.114	-.046	.056	.040	-.988	.355	-.440	.023	.050	.046
27	41.199	141.223	1.128	-.088	-.035	-.064	.072	.063	-.185	.016	1.082	.019	.066	.059	-.977	.374	-.225	.196	.102	.090
28	40.237	141.376	.943	-.046	-.013	-.023	.026	.037	-.204	-.023	.932	.029	.025	.021	-1.021	-.007	-.362	.285	.034	.022
29	40.184	140.223	1.260	.079	.012	-.131	.031	.034	-.232	-.141	1.005	.078	.178	.029	-.381	.153	.120	.146	.023	.026
30	39.345	141.575	.904	-.020	-.006	-.033	.028	.036	-.091	-.002	.895	-.005	.024	.031	-.135	.117	-.680	-.010	.081	.102
32	39.072	140.386	1.010	.067	.054	.051	.123	.127	-.108	.053	1.060	.165	.133	.137	-.026	-.014	-.121	.217	.128	.131

Table 4-1 (continued.)

8 min

	Lat ° '	Lon ° '	Cu	Cv	Du	Dv	ErrC	ErrD	Eu	Ev	Fu	Fv	ErrE	ErrF	Au	Av	Bu	Bv	ErrA	ErrB
33	38. 293	141. 111	1. 313	. 221	. 072	. 015	. 027	. 031	. 513	. 210	1. 137	. 075	. 155	. 026	. 636	. 258	−. 027	. 185	. 022	. 022
34	38. 508	139. 476	1. 275	. 327	. 085	−. 111	. 078	. 071	. 196	. 138	1. 138	−. 008	. 036	. 031	−. 730	−. 325	. 047	. 147	. 093	. 085
35	38. 180	140. 131	1. 063	. 078	. 006	−. 009	. 048	. 051	. 038	. 027	1. 152	. 121	. 048	. 051	−. 117	−. 060	−. 092	. 106	. 054	. 057
36	37. 226	139. 495	1. 098	. 065	. 027	. 004	. 016	. 021	. 007	−. 056	1. 096	. 031	. 060	. 024	. 056	−. 110	. 003	. 039	. 016	. 020
40	36. 503	140. 145	. 982	. 036	. 030	. 016	. 035	. 037	. 041	. 062	1. 026	. 054	. 063	. 067	. 802	. 062	−. 005	. 087	. 075	. 080
42	35. 474	140. 352	1. 431	. 116	−. 117	−. 120	. 055	. 076	−. 489	−. 113	1. 275	. 194	. 065	. 090	. 435	−. 272	−. 078	. 262	. 072	. 099
47	33. 456	135. 283	. 808	−. 049	−. 047	−. 031	. 075	. 080	. 054	−. 003	. 895	−. 052	. 073	. 078	. 800	. 018	. 151	. 049	. 184	. 197
50	38. 009	138. 272	. 907	. 011	−. 029	. 001	. 121	. 092	−. 046	−. 070	. 864	−. 105	. 076	. 058	. 128	−. 030	−. 046	−. 147	. 088	. 067
51	35. 446	138. 377	1. 091	−. 020	. 209	. 013	. 068	. 080	. 127	−. 068	1. 266	−. 053	. 068	. 080	−. 054	−. 164	−. 102	−. 014	. 179	. 209
53	35. 540	137. 192	1. 094	−. 078	. 011	−. 035	. 147	. 180	. 014	−. 131	1. 081	−. 076	. 226	. 278	−. 074	−. 034	−. 075	. 035	. 141	. 173
55	36. 117	136. 181	1. 068	. 222	. 093	−. 011	. 029	. 054	. 007	−. 033	1. 083	. 146	. 035	. 065	−. 360	−. 210	. 177	. 165	. 044	. 082
57	34. 579	134. 497	. 939	−. 003	. 084	−. 034	. 075	. 081	. 003	−. 004	1. 072	. 031	. 106	. 114	−. 101	−. 021	−. 137	−. 003	. 134	. 144
58	35. 248	134. 187	1. 008	−. 039	. 070	−. 024	. 027	. 024	−. 010	−. 058	1. 065	−. 091	. 097	. 031	−. 339	−. 064	. 080	−. 006	. 031	. 027
59	34. 467	133. 474	. 931	−. 031	−. 018	. 072	. 060	. 093	−. 010	−. 030	1. 046	. 020	. 078	. 122	−. 093	−. 012	−. 035	−. 045	. 108	. 168
61	34. 536	132. 101	. 937	−. 087	. 010	. 005	. 034	. 041	−. 004	. 036	. 992	−. 149	. 058	. 070	−. 455	−. 100	. 376	−. 009	. 050	. 060
62	34. 296	132. 194	1. 006	−. 106	. 052	. 022	. 030	. 064	−. 065	−. 015	1. 136	−. 024	. 037	. 078	−. 201	. 030	. 287	−. 021	. 030	. 063
63	34. 174	131. 253	. 948	−. 065	. 038	. 051	. 023	. 033	. 028	. 084	1. 045	−. 140	. 116	. 056	−. 258	−. 051	. 295	−. 053	. 035	. 028
64	32. 513	129. 451	1. 108	−. 130	−. 063	. 009	. 024	. 034	−. 110	. 110	1. 012	−. 133	. 121	. 054	. 246	. 037	. 195	−. 052	. 015	. 024
65	32. 490	130. 396	1. 207	. 023	. 039	−. 002	. 060	. 112	−. 118	. 056	1. 027	−. 040	. 072	. 134	. 148	−. 030	. 207	−. 066	. 025	. 046
66	32. 156	130. 466	1. 230	−. 035	. 027	−. 031	. 074	. 079	−. 010	. 027	. 935	−. 161	. 091	. 096	. 143	−. 096	. 176	. 036	. 053	. 056
67	31. 516	131. 176	1. 247	. 083	. 076	. 013	. 086	. 082	−. 061	−. 023	. 964	−. 078	. 080	. 077	. 460	−. 133	−. 002	−. 123	. 067	. 064
68	32. 557	131. 525	1. 063	−. 087	. 111	. 053	. 083	. 075	−. 082	−. 051	. 885	−. 149	. 121	. 109	−. 016	−. 083	−. 202	−. 105	. 064	. 058
70	33. 263	132. 382	1. 146	. 083	. 028	. 008	. 085	. 074	−. 040	−. 027	1. 000	. 008	. 079	. 069	. 223	−. 005	. 050	−. 008	. 079	. 069

Table (continued.)

8 min

	Lat ° '	Lon ° '	Cu	Cv	Du	Dv	ErrC	ErrD	Eu	Ev	Fu	Fv	ErrE	ErrF	Au	Av	Bu	Bv	ErrA	ErrB
71	33. 385	133. 488	. 989	. 022	. 024	−. 009	. 054	. 045	. 069	−. 048	1. 149	−. 050	. 089	. 074	. 268	−. 039	. 061	. 093	. 053	. 044
72	32. 484	132. 456	. 883	. 010	. 068	. 023	. 082	. 094	−. 030	. 037	. 803	−. 062	. 076	. 088	. 475	−. 057	. 001	−. 020	. 072	. 083
73	33. 359	134. 220	. 999	. 032	. 084	. 090	. 052	. 066	. 017	. 000	. 936	−. 045	. 040	. 051	. 310	−. 092	−. 199	. 010	. 044	. 055
74	34. 172	134. 408	. 897	. 002	. 025	. 025	. 078	. 066	. 004	−. 009	1. 087	. 038	. 073	. 062	. 235	−. 015	−. 043	. 227	. 200	. 169
76	43. 098	142. 364	1. 152	. 066	−. 109	−. 079	. 151	. 122	−. 250	−. 042	1. 165	. 071	. 129	. 104	−. 143	−. 180	. 254	−. 047	. 132	. 107
78	43. 380	145. 102	1. 202	. 110	−. 124	−. 052	. 067	. 089	−. 134	−. 036	2. 112	. 214	. 114	. 151	. 010	. 054	−. 559	. 025	. 033	. 044
80	41. 267	140. 086	1. 357	−. 114	. 042	−. 041	. 054	. 051	−. 281	−. 020	1. 006	−. 045	. 064	. 037	. 740	. 274	. 319	−. 133	. 064	. 055
81	40. 418	140. 069	1. 249	. 022	−. 018	−. 120	. 057	. 059	. 056	. 045	. 962	. 049	. 037	. 038	−1. 034	−. 073	. 401	. 304	. 078	. 081
85	30. 440	131. 040	. 864	−. 050	. 000	. 062	. 081	. 093	−. 026	. 018	. 729	−. 067	. 086	. 099	. 034	−. 308	−. 223	−. 064	. 104	. 120
87	36. 115	133. 135	1. 066	−. 072	−. 063	. 075	. 084	. 063	. 120	−. 022	. 825	−. 018	. 101	. 076	. 117	. 269	. 027	−. 037	. 089	. 067
88	35. 351	138. 039	. 957	−. 064	. 138	−. 098	. 189	. 102	−. 063	−. 114	1. 172	−. 017	. 280	. 152	. 099	. 063	−. 199	. 087	. 268	. 146
89	33. 199	129. 386	1. 048	−. 061	−. 097	. 020	. 062	. 089	−. 101	. 076	1. 284	−. 072	. 072	. 103	−. 109	−. 029	. 354	−. 070	. 043	. 062
90	34. 564	133. 122	. 945	−. 069	. 069	. 045	. 054	. 053	. 041	−. 059	1. 074	−. 003	. 082	. 081	−. 211	−. 003	. 140	. 006	. 089	. 087
91	43. 122	145. 045	. 876	. 020	−. 125	−. 042	. 126	. 125	−. 170	. 051	1. 278	. 086	. 115	. 113	. 107	−. 114	. 060	. 112	. 120	. 119
92	35. 570	136. 290	1. 111	. 005	. 045	−. 045	. 022	. 036	. 028	−. 004	1. 113	−. 128	. 051	. 084	−. 289	−. 078	. 116	. 095	. 037	. 060
94	34. 553	139. 539	1. 237	. 001	. 111	. 051	. 087	. 141	−. 156	−. 066	1. 060	. 125	. 097	. 158	. 319	−. 408	−. 059	. 111	. 154	. 250
101	34. 070	139. 307	1. 101	−. 104	−. 046	. 033	. 021	. 028	−. 162	. 012	1. 018	−. 056	. 020	. 028	−. 123	−. 180	−. 046	. 145	. 044	. 061
103	34. 417	138. 097	1. 206	. 077	−. 111	−. 267	. 115	. 104	−. 052	−. 035	. 975	. 179	. 236	. 214	. 625	. 046	−. 512	. 009	. 289	. 262
201	35. 152	139. 575	1. 437	. 051	−. 051	−. 037	. 032	. 038	−. 214	−. 068	1. 320	. 079	. 037	. 044	. 087	−. 436	. 034	. 154	. 039	. 046
202	39. 065	141. 124	. 912	−. 298	. 001	−. 017	. 011	. 014	−. 096	. 044	1. 007	−. 304	. 010	. 012	. 125	. 071	. 027	. 206	. 010	. 012
203	36. 061	140. 055	1. 059	. 113	−. 003	. 000	. 007	. 008	. 041	. 013	1. 005	. 082	. 007	. 009	. 721	−. 040	−. 015	. 110	. 015	. 018
204	31. 252	130. 529	1. 088	−. 010	−. 036	. 079	. 016	. 022	. 000	−. 042	. 959	−. 146	. 016	. 022	. 380	−. 198	. 066	−. 006	. 010	. 014
205	43. 545	144. 116	1. 233	. 000	−. 320	−. 107	. 023	. 031	−. 220	. 037	1. 604	. 203	. 019	. 026	. 010	−. 053	−. 511	−. 112	. 010	. 014

Table 4-1 (continued.)

8 min

	Lat ° '	Lon ° '	Cu	Cv	Du	Dv	ErrC	ErrD	Eu	Ev	Fu	Fv	ErrE	ErrF	Au	Av	Bu	Bv	ErrA	ErrB
206	34. 440	138. 480	. 993	−. 303	. 187	−. 134	. 024	. 028	. 003	−. 074	1. 024	−. 316	. 041	. 049	. 738	−. 286	−. 254	. 229	. 094	. 105
208	34. 370	138. 110	1. 342	. 167	−. 160	−. 211	. 027	. 034	−. 148	−. 154	1. 218	. 042	. 037	. 046	. 631	−. 026	−. 493	. 173	. 048	. 059
209	36. 041	138. 266	1. 147	−. 014	. 166	−. 014	. 010	. 013	. 073	−. 099	1. 330	−. 032	. 016	. 020	−. 137	−. 223	. 105	. 063	. 019	. 024

Table 4-1 (continued.)

4 min

	Lat ° '	Lon ° '	Cu	Cv	Du	Dv	ErrC	ErrD	Eu	Ev	Fu	Fv	ErrE	ErrF	Au	Av	Bu	Bv	ErrA	ErrB
1	31. 237	130. 108	. 863	−. 002	−. 011	. 004	. 062	. 055	−. 020	. 054	. 925	−. 038	. 217	. 051	. 371	−. 046	. 233	. 103	. 060	. 051
2	33. 250	130. 185	. 969	−. 027	−. 052	−. 017	. 104	. 093	−. 081	−. 131	. 977	−. 160	. 129	. 115	−. 012	. 056	. 110	−. 147	. 152	. 136
3	35. 246	133. 598	1. 048	−. 020	−. 017	. 083	. 121	. 189	. 042	−. 002	. 983	. 130	. 098	. 152	−. 267	−. 073	. 034	−. 126	. 125	. 194
4	33. 566	133. 393	1. 102	. 199	−. 183	−. 037	. 045	. 053	. 014	−. 029	1. 078	−. 052	. 081	. 047	. 217	. 038	−. 196	−. 021	. 032	. 029
8	38. 013	139. 289	1. 079	. 001	−. 004	−. 046	. 078	. 085	−. 011	. 023	1. 035	. 031	. 080	. 088	−. 147	−. 170	. 385	. 191	. 232	. 255
12	45. 254	141. 027	1. 108	−. 158	−. 182	. 006	. 126	. 137	−. 122	. 017	1. 208	−. 136	. 111	. 121	−. 331	−. 002	. 281	−. 108	. 087	. 094
13	44. 420	142. 023	1. 185	−. 024	. 075	. 031	. 071	. 101	−. 392	. 148	1. 524	. 054	. 237	. 113	−. 296	. 167	. 569	. 031	. 052	. 065
14	44. 120	143. 025	. 792	−. 038	−. 249	−. 052	. 239	. 278	−. 148	−. 157	1. 007	−. 025	. 195	. 226	−. 149	. 109	−. 082	−. 088	. 137	. 160
15	43. 504	141. 355	. 963	. 009	. 016	. 096	. 145	. 128	. 102	. 079	1. 274	. 205	. 213	. 112	−. 228	. 087	. 323	−. 150	. 097	. 104
18	43. 162	140. 347	. 975	−. 074	−. 113	−. 001	. 083	. 082	−. 052	. 004	1. 019	−. 135	. 148	. 058	−. 465	. 081	. 297	−. 169	. 065	. 053
19	43. 046	141. 510	1. 221	−. 122	. 050	. 081	. 054	. 114	−. 057	−. 334	1. 694	. 128	. 102	. 121	. 085	−. 080	. 603	−. 061	. 036	. 064
20	42. 592	143. 201	1. 003	−. 021	−. 009	. 121	. 114	. 117	−. 015	−. 009	1. 538	. 190	. 197	. 105	. 105	−. 062	. 161	. 079	. 099	. 108
22	42. 318	142. 139	. 894	. 133	. 018	. 132	. 090	. 229	. 045	−. 189	1. 691	. 155	. 075	. 190	. 215	−. 213	. 310	−. 142	. 030	. 076
23	42. 309	140. 558	. 725	−. 041	. 162	. 041	. 237	. 230	−. 084	−. 230	. 947	. 020	. 255	. 248	. 204	. 017	. 042	. 031	. 232	. 225
25	42. 242	140. 007	1. 093	−. 035	−. 005	−. 003	. 047	. 056	. 048	. 012	. 996	−. 032	. 064	. 041	. 246	. 235	. 491	−. 060	. 043	. 051
26	41. 574	140. 556	1. 095	−. 151	−. 039	. 012	. 073	. 081	−. 171	. 050	1. 081	−. 037	. 094	. 070	−. 745	. 218	−. 403	. 008	. 093	. 091
27	41. 199	141. 223	1. 065	−. 042	. 068	−. 032	. 141	. 179	−. 168	. 064	1. 070	−. 014	. 126	. 160	−. 705	. 396	−. 348	. 065	. 170	. 216
28	40. 237	141. 376	. 882	. 041	. 058	−. 041	. 074	. 059	−. 229	. 019	. 962	. 008	. 063	. 033	−. 925	. 092	−. 223	. 133	. 082	. 052
29	40. 184	140. 223	1. 161	. 079	−. 122	−. 065	. 057	. 065	−. 273	−. 038	1. 008	. 058	. 268	. 057	−. 255	. 115	. 153	. 065	. 045	. 048
30	39. 345	141. 575	. 888	−. 017	−. 017	−. 016	. 039	. 055	−. 095	. 014	. 891	−. 002	. 031	. 044	−. 043	. 132	−. 603	−. 001	. 047	. 068
32	39. 072	140. 386	. 968	−. 018	. 029	. 098	. 283	. 274	−. 097	−. 079	1. 061	. 127	. 232	. 224	−. 050	−. 105	−. 140	. 086	. 207	. 200
33	38. 293	141. 111	1. 414	. 130	. 105	. 072	. 108	. 134	. 608	. 231	1. 165	. 132	. 119	. 109	. 829	. 181	−. 014	. 161	. 068	. 085
34	38. 508	139. 476	1. 308	. 502	−. 094	. 021	. 096	. 097	. 186	. 217	1. 119	−. 018	. 084	. 053	−. 827	−. 362	. 368	. 045	. 093	. 086

Table 4-1 (continued.)

4 min

	Lat ° '	Lon ° '	Cu	Cv	Du	Dv	ErrC	ErrD	Eu	Ev	Fu	Fv	ErrE	ErrF	Au	Av	Bu	Bv	ErrA	ErrB
35	38. 180	140. 131	1. 074	. 130	−. 038	−. 019	. 127	. 159	. 021	. 100	1. 215	. 148	. 124	. 156	−. 142	−. 045	−. 138	. 045	. 102	. 128
36	37. 226	139. 495	1. 091	. 022	. 015	−. 006	. 039	. 049	. 071	. 127	1. 075	. 059	. 159	. 055	−. 010	−. 097	−. 020	−. 002	. 035	. 043
40	36. 503	140. 145	. 933	−. 002	. 018	. 009	. 108	. 111	. 050	. 027	1. 025	. 029	. 155	. 159	. 635	−. 052	. 027	. 079	. 143	. 147
50	38. 009	138. 272	. 881	−. 082	−. 081	. 024	. 168	. 141	−. 143	−. 038	. 788	−. 085	. 147	. 123	. 061	. 041	−. 082	−. 081	. 136	. 114
55	36. 117	136. 181	1. 036	. 333	. 128	−. 059	. 096	. 131	−. 005	−. 112	1. 011	. 403	. 102	. 139	−. 371	−. 219	. 173	. 378	. 168	. 230
58	35. 248	134. 187	. 959	. 017	. 044	−. 019	. 056	. 066	. 062	−. 092	1. 085	−. 060	. 138	. 065	−. 303	−. 060	. 116	. 007	. 056	. 059
61	34. 536	132. 101	. 928	−. 042	−. 022	. 042	. 055	. 047	−. 031	. 024	1. 002	−. 148	. 068	. 058	−. 455	−. 036	. 401	−. 002	. 096	. 083
62	34. 296	132. 194	. 964	−. 037	−. 035	. 020	. 047	. 077	. 021	−. 032	1. 159	−. 001	. 048	. 078	−. 046	. 122	. 218	−. 067	. 061	. 099
63	34. 174	131. 253	. 912	−. 122	. 039	. 023	. 074	. 075	. 022	. 161	1. 064	−. 121	. 115	. 116	−. 142	−. 023	. 137	−. 010	. 180	. 182
64	32. 513	129. 451	1. 028	−. 103	−. 101	−. 052	. 031	. 040	. 076	. 282	. 901	−. 092	. 080	. 047	. 248	. 045	. 120	−. 066	. 026	. 035
65	32. 490	130. 396	1. 199	−. 034	−. 115	−. 046	. 125	. 170	−. 014	. 073	1. 039	−. 026	. 069	. 094	. 130	−. 031	. 182	−. 066	. 048	. 065
66	32. 156	130. 466	1. 024	. 053	. 048	−. 047	. 149	. 207	. 050	−. 103	. 879	−. 174	. 113	. 157	. 101	−. 014	. 232	. 042	. 095	. 132
67	31. 516	131. 176	1. 130	−. 023	. 117	−. 191	. 149	. 141	. 010	−. 151	. 820	−. 069	. 100	. 095	. 325	−. 175	−. 198	. 002	. 115	. 109
68	32. 557	131. 525	1. 044	. 041	−. 016	. 005	. 092	. 079	−. 051	−. 013	. 970	−. 045	. 104	. 089	−. 045	−. 065	−. 306	−. 108	. 091	. 078
70	33. 263	132. 382	. 929	. 106	−. 009	. 036	. 189	. 143	−. 004	−. 103	. 902	−. 014	. 125	. 095	. 182	−. 101	. 026	−. 010	. 144	. 109
71	33. 385	133. 488	. 972	−. 102	−. 067	−. 103	. 103	. 139	. 121	. 006	1. 037	−. 007	. 093	. 127	. 172	−. 126	. 037	. 028	. 066	. 089
72	32. 484	132. 456	. 640	. 008	. 034	−. 038	. 212	. 180	−. 059	. 036	. 671	−. 050	. 160	. 135	. 249	−. 088	. 006	. 031	. 173	. 147
73	33. 359	134. 220	1. 063	. 027	−. 016	. 012	. 077	. 093	. 015	−. 064	. 999	−. 114	. 071	. 086	. 199	−. 124	−. 257	−. 002	. 065	. 079
76	43. 098	142. 364	. 891	. 027	. 056	−. 074	. 233	. 230	−. 012	−. 042	1. 001	. 080	. 250	. 247	−. 094	−. 150	. 121	. 018	. 186	. 184
78	43. 380	145. 102	1. 407	. 144	−. 172	−. 044	. 103	. 128	−. 146	−. 012	2. 291	. 121	. 128	. 160	. 093	. 144	−. 578	. 056	. 053	. 066
80	41. 267	140. 086	1. 241	−. 070	−. 105	. 016	. 146	. 159	−. 218	−. 016	. 967	. 095	. 109	. 119	. 749	. 103	. 294	. 004	. 149	. 162
81	40. 418	140. 069	1. 194	. 033	−. 165	−. 076	. 097	. 107	. 075	−. 059	1. 103	. 039	. 082	. 090	−. 905	−. 051	. 575	. 130	. 128	. 140
85	30. 440	131. 040	. 656	. 123	−. 083	. 053	. 161	. 212	−. 086	. 022	. 536	−. 068	. 134	. 177	. 048	−. 165	−. 116	. 015	. 150	. 198

Table 4-1 (continued.)

4 min

	Lat ° ,	Lon ° ,	Cu	Cv	Du	Dv	ErrC	ErrD	Eu	Ev	Fu	Fv	ErrE	ErrF	Au	Av	Bu	Bv	ErrA	ErrB
87	36. 115	133. 135	. 744	. 103	. 123	. 067	. 225	. 279	−. 002	−. 057	. 530	−. 011	. 208	. 257	. 304	. 154	−. 012	−. 025	. 129	. 160
89	33. 199	129. 386	1. 067	. 063	−. 078	. 001	. 154	. 171	−. 028	. 005	1. 268	−. 033	. 178	. 198	−. 051	−. 078	. 337	−. 034	. 122	. 135
90	34. 564	133. 122	. 912	. 036	−. 008	−. 028	. 113	. 127	. 045	. 059	1. 005	. 012	. 129	. 144	−. 130	. 071	. 172	. 081	. 147	. 164
91	43. 122	145. 045	. 852	. 005	. 089	. 044	. 227	. 247	−. 275	. 000	1. 057	. 048	. 196	. 213	. 054	−. 209	. 061	. 070	. 215	. 234
92	35. 570	136. 290	1. 116	. 000	. 029	−. 071	. 060	. 096	. 016	. 018	1. 021	−. 050	. 061	. 096	−. 293	. 028	. 178	. 054	. 083	. 132
101	34. 070	139. 307	1. 057	−. 041	−. 047	. 055	. 046	. 057	−. 146	. 008	. 926	−. 047	. 039	. 049	−. 093	−. 099	−. 068	. 050	. 066	. 083
201	35. 152	139. 575	1. 345	−. 032	−. 137	−. 011	. 145	. 166	−. 290	. 008	1. 251	−. 013	. 123	. 140	−. 010	−. 234	. 085	. 138	. 122	. 138
202	39. 065	141. 124	. 766	−. 506	−. 004	. 011	. 030	. 035	−. 063	. 097	. 854	−. 535	. 027	. 030	. 178	−. 051	. 136	. 114	. 020	. 022
203	36. 061	140. 055	1. 085	. 176	. 007	. 003	. 027	. 031	. 077	. 013	. 994	. 135	. 023	. 026	. 576	−. 014	−. 035	. 091	. 040	. 046
204	31. 252	130. 529	1. 065	−. 025	−. 049	. 012	. 024	. 032	−. 046	−. 044	. 835	−. 099	. 021	. 027	. 277	−. 177	. 035	. 004	. 017	. 022
205	43. 545	144. 116	1. 262	. 051	−. 339	. 007	. 029	. 038	−. 260	. 025	1. 664	. 200	. 031	. 040	. 033	−. 025	−. 531	−. 070	. 017	. 022
208	34. 370	138. 110	1. 363	. 156	−. 270	−. 127	. 081	. 094	−. 270	−. 140	1. 178	. 047	. 113	. 129	. 577	−. 158	−. 344	. 261	. 110	. 127
209	36. 041	138. 266	1. 088	−. 018	. 126	−. 047	. 029	. 034	. 027	−. 071	1. 261	−. 079	. 044	. 051	−. 159	−. 156	. 094	. 056	. 052	. 060

Latitude, Longitude : 31.237 means 31 deg 23.7 min.

Xu means in-phase part and Xv means imaginary part.

ErrX means 95% confidence level.

Cu and Fu are added 1.0.

Station number < 200 : First order geomagnetic stations (GSI)
201 : Kanozan (GSI)
202 : Mizusawa (GSI)
203 : Tsukuba (GSI)
204 : Kanoya (JMA)
205 : Memanbetsu (JMA)
206 : Matsuzaki (JMA)
208 : Omaezaki (JMA)
209 : Yatsugatake (ERI)

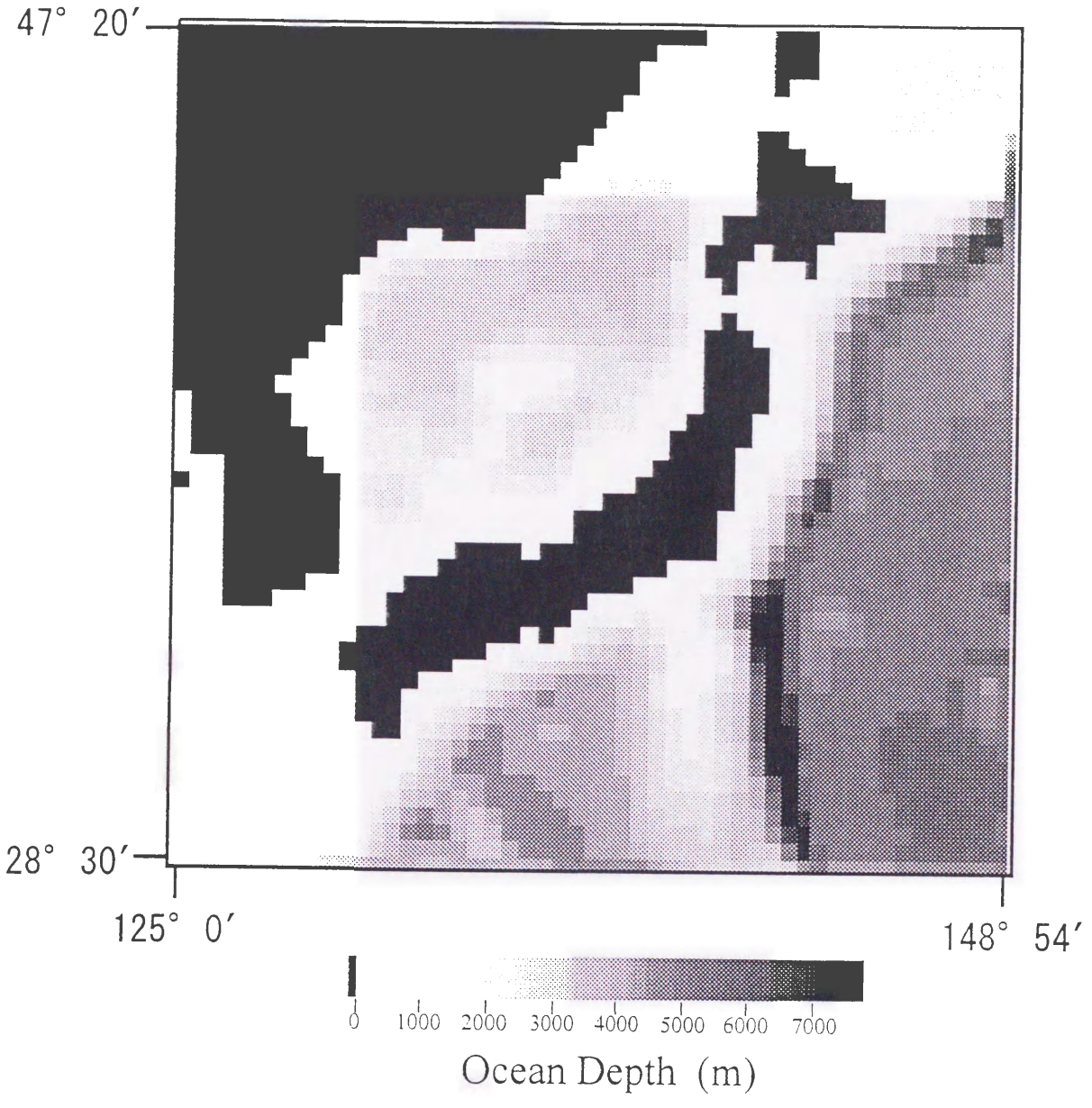

Figure 4-7 Ocean depth used in this study at the period of 32 min

Table 4-2 Configuration of each conductance and depth of sea water

Depth of Sea	Mean value
0 < d	(1000 ohm. m)
-100 < d < 0	50 m
-200 < d < -100	150 m
-400 < d < -200	300 m
-700 < d < -400	550 m
-1000 < d < -700	850 m
-1500 < d < -1000	1250 m
-2000 < d < -1500	1750 m
-2500 < d < -2000	2250 m
-3000 < d < -2500	2750 m
-3500 < d < -3000	3250 m
-4000 < d < -3500	3750 m
-4500 < d < -4000	4250 m
-5000 < d < -4500	4750 m
-5500 < d < -5000	5250 m
-6000 < d < -5500	5750 m
-6500 < d < -6000	6250 m
-7000 < d < -6500	6750 m
-7500 < d < -7000	7250 m
d < -7500	7750 m

conductance = (depth × σ_{sw} + (10000 - depth) × σ_L) / (skin depth × σ_L)

σ_{sw} = 3.3S / m

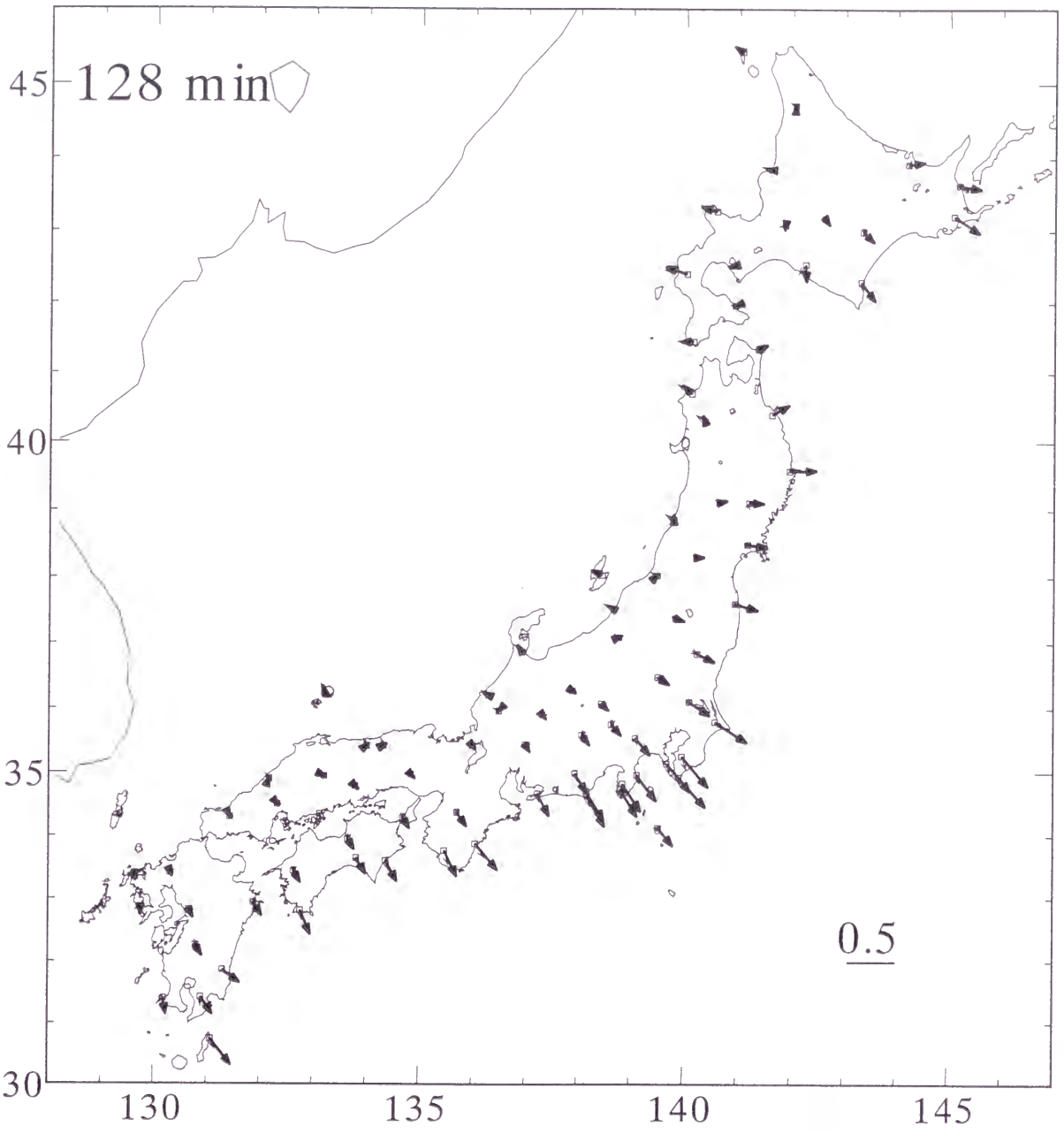

Figure 4-8 (a) Induction arrows of the thin-sheet model calculation
The thick line with a large arrowhead shows a real part and the thin line with a small arrowhead shows an imaginary part

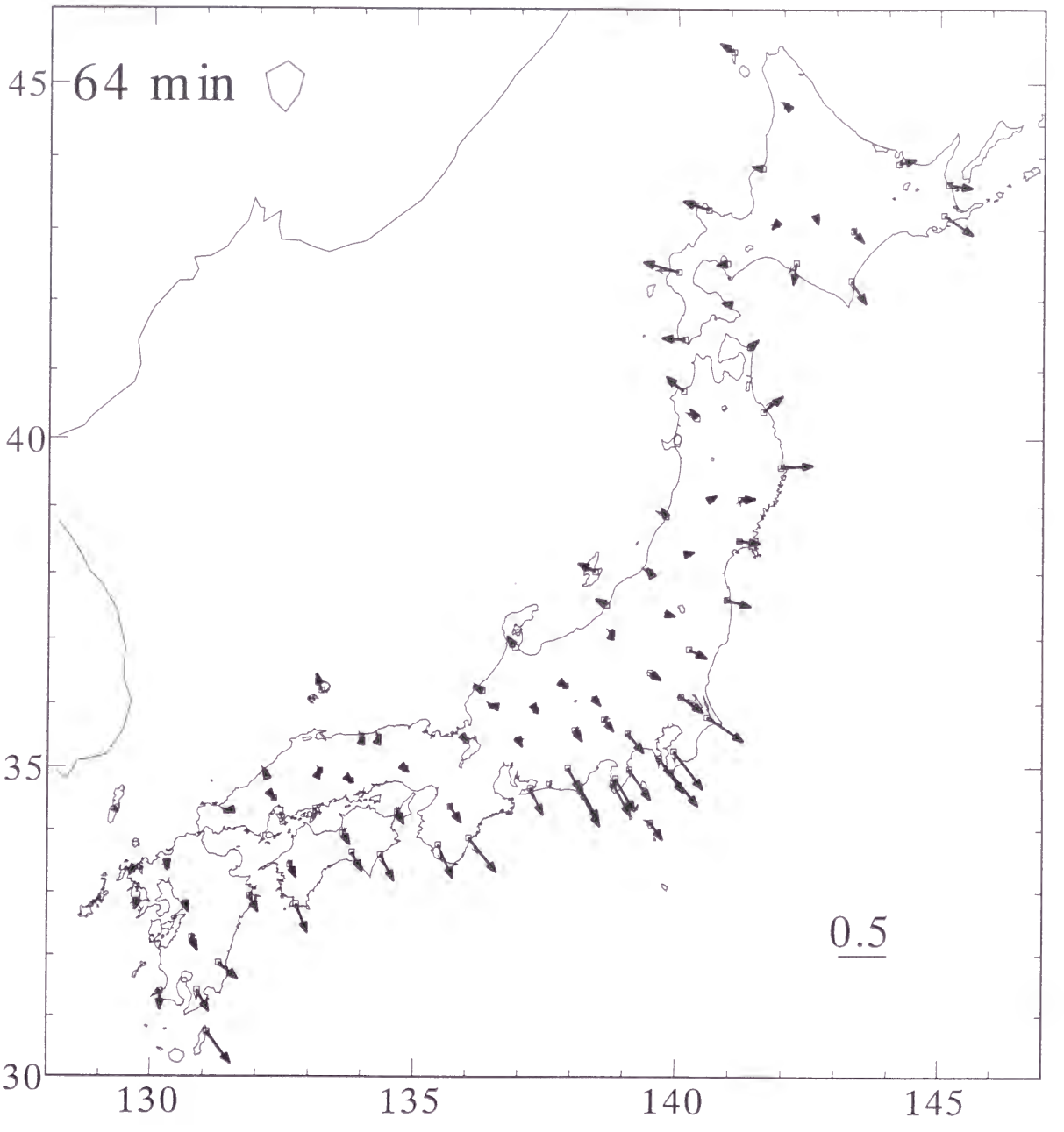

Figure 4-8 (b) Induction arrows of the thin-sheet model calculation
The thick line with a large arrowhead shows a real part and the thin line with a small arrowhead shows an imaginary part

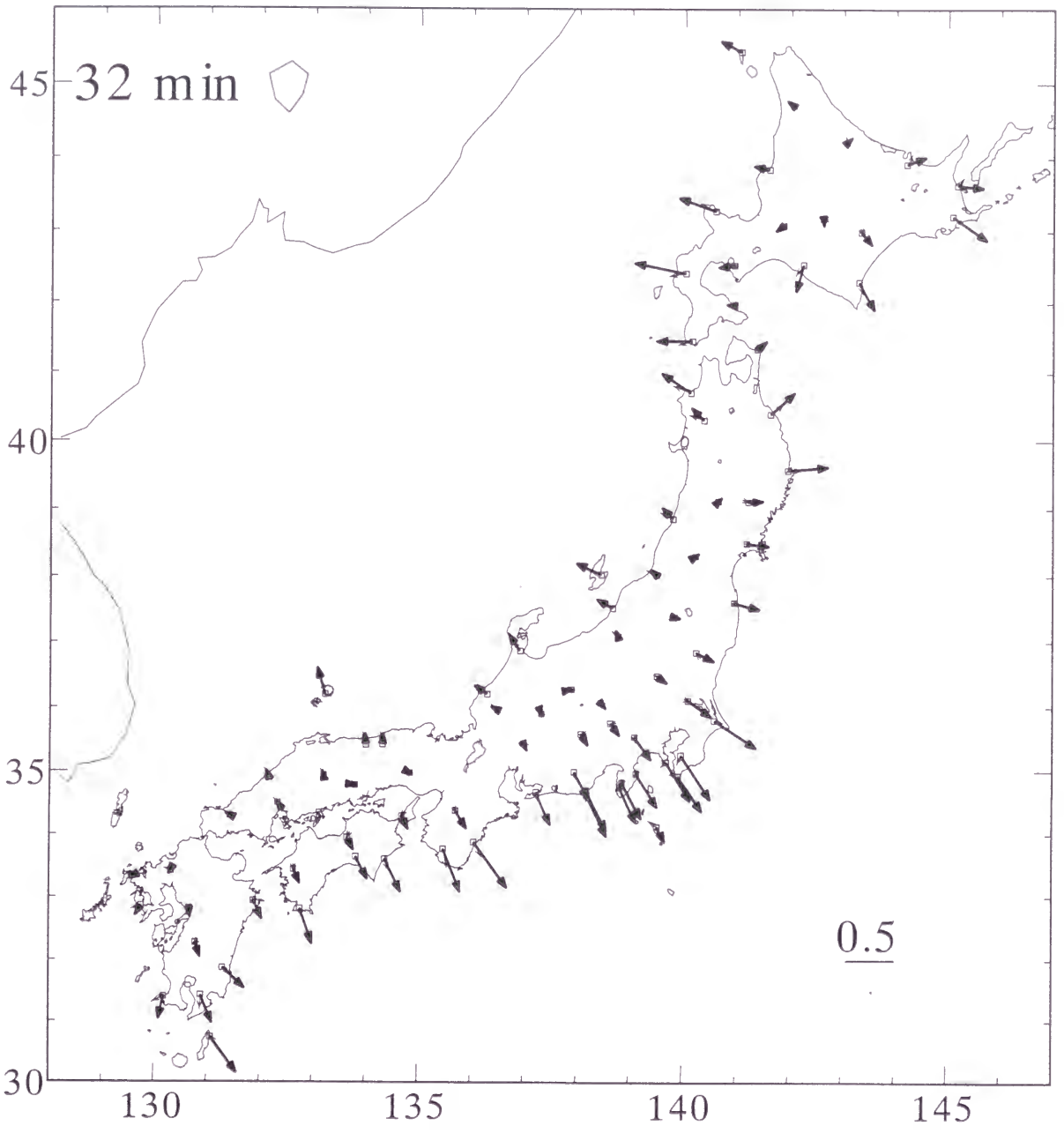

Figure 4-8 (c) Induction arrows of the thin-sheet model calculation
The thick line with a large arrowhead shows a real part and the thin line with a small arrowhead shows an imaginary part

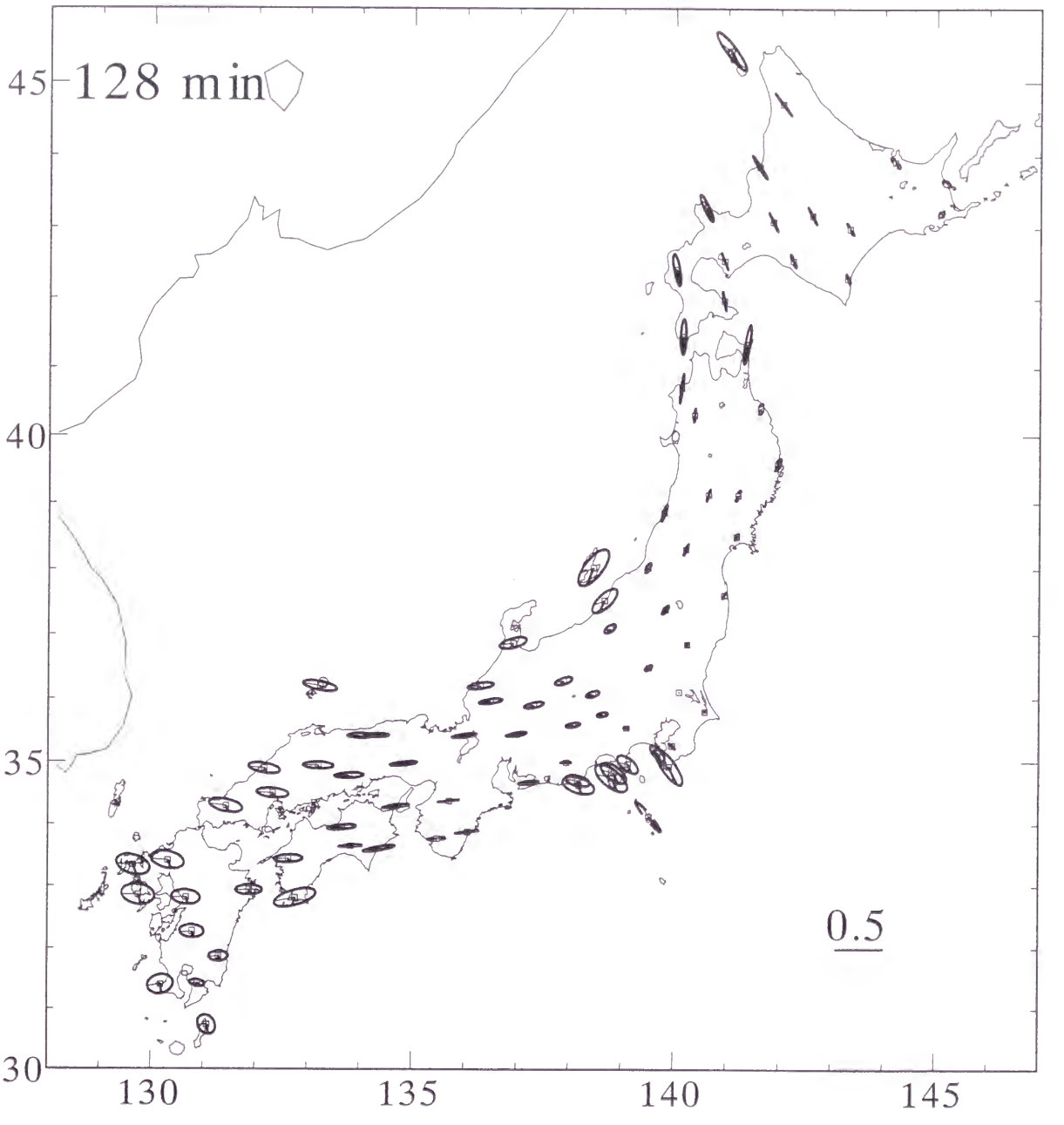

Figure 4-9 (a) Anomalous ellipses of the horizontal transfer functions of the thin-sheet model calculation (real part)

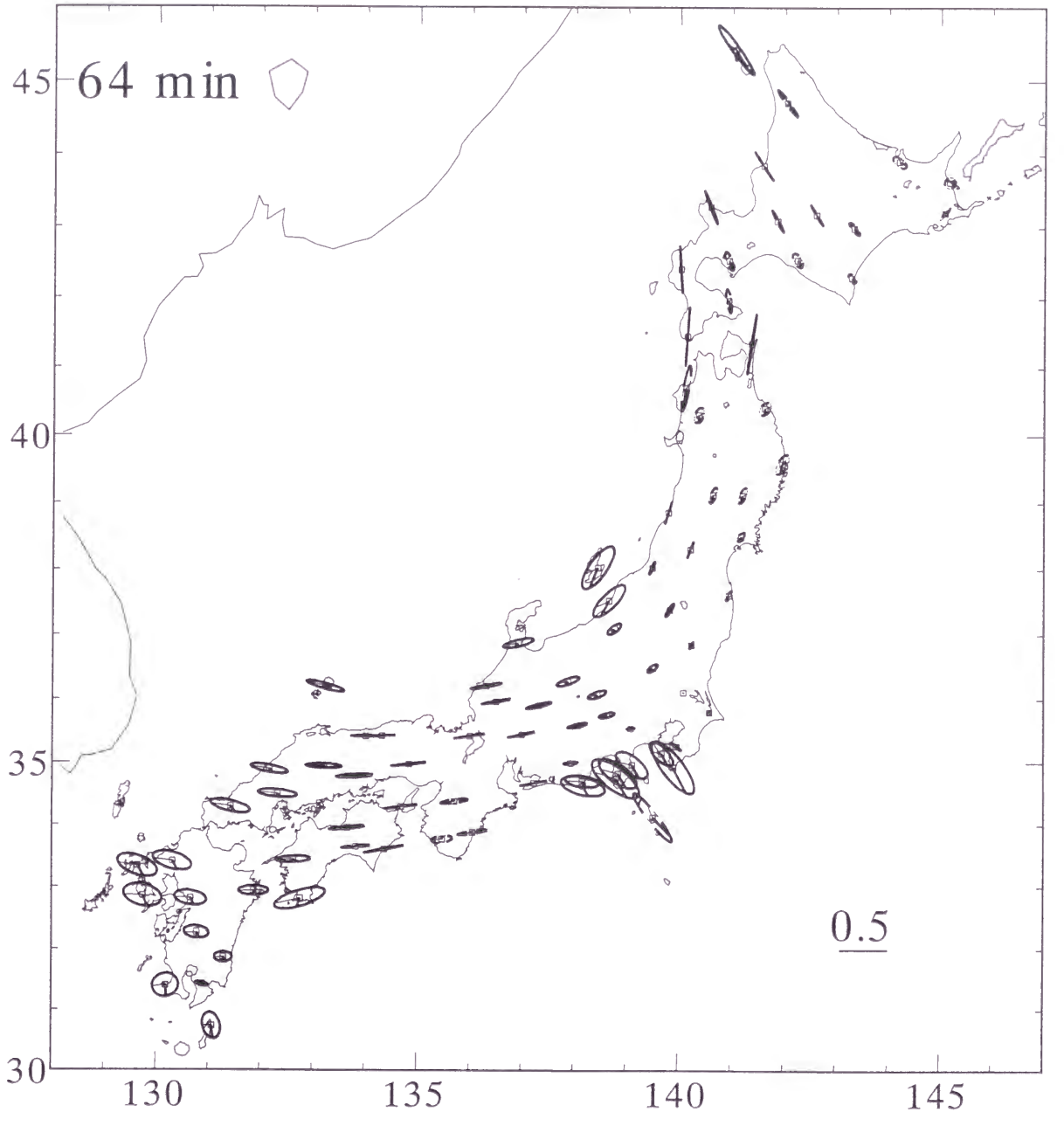

Figure 4-9 (b) Anomalous ellipses of the horizontal transfer functions of the thin-sheet model calculation (real part)

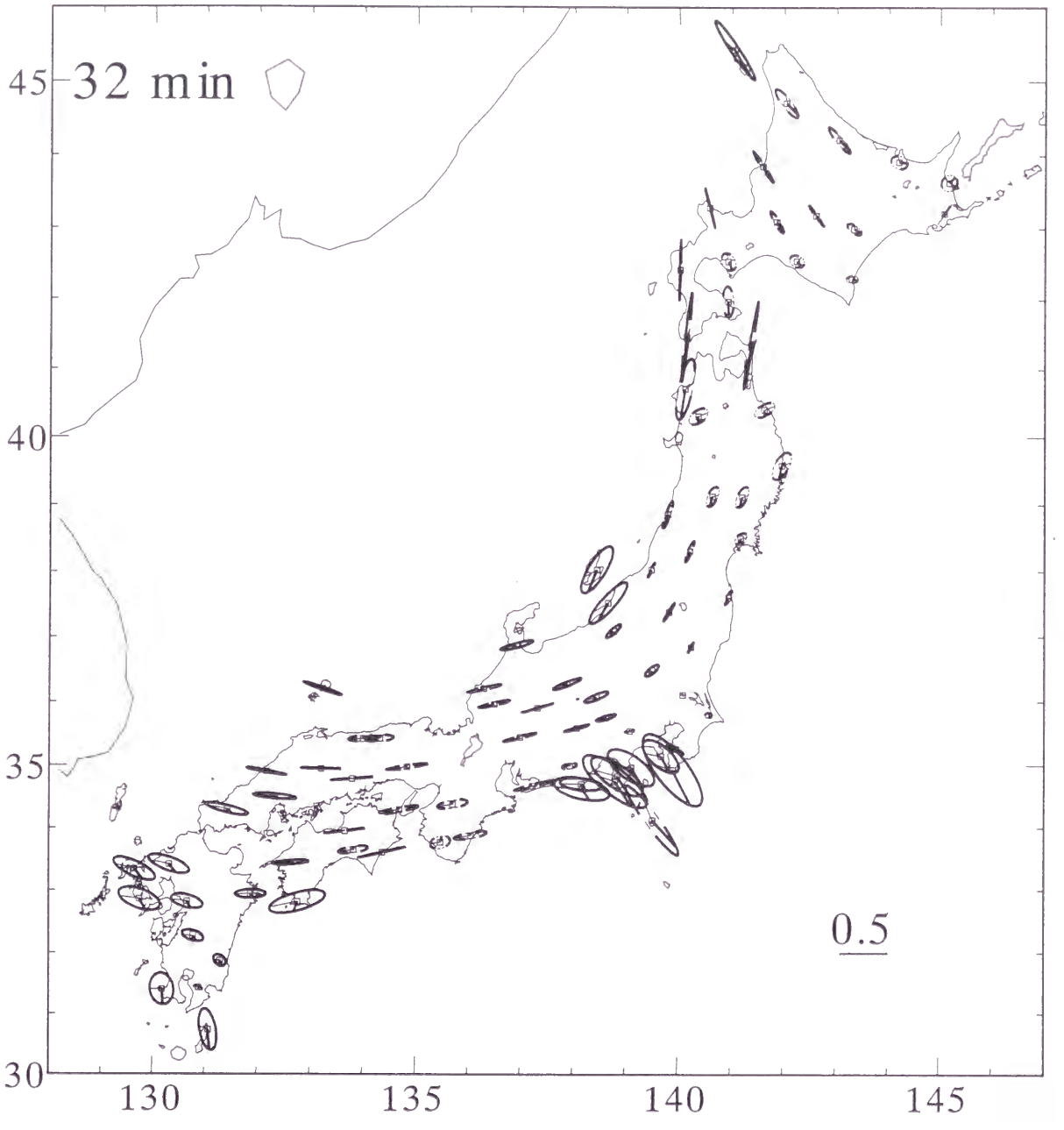

Figure 4-9 (c) Anomalous ellipses of the horizontal transfer functions of the thin-sheet model calculation (real part)

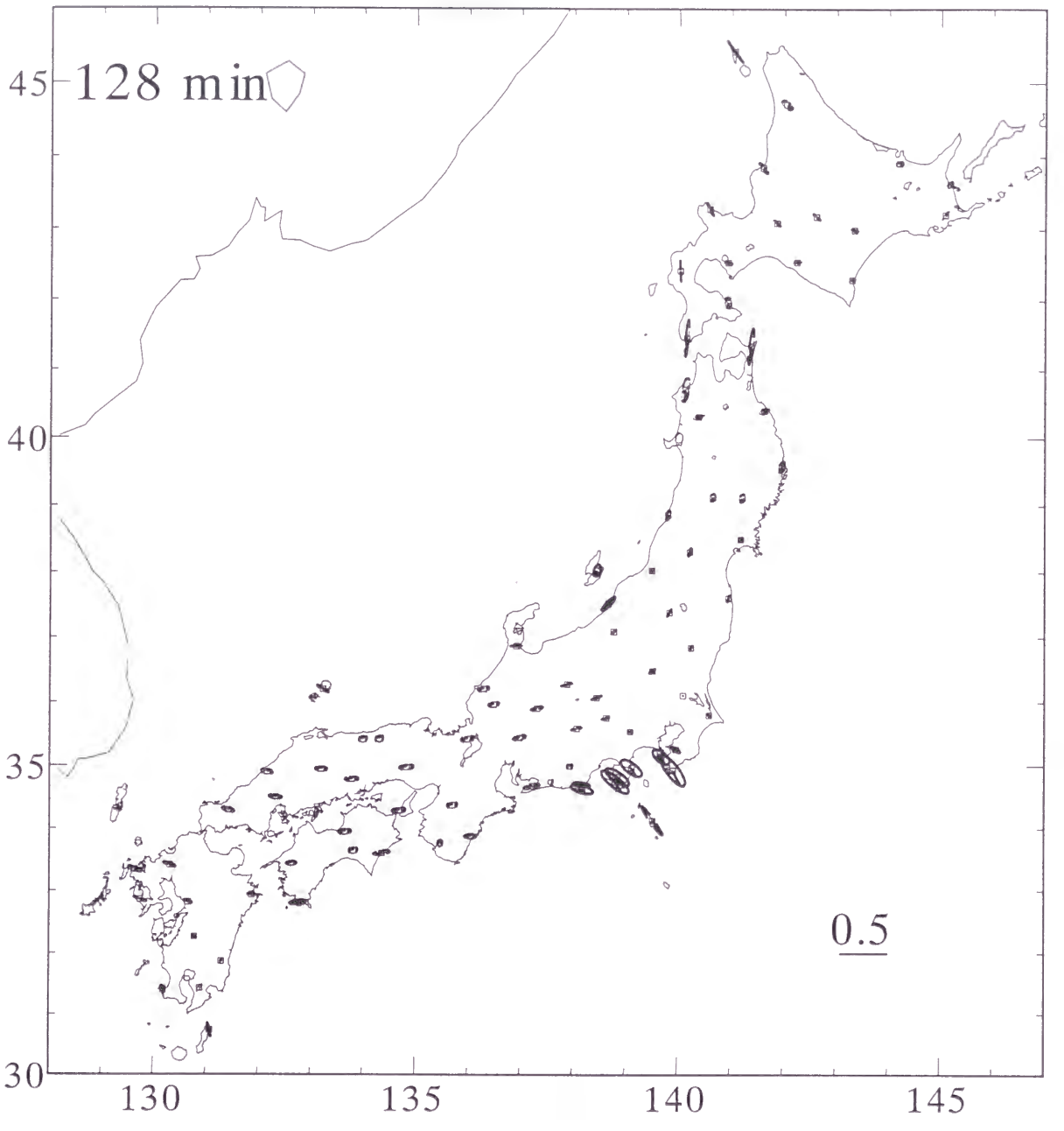

Figure 4-10 (a) Anomalous ellipses of the horizontal transfer functions of the thin-sheet model calculation (imaginary part)

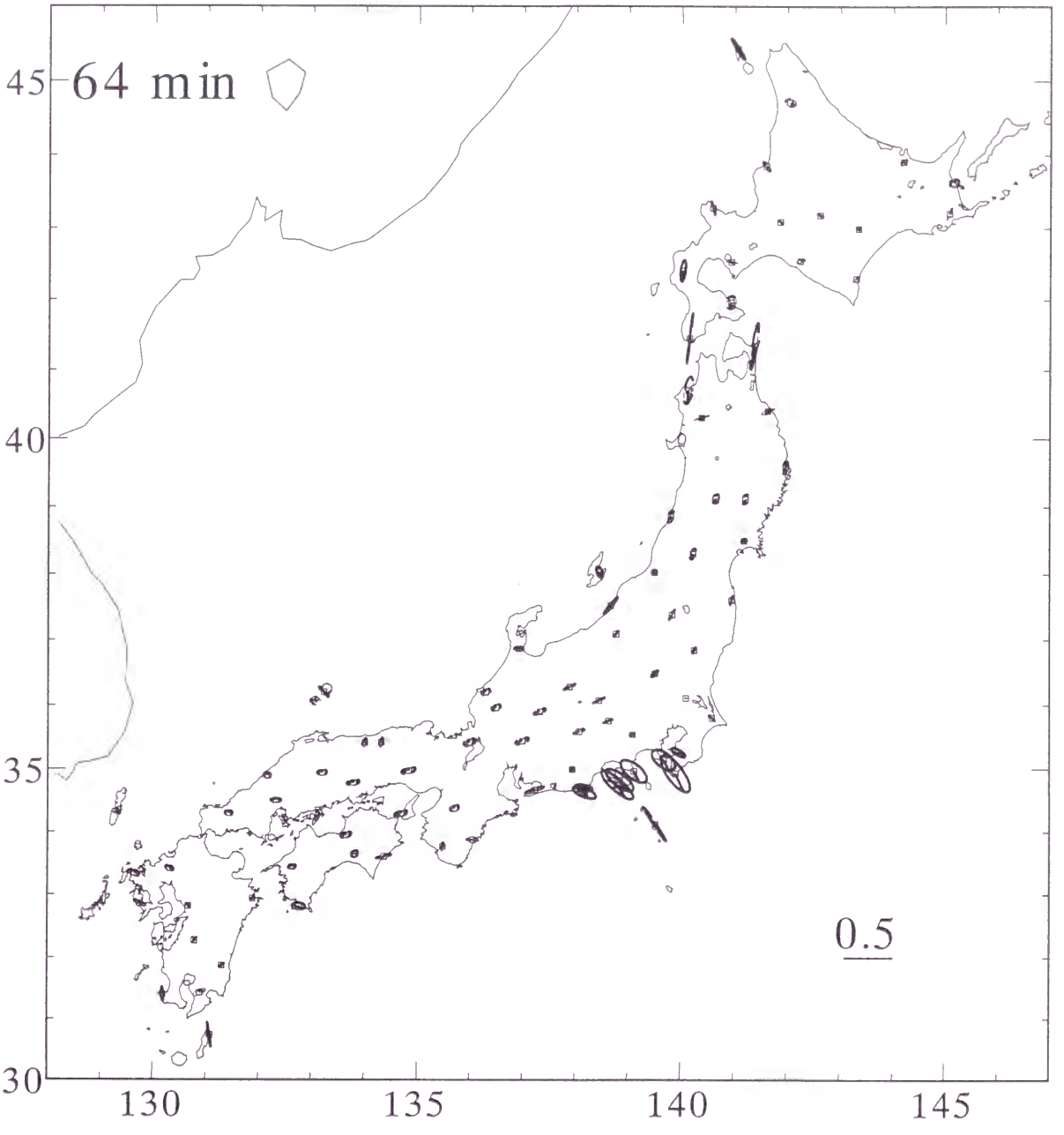

Figure 4-10 (b) Anomalous ellipses of the horizontal transfer functions of the thin-sheet model calculation (imaginary part)

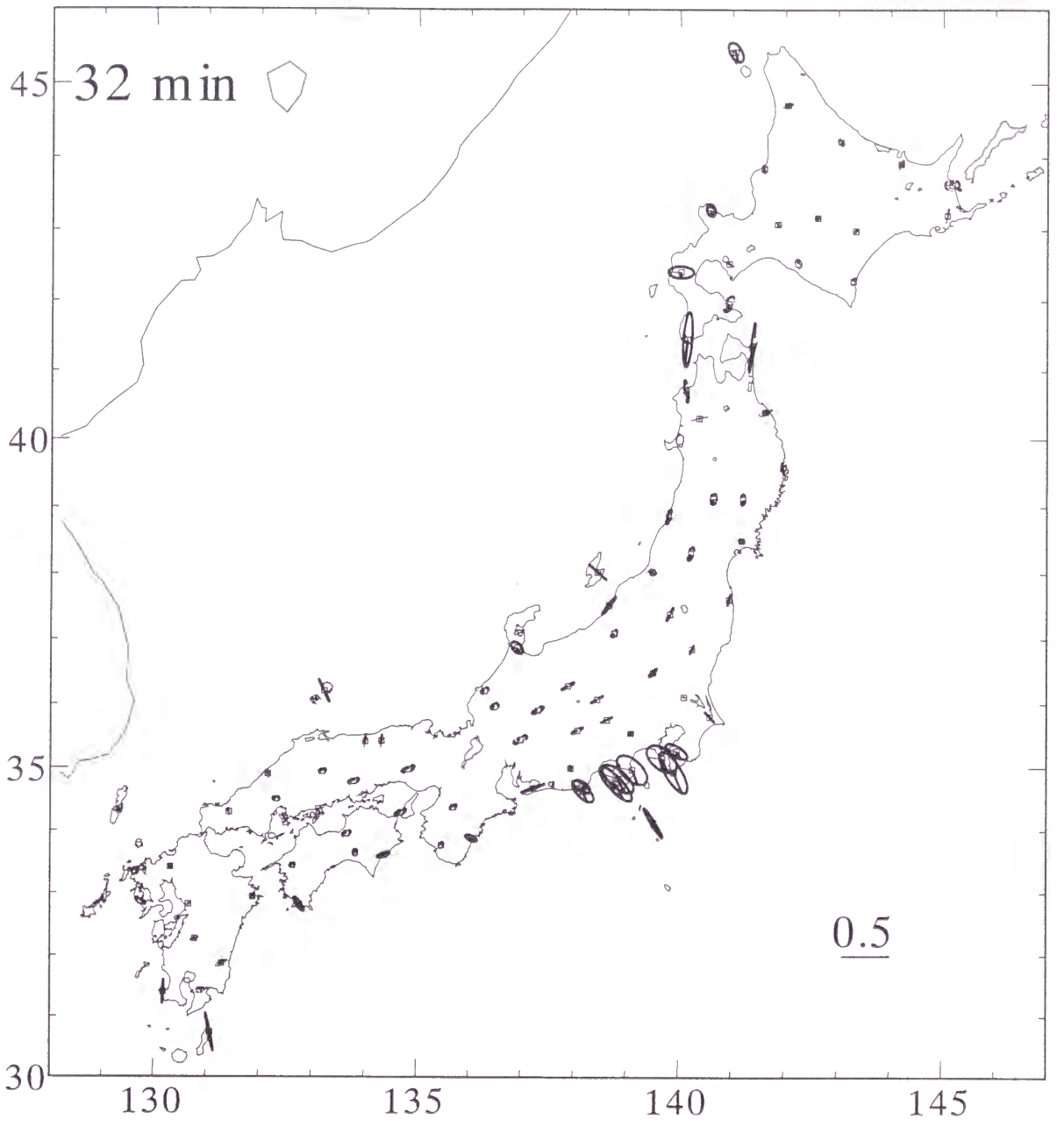

Figure 4-10 (c) Anomalous ellipses of the horizontal transfer functions of the thin-sheet model calculation (imaginary part)

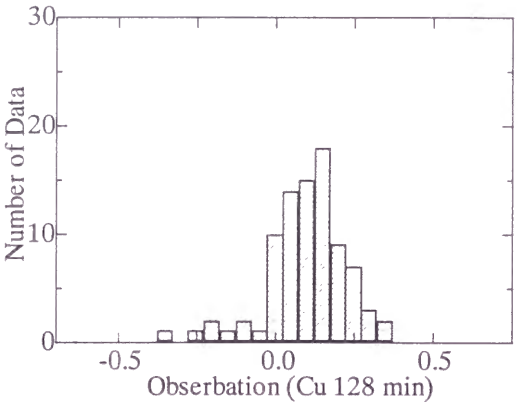

mean=.0989 SD=.1249

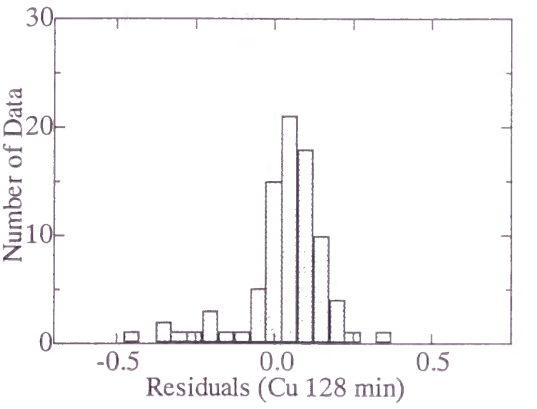

mean=.0457 SD=.1652

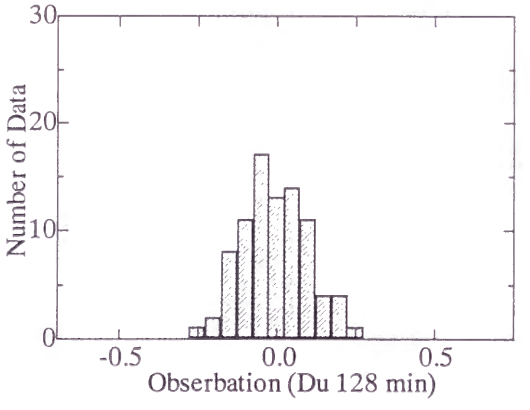

mean=-.0041 SD=.1031

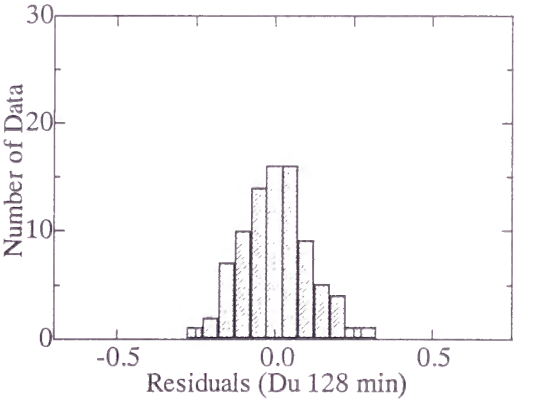

mean=.0025 SD=.1058

Figure 4-11 (a) Histograms of the observed and the residual transfer functions. Each mean value and SD are shown. The real part is donated with suffix *u*.

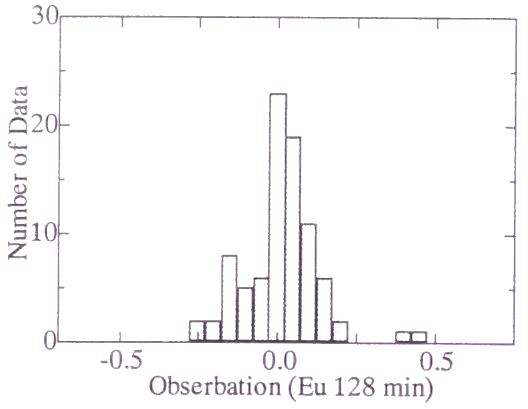

mean-.0168 SD=.1173

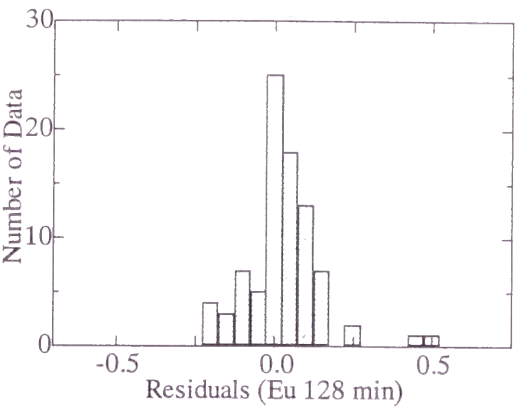

mean=.0287 SD=.1171

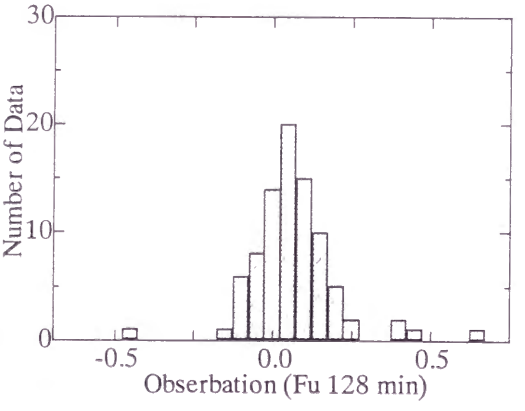

mean=.0671 SD=.1399

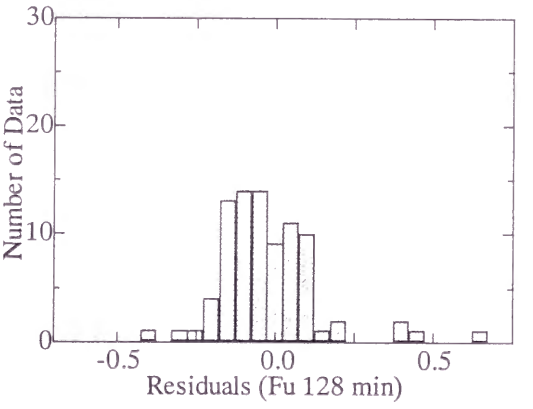

mean=-.0074 SD=.1912

Figure 4-11 (b) Histograms of the observed and the residual transfer functions. Each mean value and SD are shown. The real part is donated with suffix *u*.

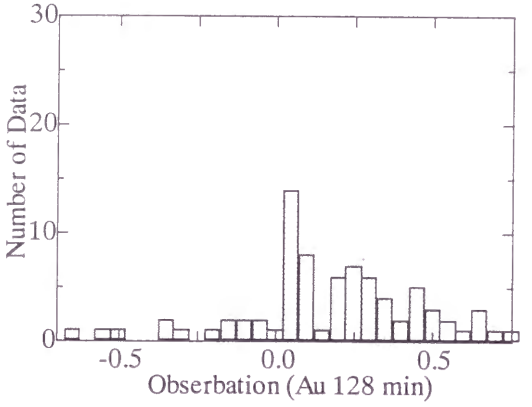

mean=.2130 SD=.3671

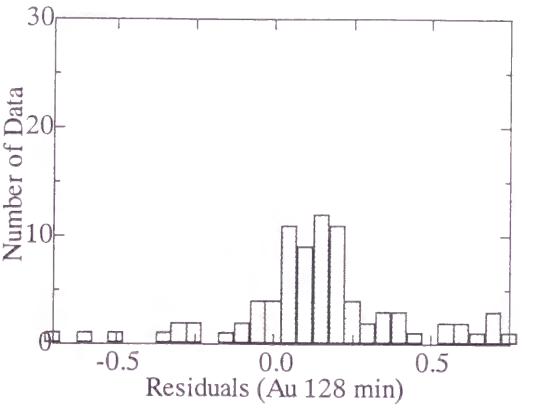

mean=.1290 SD=.2823

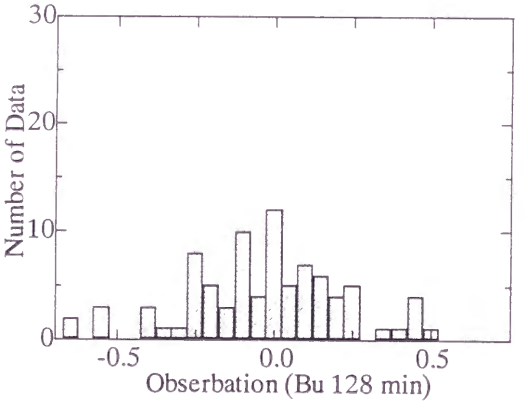

mean=-.0295 SD=.2477

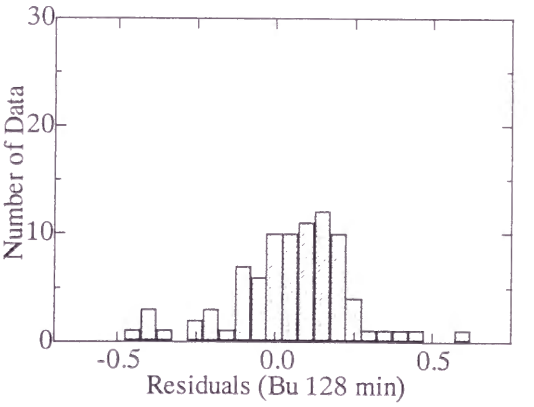

mean=.0468 SD=.1829

Figure 4-11 (c) Histograms of the observed and the residual transfer functions. Each mean value and SD are shown. The real part is donated with suffix *u*.

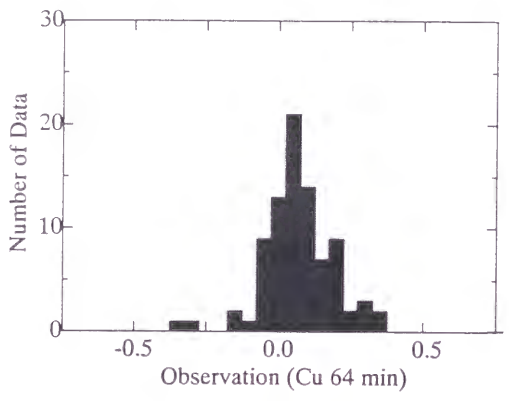

mean=.1170 SD=.1197

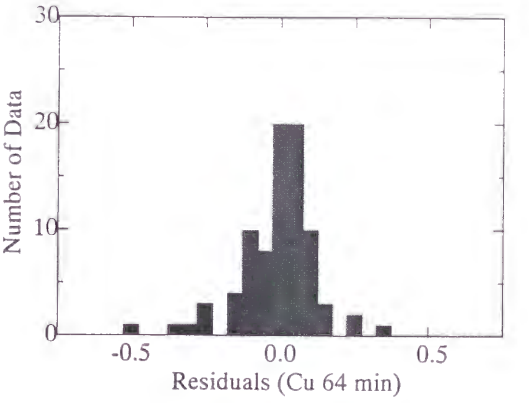

mean=.0529 SD=.1624

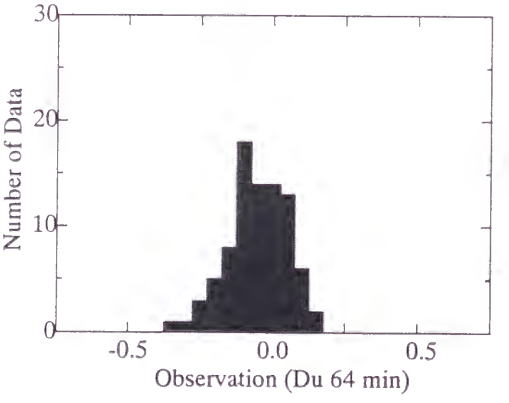

mean=-.0035 SD=.1004

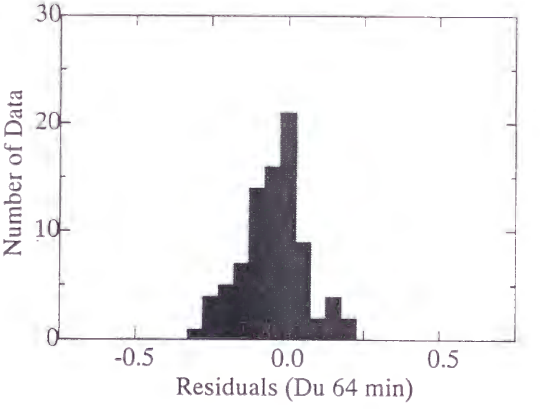

mean=.0050 SD=.1021

Figure 4-11 (d) Histograms of the observed and the residual transfer functions. Each mean value and SD are shown. The real part is donated with suffix *u*.

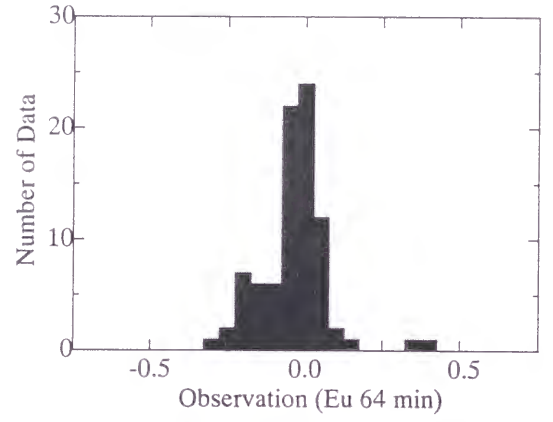

mean=.0125 SD=.1089

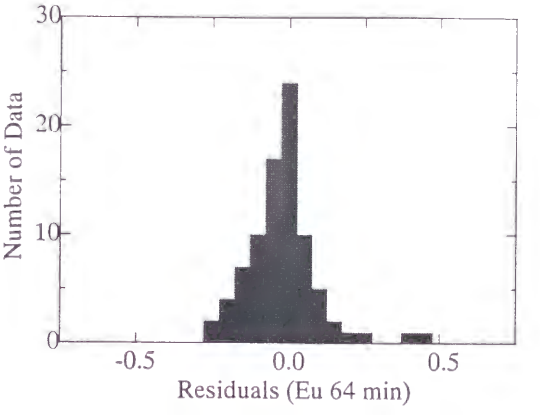

mean=.0301 SD=.1154

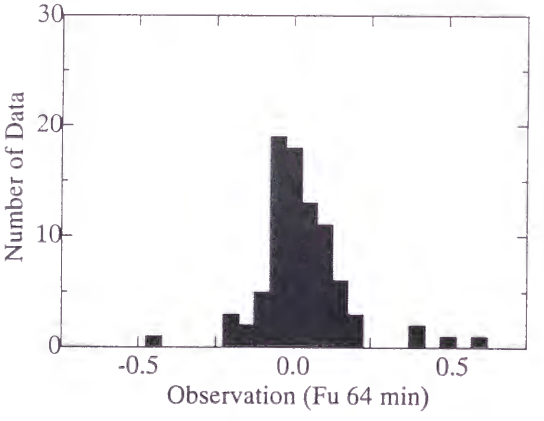

mean=.0755 SD=.1408

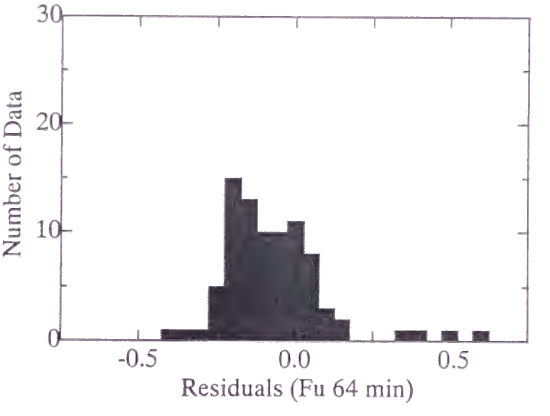

mean=-.0084 SD=.1994

Figure 4-11 (e) Histograms of the observed and the residual transfer functions. Each mean value and SD are shown. The real part is donated with suffix *u*.

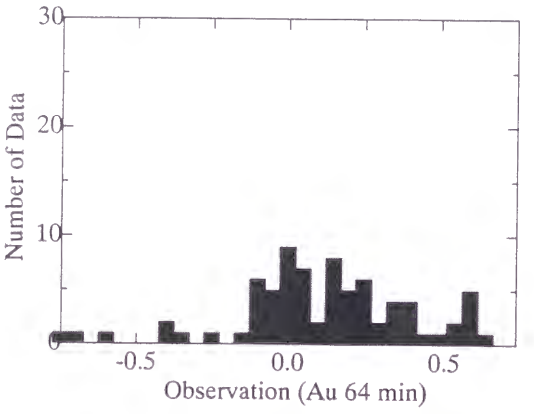

mean=.2068 SD=.3824

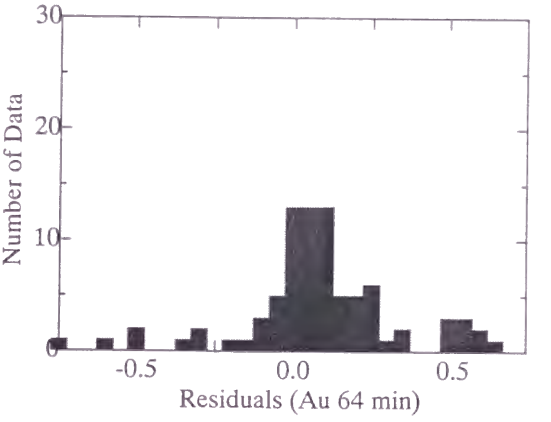

mean=.1187 SD=.2744

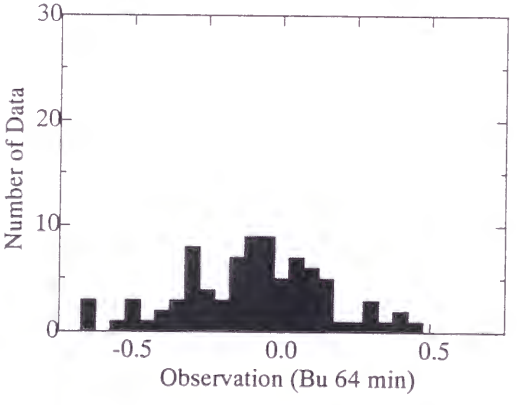

mean=-.0409 SD=.2422

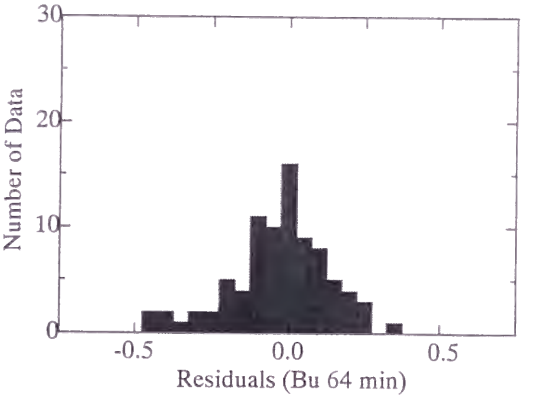

mean=.0220 SD=.1595

Figure 4-11 (f) Histograms of the observed and the residual transfer functions. Each mean value and SD are shown. The real part is donated with suffix *u*.

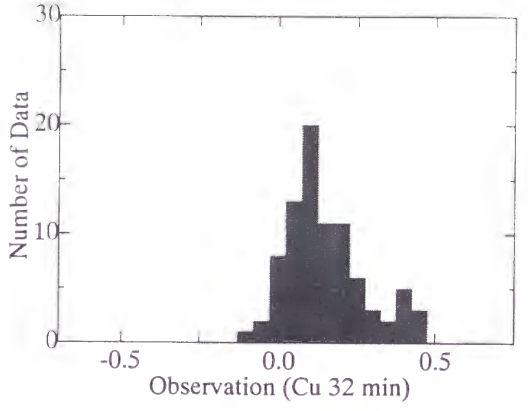

mean=.1498 sd=.1256

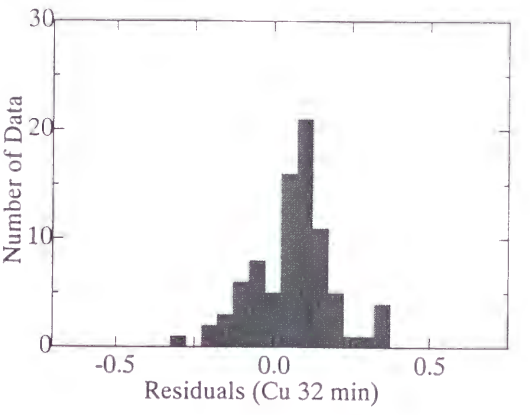

mean=.0745 sd=.1590

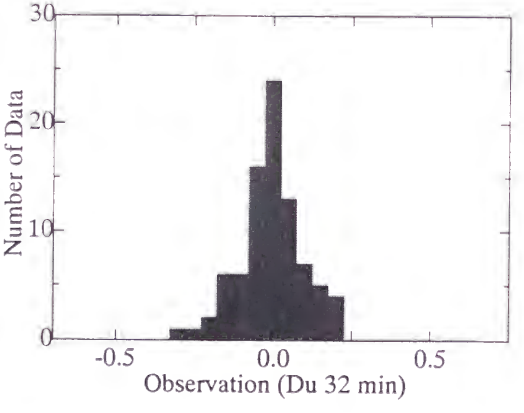

mean=-.0038 sd=.1002

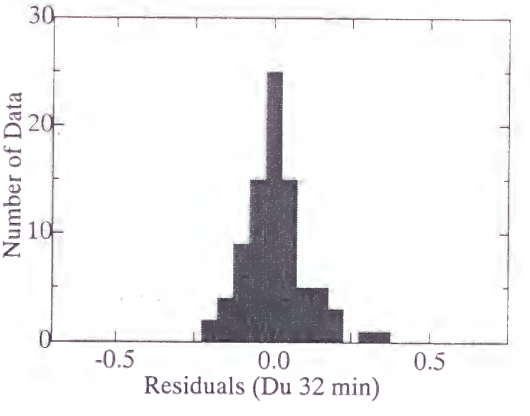

mean=.0081 sd=.0951

Figure 4-11 (g) Histograms of the observed and the residual transfer functions. Each mean value and SD are shown. The real part is donated with suffix *u*.

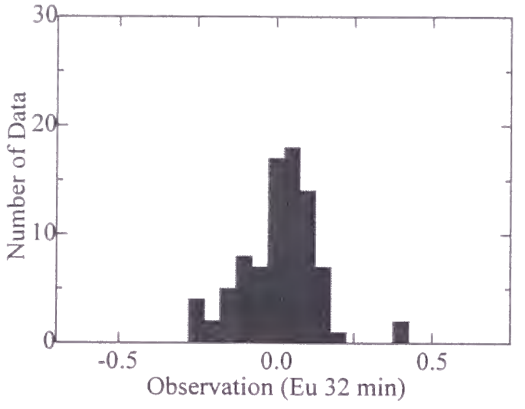

mean=.0104 sd=.1219

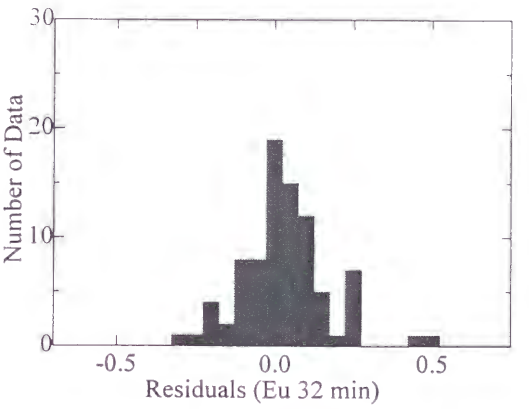

mean=.0325 sd=.1333

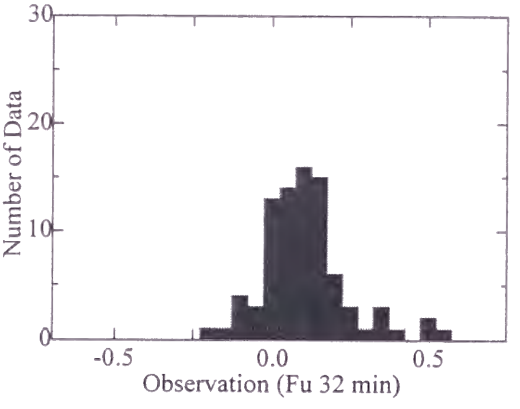

mean=.1158 sd=.1556

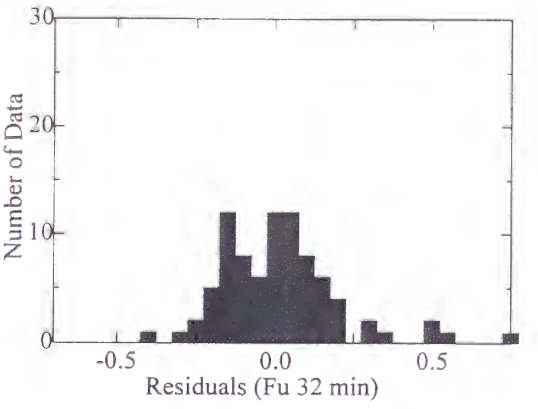

mean=.0284 sd=.2193

Figure 4-11 (h) Histograms of the observed and the residual transfer functions. Each mean value and SD are shown. The real part is donated with suffix *u*.

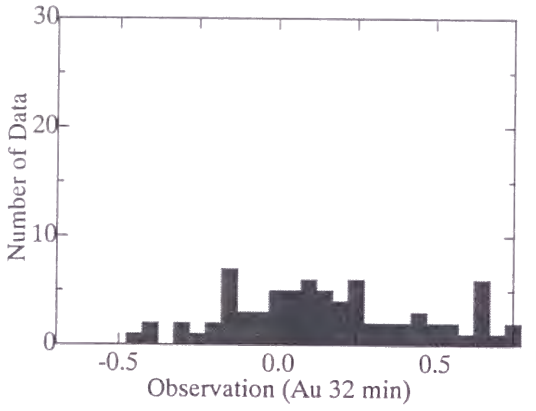

mean=.1381 sd=.4501

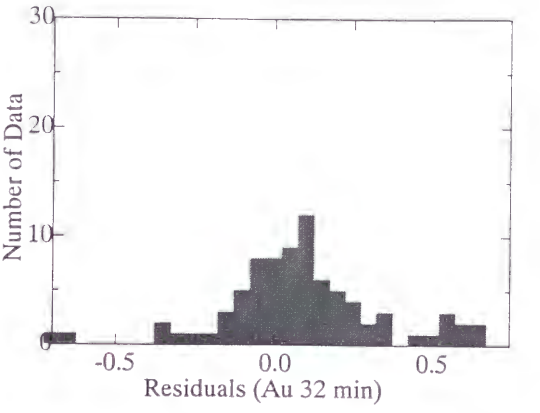

mean=.0473 sd=.3248

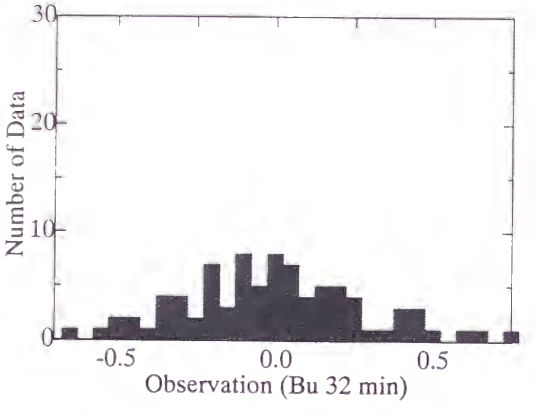

mean=-.0055 sd=.2825

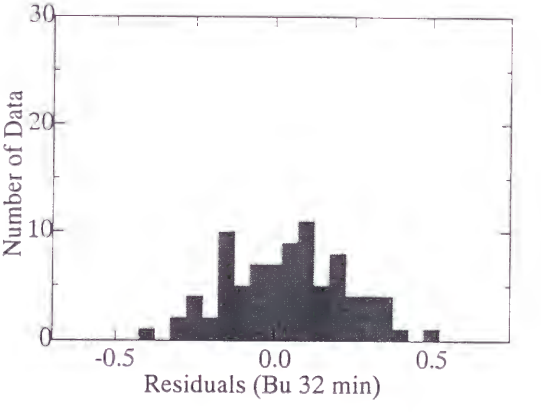

mean=.0433 sd=.1854

Figure 4-11 (i) Histograms of the observed and the residual transfer functions. Each mean value and SD are shown. The real part is donated with suffix *u*.

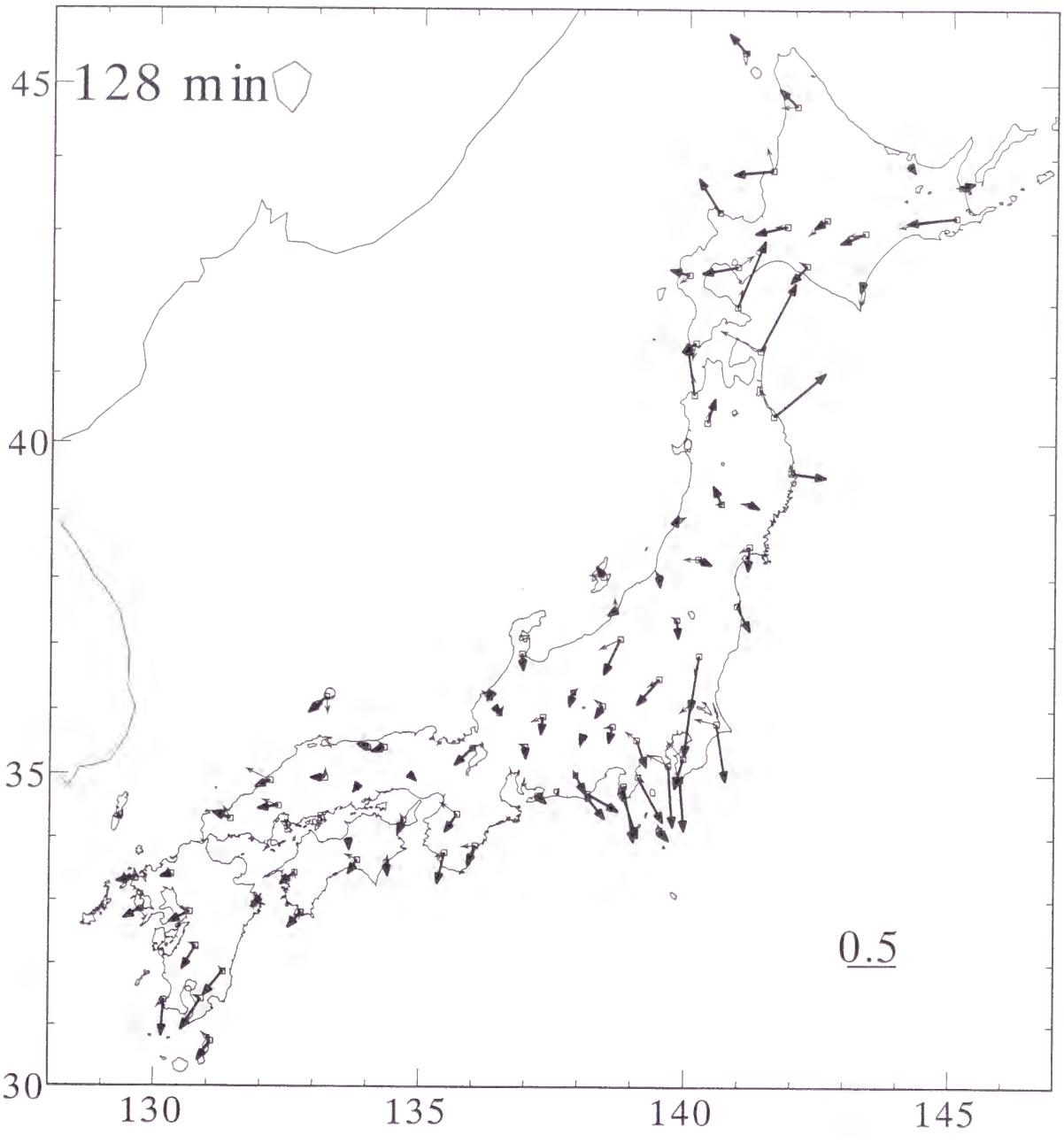

Figure 4-12 (a) Residual remote reference induction arrows
The thick line with a large arrowhead shows a real part and the thin line with a small arrowhead shows an imaginary part.

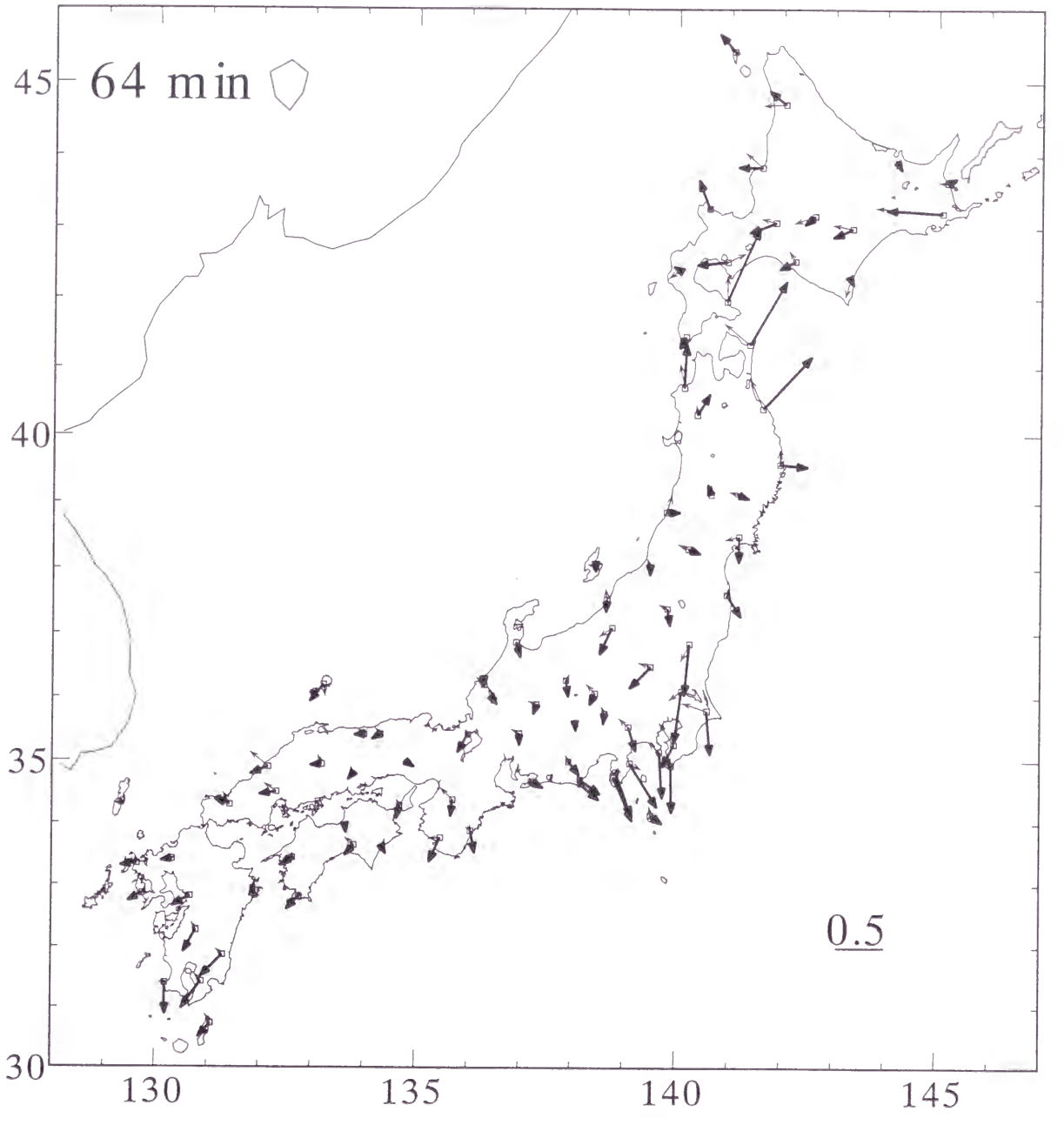

Figure 4-12 (b) Residual remote reference induction arrows
The thick line with a large arrowhead shows a real part and the thin line with a small arrowhead shows an imaginary part.

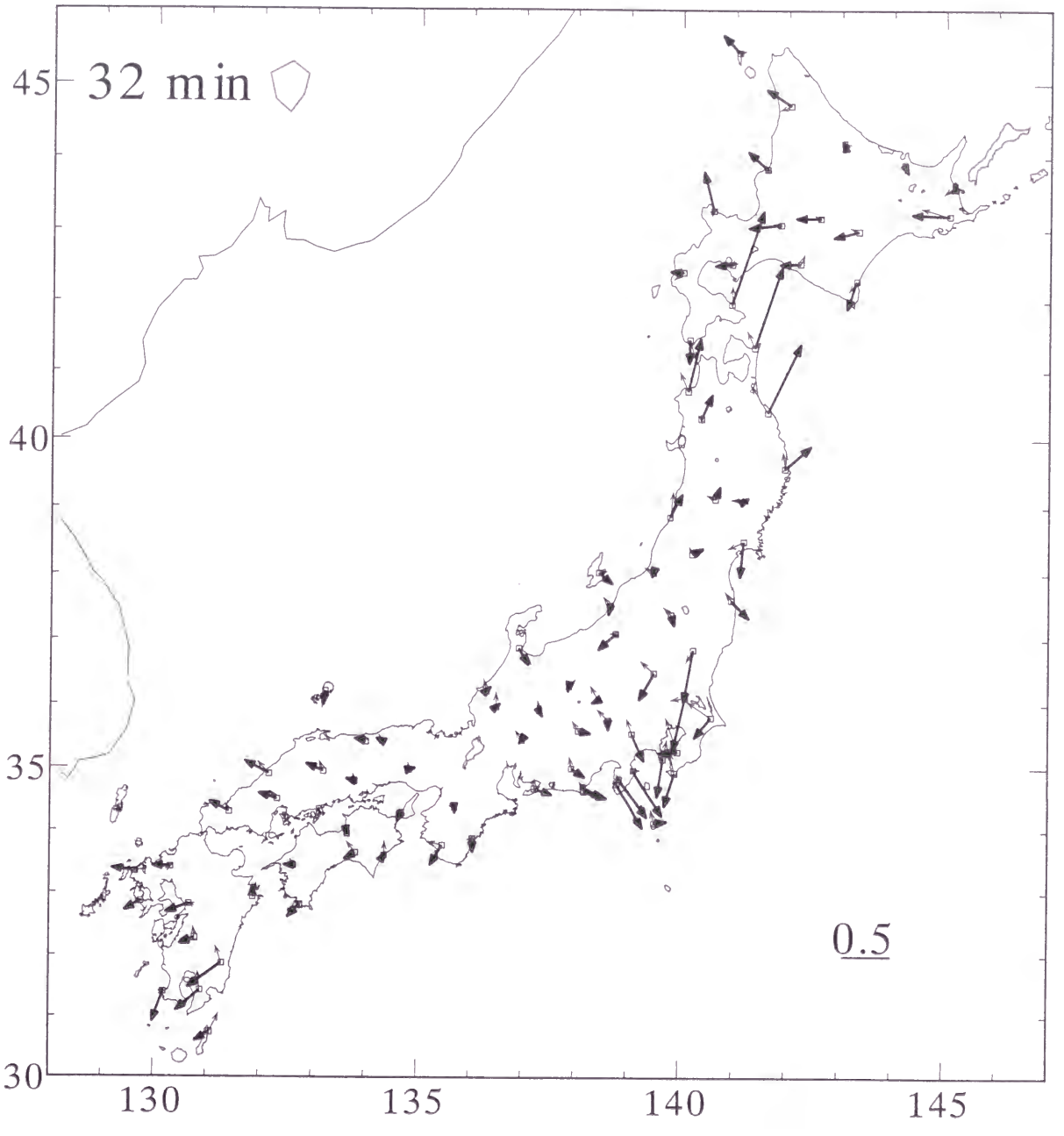

Figure 4-12 (c) Residual remote reference induction arrows
The thick line with a large arrowhead shows a real part and the thin line with a small arrowhead shows an imaginary part.

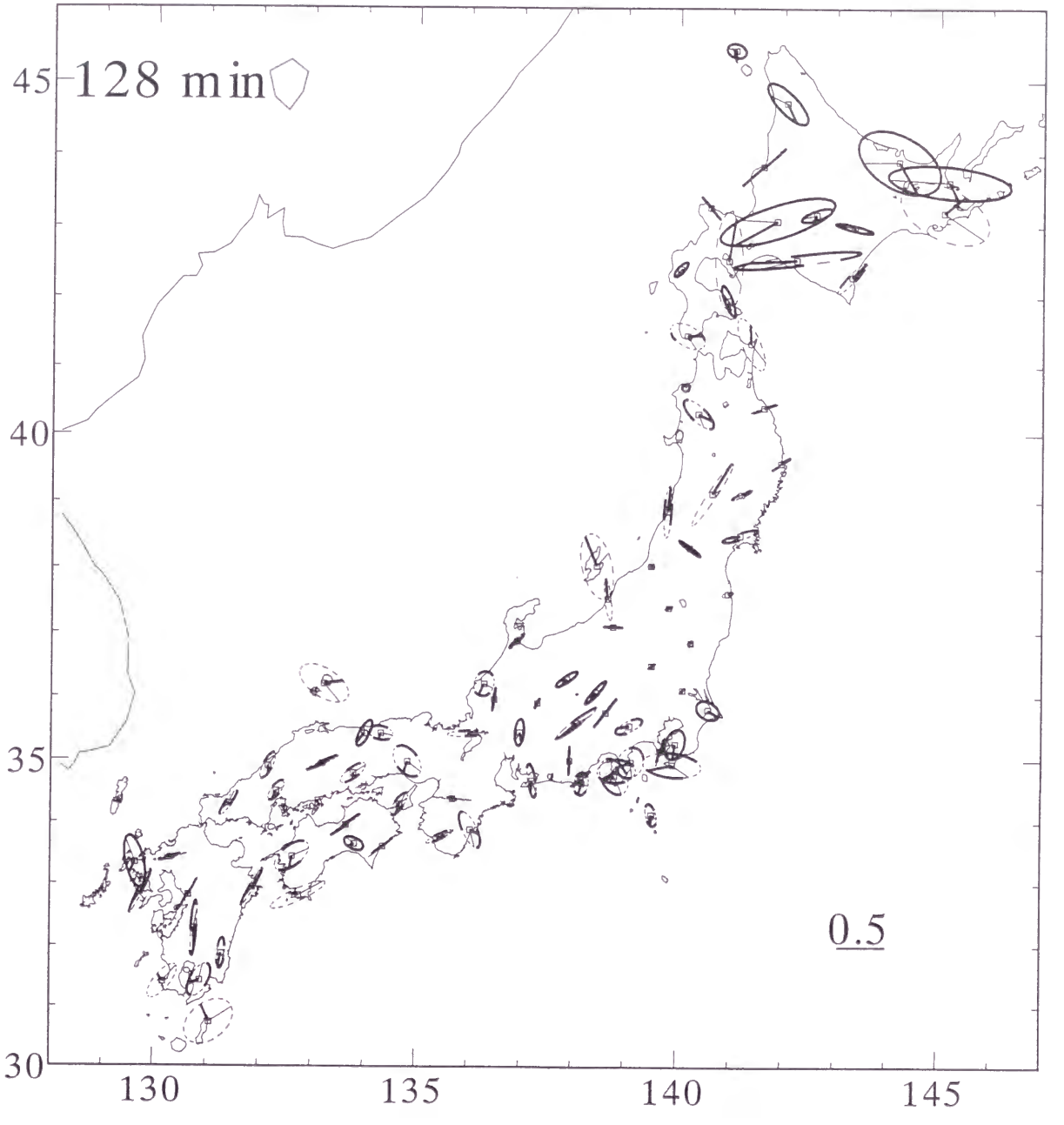

Figure 4-13 (a) Residual anomalous ellipses of the horizontal transfer functions (real part)

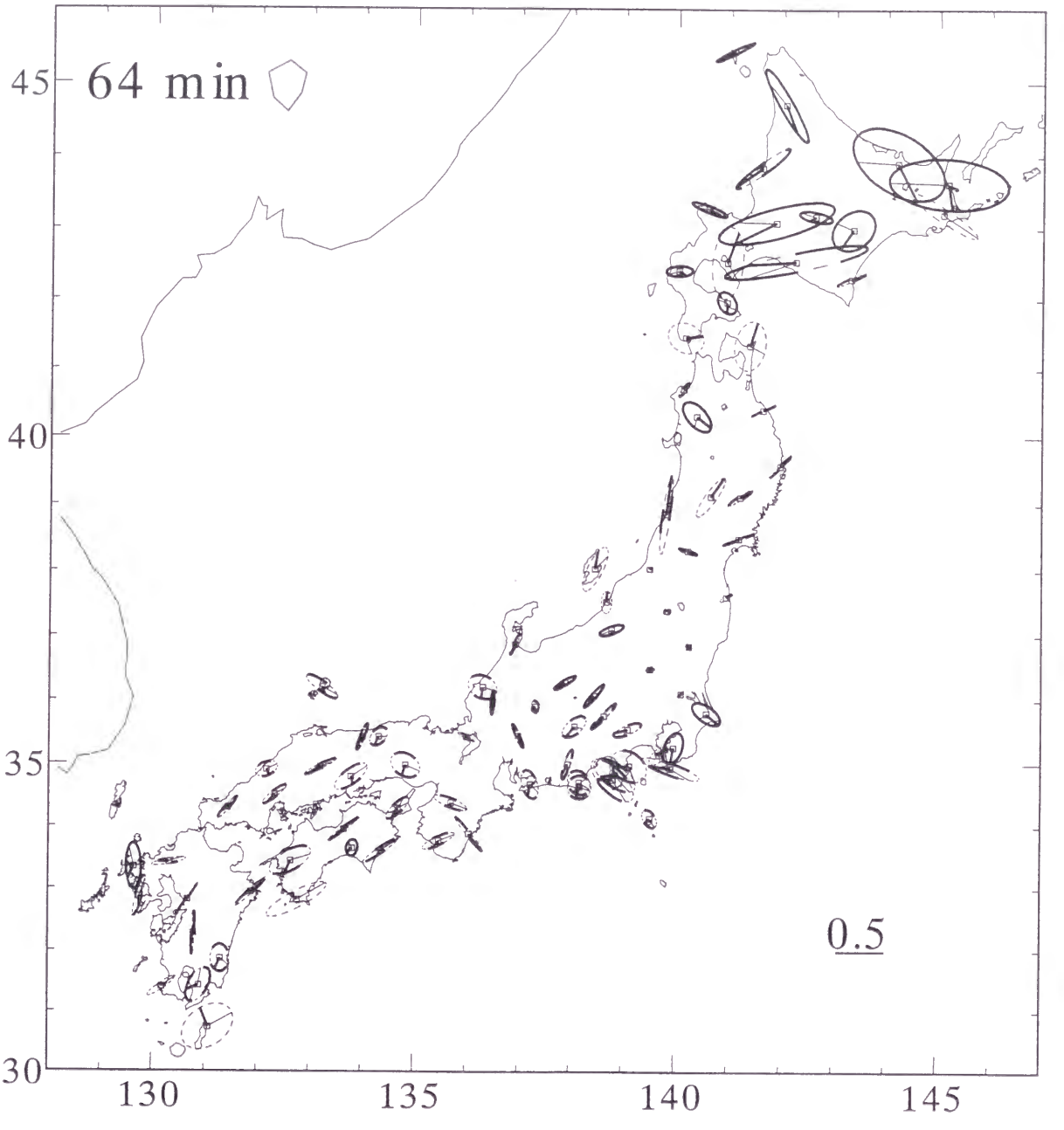

Figure 4-13 (b) Residual anomalous ellipses of the horizontal transfer functions (real part)

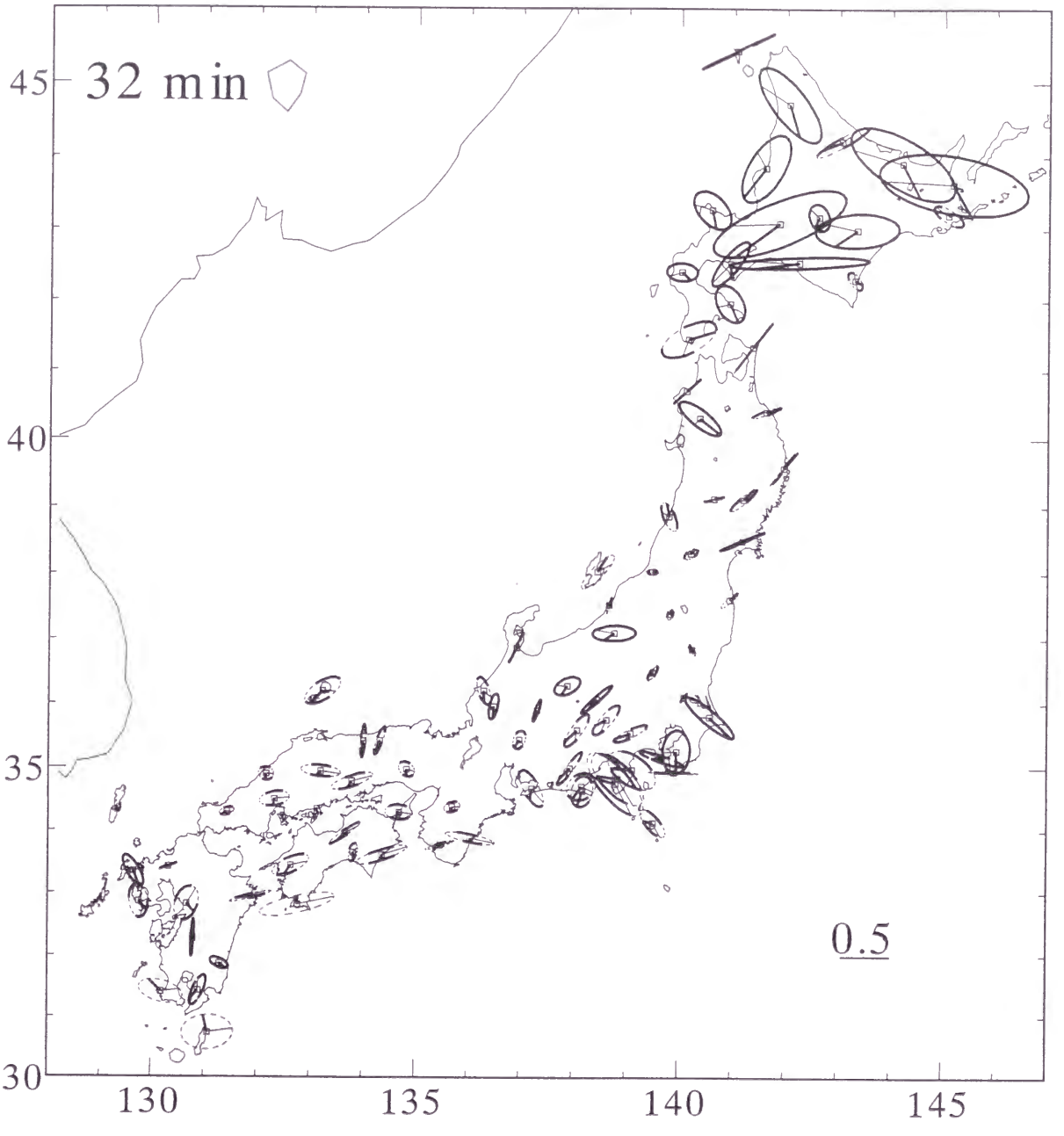

Figure 4-13 (c) Residual anomalous ellipses of the horizontal transfer functions (real part)

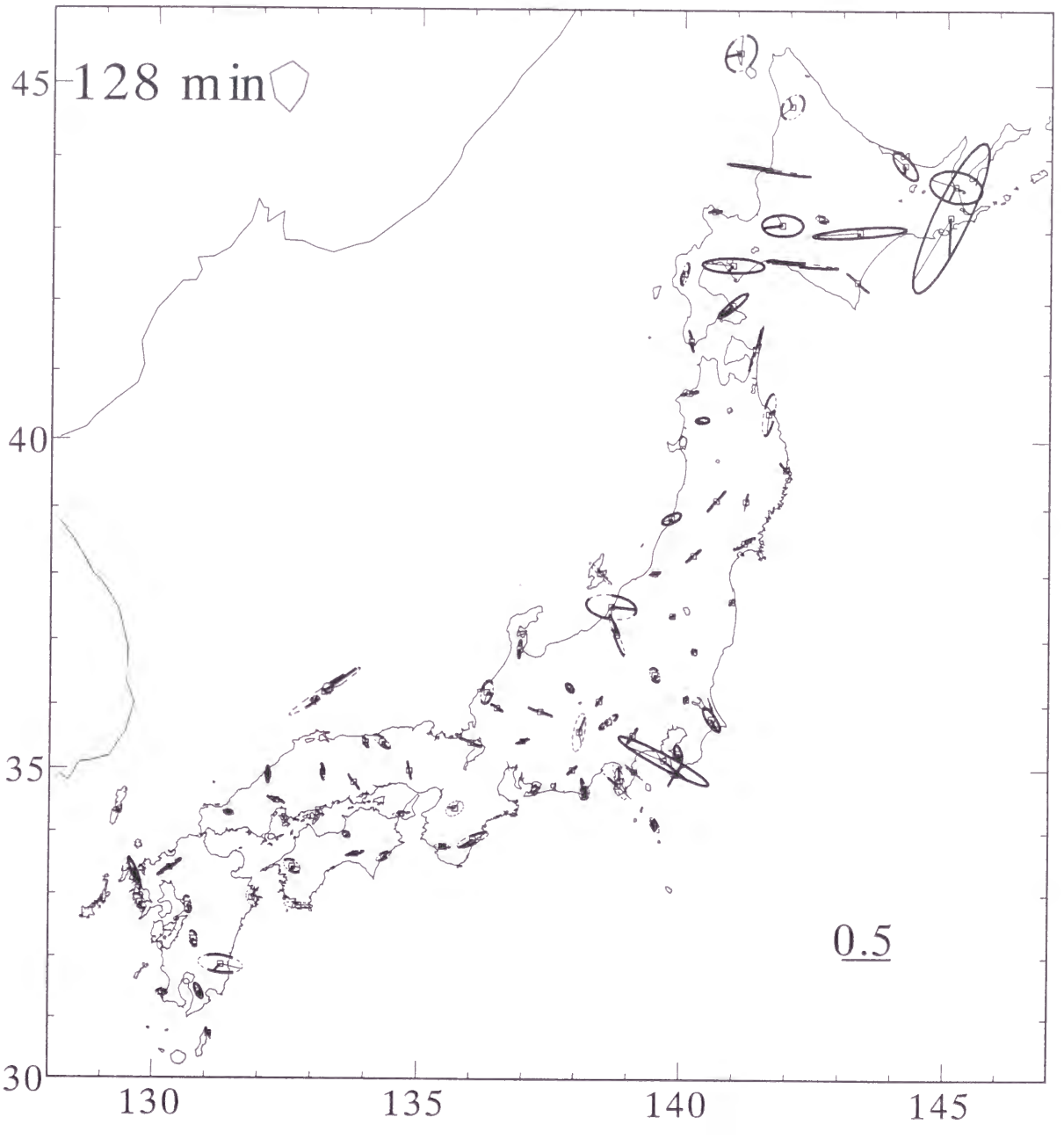

Figure 4-14 (a) Residual anomalous ellipses of the horizontal transfer functions (imaginary part)

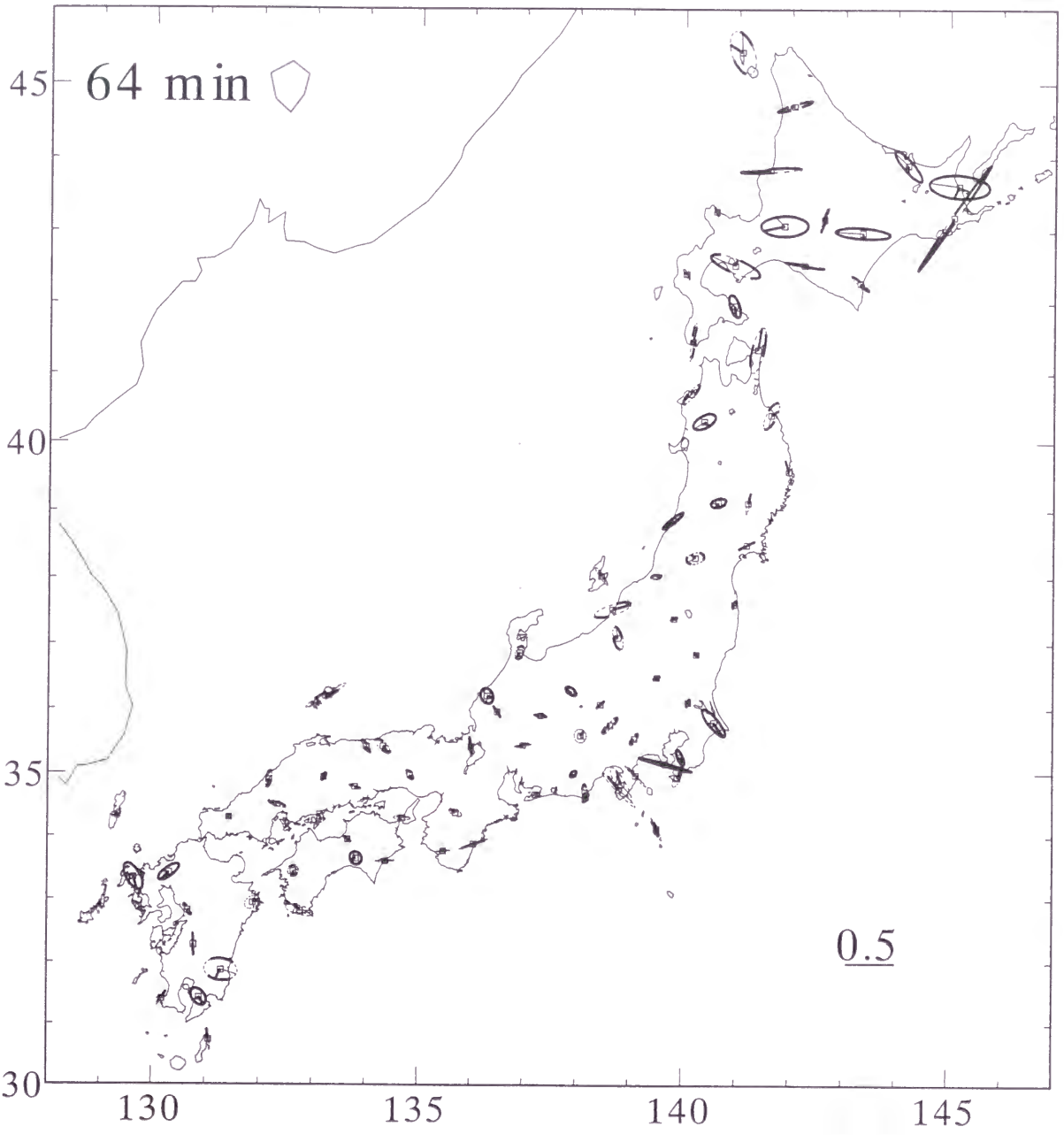

Figure 4-14 (b) Residual anomalous ellipses of the horizontal transfer functions (imaginary part)

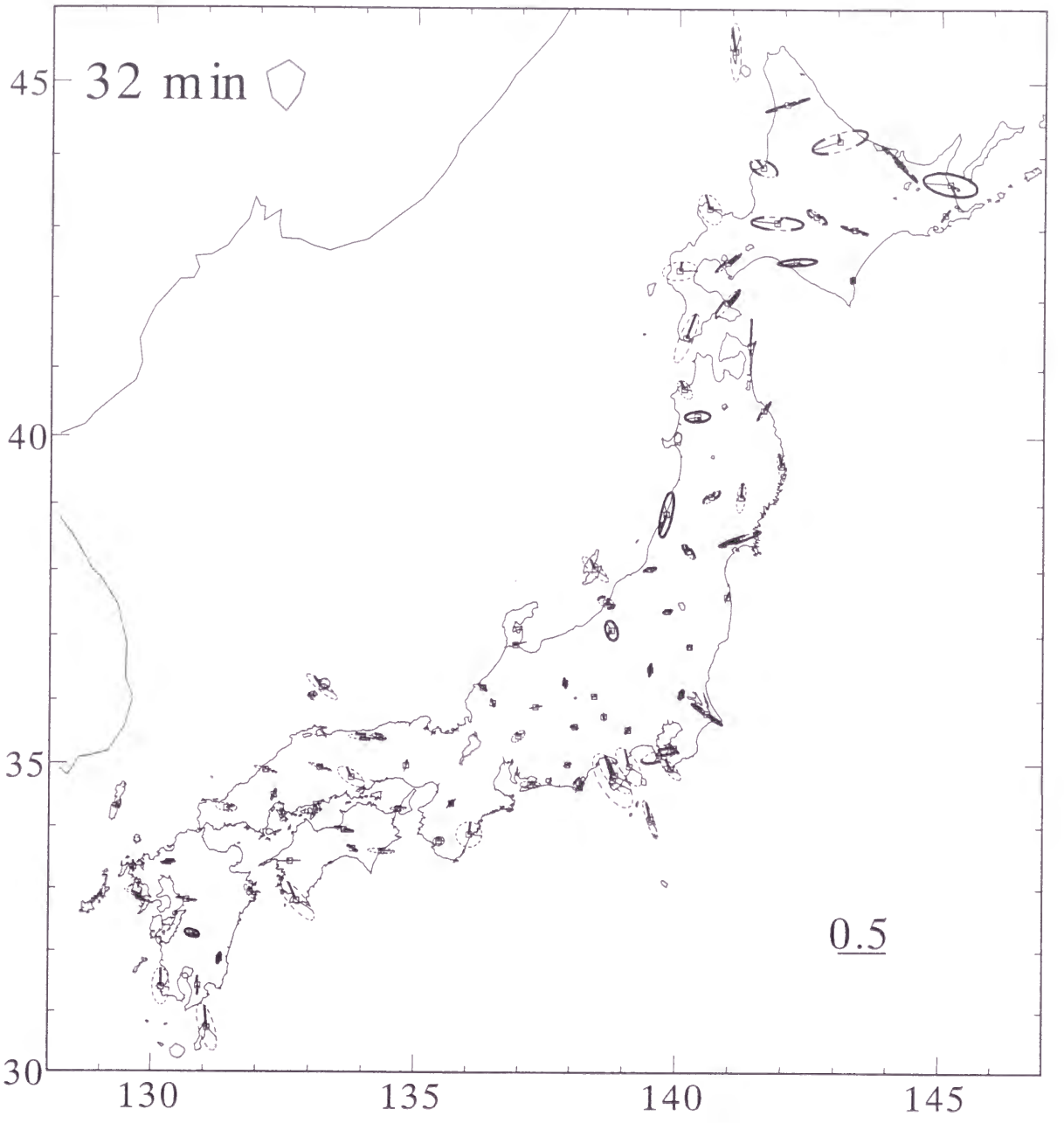

Figure 4-14 (c) Residual anomalous ellipses of the horizontal transfer functions (imaginary part)

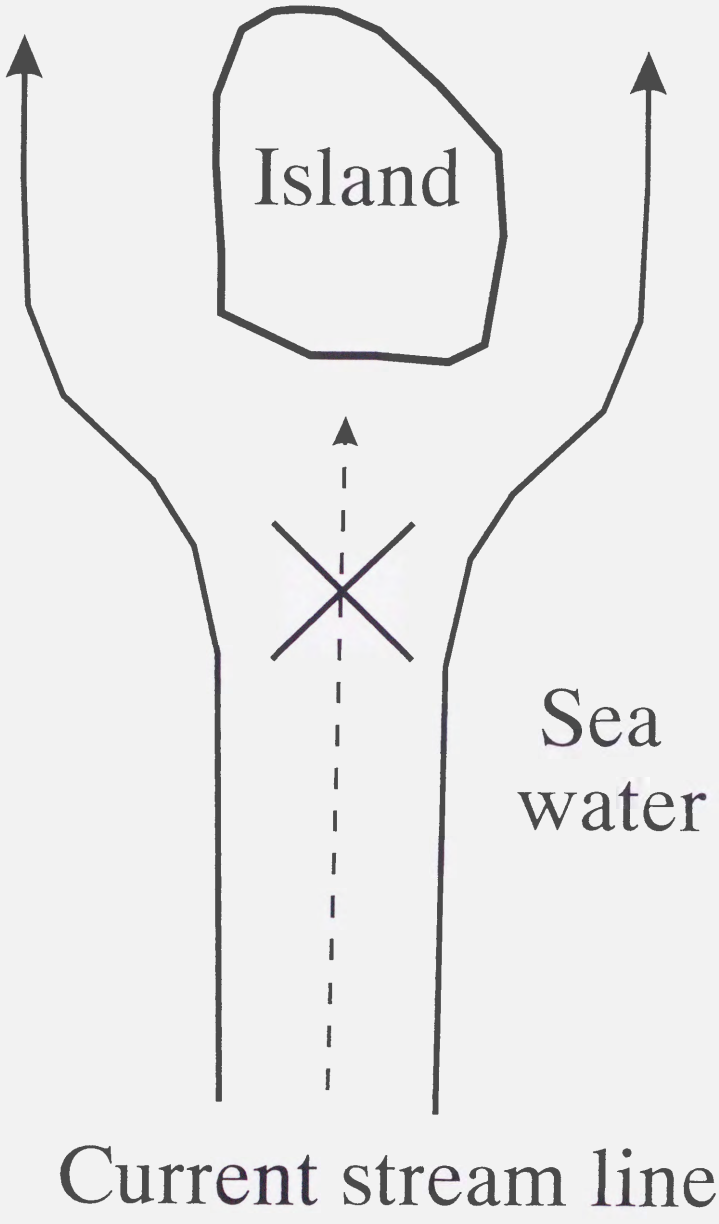

Figure 5-1 Schematic explanation of electric current around an island

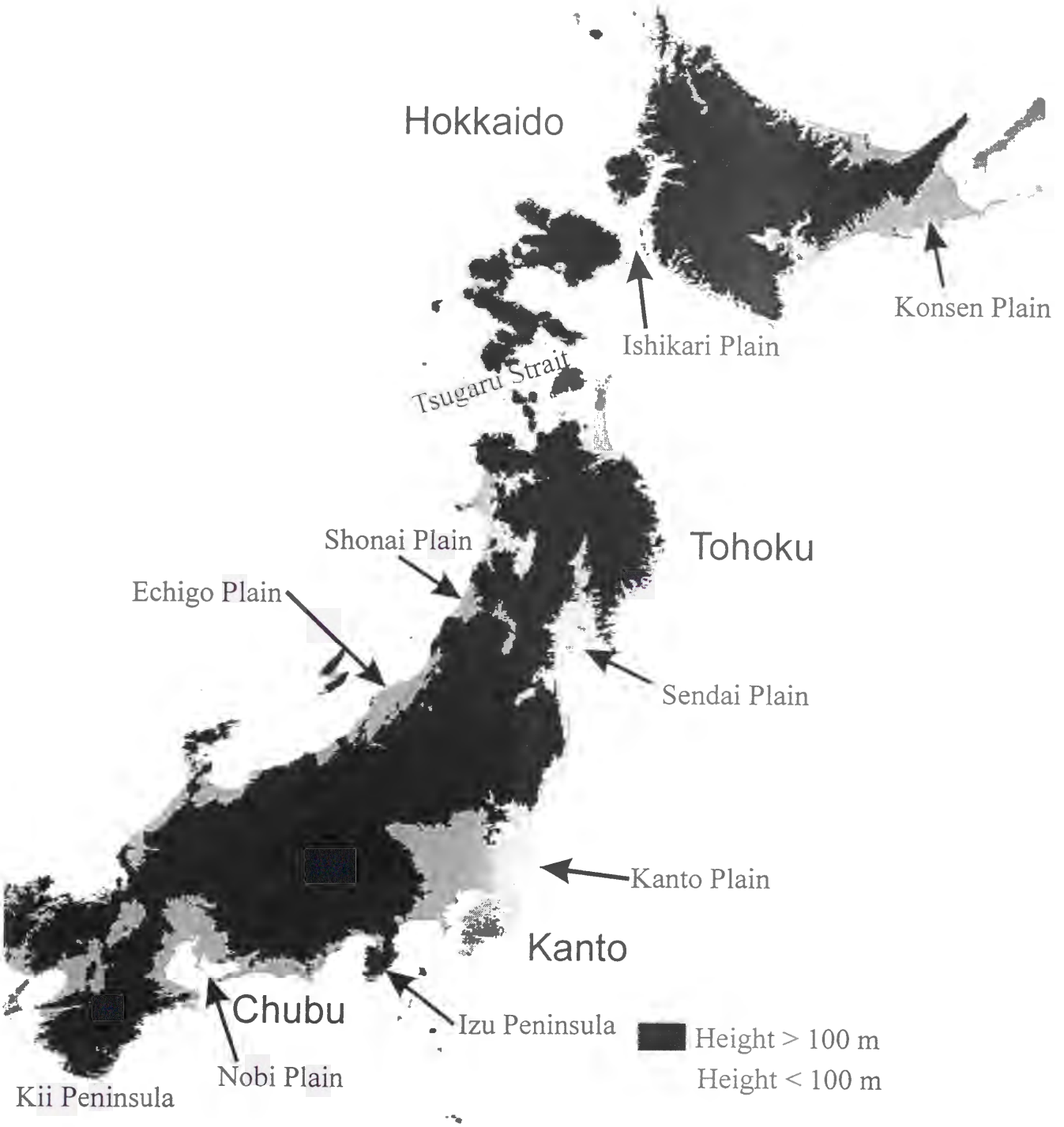

Figure 5-2 Topographic features in eastern Japan

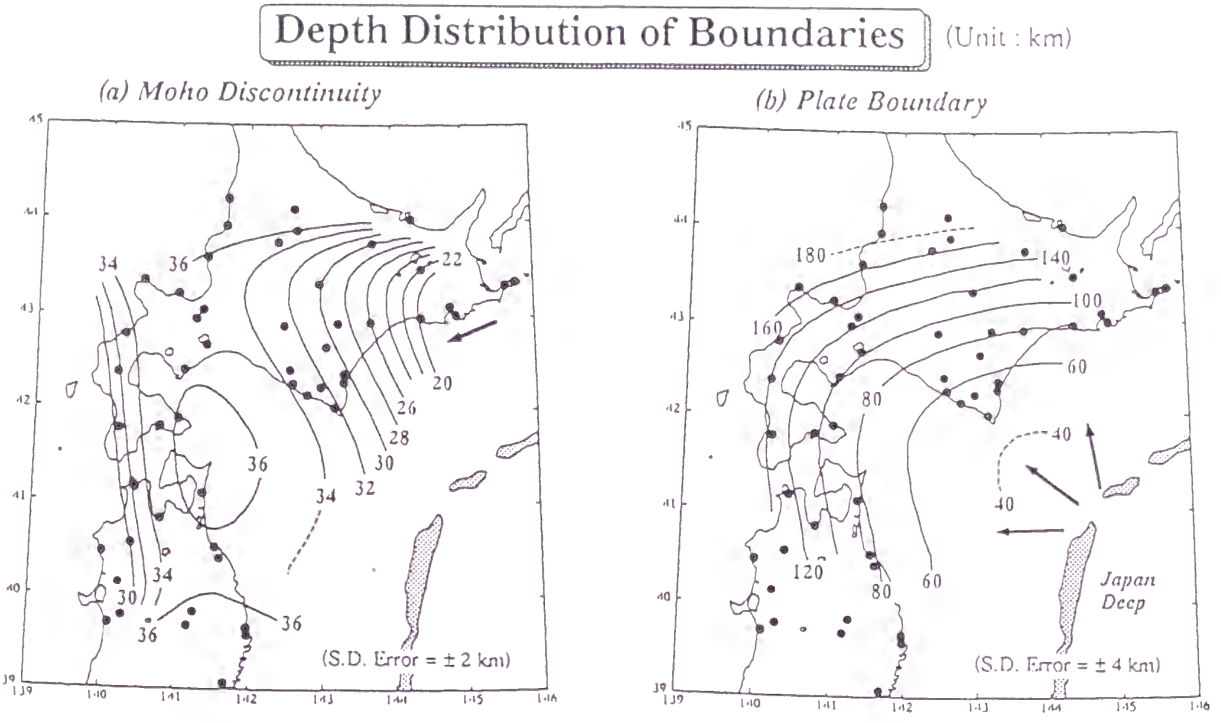

Figure 5-3 Depth of the Moho discontinuity and the upper plate boundary
(after Miyamachi et al., 1993)

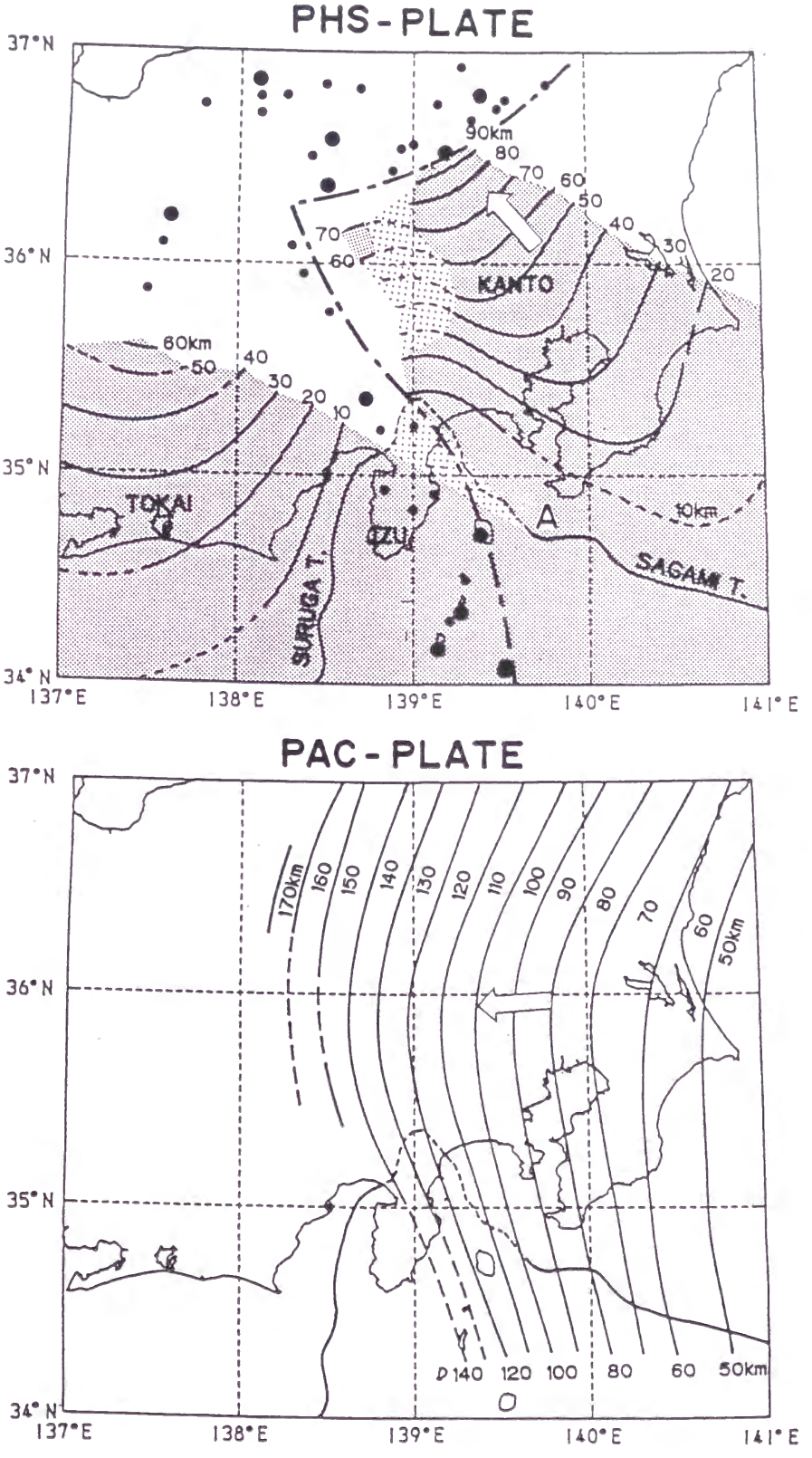

Figure 5-4 Depth of the upper boundary of the Philippine Sea plate (PHS) and the Pacific ocean plate (PAC) (after Ishida, 1992)

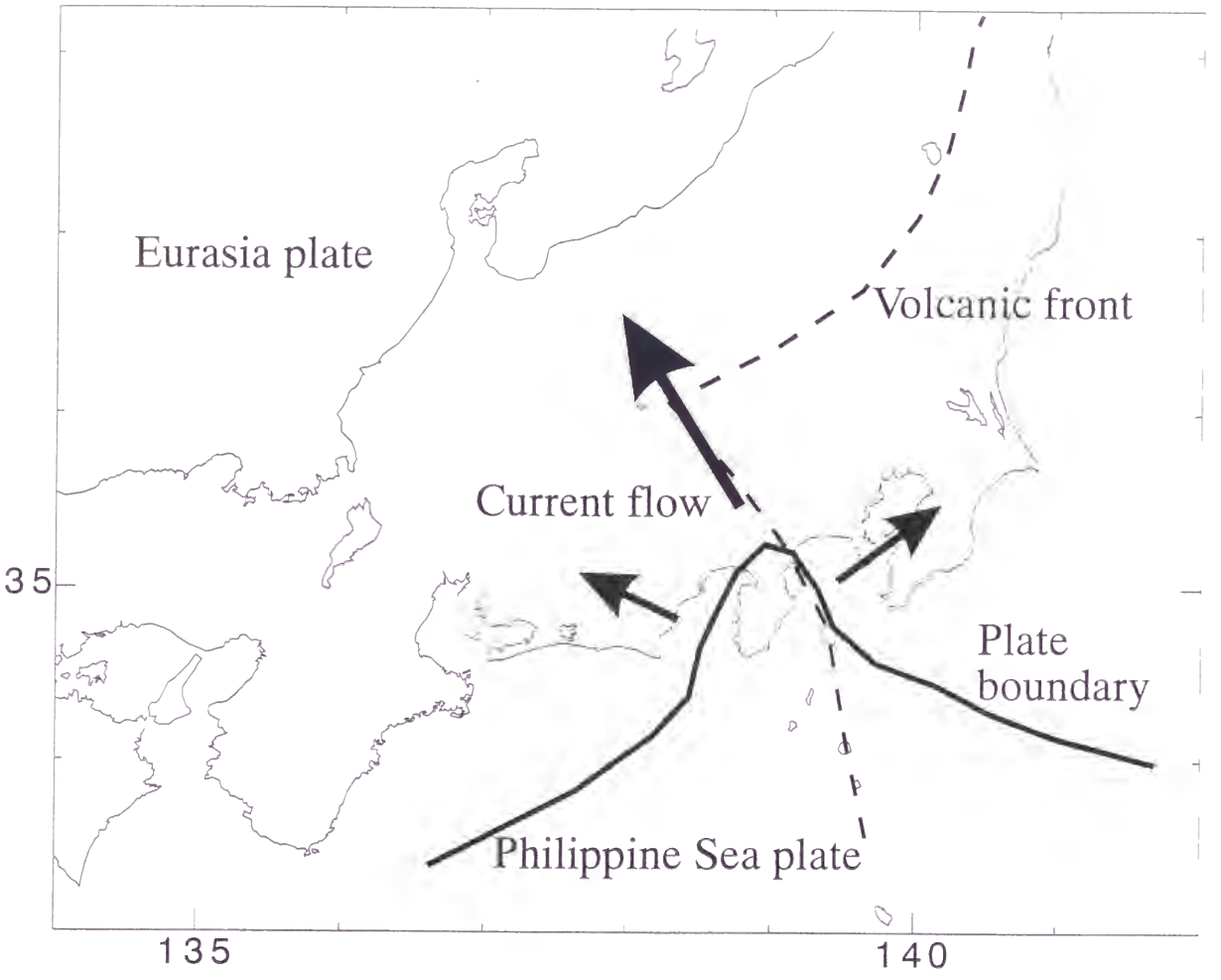

Figure 5-5 Plate boundary of the Philippine Sea plate and the Eurasian plate (thick line), volcanic front (broken line) and schematic explanation of electric currents (arrows) in Kanto and Chubu Districts associated with the Philippine Sea plate.

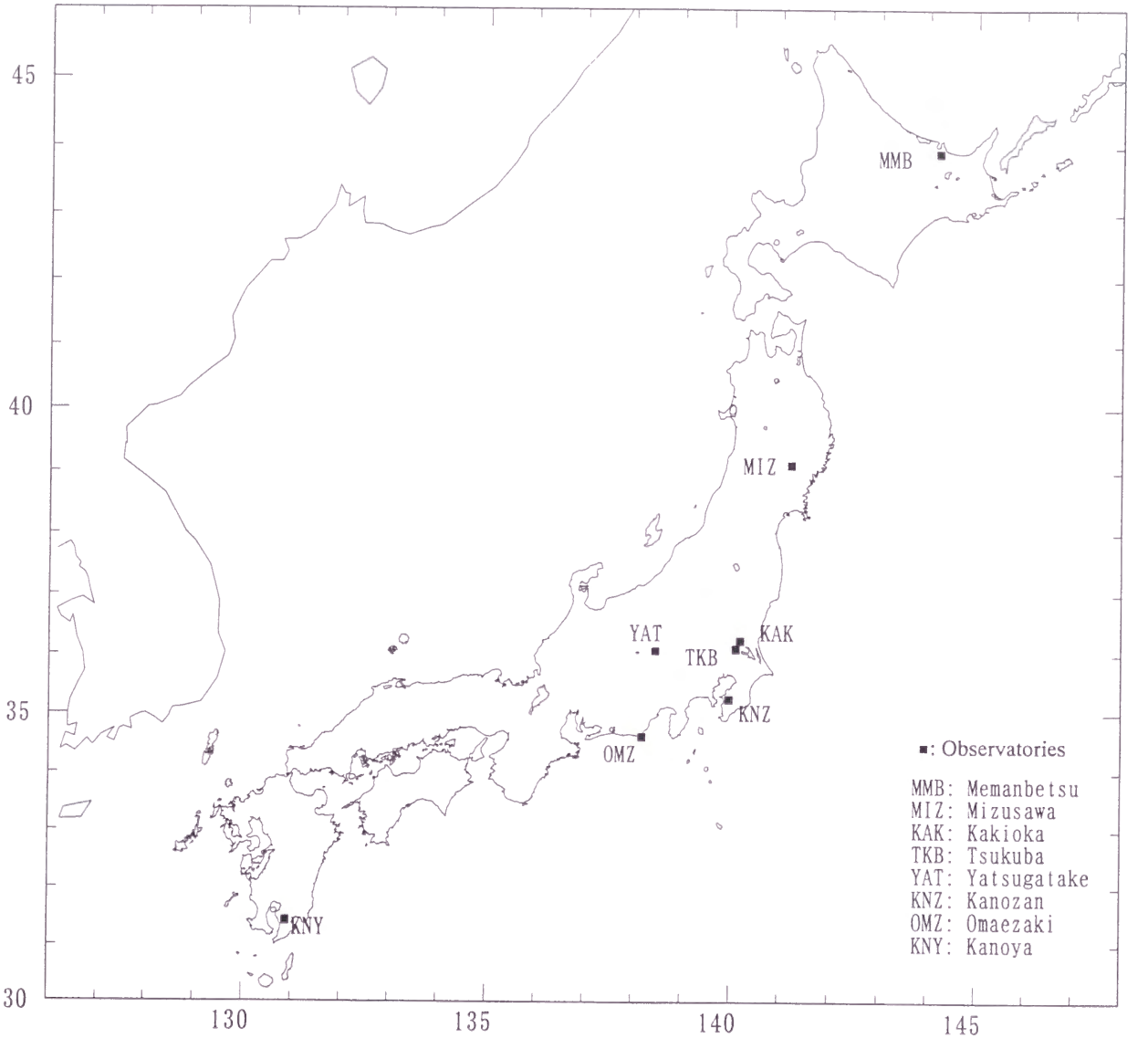

Figure 6-1 Locations of the geomagnetic observatories

Figure 6-2 (a) Semimonthly single-station transfer functions A and B (1989-1992)
The real and imaginary parts are donated with suffixes u and v, respectively.

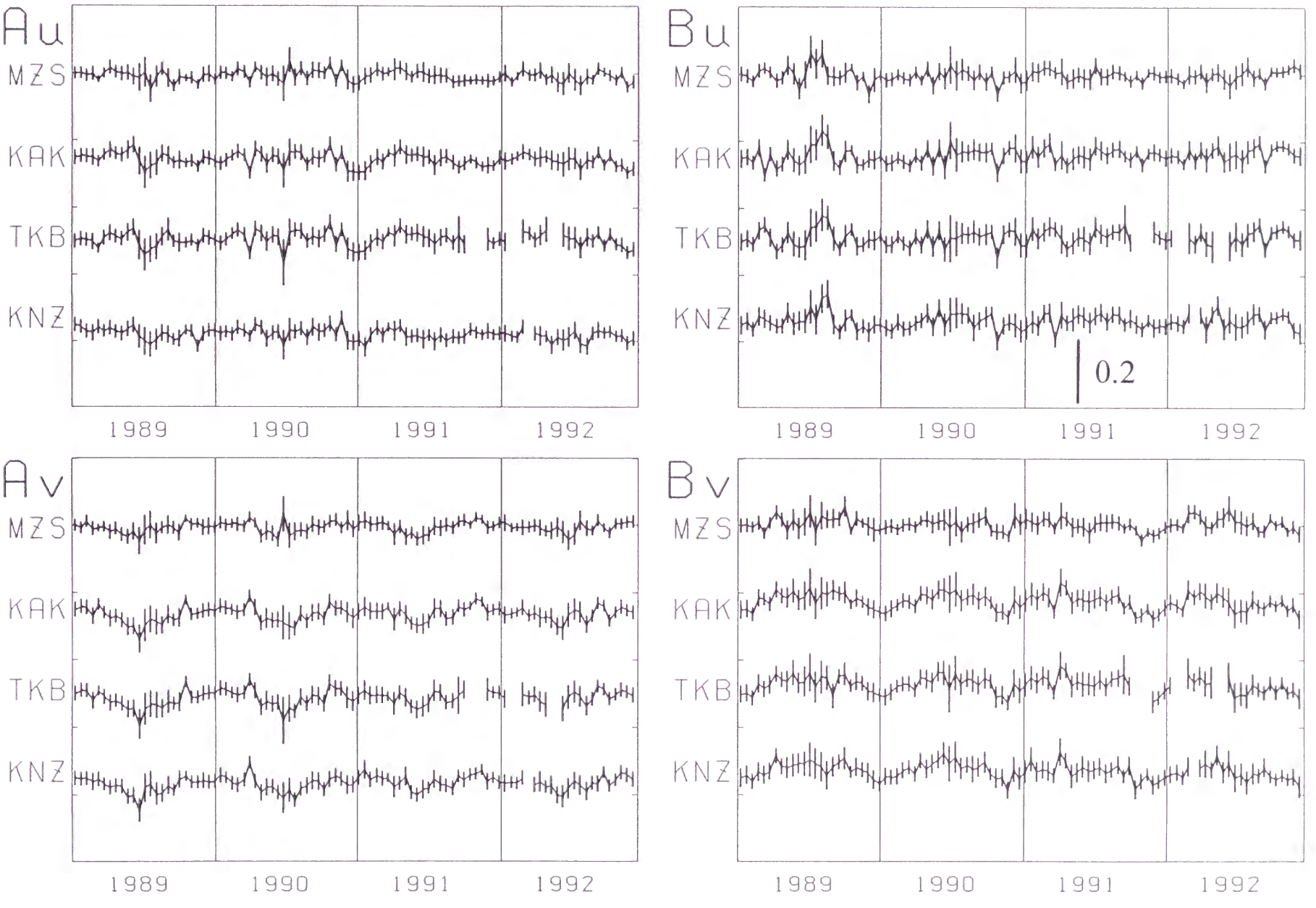

Figure 6-2 (b) Semimonthly single-station transfer functions *A* and *B* (1989-1992)
The real and imaginary parts are donated with suffixes *u* and *v*, respectively.

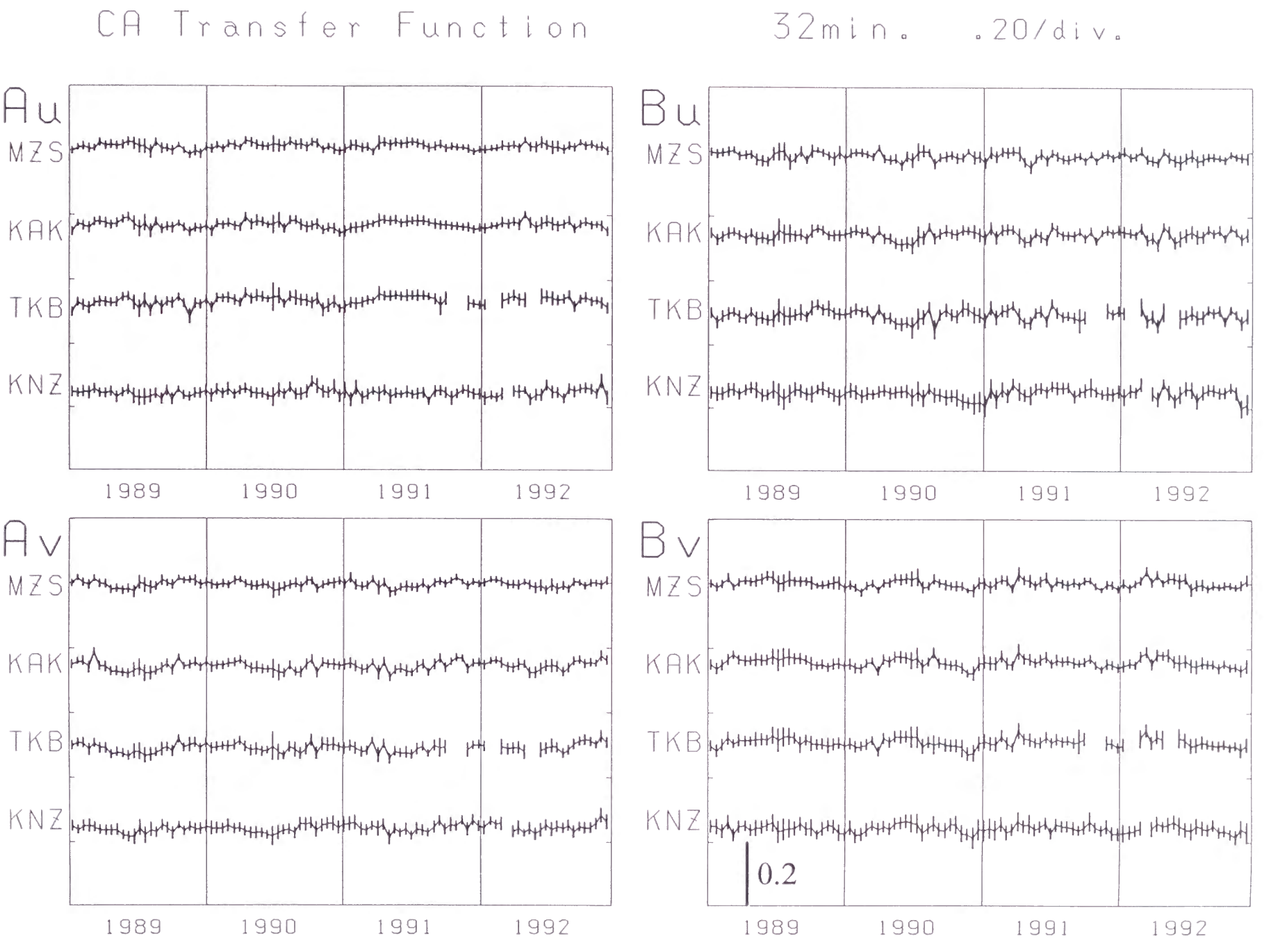

Figure 6-2 (c) Semimonthly single-station transfer functions *A* and *B* (1989-1992)
The real and imaginary parts are donated with suffixes *u* and *v*, respectively.

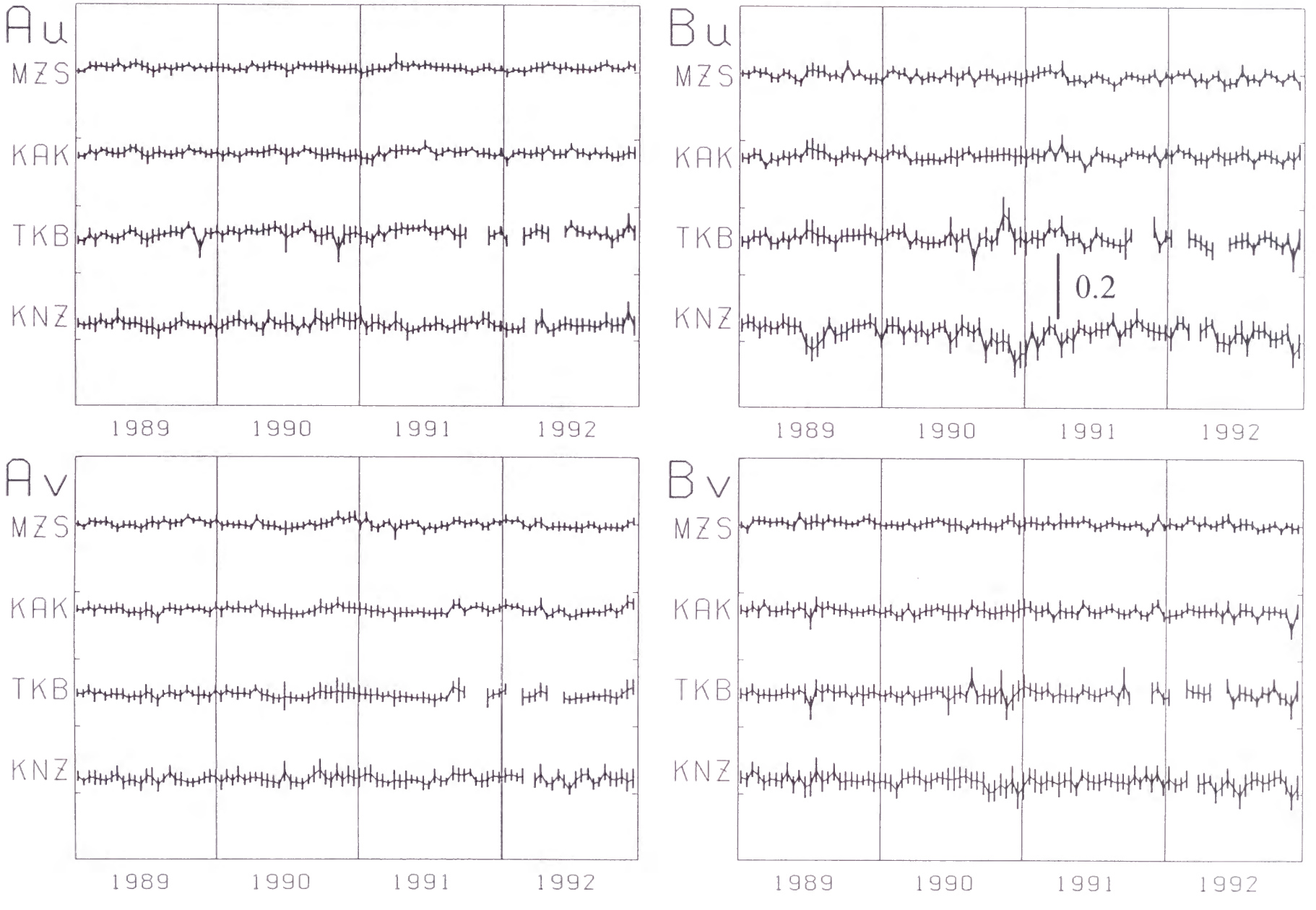

Figure 6-2 (d) Semimonthly single-station transfer functions *A* and *B* (1989-1992)
The real and imaginary parts are donated with suffixes *u* and *v*, respectively.

Figure 6-2 (e) Semimonthly single-station transfer functions A and B (1989-1992)
The real and imaginary parts are donated with suffixes u and v, respectively.

Figure 6-2 (f) Semimonthly single-station transfer functions *A* and *B* (1989-1992)
The real and imaginary parts are donated with suffixes *u* and *v*, respectively.

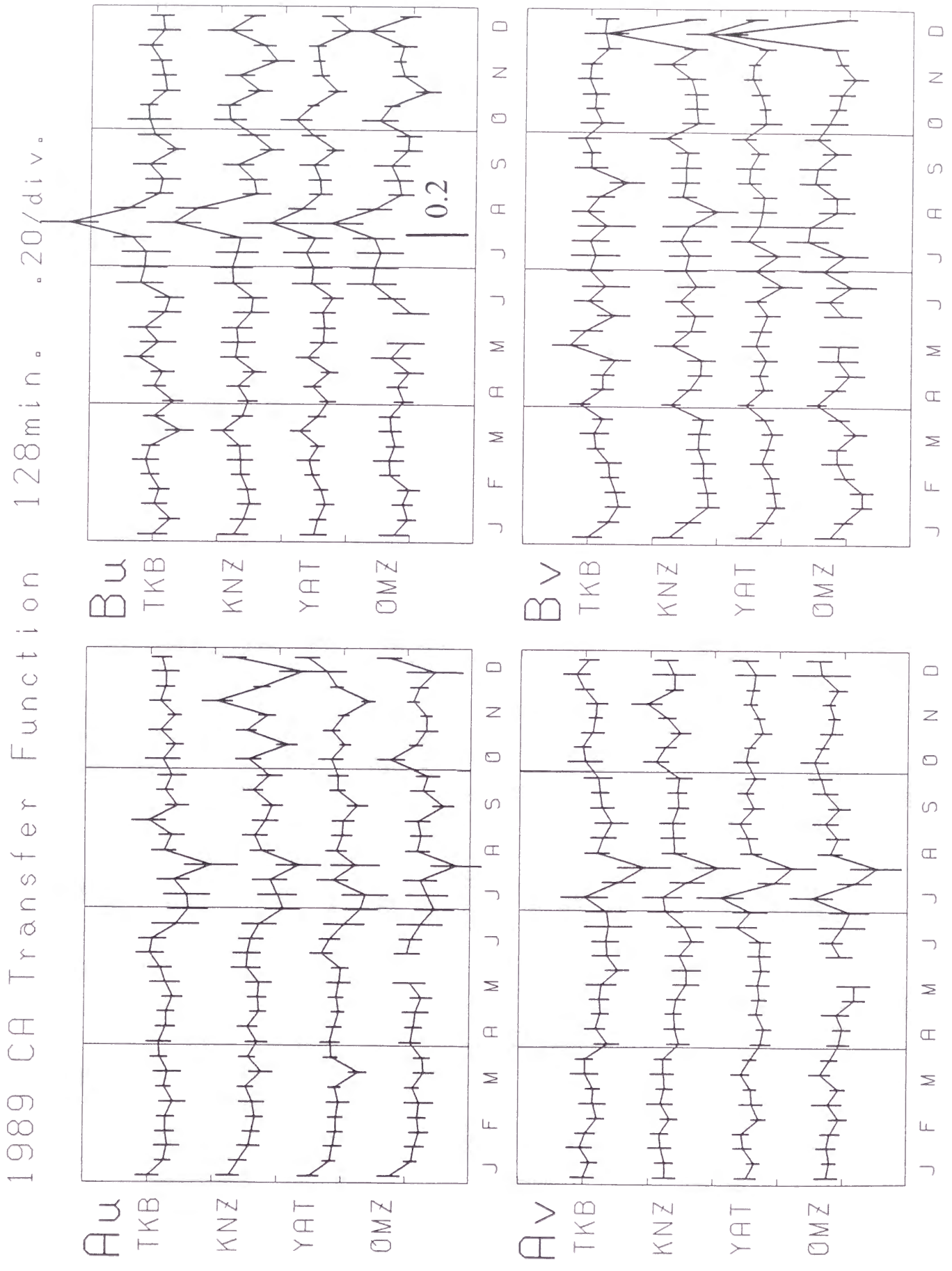

Figure 6-3 (a) Temporal changes of single-station transfer functions A and B in 1989. The real and imaginary parts are donated with suffixes u and v, respectively.

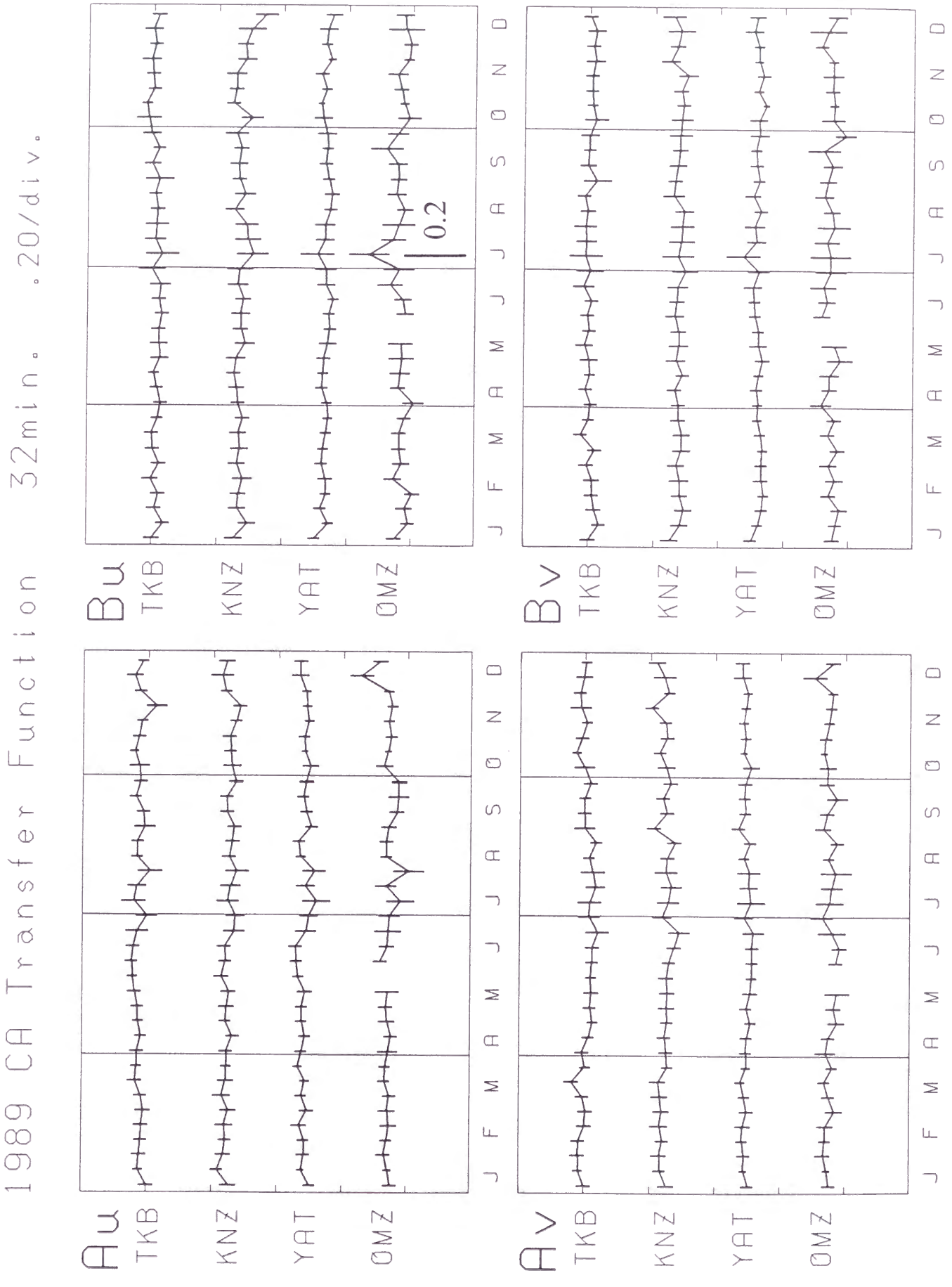

Figure 6-3 (b) Temporal changes of single-station transfer functions A and B in 1989. The real and imaginary parts are donated with suffixes u and v, respectively.

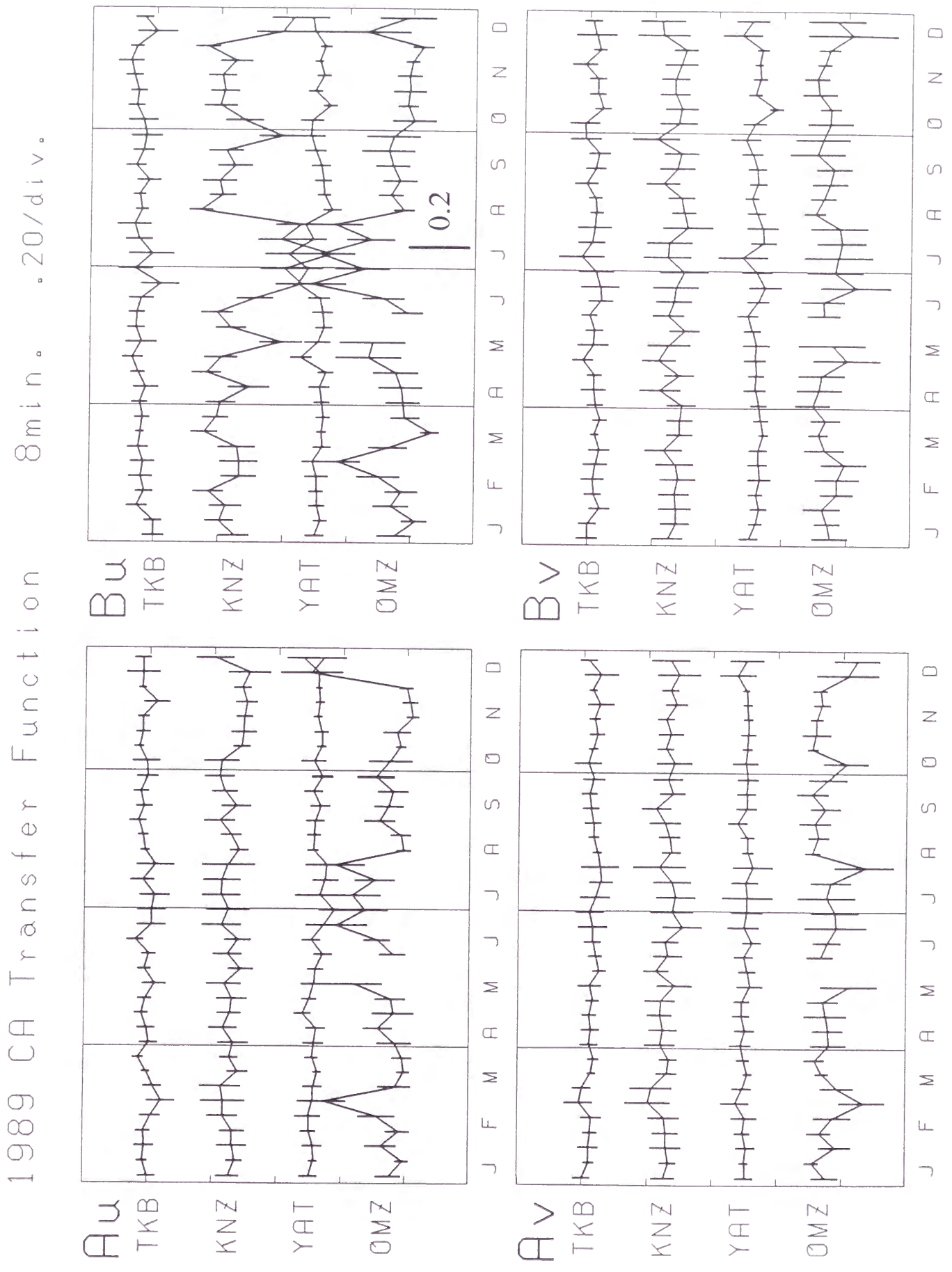

Figure 6-3 (c) Temporal changes of single-station transfer functions A and B in 1989. The real and imaginary parts are donated with suffixes u and v, respectively.

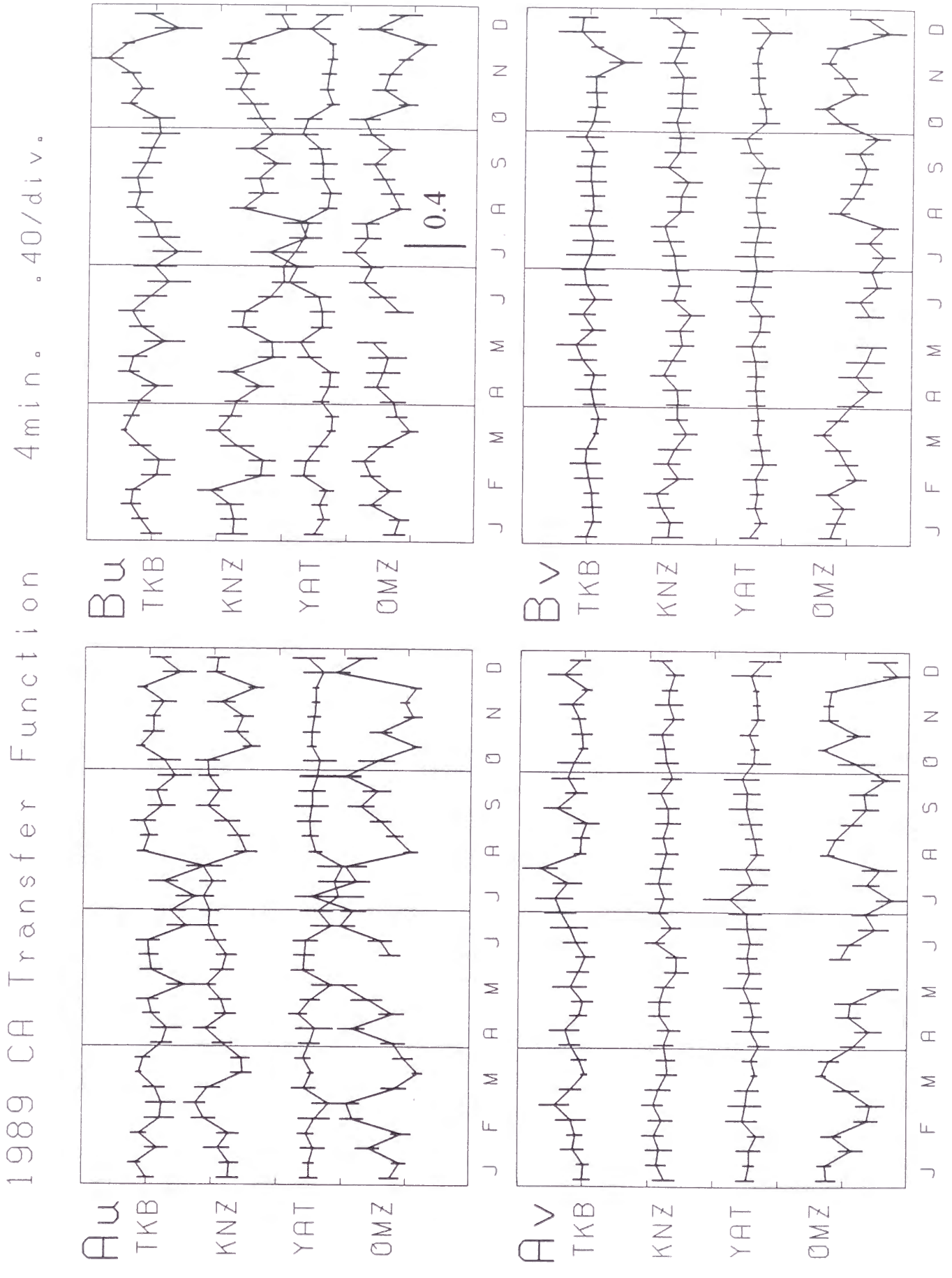

Figure 6-3 (d) Temporal changes of single-station transfer functions A and B in 1989. The real and imaginary parts are donated with suffixes u and v, respectively.

Table 6-1 Correlation coefficients between the temporal changes of *Au* and *Bu* at Tsukuba and those at each observatory.

Obsevatories	Period	Correlation coefficients	
		Au	*Bu*
TKB-MZS	64 min	0.43	0.55
	4 min	-0.26	0.22
TKB-KAK	64 min	0.90	0.97
	4 min	0.90	0.60
TKB-KNZ	64 min	0.64	0.67
	4 min	-0.74	0.70

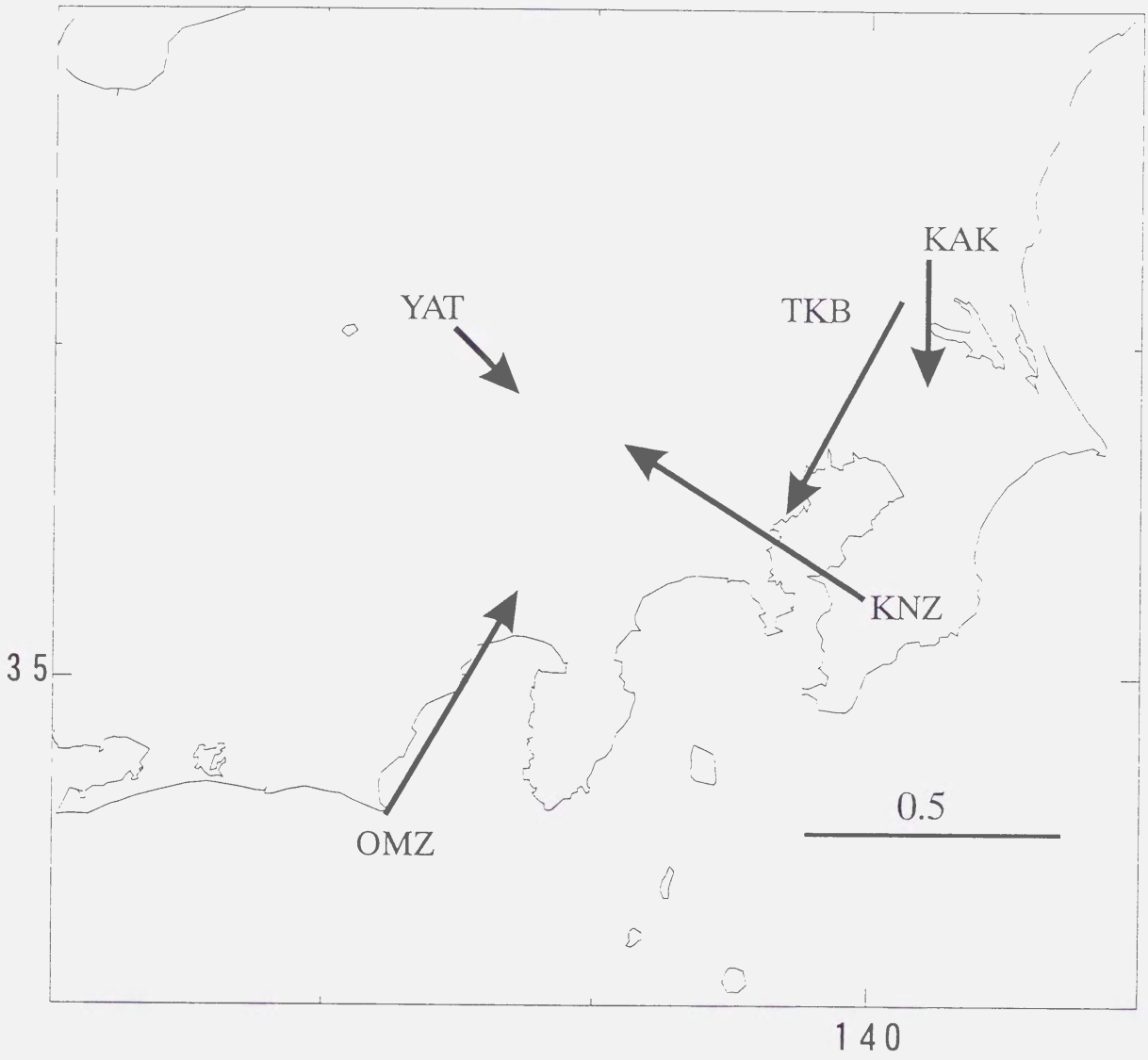

Figure 6-4 Difference induction arrows between July and August, 1989 (rel part).

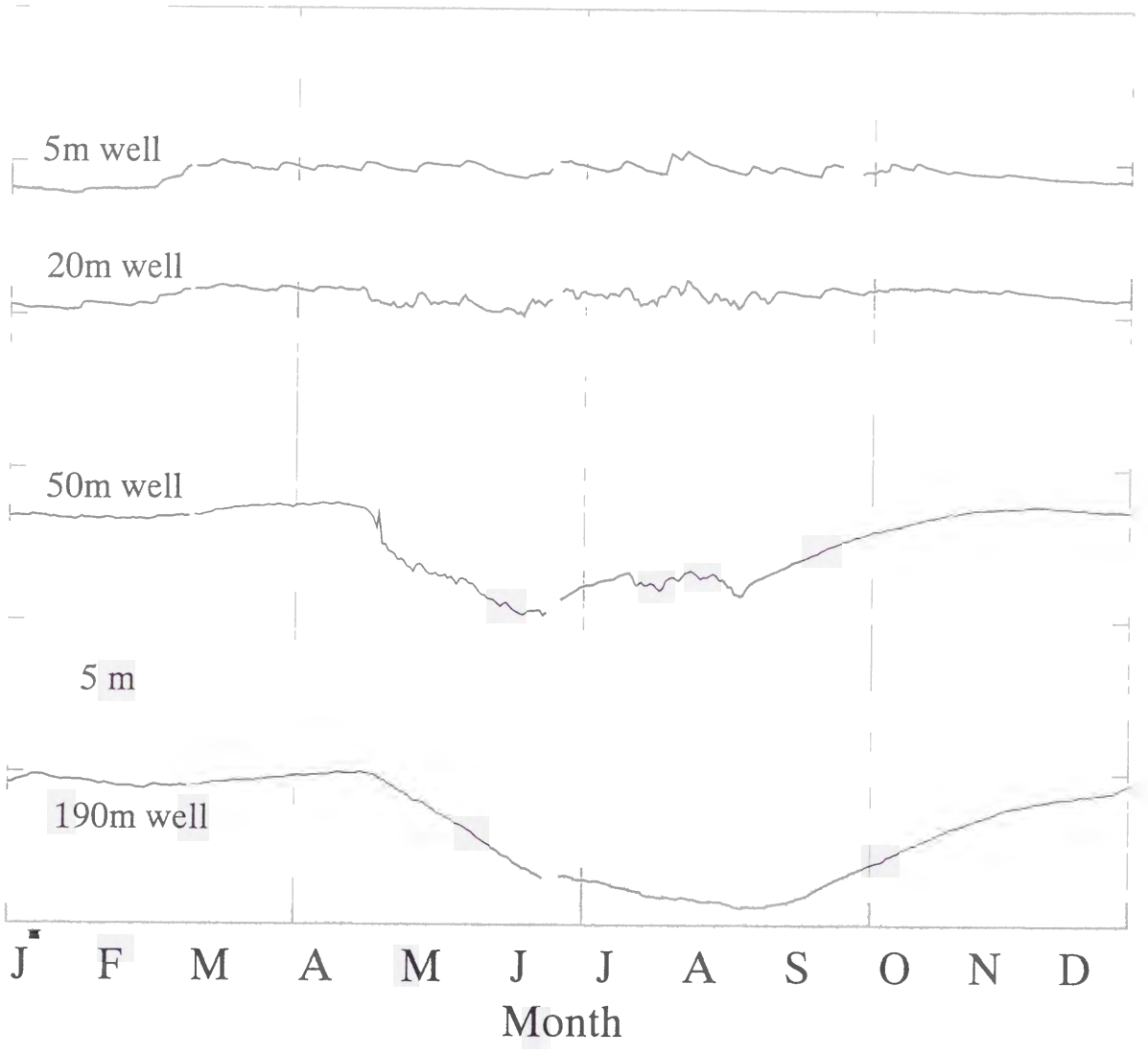

Figure 6-5 Underground water level at Tsukuba in 1989
Each well has different depth.

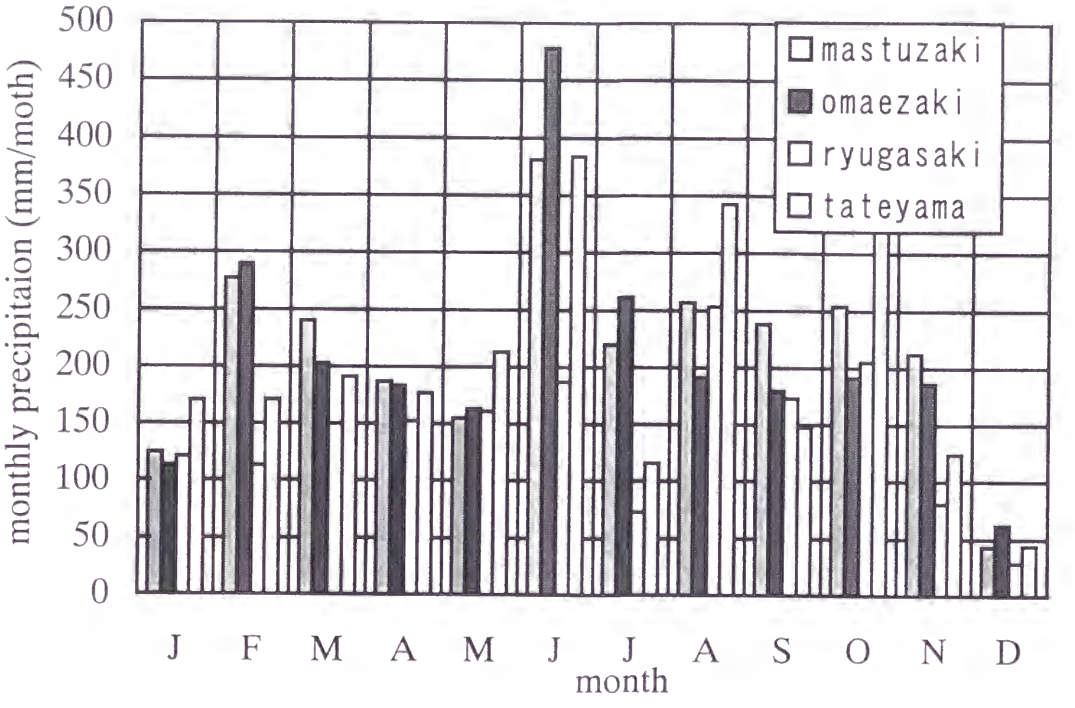

(a)

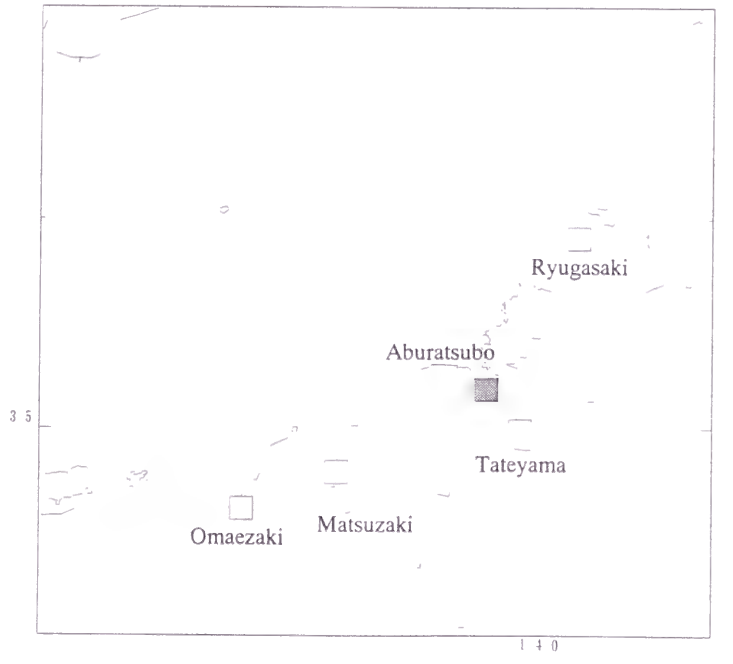

(b)

Figure 6-6 (a) Monthly precipitaion in 1989 and (b) observation sites
(after Japan Meteorological Agency, 1990)

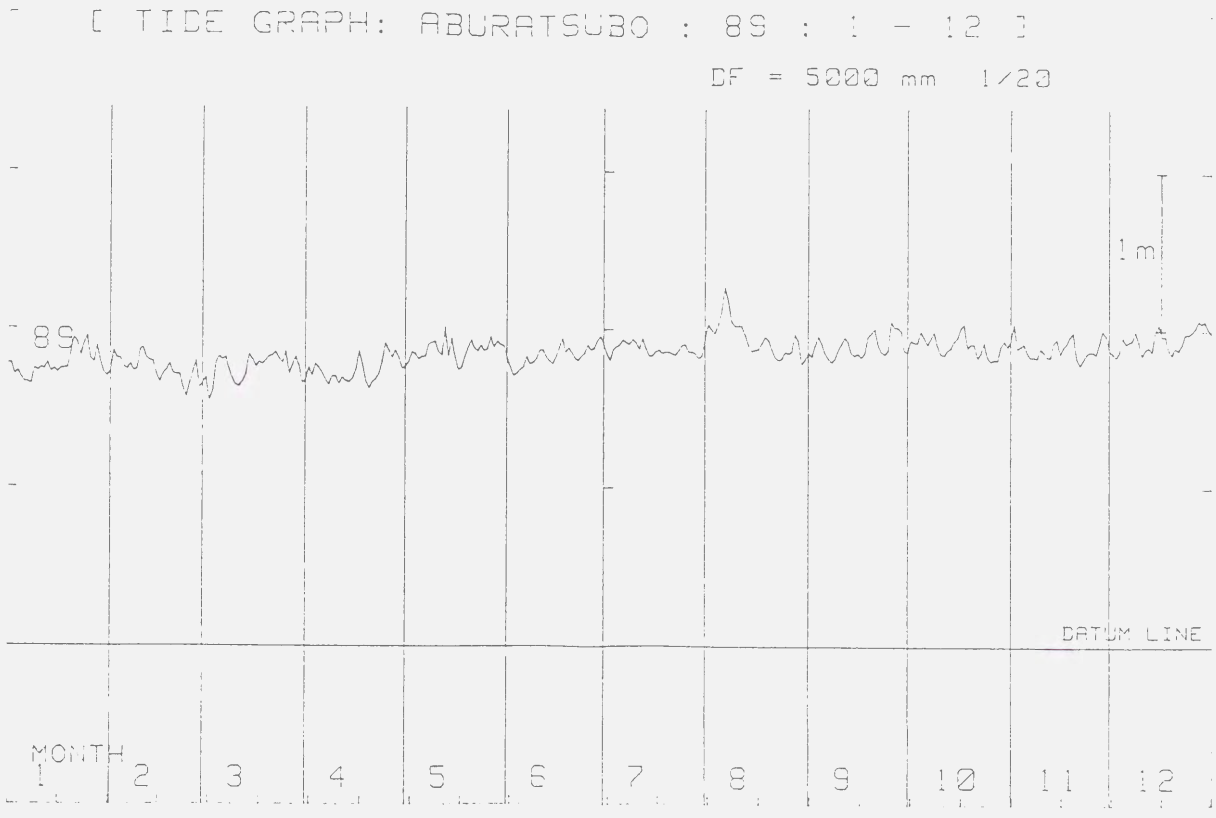

Figure 6-7 Daily sea level at Aburatsubo Tide station operated by the GSI in 1989
A peak in August was caused by low atmospheric pressure of a typhoon.

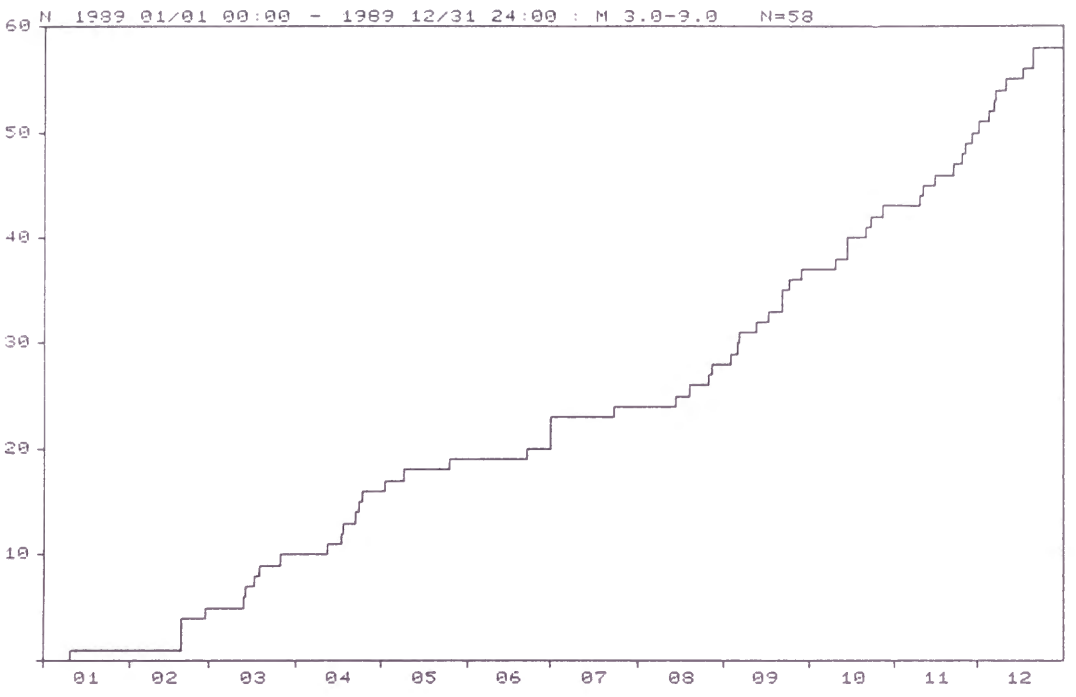

(a)

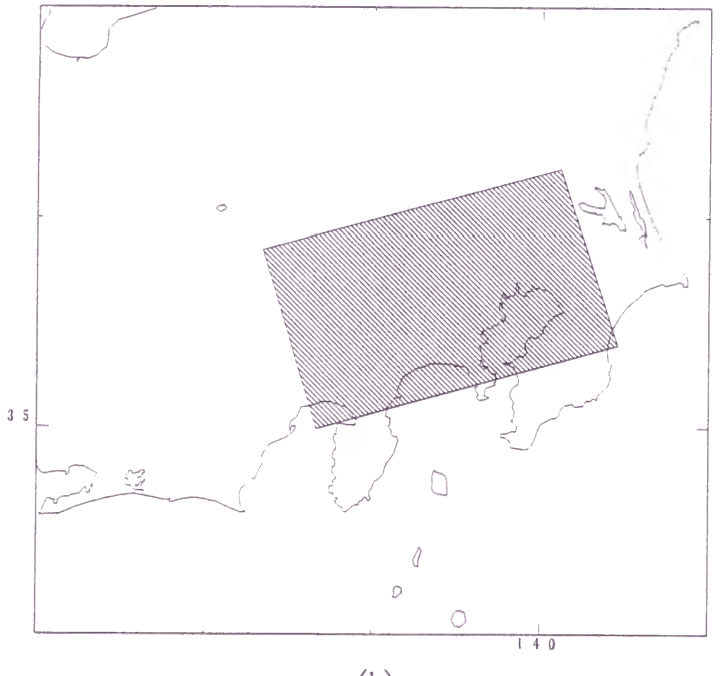

(b)

Figure 6-8 (a) Cumulative number of earthquakes (M>3, 0< Depth <200 km) occurred in the shadowed area in (b) (after SEIS-PC [Ishikawa *et al.*, 1985]).

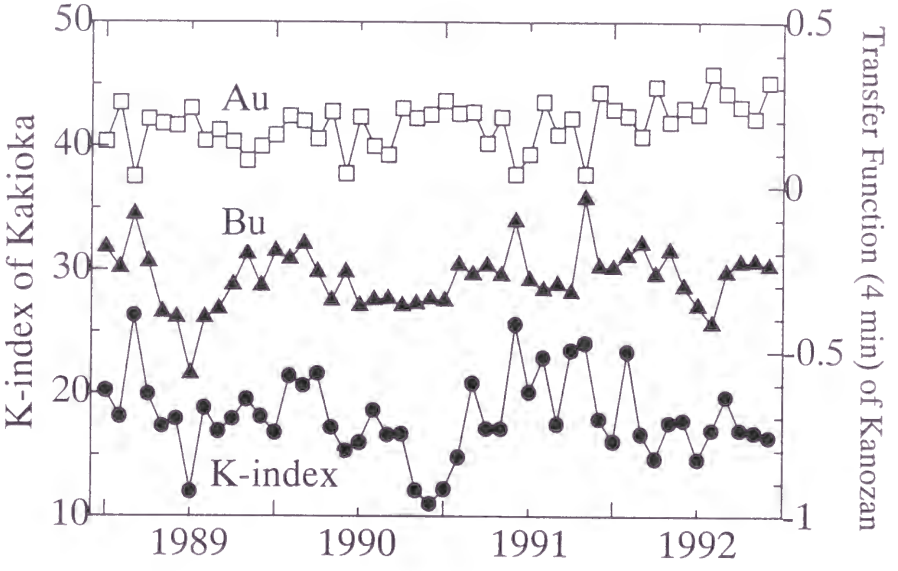

(a) Monthly transfer functions of Kanozan and K-index of Kakioka

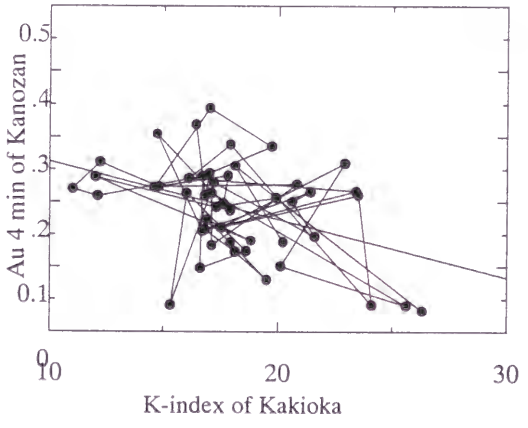

Correlation coeficient = -0.406

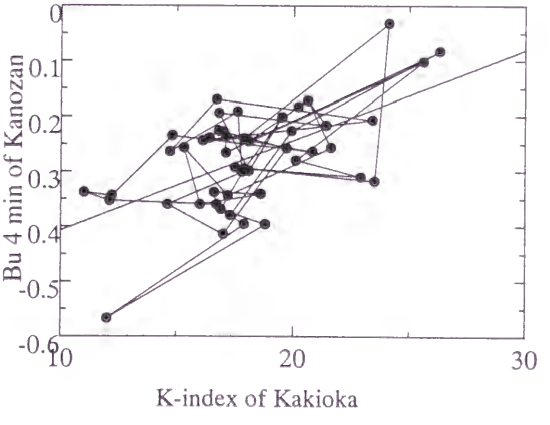

Correlation coeficient = 0.587

(b) Correlation charts of (a)

Figure 6-9 Correlation between temporal changes of K-index at Kakioka and those of transfer functions of Kanozan

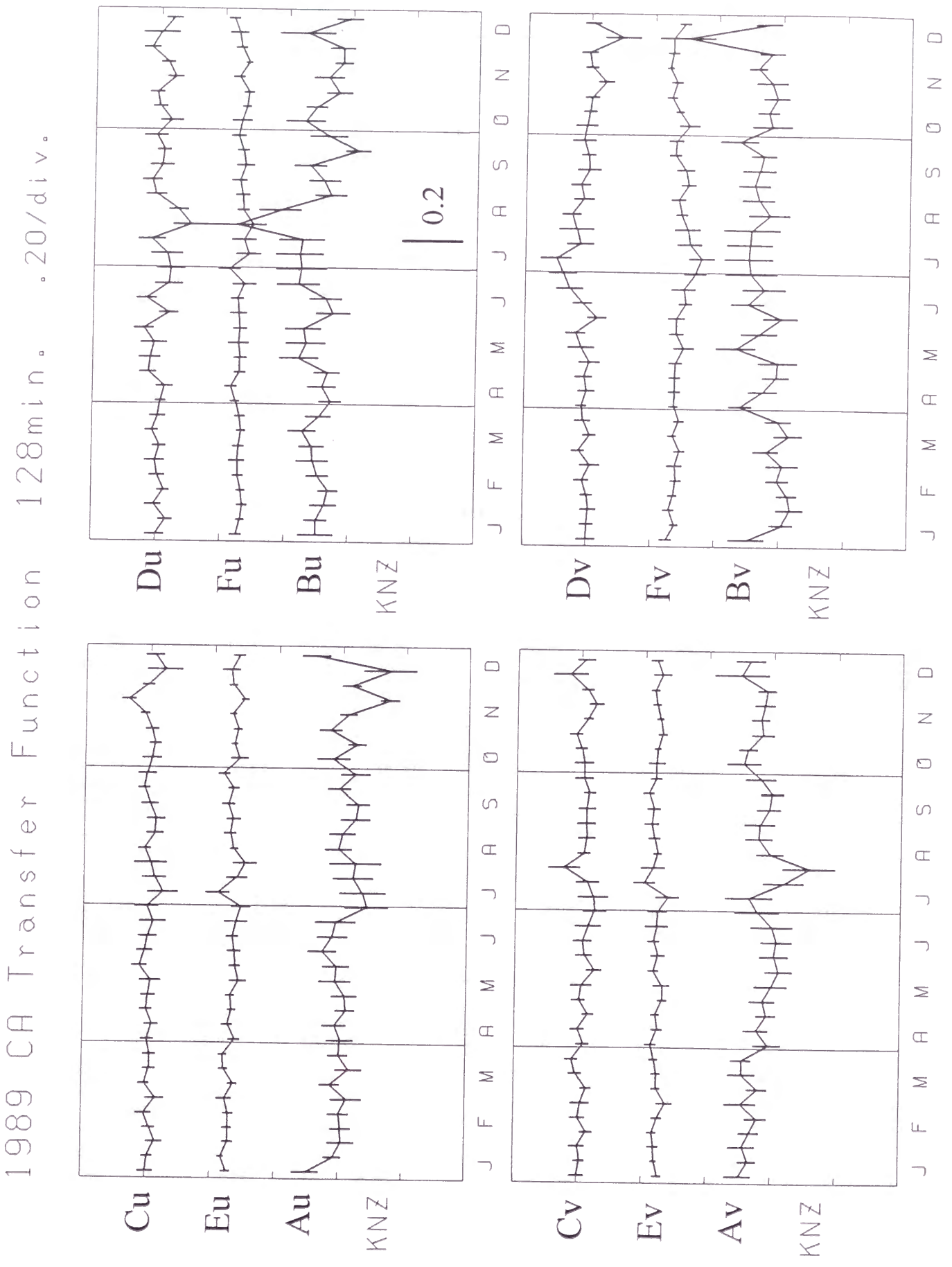

Figure 6-10 (a) Temporal changes of interstation transfer functions of Kanozan in 1989. The real and imaginary parts are donated with suffixes *u* and *v*, respectively. The reference station is Kakioka.

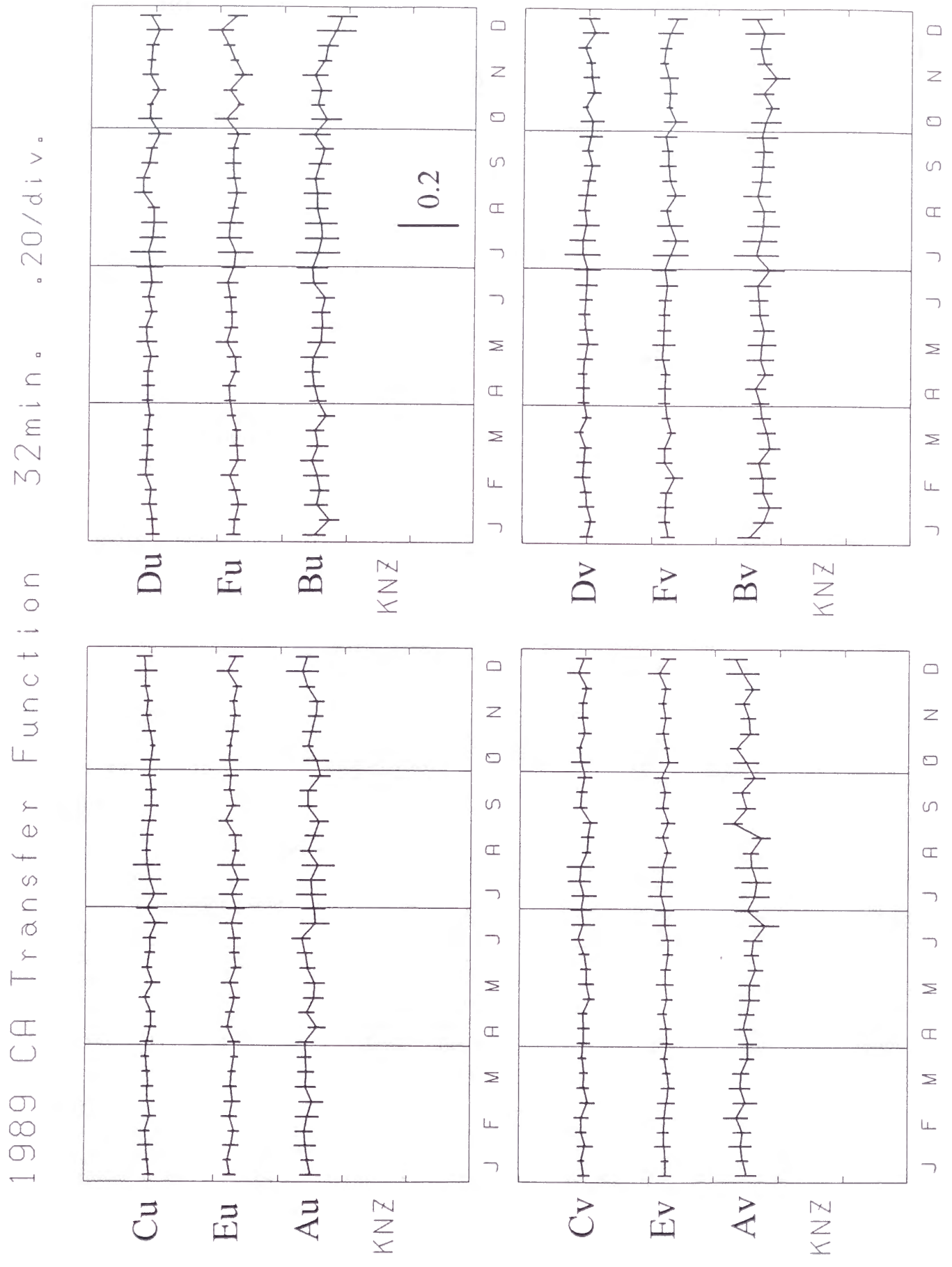

Figure 6-10 (b) Temporal changes of interstation transfer functions of Kanozan in 1989. The real and imaginary parts are donated with suffixes *u* and *v*, respectively. The reference station is Kakioka.

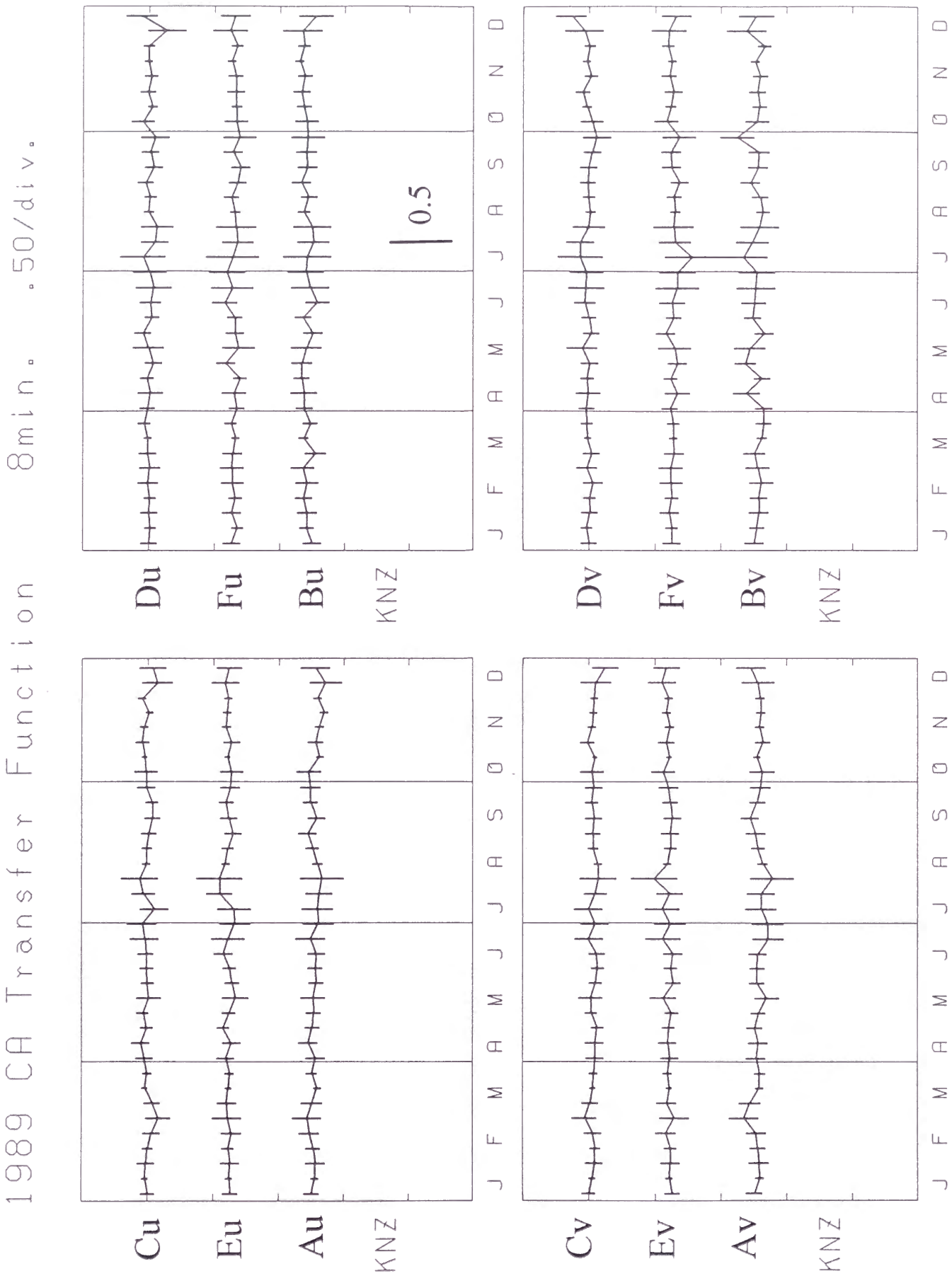

Figure 6-10 (c) Temporal changes of interstation transfer functions of Kanozan in 1989. The real and imaginary parts are donated with suffixes *u* and *v*, respectively. The reference station is Kakioka.

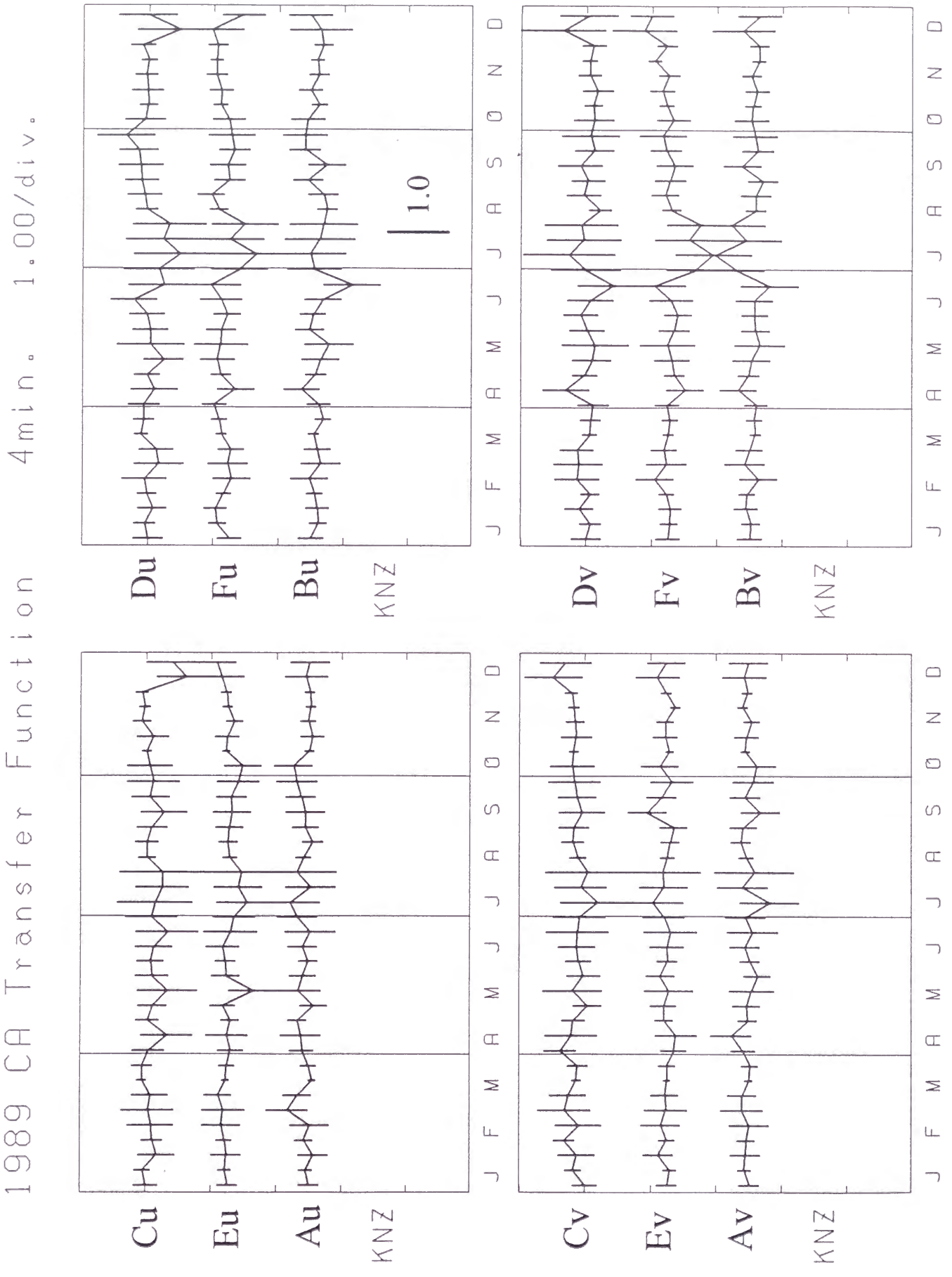

Figure 6-10 (d) Temporal changes of interstation transfer functions of Kanozan in 1989. The real and imaginary parts are donated with suffixes *u* and *v*, respectively. The reference station is Kakioka.

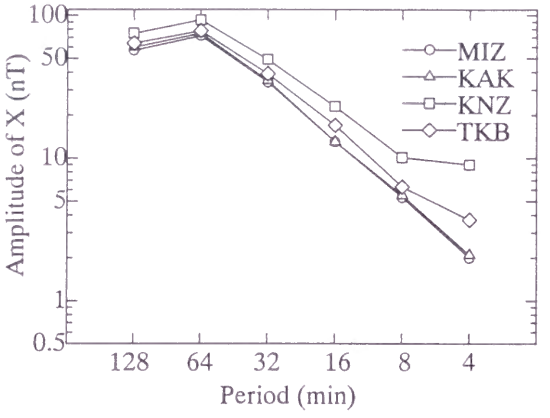

(a) X component

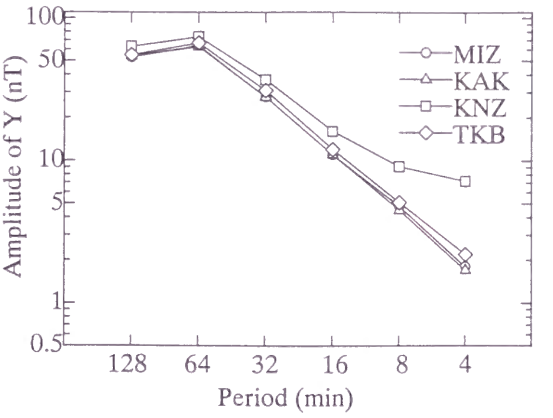

(b) Y component

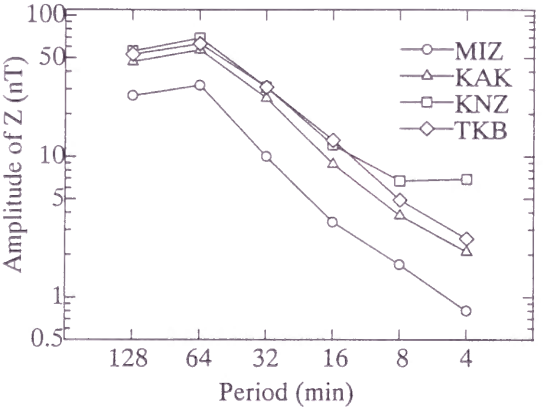

(c) Z component

Figure 6-11 Average amplitude of the three geomagnetic components

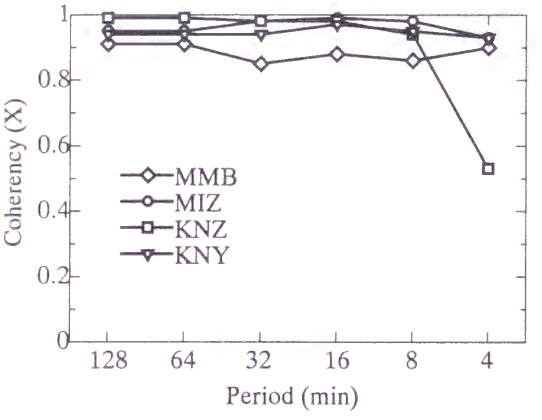

(a) X component

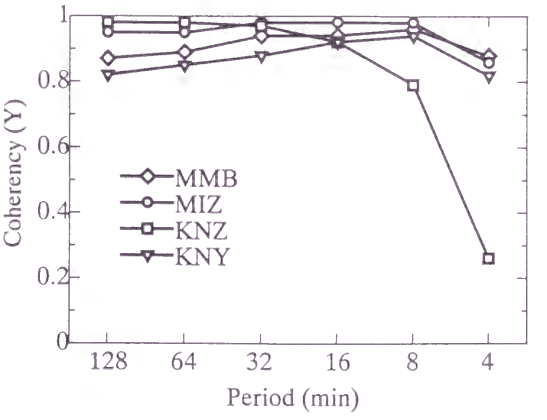

(b)Y component

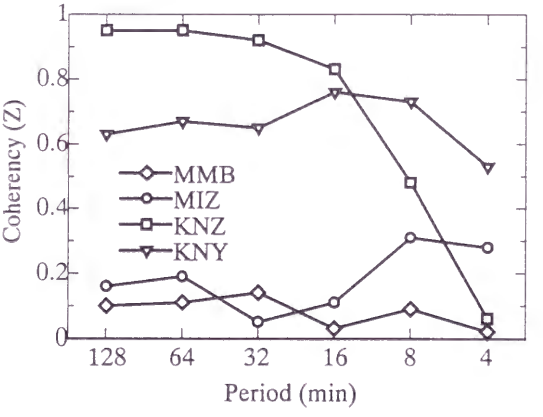

(c) Z component

Figure 6-12 Coherency squared of the horizontal components between Kakioka and each observatory

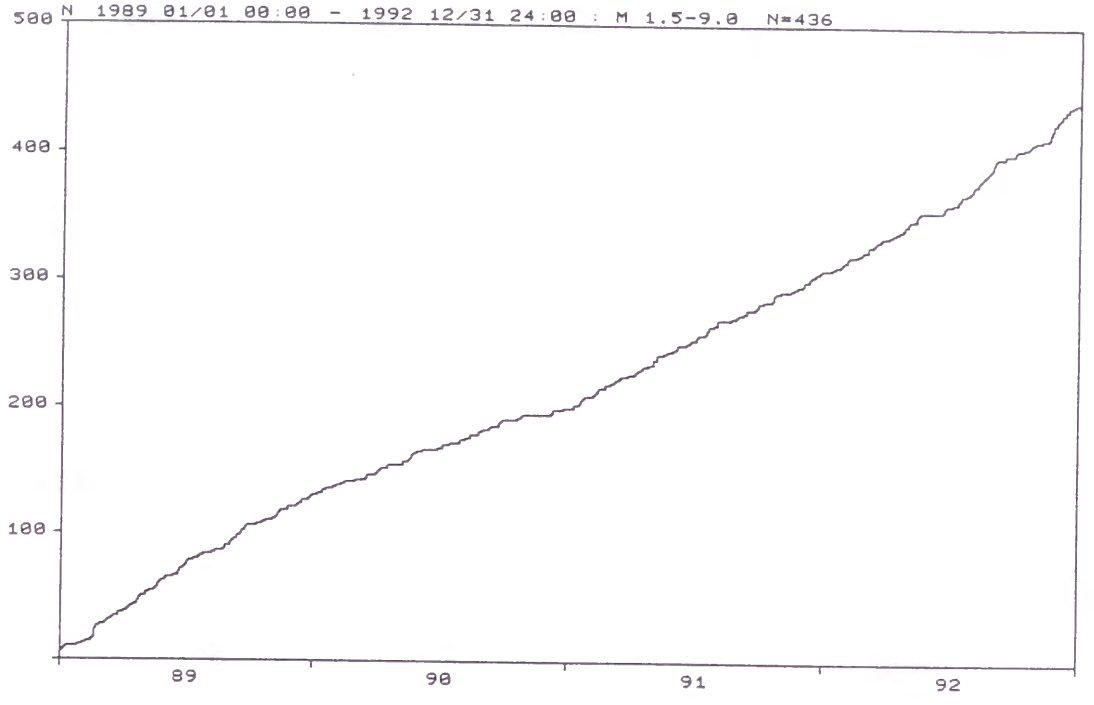

(a)

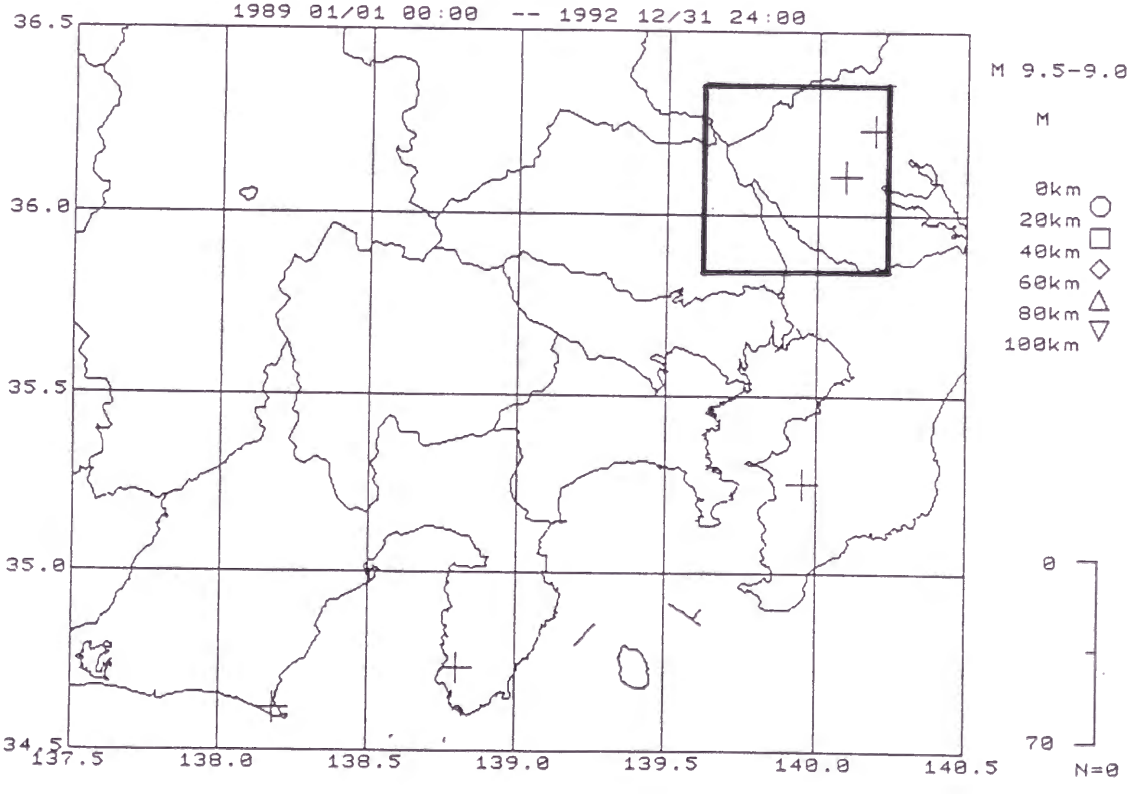

(b)

Figure 6-13 (a) Cumulative number of earthquakes (M>1.5, 0< Depth <200 km) occurred in the rectangle area in (b) (after SEIS-PC [Ishikawa *et al.*, 1985])

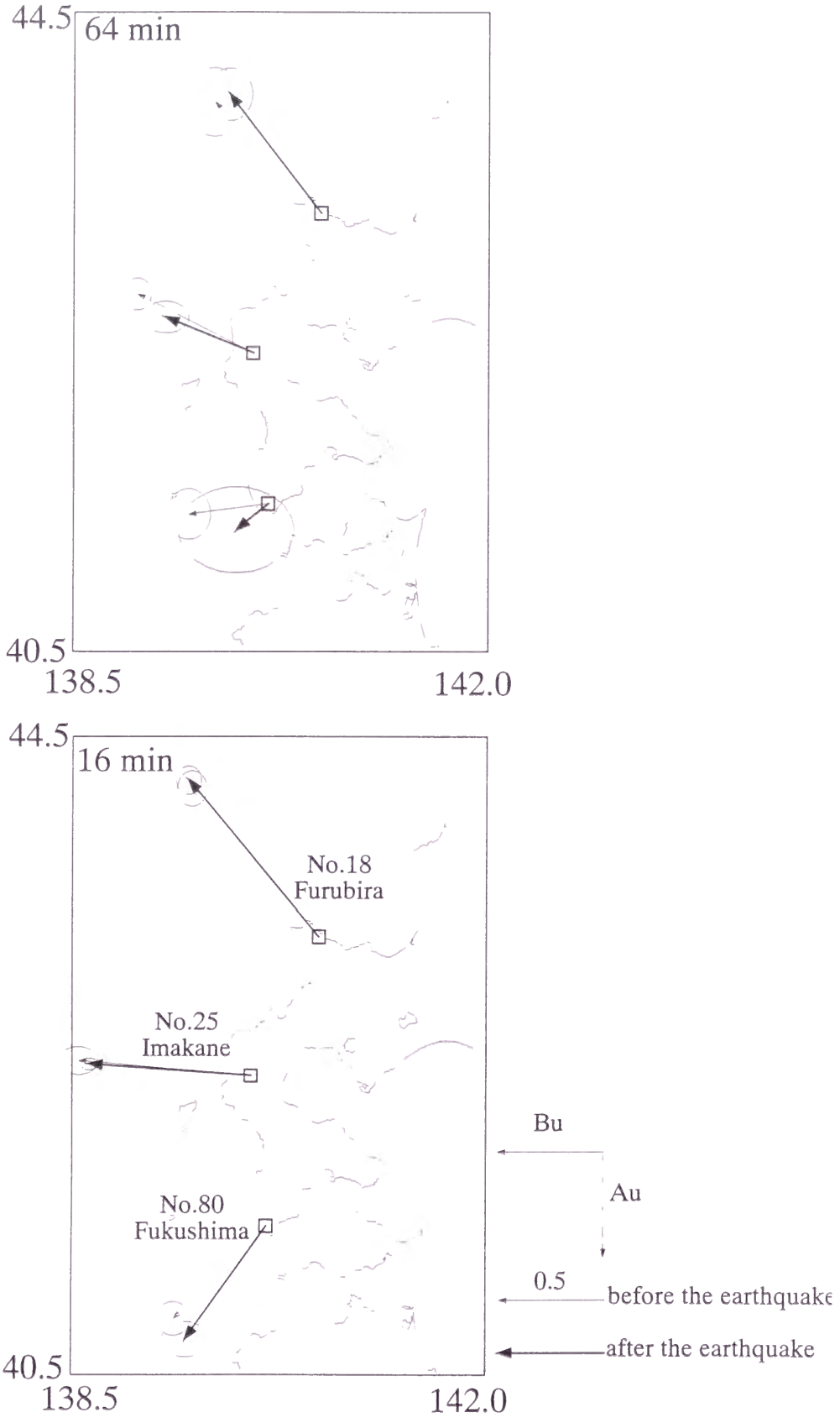

Figure 6-14 (a) Induction arrows of the vertical field, before and after the earthquake (real part). Ellipses shows the 95 % confidence intervals.

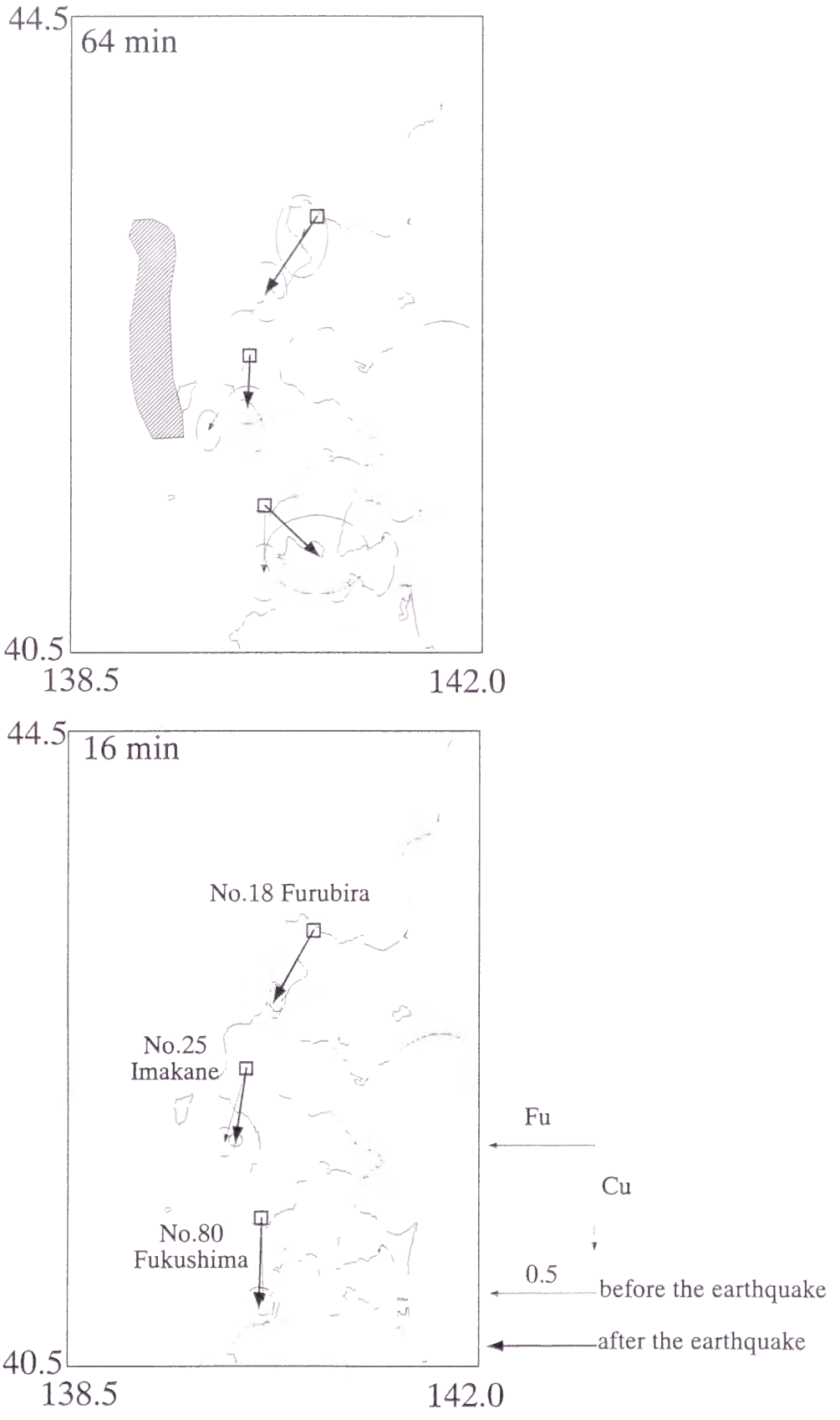

Figure 6-14 (b) Induction arrows of the the horizontal field, before and after the earthquake (real part). Ellipses shows the 95 % confidence intervals. The hatched area shows the after shock region of the earthquake.

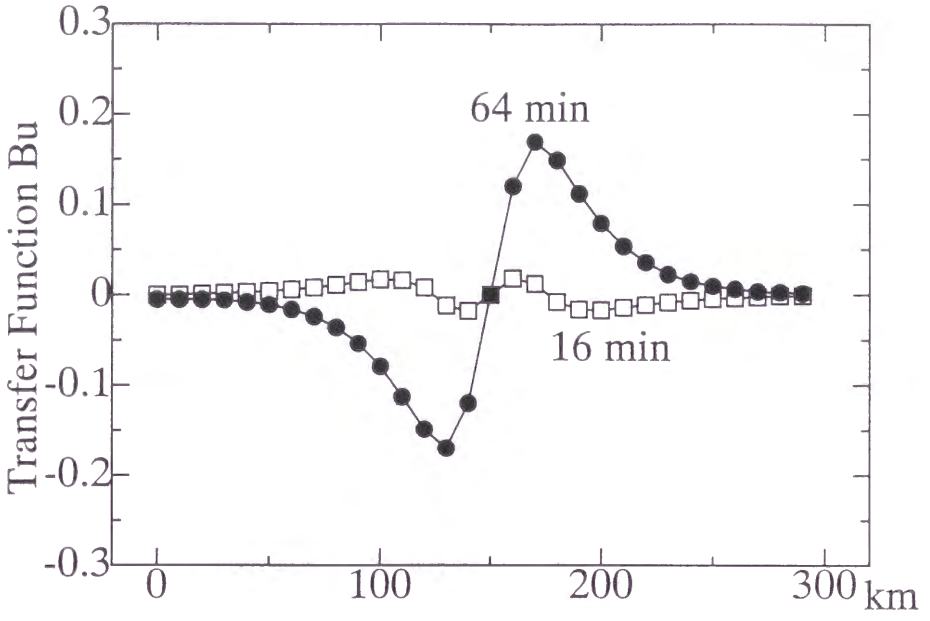

(a) Result of model in (b)

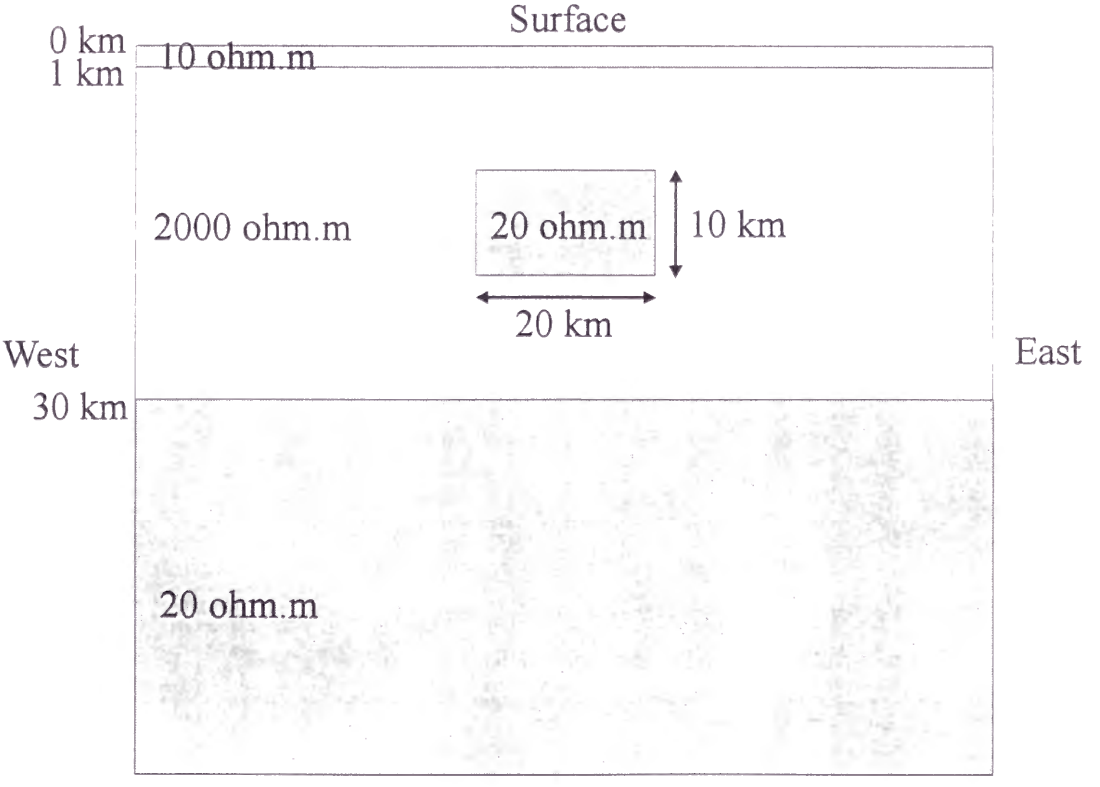

(b) Conductivity model

Figure 6-15 Two dimensional model simulation (real part).
This situation status is before the occurance of the earthquake.